Kappa opioid signaling in the brainstem and spinal cord for itch and pain

by

Eileen K Nguyen

B.S., University of California, Los Angeles, 2014

Submitted to the Graduate Faculty of the

School of Medicine in partial fulfillment

of the requirements for the degree of

Doctor of Medicine

University of Pittsburgh

2021

UNIVERSITY OF PITTSBURGH

SCHOOL OF MEDICINE

This dissertation was presented

by

Eileen K Nguyen

It was defended on

July 9, 2021

and approved by

Dr. Rebecca P. Seal, PhD, Associate Professor, Department of Neurobiology, School of Medicine

Dr. Michael S. Gold, PhD, Professor, Department of Neurobiology, School of Medicine

Dr. Bradley K. Taylor, PhD, Professor, Department of Anesthesiology, School of Medicine

Dr. Grace Lim, MD, Associate Professor, Department of Anesthesiology, School of Medicine

Dr. Sung Han, Assistant Professor, Salk Institute for Biological Sciences

Dissertation Director: Dr. Sarah E. Ross, PhD, Associate Professor, Department of Neurobiology, School of Medicine

Kappa signaling in the brainstem and spinal cord for itch and pain

Eileen K Nguyen, PhD

University of Pittsburgh, 2021

In the following dissertation I examine two of my primary studies that highlight the importance of *opioid balance* in itch and pain. In particular, these two studies focus on neurons that participate in kappa-opioid receptor signaling. In Part I, I describe the role of dynorphin spinal cord neurons in the modulation of itch. In Part II, I focus on neurons in the brainstem containing the kappa-opioid receptor and their role in the modulation of itch and pain.

In Part I, I discuss the role of neurons in the spinal cord that participate in kappa signaling that are modulated by mu agonists such as morphine. For this study, we used animal models and found that neuraxial morphine causes itch through spinal neurons and not mast cells. In particular, we found that spinal dynorphin (Pdyn) neurons are both necessary and sufficient for morphine-induced itch in mice. Agonism of the kappa-opioid receptor alleviated morphine-induced itch in mice and nonhuman primates. Thus, our work revealed that morphine causes itch through a mechanism of disinhibition of a kappa-sensitive pathway within the spinal cord. This mechanism, in which a mu agonist reduces the impact of endogenous dynorphin, is illustrative of the delicate balance between mu and kappa tone that, when accidentally disrupted, elicits abnormal itch sensations.

In Part II, I describe a cellular circuit involving brainstem neurons containing the kappa-opioid receptor that inhibits pain and itch in mice. Using a combination of molecular, tracing, and behavioral approaches, we found that spinally-projecting neurons in the medulla containing the kappa-opioid receptor inhibit itch and pain. With chemogenetic inhibition, we determined

that these neurons are required for stress-induced analgesia. Furthermore, we found a dynorphinergic pathway arising from the midbrain that modulates nociception within the medulla. These discoveries highlight the role of kappa signaling in the brainstem modulate itch and pain.

Thus, both investigations, centered in the brainstem and in the spinal cord, emphasize the importance the balance between endogenous opioids in normal somatosensory functions.

Table of Contents

List of Tables

List of Figures

Preface

This dissertation covers two major projects that I have worked on as a student. In my eyes, they have both challenged me and are equally interesting. Having divided my time across both projects throughout the duration of my studies, I believe it is worthwhile to dedicate space for them both in this dissertation. Initially, I viewed these two projects, one focused on a brainstem structure, the other on a specific population of spinal neurons, as distinct and separate questions. However, I now appreciate their similarities and how they both harmonize the idea that opioid homeostasis is integral to normal somatosensory functions. In both the brainstem and in the spinal cord, an imbalance between opioid signaling can engender itch pathology. The neuronal underpinnings of these disorders have formed the basis of my investigations. Together, I hope that both of these projects may shed light on a small part of our natural world.

Acknowledgements

I would like to express my special appreciation and gratitude to my advisor, Professor Sarah Elizabeth Ross. She has been a tremendous mentor. I would like to thank her for encouraging my research and for allowing me to grow as a scientist. She created a vibrant, engaging, and fun environment for me to conduct these studies. She has given me space and freedom to explore things and discover my own research potential. Due to her support, I have learned to appreciate the process of creating knowledge. I have learned, above all, to aim to do science with integrity, such that it will stand the test of time -- to do science that may, someday, improve human health. The outstanding mentorship I have received from her is a debt I can only pay forward.

I would also like to thank three important groups of people, without whom this dissertation would not have been possible: my committee, my colleagues, and my family.

I wish to thank the members of my dissertation committee: Professors Rebecca Seal (the chair of this committee), Michael Gold, Bradley Taylor, Grace Lim, and Sung Han. They have all generously offered their time, support, guidance and good will throughout the preparation and review of this document. They have each significantly contributed to my development, training, and confidence as a researcher and, from the bottom of my heart, I am grateful to them.

I have been lucky to have the support and encouragement from my friends and colleagues, both in and outside of the lab. From camaraderie to intellectual and technical help, I have received immense support from all members of the Ross Laboratory. I thank them, the Pain Center, and the Neurobiology Department for fostering an exciting and encouraging workplace. I also thank all my friends, both in and outside of Pittsburgh, who have actively supported me

through my training by listening to my practice presentations and carefully reviewing my applications.

My family, including my parents and both my maternal and paternal grandparents, who came to the United States as Vietnamese refugees, have made extraordinary sacrifices for me to have a chance to work towards something meaningful and something that I love. I owe much of my happiness and fulfillment to my family: Mom, Dad, Nick, and Neal. They have allowed me to appreciate the joy of working hard and creating a meaningful life. They raised me to be thoughtful, positive, and earnest. I thank them for always cheering me on, for their guidance, and for sending me dozens of California pastries over the years.

I want to thank my partner and husband, Lior Schenk, who moved to Pittsburgh in support of my academic dreams. Together, we have braved the world, made sense of its complexity, and conquered many of its challenges. He is my greatest gift, my love and light, and I am so lucky and honored to have married him.

To all of these individuals, I thank them for *everything* that helped me get to this day.

1.0 Introduction to morphine-induced itch

Opioids have been used to control pain for millennia. Today, they are used for numerous types of pain, including acute, chronic, pre-, peri-, and post- operative, and cancer pain. Unfortunately, the use of opioids is not without side effects. These side effects range from debilitating, such as constipation and nausea, to deadly, such as sedation and respiratory depression (Colvin, Bull, and Hales 2019; Els et al. 2017; Baldini, Von Korff, and Lin 2012; Dahan et al. 2004; Dahan, Aarts, and Smith 2010). Additionally, opioid medications are extremely addictive and have contributed to the world-wide opioid epidemic (Alam and Juurlink 2016). Thus, clinical efforts to reduce the use and abuse of these drugs have spurred research into alternative treatments and well as alternative routes for the administration of opioid drugs (E. C. Sun et al. 2016; Mudumbai et al. 2016).

One attempt to circumvent these adverse side effects has been the neuraxial (epidural and intrathecal) route of administration of opioids. The neuraxial route of administration is often preferred due to a decreased risk of constipation, nausea, respiratory depression, and dependence (de Leon-Casasola, Karabella, and Lema 1996; C. L. Wu et al. 2004; Niiyama et al. 2005; Bujedo 2012; Bujedo 2014). Moreover, because a catheter can be placed directly into the neuraxis, a smaller dose of opioid analgesics can be used for rapid and effective pain management (Fassoulaki et al. 2004; Chadwick and Ready 1988; Chestnut 2005). Compared with parenteral opioid administration, such as through an intravenous (IV), intramuscular (IM), or subcutaneous (SC) route, the intrathecal (IT) route of administration uses a fraction of the dose required due to its improved bioavailability (Stevens and Ghazi 2000).

1.1 Clinical indications for neuraxial opioid drug use

Neuraxial opioids are frequently administered for abdominal and lower extremity surgeries (Sarma and Boström 1993; Fassoulaki et al. 2004; Dualé et al. 2003; Chadwick and Ready 1988; Grant and Checketts 2008). For these procedures, the use of neuraxial analgesia, rather than parenteral analgesia, has been associated with improved postoperative outcomes such decreased length of hospital stay and reduced need for parenteral opioids postoperatively (de Leon-Casasola, Karabella, and Lema 1996; Jørgensen et al. 2000; Chestnut 2005).

1.2 Epidemiology and burden of opioid-induced pruritus

Although neuraxial opioids are frequently used in acute perioperative pain, they also have side effects. These side effects include pruritus (Ballantyne, Loach, and Carr 1988; Szarvas, Harmon, and Murphy 2003; Kumar and Singh 2013; Ganesh and Maxwell 2007), nausea (25%), sedation (17%), urinary retention (19%), and, very rarely, respiratory depression (3%) (Yurashevich and Habib 2019; Chestnut 2005; Mugabure Bujedo 2012). Although pruritus is occasionally observed with parenteral opioid use (Tarcatu et al. 2007; Jannuzzi 2016), it is an extremely common side effect of neuraxial opioids, with an incidence ranging from 30-85%, depending on the dose and lipophilicity of the opioid administered (Kumar and Singh 2013; Yeh et al. 2000; Shah, Sia, and Chong 2000). Dose-response relationships between spinal morphine, analgesic duration, and pruritus have indicated that escalating doses of morphine improve analgesia, but are correlated with higher incidences and severity of pruritus (Jiang et al. 1991; Sultan et al. 2016). This relationship suggests that the duration of analgesia of neuraxial

morphine can be improved with increased doses, but must be weighed against increasing side effects.

Due to the widespread use of neuraxial opioids in the childbirth setting, opioid-induced pruritus is most frequently observed among obstetric patients (Tubog et al. 2018; Wells, Paech, and Evans 2004; Yurashevich and Habib 2019; S Charuluxananan et al. 2000) (Table 1), where it has an incidence of up to 85% (Yeh et al. 2000), and is primarily dose-dependent (Jiang et al. 1991; Sultan et al. 2016). Pruritus is also frequently reported among orthopedic patients receiving neuraxial opioids (30-70%) (Kaye et al. 2019; Szarvas et al. 2003) for enhanced recovery after surgery (ERAS). The incidence of pruritus in patients receiving neuraxial morphine is more common among female patients (60-85%) (Tubog et al. 2018; Wells, Paech, and Evans 2004; Yurashevich and Habib 2019; Charuluxananan et al. 2000), which mirrors the incidence and burden of chronic pain that also disproportionately affects women. Differences in estrous cycle, which could affect the sensitivity of the mu-opioid receptor to opioid drugs (LaBella, Kim, and Templeton 1978), have been proposed to underlie these differences, yet the extent to which non-biological factors could also contribute to disparities in experiences of pruritus warrants further investigation.

In contrast to the high frequency of neuraxial opioid-induced itch, parenteral opioid-induced pruritus occurs in less than 10% of patients on long-term opioid therapy, such as patients receiving intravenous (IV) morphine for vaso-occlusive crisis in sickle cell disease (Krajnik and Zylicz 2001; Werawatganon and Charuluxanun 2005). Unlike neuraxial opioid-induced pruritus, which is observed following a single dose of opioids, parenteral opioid-induced pruritus is mostly observed among patient populations on chronic opioid use (Werawatganon and Charuluxanun 2005; Hong, Flood, and Diaz 2008). In addition to patients with sickle cell

disease, these groups include individuals who chronically take oral and parenteral opioids for pain, such as cancer patients and those with opioid dependence (Galloway and Yaster 2000; Watcha and White 1992; Koch et al. 2008).

Among patients on continuous morphine infusion during vaso-occlusive crises in sickle cell disease, pruritus was the most common reason for switching medications to another opioid class: for example, from morphine to a semi-synthetic opioid such as hydromorphone (DiGiusto et al. 2014) In these settings, the development of pruritus may be associated with central sensitization to opioids that may occur independently of tolerance to opioid-induced analgesia (Schmelz and Paus 2007). Proposed mechanisms include sensitization of itch-responsive circuits within the spinal dorsal horn following chronic use (Ikoma et al. 2006). In particular, central, but not peripheral, mu-opioid receptors have recently been implicated in modulation of dermatitis and lymphoma-induced chronic itch (Wang et al. 2021). Further research is necessary to elucidate the contribution of these central pathways to chronic opioid-induced pruritus. Thus, while pruritus is most common following neuraxial opioid administration, it also poses a troublesome side effect for a small number of patients, such as those with sickle cell disease on parenteral opioids.

Polymorphisms of OPRM1 on opioid-induced analgesia and pruritus

Sequencing of the *OPRM1* gene, which encodes the mu-opioid receptor, indicates that certain polymorphisms may be associated with protection against the side effect of pruritus (Tsai et al. 2010; Pettini et al. 2018). For example, genetic association studies have focused on the A118G polymorphism of *OPRM1* (Tsai et al. 2010; Pettini et al. 2018). The recessive G allele in this polymorphism is associated with lower incidences of pruritus among obstetric patients receiving epidural (4.8%) and spinal (0-50%) morphine (Tsai et al. 2010; Pettini et al. 2018).

This variant is further associated with reduced sensitivity to the analgesic effects of opioids (Sia et al. 2008), suggesting that the A118G polymorphism may give rise to a mu-opioid receptor that is generally less responsive to opioid medications. However, given the heterogeneity among clinical populations receiving opioid analgesia and their self-reported experiences for both pain and itch, many of these studies are underpowered to provide definitive conclusions about these polymorphism relationships (Wong et al. 2010; Kung et al. 2018). In mice, distinct splice variants of the mu-opioid receptor, *MOR1D* and *MOR1*, have been shown to differentially modulate morphine-induced itch and morphine-induced analgesia, respectively (Liu et al. 2011). However, the contributions of these splice variants have not been characterized in humans. Additional large population genetic association studies are necessary to further assess the clinical significance and utility of identifying genetic variations on acute postoperative pain management and risk for opioid-related side effects.

Differences in opioid medications and pruritus

Opioid-induced pruritus is observed following the use of intrathecally administered hydrophilic opioids (such as morphine) and lipophilic opioids (such as fentanyl and sufentanil) (Mulroy, Larkin, and Siddiqui 2001; Gulhas et al. 2007). The high incidence of pruritus following morphine (60-85%) (Waxler et al. 2005; Jannuzzi 2016; Ganesh and Maxwell 2007; Szarvas, Harmon, and Murphy 2003; Ballantyne, Loach, and Carr 1988) and lipophilic opioids (60-90%) (Mulroy, Larkin, and Siddiqui 2001; Gulhas et al. 2007) suggests a common mu-sensitive pathway modulates pruritus in response to these medications (Table 1). However, a key difference between these two classes of opioid drugs is the onset of pruritus; pruritus occurs within hours up to several days in patients receiving epidural and spinal morphine (Slappendel et al. 2000; Waxler et al. 2005), whereas with lipid-soluble opioids, the onset of pruritus can occur

as rapidly as within minutes of administration (Gulhas et al. 2007; Wells, Paech, and Evans 2004). These differences reflect the pharmacokinetics of these intrathecally-administered opioid medications; microdialysis studies in pigs (Ummenhofer et al. 2000) (using equimolar doses of morphine, fentanyl, and sufentanil) have revealed that spinal exposure to morphine was greater than lipophilic opioids due to its low spinal cord distribution volume and slow clearance into the plasma. Fentanyl and sufentanil were found to rapidly clear into the plasma and epidural fat, respectively, reducing their spinal bioavailability (Ummenhofer et al. 2000). In a clinical study examining the clearance of opioid medications from the CSF, volunteers receiving an intrathecal injection of both morphine and fentanyl (50 μg each), the ratio of morphine to fentanyl in the CSF increased over time (reaching 4:1 within two hours) (Eisenach et al. 2003). These differences support the suitability of neuraxial morphine for acute postoperative pain, such as for ERAS (Tang et al. 2020) and in obstetric settings (Sutton and Carvalho 2017), due to its superior bioavailability, but its long elimination time must be considered against its delayed adverse effects, such as pruritus.

Table 1. Incidence of parenteral and neuraxial opioid-induced pruritus.

Route	Opioid	Incidence of pruritus	Onset	Mechanism
Parenteral	Morphine (0.05 mg·kg^{-1}·h^{-1} IV)	<10% (Krajnik and Zylicz 2001; Werawatganon and Charuluxanun 2005)	Apparent with chronic use (Werawatganon and Charuluxanun 2005; Hong, Flood, and Diaz 2008)	Peripheral (histamine dependent) (Ennis et al. 1991; Philbin et al. 1982; Baldo and Pham 2012)
Neuraxial	Morphine (1.5-5 mg epidural; 50-200 μg IT)	60-85% (Waxler et al. 2005; Jannuzzi 2016; Ganesh and Maxwell 2007; Szarvas, Harmon, and Murphy 2003; Ballantyne, Loach, and Carr 1988)	Hours to days (Slappendel et al. 2000; Waxler et al. 2005)	Central/spinal (Kumar and Singh 2013; Wang et al. 2021; Nguyen et al. 2021)
Neuraxial	Lipid-soluble (fentanyl and sufentanil) (20-100 μg epidural; 10-20 μg IT)	60-90%(Mulroy, Larkin, and Siddiqui 2001; Gulhas et al. 2007)	Rapid (within minutes to 4 hours) (Gulhas et al. 2007; Wells, Paech, and Evans 2004)	Central/spinal (Kumar and Singh 2013; Wang et al. 2021; Nguyen et al. 2021)

1.3 Mechanisms for opioid-induced pruritus

1.3.1 Role of mast cells

It has been proposed that release of histamine underlies opioid-induced pruritus (Galloway and Yaster 2000), although route of administration might lead to differential impact of mast cells on pruritus (Figure 1). Intramuscular and subcutaneous morphine have been shown to evoke pruritus and vasodilation at the injection site (Melo et al. 2018). One study that performed *in vivo* microdialysis in human skin found that intradermal injections of morphine led

to dose-dependent increases in local histamine and itch sensations (Blunk et al. 2004). Similarly, examination of blood samples from patients with parenteral exposure to opioids has also revealed an elevation in histamine levels (Ennis et al. 1991; Philbin et al. 1982; Baldo and Pham 2012). Lastly, *in vitro* studies in both human and rodent models have confirmed that opioids, such as morphine, act directly on mast cells to drive degranulation and histamine release (Lansu et al. 2017; Grosman 1981; Hermens et al. 1985).

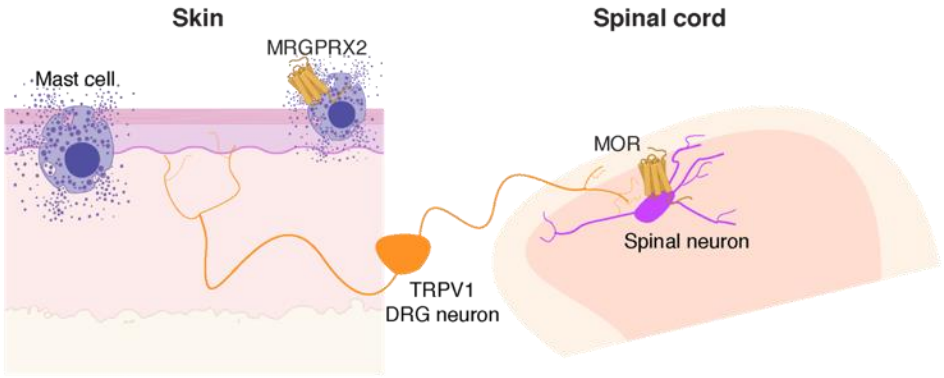

Figure 1. Proposed mechanisms of opioid-induced pruritus.

Mechanisms by which opioids could drive pruritus in the skin, dorsal root ganglia (DRG), and spinal cord dorsal horn. In the skin, systemic opioids can cause mast cell degranulation through activation of Mas-Related G Protein-Coupled Receptor-X2 (MRGPRX2) on mast cells. Neuraxial opioids are proposed to drive itch through spinal neurons containing the mu-opioid receptor (MOR) in the spinal cord dorsal horn.

Only recently, however, has it become clear how opioids could directly activate mast cells. Morphine was recently found to induce mast cell degranulation through activation of mas-related G protein-coupled receptor X2 (MRGPRX2), a primate-exclusive G protein-coupled receptor (GPCR), rather than canonical opioid receptors (such as the mu-opioid receptor) (Lansu et al. 2017). Binding of opioids to MRGPRX2 leads to increases in intracellular calcium in mast cells

(Lansu et al. 2017). This is thought to occur through the phospholipase C-beta pathway, which results in the release of mediators, such as histamine (Porebski et al. 2018) MRGPRX2 is implicated in itch and pain (Meixiong et al. 2019), and the restricted expression of MRGPRX2 on mast cells, which can be activated in the absence of atopy (Porebski et al. 2018), such as by direct binding of opioids (Lansu et al. 2017), establishes a mechanism for how opioids can directly act on mast cells to give rise to pruritus (Figure 2). The expression of MRGPRX2 on mast cells may also underlie anaphylaxis following opioid administration, which comprised 2.6% of all cases of anaphylaxis due to anesthetics (Laxenaire et al. 1990). For these reasons, MRGPRX2 should be considered a target for IgE-independent allergic reactions to perioperative drugs such as morphine administered subcutaneously and intravenously.

However, for neuraxial opioids, the evidence that a mast cell-dependent mechanism underlies pruritus is less compelling. In humans, the neuraxial administration of fentanyl, a lipophilic and synthetic opioid, evokes pruritus even though fentanyl does not cause mast cell degranulation and histamine release as morphine does (Rosow et al. 1982; Hermens et al. 1985; Warner et al. 1991; Flacke et al. 1987). Furthermore, clinical plasma concentrations of morphine are orders of magnitude smaller than CSF concentrations following neuraxial morphine administration (<0.01%) (Sjöström et al. 1987; Bernards et al. 2003) and the concentration of morphine detected in the plasma is likely insufficient to cause mast cell degranulation, as suggested by in vitro studies (Figure 2) (Lansu et al. 2017; Grosman 1981; Hermens et al. 1985). Mast cell-mediated pruritus following the local injection of opioids, as seen following intradermal injections of morphine, is restricted to the site of injection (Blunk et al. 2004), and does not explain how neuraxial opioids, frequently administered into lumbar segments, evoke pruritus in other dermatomes, including those innervating facial regions (Ballantyne, Loach, and

Carr 1988; Szarvas, Harmon, and Murphy 2003; Ganesh and Maxwell 2007). Lastly, genetically modified mice lacking mast cells scratch at levels similar to controls in response to intrathecal morphine (Nguyen et al. 2021). Therefore, a mast cell-dependent mechanism does not explain the prevalence and spread of neuraxial opioid-induced pruritus.

Taken together, although there is evidence that histamine release from mast cells may cause itch from peripheral (subcutaneous, oral, and intravenous) opioids, this process is unlikely to contribute to neuraxial opioid-induced pruritus.

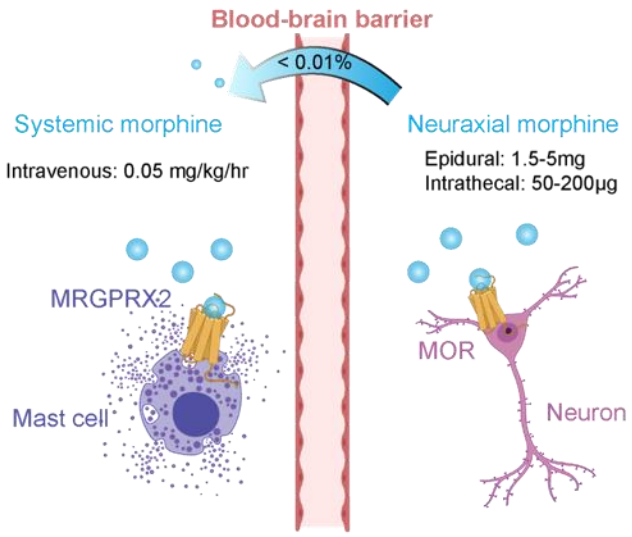

Figure 2. Systemic and neuraxial opioid-induced pruritus are separately modulated.

Systemic (oral, subcutaneous, and parenteral) morphine may drive pruritus through the engagement of Mas-Related G Protein-Coupled Receptor-X2 (MRGPRX2) on mast cells. Neuraxial (epidural and intrathecal) opioid-induced pruritus, on the other hand, is likely driven by spinal neurons containing the mu-opioid receptor (MOR) because less than 0.01% of the peak concentration detected in the CSF is detected in the plasma following neuraxial opioid administration.

1.3.2 Central mechanisms of opioid-induced pruritus

With neuraxial morphine-morphine induced itch, it has been proposed that the nervous system could be responsible for mediating the sensation of itch through the binding of opioids to the mu opioid receptor (Ko 2015; Kumar and Singh 2013) (Figure 2). The analgesic benefits of opioids are mediated through the nervous system (Pathan and Williams 2012; Pan, Hirakawa, and Fields 2000); therefore, it is plausible that pruritus, the unwanted sensory symptom, may also be neuronally-mediated. To add, although both intrathecal and epidural opioids cause pruritus (Ballantyne, Loach, and Carr 1988; Szarvas, Harmon, and Murphy 2003), pruritus occurs much more commonly with the intrathecal route of administration (Simmons et al. 2012). This observation suggests that the pruritus occurs due to a direct effect of the opioid within the neuraxis.

Further evidence for a neuronal mechanism is the clinical observation that opioid lipophilicity is associated with the onset of pruritus among patients. For example, lipophilic opioids such as fentanyl, which more readily cross the blood brain barrier, are associated with a more rapid onset and shorter duration of pruritus than hydrophobic opioids such as morphine (Asokumar et al. 1998; Wells, Paech, and Evans 2004; Shah, Sia, and Chong 2000; Kumar and Singh 2013), consistent with a neural mechanism of action. These clinical observations further support the idea that two separate mechanisms underlie opioid-induced pruritus from different routes of administration.

1.3.2.1 Opioid-induced pruritus mediated by primary afferents

Primary sensory neurons respond directly to itch-inducing agents. For example, a class of TRPV1-containing C-fibers that innervate the skin expresses the histamine receptor (H1R),

which can be activated by histamine (Shim and Oh 2008; Davidson and Giesler 2010). Upon activation with histamine, these neurons transmit pruriceptive information to the superficial layers of the spinal cord and this information ascends through the spinothalamic tracts to target the primary sensory and cingulate cortices (Schmelz et al. 1997). Thus, if opioid-induced pruritus causes the release of histamine, then peripheral opioid-induced itch may occur through this pathway (Figure 1). Consistent with this view, intradermal injection of the mu-opioid receptor agonist, DAMGO, elicits itch in mice that is abrogated with the ablation of TRPV1-expressing fibers (Melo et al. 2018). Furthermore, the administration of capsaicin, a TRPV1 agonist, reduced scratching in response to intradermal DAMGO, but this was not observed following agonism of TRPA1, another channel expressed by primary afferents that has been implicated in acute and chronic itch (Melo et al. 2018; Wilson et al. 2013, 2011). These findings suggest that for subcutaneous, oral, and intravenous opioids, itch likely occurs through TRPV1 sensory neurons following the release of histamine from mast cells (Ennis et al. 1991; Philbin et al. 1982; Baldo and Pham 2012). However, given the weak association between neuraxial opioids and histamine release in the systemic circulation (Rosow et al. 1982; Hermens et al. 1985; Warner et al. 1991; Flacke et al. 1987), H1R-expressing sensory neurons are not likely to be involved in neuraxial opioid-induced pruritus.

Presently, neuraxial opioids are not believed to act directly on mu-opioid receptor expressing sensory neurons to elicit itch. Conditional deletion of the mu-opioid receptor from TRPV1 and somatostatin neurons, which have been implicated in itch signaling, did not affect intrathecal morphine-induced itch in mice (Wang et al. 2021). In support of this view, other studies have suggested that rather than direct modulation of these peripheral sensory neurons, neuraxial opioids may influence pruriceptive processing centrally. One study, performed in rats,

identified that neuraxial morphine augmented the activity in trigeminothalamic tract neurons in response to itch stimuli (Moser and Giesler 2013). Trigeminothalamic tract neurons are analogous to spinothalamic tract neurons in the spinal cord, but relay information pertaining to the head and neck regions rather than the body. It was found that intrathecal morphine caused these neurons to increase their ongoing activity to pruritogens applied to the skin (Moser and Giesler 2013). Intrathecal morphine also enhanced responses to innocuous mechanical stimuli, suggesting that opioids may also cause sensitization to touch-evoked itch (Moser and Giesler 2013). Another study in mice also examined the role of TRPV1 antagonists and neuraxial morphine-induced itch (Sakakibara et al. 2019). In this study, it was observed that the intrathecal delivery of a TRPV1 antagonist reduced morphine-induced itch in mice. Together, these studies suggest that neuraxial morphine can evoke sensitization of central pathways, leading to an enhancement of responsiveness within these circuits to peripheral stimulation.

1.3.2.2 Opioid pharmacology as a key to understanding spinal circuitry

It is curious that opioids suppress pain, but evoke itch. Conversely, intense pain can also suppress itch (Liu and Ji 2013; Graham, Goodell, and Wolff 1951). Previously, it was believed that itch occurs due to a reduction in pain signaling (Ikoma et al. 2006). However, detailed pharmacological investigations have largely ruled out this theory (Ko and Naughton 2000; Liu et al. 2011). Several studies have shown that mu-opioid agonists, such as morphine, elicit itch, but delta- and kappa-opioid receptor agonists, which also produce analgesia (Woolf 2009), do not cause scratching behavior (Ko 2015; Ko et al. 2003; Ko and Naughton 2000). Instead, selective kappa-opioid receptor agonists have been shown to suppress itch in preclinical models (Kamei and Nagase 2001; Ko and Husbands 2009; Kardon et al. 2014) and have been approved to treat chronic pruritus in Japan (Cowan, Kehner, and Inan 2015). Notably, mu and kappa-opioid

receptors often exert opposing effects in several regions of the central nervous system; whereas mu-opioid receptor agonists produce analgesia, euphoria, and itch, kappa-opioid receptor agonists are anti-pruritic and dysphoric (Pfeiffer et al. 1986; Pan 1998). Clearly, a simple model whereby a suppression of pain is sufficient to evoke itch does not explain these observations. The differential roles of these opioid receptors and their agonism in the context of itch underscores that opioid-induced pruritus is a complex and active process.

1.3.2.3 Neuronal disinhibition underlies neuraxial opioid-induced itch

The mechanisms of opioid-induced itch at the level of the dorsal horn have only recently begun to be examined. One study in mice suggested that neuraxial morphine causes itch through activation of gastrin-releasing peptide receptor (GRPR) neurons in the dorsal horn (Liu et al. 2011), an excitatory population that is involved in mediating itch (Sun and Chen 2007; Pagani et al. 2019) (Figure 3). This study suggested that neuraxial morphine could induce heterodimerization of the mu-opioid receptor (MOR) with GRPR, activating the PLCβ3 and IP3R3 pathway, resulting in itch (Liu et al. 2011). However, recent sequencing (Sathyamurthy et al. 2018; Häring et al. 2018) and neurochemical studies (Wang et al. 2020) cast doubt on this possibility and, mechanistically, binding of morphine to the mu opioid receptor causes hyperpolarization, rather than activation, of neurons (Al-Hasani and Bruchas 2011; Torrecilla et al. 2008). Thus, the notion that opioids cause itch through heterodimerization of MOR and GRPR remains controversial (Ko 2015).

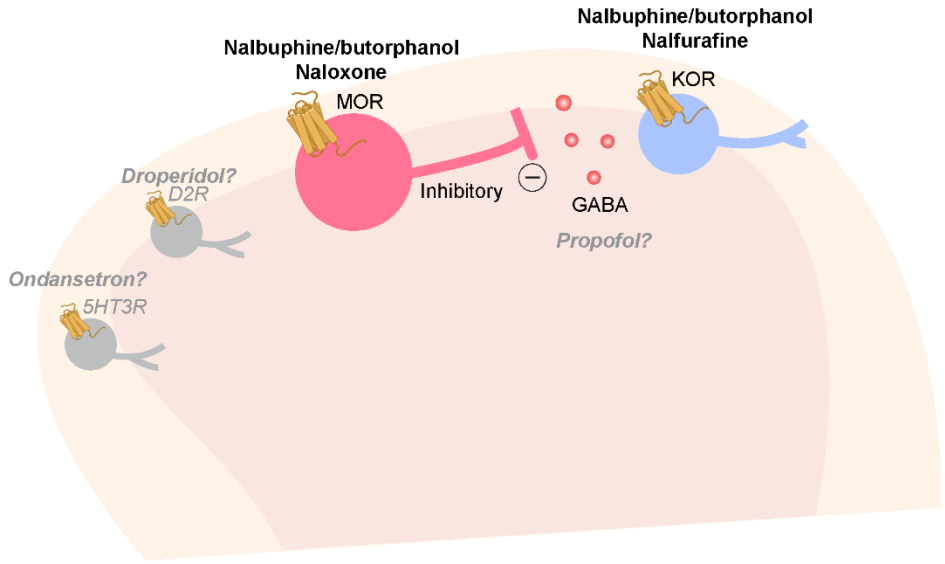

Figure 3. Mechanisms of action of proposed therapies for neuraxial opioid-induced pruritus.

Antagonists (naloxone) of the mu-opioid receptor (MOR) are proposed to act on MOR-expressing inhibitory neurons to relieve pruritus. Propofol may potentiate the inhibitory action of these inhibitory neurons to suppress itch. Mixed antagonist-agonists (nalbuphine and butorphanol) inhibit itch through antagonism of MOR and agonism of the kappa-opioid receptor (KOR). Dopamine and serotonin receptor antagonists (droperidol and ondansetron, respectively) are thought to exert their action on spinal neurons, although this has not been tested directly.

Alternatively, molecularly defined inhibitory neurons have been implicated in the modulation of itch. For example, inhibitory neurons containing dynorphin (Pdyn) and neuropeptide Y (Npy) have been shown to be important for the inhibition of chemical (Kardon et al. 2014; Ross et al. 2010; Huang et al. 2018) and mechanical itch (Acton et al. 2019; Bourane et al. 2015), respectively. When either Pdyn neurons or Npy neurons are lost during development, mice show spontaneous scratching behavior suggesting that these populations are involved in the tonic inhibition of itch (Ross et al. 2010; Bourane et al. 2015; Kardon et al. 2014; Huang et al. 2018; Acton et al. 2019). In a recent study, selective removal of the mu-opioid receptor from inhibitory neurons (neurons that produce GABA, gamma-amino butyric acid) abolished opioid-induced itch in a mouse model (Wang et al. 2021). A second study focused on a subset of

inhibitory neurons containing dynorphin, the endogenous peptide for the kappa-opioid receptor (Nguyen et al. 2021). In this study, the expression of the mu-opioid receptor was found to be required for morphine-induced itch (Nguyen et al. 2021). Kappa-opioid signaling alleviated morphine-induced itch in both mice and non-human primates (Nguyen et al. 2021). Therefore, emerging evidence highlights that opioids could cause itch through inhibition of inhibitory neurons; rather than through MOR/GRPR heterodimerization, there is now compelling evidence that opioids cause itch through a mechanism of neuronal disinhibition (Figure 3).

These two recent studies, from two independent groups, highlight the role of inhibitory neurons in the spinal cord as the crucial mediators of opioid-induced itch. To date, they provide the most compelling evidence for how a spinal mechanism is responsible for neuraxial opioid-induced itch.

1.4 Treatments for opioid-induced pruritus

Given the dose-dependent nature of opioid-induced pruritus, clinicians have managed to control unwanted side effects by tightly titrating the dose needed to optimize analgesia. Furthermore, multimodal analgesia has also been shown to be effective at both managing pain and reducing the side effect of pruritus. For example, the addition of a local anesthetic, such as bupivacaine, with the opioid analgesic appears to reduce the severity of pruritus in the immediate postoperative period (Mulroy, Larkin, and Siddiqui 2001; Asokumar et al. 1998). However, the half-lives of these local anesthetics are short compared to opioids (Liu et al. 1996; DeSousa 2014; Smith et al. 2008), and thus it is challenging to determine whether local anesthetics reduce the pruritus caused by opioids or simply reduce sensation more generally. Despite efforts to

reduce the dose of opioids administered and to apply a multi-modal approach to neuraxial analgesia, pruritus as a side effect persists. For these patients, the most common treatment options are described below (Table 2).

Table 2. Frequently prescribed treatments for opioid-induced pruritus.

Examples and sites of action are listed. H1R, histamine receptor; 5HT3R, 5-hydroxytryptamine receptor 3A; D2R, dopamine receptor; GABA, gamma-aminobutyric acid; PONV, postoperative nausea and vomiting.

Class	Example (recommended dose and route)	Site of Action	Recommended appropriate clinical use	Notes
H1R antagonist	Diphenhydramine (25 mg IV)	Peripheral	Parenteral morphine	Sedation is a common and problematic side effect (Anwari and Iqbal 2003; Jannuzzi 2016; Roth et al. 1987)
Mu antagonist	Naloxone (0.25-2 $\mu g \cdot kg^{-1} \cdot h^{-1}$ IV)	Central	Parenteral and neuraxial opioids	Limited by reduction in analgesia (Gan et al. 1997)
Mixed mu antagonist, kappa agonist	Nalbuphine (1-5 mg IV), butorphanol (.2-2 mg IV)	Central	Neuraxial opioids	Highly effective anti-pruritic, without major reductions in analgesia, but can cause drowsiness (Jannuzzi 2016; Cohen et al. 1992; Lee et al. 2007)
5HT3R antagonist	Ondansetron (4 mg IV)	Central	Neuraxial opioids	Does not decrease the incidence of pruritus, but prophylactic treatment may reduce severity (George, Allen, and Habib 2009; Somrat Charuluxananan et al. 2003; Sarvela et al. 2006; Yeh et al. 2000; Yazigi et al. 2002; Siddik-Sayyid et al. 2007; Kyriakides, Hussain, and Hobbs 1999) and reduce PONV
Selective kappa agonist (preclinical)	Nalfurafine (in primates: 0.1-1 μg/kg IV; 0.3 μg IT; in mice: 40 ng IT)	Central	Neuraxial opioids	Clinically approved for pruritus of systemic disease in Japan (Cowan, Kehner, and Inan 2015). Effectively treats morphine-induced itch in preclinical models without affecting analgesia (Nguyen et al. 2021)
D2R antagonist	Droperidol (1.25 mg IV)	Central	Neuraxial opioids	Data limited, but has been observed to reduce incidence of pruritus (Horta and Vianna 2003; Horta, Ramos, and Gonçalves 2000; Horta et al. 2006)
Inhibition of neuronal activity	Gabapentin (1200 mg PO)	Central	Neuraxial opioids	Effective for pruritus in systemic disease (Anand 2013), but effectiveness is unclear for opioid-induced pruritus (Chiravanich, Oofuvong, and Kovitwanawong 2012; Sheen et al. 2008)

Table 2. Frequently prescribed treatments for opioid-induced pruritus. (continued)

Potentiation of GABAAR	Propofol (10-30 mg IV)	Central	Neuraxial opioids	Controversial; reduces incidence of pruritus in patients undergoing some elective surgeries (Törn et al. 1994; Borgeat et al. 1992), but not cesarean delivery (Warwick, Kearns, and Scott 1997)

1.4.1 Antihistamines

The role of antihistamines in neuraxial opioid-induced pruritus is contested. Antihistamines reduce diaphoresis and wheal-and-flare responses to parenteral opioids (Philbin et al. 1982), and many providers continue to use antihistamines to manage pruritus induced by opioids. Nevertheless, the appropriateness of this practice in the setting of neuraxial opioid-induced pruritus is questionable (McNicol et al. 2003). Several studies indicate that H1R antagonists, such as diphenhydramine and promethazine, reduce itch in obstetric patients who receive neuraxial opioids (Liao et al. 2011; Horta et al. 2006; Eldor et al. 1994; Millington et al. 2018). However, antihistamines have also been shown to cause sedation (Anwari and Iqbal 2003; Jannuzzi 2016; Roth et al. 1987), and it has been observed that the sedating effects of antihistamines have caused patients to verbally deny itch, but continue to scratch or that patients report itchiness in between periods of sleep (Roth et al. 1987; Ballantyne, Loach, and Carr 1988; Horta et al. 2006). Thus, it is possible that the apparent reduction in itch with antihistamine treatment seen in some studies may, in fact, be secondary to drowsiness (Kamei et al. 2005).

Comparisons between the effectiveness of mixed kappa agonist-mu antagonists and antihistamines for the management of neuraxial opioid-induced pruritus have revealed major limitations of antihistamine treatment for this form of pruritus (Eldor et al. 1994; Dunteman,

Karanikolas, and Filos 1996; Liao et al. 2011; Somrat et al. 1999; Horta et al. 2006; Juneja, Ackerman, and Bellinger 1991). In spite of these limitations, they continue to be prescribed for both peripheral and central opioid-induced pruritus (Millington et al. 2018; Kumar and Singh 2013). Given new evidence that spinal neurons mediate neuraxial opioid-induced pruritus (Ko 2015; Wang et al. 2021; Nguyen et al. 2021), antihistamines likely have no role in the treatment of neuraxial opioid-induced pruritus, but they may have a key role in the treatment of subcutaneous, oral, and intravenous morphine-induced pruritus.

1.4.2 Mu-opioid receptor antagonists

To date, the most effective treatments for opioid-induced pruritus have included pharmacological agents that antagonize the mu-opioid receptor, which pose disadvantages in that they can reverse analgesia (Cohen et al. 1992; Miller and Hagemann 2011). Clinically, mu-opioid receptor antagonists have also been shown to be effective for the management of parenteral opioid-induced pruritus (Dunteman, Karanikolas, and Filos 1996). For patients on parenteral opioid therapy, such as patients with sickle cell disease, the co-administration of the opioid analgesic and its antagonist helps to mitigate pruritus, (Koch et al. 2008) particularly when small doses are infused (e.g. naloxone 0.25-2 $\mu g \cdot kg^{-1} \cdot h^{-1}$ intravenous push) (Kjellberg and Tramèr 2001; Maxwell et al. 2005). Naloxone is also effective at reducing wheal and flare responses caused by morphine (Levy et al. 1989). These findings highlight the utility of mu-opioid receptor antagonists in the management of peripherally mediated and histamine-dependent opioid induced pruritus.

Mu-opioid receptor antagonists are also effective for the treatment of pruritus induced by neuraxial opioid administration (Ganesh and Maxwell 2007; Kumar and Singh 2013). Naloxone

and naltrexone are direct opioid receptor antagonists often used to reduce both the frequency and severity of pruritus evoked by neuraxial opioid analgesia (Miller and Hagemann 2011). Unfortunately, these antagonists, at doses that are clinically effective at reversing pruritus, may also reverse the analgesic effects of opioids (Gan et al. 1997) (e.g., complete reversal for opioid-induced respiratory depression at doses of naloxone 0.1 mg/kg intravenous push) (Rzasa Lynn and Galinkin 2018). In non-human primates, the one-time administration of a selective mu-opioid receptor antagonist, such as nalmefene, produced a 10-fold rightward shift in both morphine-induced scratching and analgesia (M. C. Ko and Naughton 2000). Furthermore, the mean pK_B (an estimate of antagonist affinity) of nalmefene was found to be similar for both scratching and thermal nociception endpoints (M. C. Ko and Naughton 2000), indicative of a circumscribed window for the management of itch without affecting analgesia by mu-opioid receptor antagonism, making these agents suboptimal for the treatment of pruritus in obstetric patients. Thus, optimal doses of mu antagonists, such as naloxone or naltrexone, to relieve clinical pruritus often come with a risk-benefit discussion with patients about their preferential priorities on pain control versus itch.

Alternatively, mixed opioid receptor agonists, such as nalbuphine (1-5 mg IV) (S Charuluxananan et al. 2001) and butorphanol (0.2-2 mg IV) (Lawhorn et al. 1991) are also clinically effective therapies for neuraxial opioid-induced pruritus (Jannuzzi 2016; Cohen et al. 1992; Lee et al. 2007). They are frequently used due to their improved ability to manage pruritus without reducing analgesia compared to selective mu-opioid receptor antagonists (Cohen et al. 1992). Nalbuphine is a mixed antagonist of the mu-opioid receptor and agonist of the kappa-opioid receptor and due to its partial antagonism of the mu-opioid receptor, reversal of analgesia remains a concern (Kendrick et al. 1996). Another potential limitation of nalbuphine is its

sedating side effect (Kjellberg and Tramèr 2001; Jannuzzi 2016), although this is only observed when a high dose (10 mg/70 kg) is used (Goletiani et al. 2007), which is beyond the range used to manage pruritus clinically (Tubog et al. 2018). In contrast, butorphanol is a partial agonist of both the mu- and kappa-opioid receptors. Similar to nalfurafine, butorphanol has also been reported as an effective treatment of opioid-induced pruritus, particularly among pediatric patients (Gunter et al. 2000; Bailey et al. 1994). Thus, nalfurafine and butorphanol may pose therapeutic advantages over selective mu antagonists due to their agonism of the kappa opioid receptor and the ability to directly modulate spinal itch circuits.

Notably, both opioid antagonists and mixed agonist-antagonists are effective for other clinical instances of pruritus, including those associated with systemic disease or of dermatologic origin. Nalbuphine, for example, is effective at managing pruritus among patients with end stage renal disease (Hawi et al. 2015; Reszke and Szepietowski 2018) and contact dermatitis (Inan et al. 2019). These observations suggest that different forms of pruritus (spanning from systemic disease to drug-induced) converge on a common itch pathway that depend on central opioid signaling, likely centered upon the involvement of endogenous endorphin and dynorphin tone. Presently, the use of nalbuphine for the clinical management of opioid-induced pruritus is off-label, despite its effectiveness for the prevention and severity of pruritus (Jannuzzi 2016). As is the case with many drugs frequently used for anesthesia that lack FDA labeling (Smith et al. 2012), a new drug indication of nalbuphine for pruritus would only facilitate its widespread use within clinical practice.

1.4.3 Selective kappa opioid receptor agonists

The dynorphin-kappa-opioid receptor system has been heavily implicated in itch. Pharmacologic and genetic manipulations of spinal dynorphin-expressing neurons in mice have uncovered that spinal dynorphin is required for the inhibition of itch (Kardon et al. 2014; Huang et al. 2018). In rodent and non-human primate models, selective kappa-opioid receptor agonists, such as nalfurafine, have been shown to be important for the inhibition of several forms of chemical, immunologic, and drug-induced (including opioid-induced) itch (Umeuchi et al. 2003; Togashi et al. 2002; Ko and Husbands 2009). Clinically, nalfurafine (2.5 or 5.0 μg PO) (Kozono, Yoshitani, and Nakano 2018) has been shown to be effective for the treatment of uremic and cholestatic pruritus in Japan (Cowan, Kehner, and Inan 2015).

Emerging evidence in preclinical models, involving both mice and non-human primates, indicate that the intrathecal and systemic administration kappa-opioid receptor agonists can reduce morphine-induced itch without reducing morphine-induced analgesia (Ko and Husbands 2009; Akiyama et al. 2015; Nguyen et al. 2021). In preclinical models, nalfurafine has been found to restore dynorphin signaling disrupted by neuraxial mu-opioid receptor agonists, such as morphine (Nguyen et al. 2021). These preclinical findings indicate that selective kappa-opioid receptor agonists should be further considered for opioid-induced pruritus in the future.

Presently, however, nalfurafine does not have approval by the European Medicines Agency or Federal Drug Administration for clinical use in Europe and the United States, respectively (Mores et al. 2019). One concern has been its sedating effects, which has been observed following long-term use in dogs (European Medicines Agency. Assessment Report: Winfuran. European Medicines Agency. Committee for Medicinal Products for Human Use; 2013), but this has not been a consistent finding in other animal models and in patients (Brust et

al. 2016; Kozono, Yoshitani, and Nakano 2018; Ko and Husbands 2009) In European trials, nalfurafine (5 μg PO) did not significantly reduce the severity of uremic pruritus compared to placebo over 8 weeks. (European Medicines Agency. Assessment Report: Winfuran. European Medicines Agency. Committee for Medicinal Products for Human Use; 2013) However, one key difference between the studies conducted in Europe and Japan (Kumagai et al. 2010) was the duration of the trial (weeks compared to days, respectively) and notably, in the European trials both the nalfurafine-treated and placebo groups exhibited significant reductions in self-reported VAS intensities of pruritus over the course of the study (European Medicines Agency. Assessment Report: Winfuran. European Medicines Agency. Committee for Medicinal Products for Human Use; 2013). Given the incidence of opioid-induced pruritus in the postoperative setting, the effectiveness of nalfurafine may be more evident in acute settings, although further testing is necessary in preclinical and clinical trials.

1.4.4 Serotonin receptor antagonists

5-hydroxytryptamine receptor (5HT3R) antagonists are frequently used to treat postoperative nausea and vomiting (PONV). Both of these side effects are observed in postoperative patients who receive neuraxial morphine (Grangier et al. 2020; Norris et al. 1994). Several studies have revealed that prophylaxis with a 5HT3R antagonist (such as ondansetron, ranging from 4-8 mg IV) does not significantly reduce the incidence of pruritus (George, Allen, and Habib 2009; Somrat Charuluxananan et al. 2003; Sarvela et al. 2006; Yeh et al. 2000; Yazigi et al. 2002; Siddik-Sayyid et al. 2007; Kyriakides, Hussain, and Hobbs 1999). A systematic review by *Bonnet et al.* of 15 randomized controlled trials suggests that 5HT3R antagonists may reduce the intensity of opioid-induced pruritus, but also concluded that the trials included in the

systematic review, such as small studies that favor the publication of positive findings, may have suffered from publication bias (Bonnet et al. 2008). Thus, there is still a lack of consensus on the clinical effectiveness of 5HT3R antagonists in opioid-induced pruritus (Bonnet et al. 2008; George, Allen, and Habib 2009).

The mechanism by which 5HT3R antagonists, such as ondansetron, alleviate itch is not clear. 5HT3R immunoreactivity has been observed in the spinal dorsal horn (Morales, Battenberg, and Bloom 1998) and the endogenous source of serotonin is thought to originate from descending fibers arising within the brainstem (Marinelli et al. 2002). Depletion of supraspinal serotonin has been shown to alleviate pruritogen-induced itch in rodents (Zhao et al. 2014), which may partially explain how antagonism of 5HT3R reduces opioid-induced itch. However, spinal neurons expressing 5HT3R and MOR have been found comprise non-overlapping populations (Häring et al. 2018), making it unlikely that agents such as ondansetron could directly reduce the activity of neurons responsible for opioid-induced itch. In rhesus monkeys, ondansetron has also been found to be ineffective at reducing morphine-induced itch, even at high doses that caused extrapyramidal effects (Ko 2015). Given these conflicting reports between human and animal models, and the lack of a cellular basis for how serotonin and opioid signaling could converge, 5HT3R antagonists are currently not considered front-line therapies for opioid-induced pruritus, and likely have a limited role in prophylaxis against opioid-induced pruritus.

1.4.5 Propofol

The effectiveness of sub-hypnotic doses of propofol (10-30mg IV) for the treatment of opioid-induced pruritus remains controversial. In one double-blind trial, propofol (10mg IV) was

observed to reduce morphine-induced pruritus compared to placebo (85% compared to 16%, respectively) (Borgeat et al. 1992). The patients in this study had received either epidural or spinal morphine for a variety of surgical procedures including gynecologic, gastrointestinal, thoracic, and orthopedic surgery (Borgeat et al. 1992). Another study also reported that propofol (10mg IV) protected against pruritus following intrathecal morphine for arthroplasty surgery (Törn et al. 1994). However, *Warwick et al.* did not confirm these findings in a double-blind study of obstetric patients; propofol (10-20mg IV) had no effect on the onset or severity of pruritus following intrathecal morphine (Warwick, Kearns, and Scott 1997) Age and sex differences among these studies may account for the variable effectiveness of the similar doses of propofol used to mitigate neuraxial morphine-induced pruritus. These studies further underscore that pruritus disproportionately occurs in younger and female obstetric patients (Tubog et al. 2018; Wells, Paech, and Evans 2004; Yurashevich and Habib 2019; S Charuluxananan et al. 2000) who may be less responsive to the antipruritic effects of propofol. Another possibility for the observed differences across studies is that the dose of propofol used may not have been adequate to achieve clinical effect. Thus, although propofol has been observed to reduces incidence of pruritus in patients receiving morphine for a variety of elective surgeries (Törn et al. 1994; Borgeat et al. 1992), its benefit in the treatment of opioid-induced pruritus within the obstetric population remains questionable (Warwick, Kearns, and Scott 1997). Recent work in rodents have revealed that neurons producing GABA are required for neuraxial opioid-induced itch (Wang et al. 2021; Nguyen et al. 2021) and the administration of propofol, through potentiation of GABA receptors, may enhance the ability of these neurons to dampen excitatory spinal circuits (Sun and Chen 2007) involved in itch transmission. Additional dose-

response studies are necessary to identify the appropriate dose of propofol for management of pruritus without sedation.

1.4.6 Gabapentin

Gabapentin has been shown to be effective for several forms of pruritus in systemic disease, including uremic pruritus, pruritus in multiple sclerosis, and pruritus of unknown origin (Anand 2013; Yesudian and Wilson 2005; Gunal et al. 2004). Its use in the treatment of neuraxial opioid-induced pruritus is less clear. Preoperative gabapentin (1200 mg PO) has been found to significantly delay the onset and reduce the incidence and severity of intrathecal morphine-induced pruritus in patients undergoing orthopedic surgery (Sheen et al. 2008) and prolong the onset of pruritus in patients receiving spinal morphine for unilateral hernia repair (Akhan et al. 2016). However, a lower dose (600 mg) was not found to significantly decrease the incidence of pruritus compared to placebo and was associated with urinary retention (Chiravanich, Oofuvong, and Kovitwanawong 2012). Further pharmacological studies in preclinical and clinical models are necessary to characterize the mechanism of action of gabapentin within the nervous system and to determine its dosing in the management of opioid-induced pruritus.

1.4.7 Dopamine D2 receptor antagonists

Droperidol (1.25 mg IV), a short-acting, potent dopamine receptor (D2R) antagonist, has been shown in several studies to be effective at reducing the incidence and severity of neuraxial opioid-induced pruritus and has previously been used for postoperative nausea and vomiting

(Horta and Vianna 2003; Horta, Ramos, and Gonçalves 2000; Horta et al. 2006). However, D2R antagonists have been reported to be effective only when small doses of opioids are administered. Sedation has been shown to increase with escalating doses of droperidol (2.5 to 5 mg IV), which may confound its antipruritic effects (Horta, Ramos, and Gonçalves 2000). Given the broad influences of supraspinal dopamine signaling on the functions of spinal and dorsal root ganglion neurons, the anti-pruritic effects observed may be non-specific (Wood 2008). Emerging evidence indicates that low doses of droperidol may be safely used; however, clinical use of droperidol in a perioperative setting is limited by an FDA black box warning issued (2001) due to its risk for sudden cardiac death (Jackson, Sheehan, and Reddan 2007). The warning will likely preclude any clinical adoption of droperidol to treat opioid-induced pruritus.

1.4.8 Emerging treatments

All existing treatment options for opioid-induced pruritus have undesirable side effect profiles. Furthermore, many of these treatments are used empirically and off-label. Due to the limitations of currently available treatments, some patients or providers may elect to forgo analgesia or opt for sub-optimal analgesia that excludes neuraxial opioids, but these practices can lead to unnecessary pain and suffering (Arendt and Segal 2008). Recent success in preclinical models suggests that nalfurafine, a selective kappa-opioid receptor agonist, may be used to manage opioid-induced pruritus without limiting opioid-induced analgesia (Nguyen et al. 2021). but further basic, translational and clinical research is required before recommendations for clinical use in opioid-induced pruritus can be made. Optimization of opioid analgesia as well as development of improved therapies for opioid-induced pruritus have the potential to significantly

improve the clinical standards of care for patients who receive opioids for the management of perioperative pain and experience pruritus as an unwanted side effect.

1.5 Summary

Pruritus following neuraxial opioids remains a highly common and dissatisfying side effect. Advancements in the understanding of mast cell biology and neuronal itch circuitry have provided clues as to how opioids can induce analgesia as well as evoke pruritus. Existing evidence suggests that parenteral opioids cause pruritus through histamine release, whereas neuraxial opioid-induced pruritus occurs through a mechanism of neuronal disinhibition in the spinal cord dorsal horn. The differential modulation of peripheral and neuraxial opioid-induced pruritus by mast cells and neurons, respectively, further highlight the complexity of the side effects of opioid use. Emerging evidence suggests that pruritus arises due to the dysregulation of opioid-sensitive pathways involving mu- and kappa-opioid receptor signaling, which parallels other forms of chronic, systemic, and drug-induced pruritus. Ultimately, a richer understanding of the genetic, molecular, and cellular underpinnings of opioid-induced pruritus may provide a basis upon which to develop improved therapies that can manage pain but do not cause itch.

2.0 Translation of models of morphine-induced itch: from mice to obstetric patients

2.1 Introduction

Neuraxial morphine and other mu opioid receptor (Oprm1) agonists are routinely administered in hospitals around the world (Waxler et al. 2005a). For instance, many pregnant women undergoing cesarean delivery in North America and Europe receive epidural or spinal morphine (Butwick, Wong, and Guo 2018; Alran et al. 2002; Kumar and Singh 2013). Moreover, epidural or spinal morphine is given as an analgesic for a large proportion of surgical procedures, including hip and knee arthroplasty (Kaye et al. 2019). Unfortunately, one of the major unwanted side effects of the spinal or epidural delivery routes is morphine-induced itch, which is observed in more than half of patients (Waxler et al. 2005b; Jannuzzi 2016; Ganesh and Maxwell 2007; Szarvas, Harmon, and Murphy 2003; Ballantyne, Loach, and Carr 1988).

Although it is clear that neuraxial morphine causes itch in humans (Waxler et al. 2005b; Jannuzzi 2016; Ganesh and Maxwell 2007; Szarvas, Harmon, and Murphy 2003; Ballantyne, Loach, and Carr 1988), the characterization of clinical endpoints for morphine-induced itch remains limited. We sought to further characterize itch dysesthesias elicited by morphine in humans and in rodents in efforts to fully assess the behavioral effects of opioids on pruritus.

2.2 Methods

Human subjects

A prospective observational approach was chosen. Written consent was obtained from all research participants and this study was approved by the University of Pittsburgh Institutional Review Board. A convenience sampling of women aged 18 years or older with scheduled cesarean sections was conducted. Exclusion criteria included chronic pain, current opioid maintenance therapy, or emergency cesarean delivery. Upon enrollment, morphine-induced itch, hyperknesis, and alloknesis were established, each using a numerical rating scale (NRS) (e.g., "How itchy do you currently feel?"). Zero indicated "no intensity (or unpleasantness) at all" and 10 indicated "the most intense (or unpleasant) itch I can imagine." Hyperknesis was assessed using a 2.0 gram von Frey monofilament applied to a distal extremity. Alloknesis was assessed using a brush (SenseLab, Somedic AB, Sweden) applied to a distal extremity. Assessments occurred during hospitalization prior to and 24 hours after cesarean delivery. Responses were de-identified, coded, and stored on a secure, web-based application on Research Electronic Data Capture (REDCap).

Mice

The studies were performed in both male and female mice 8-10 weeks of age. All animals were of the C57Bl/6 background. Even numbers of male and female mice were used for all experiments. No sex differences were found and, thus, animals were pooled. Mice were given food and water ad libitum and housed under standard laboratory conditions. The use of animals was approved by the Institutional Animal Care and Use Committee of the University of Pittsburgh.

Intradermal and intrathecal injections

For intradermal injection of chloroquine, hair was clipped from the neck or calf of each mouse at least 24 hours before the experiment. Chloroquine (100 μg in 10 μL) was administered into the nape of the neck or calf, which could be subsequently visualized by the formation of a small bubble under the skin. For intrathecal injections, hair was clipped from the back of each mouse at least 24 hours before the experiment. All intrathecal injections were delivered in a total volume of 5 μL using a 30-gauge needle attached to a luer-tip 25 μL Hamilton syringe. The needle was inserted into the tissue at a 45° angle through the fifth intervertebral space (L5 – L6). Solution was injected at a rate of 1 μL/s. The needle was held in position for 10 seconds and removed slowly to avoid any outflow of the solution. Only mice that exhibited a reflexive flick of the tail following puncture of the dura were included in behavioral analysis. These procedures were performed in awake, restrained mice.

Observation of scratching behavior

Scratching behavior was observed using a previously reported method (Kardon et al. 2014). Mice were individually placed in the observation cage (12 x 9 x 14 cm) to acclimate for 30 minutes. The mice were assigned to dosing conditions in a randomized manner. For dose-dependent subcutaneous morphine-induced itch, animals received either 5 μL morphine (0.3, 3, or 300 pmol) or saline to the nape of the neck. Scratching behavior was videotaped for 60 minutes after administration. The total numbers of scratch bouts by the hind paws at various body sites during the first 60 minutes after intrathecal morphine were counted.

Alloknesis

One hour after the intrathecal injection of morphine, mice were assessed for alloknesis. As previously described (Akiyama et al. 2012), alloknesis was assessed by delivering 3 separate

innocuous mechanical stimuli using a von Frey filament (bending force: 0.7 mN; Stoelting, USA) every 5 minutes. Each application of the von Frey filament was reported as 1 trial, yielding a total of 18 trials over 30 minutes.

Hyperknesis

One hour after the intrathecal injection of morphine, mice were assessed for hyperknesis. Chloroquine (100 μg in 10 μL) was injected intradermally into the nape of the neck or calf and scratching behavior was recorded for 30 minutes. The total number of scratch bouts by the hand paws directed to the nape of the neck was counted.

2.3 Results

2.3.1 Spinal morphine is associated with morphine induced itch, hyperknesis, and alloknesis in obstetric patients.

We found that morphine not only caused itch in women receiving spinal morphine for cesarean delivery, as previously reported (Szarvas, Harmon, and Murphy 2003; Ballantyne, Loach, and Carr 1988), but also gave rise to clinical hyperknesis, as defined by exacerbation of itch in response to punctate stimulation (Andersen et al. 2018), and clinical alloknesis, as defined by touch-evoked itch in response to brushing (Andersen et al. 2018) (Figure 4, Figure 5). These newly identified endpoints for morphine-induced itch in humans were highly correlated with overall self-reported itch ratings obtained using a numerical rating scale (Figure 5), suggesting that morphine-induced itch is accompanied by central sensitization (Andersen et al. 2018).

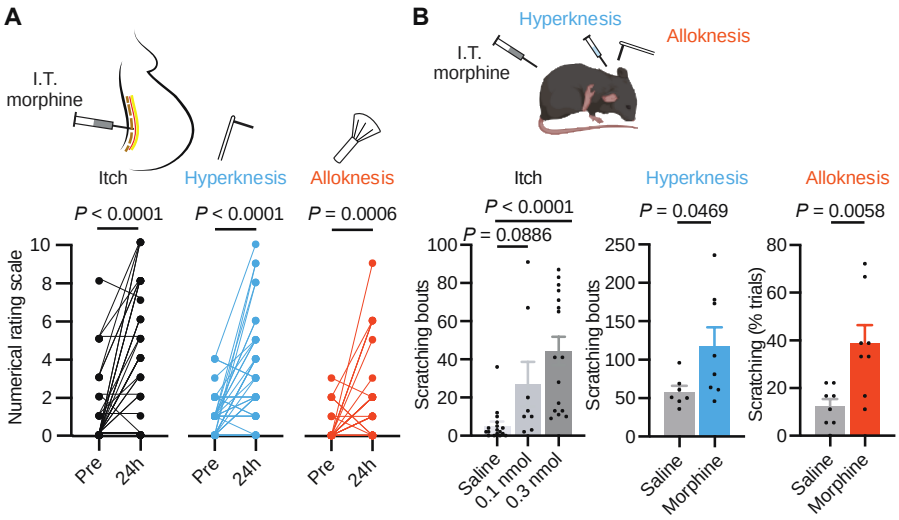

Figure 4. Novel endpoints for sensitization caused by morphine-induced itch in human subjects and in mice.

(A) I.T. morphine-induced itch, hyperknesis, and alloknesis in obstetric patients. I.T., intrathecal. *n* = 39 human subjects. **(B)** I.T. morphine-induced itch, hyperknesis, and alloknesis in mice. *n* = 7-9 mice per group. *P* value was determined by (A) Wilcoxon matched-pairs signed rank test and (B) one-way ANOVA, with Bonferroni's correction and two-tailed unpaired t-test. (A) data points represent individual human subjects pre and post spinal morphine (B) and data are mean + S.E.M with dots representing individual mice.

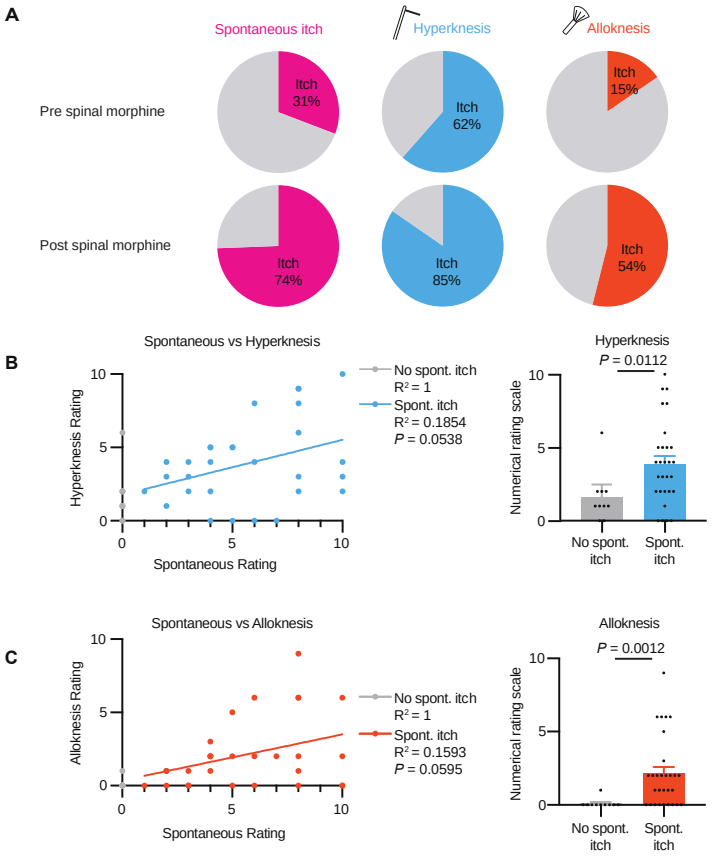

Figure 5. Morphine-induced itch, hyperknesis, and alloknesis in obstetric patients.

(A) Proportion of women reporting itch, hyperknesis, and alloknesis before and after spinal morphine. **(B** and **C)** Correlation between subjects' spontaneous score and **(B)** hyperknesis score, **(C)** and alloknesis score. *n* = 39 subjects. (B and C) *P* value was determined by a linear regression (left) and Mann-Whitney test (right). Data are mean + S.E.M with dots representing individual patients.

2.3.2 Intrathecal morphine is associated with morphine induced itch, hyperknesis, and alloknesis in mice.

Next, we reverse-translated these findings in a mouse model (with even numbers of males and females) using an analgesic dose of morphine given intrathecally (300 pmol; I.T). In addition to morphine-induced scratching behavior, consistent with previous reports (Sakakihara, Imamachi, and Saito 2016), mice showed morphine-induced hyperknesis, as demonstrated by an exacerbation of chloroquine-induced itch, as well as morphine-induced alloknesis, as revealed by

touch-evoked itch in response to a von Frey filament (Figure 4, Figure 6). Thus, morphine-induced itch in mice appears to recapitulate our observations in humans, thereby enabling detailed mechanistic investigations of this phenomenon.

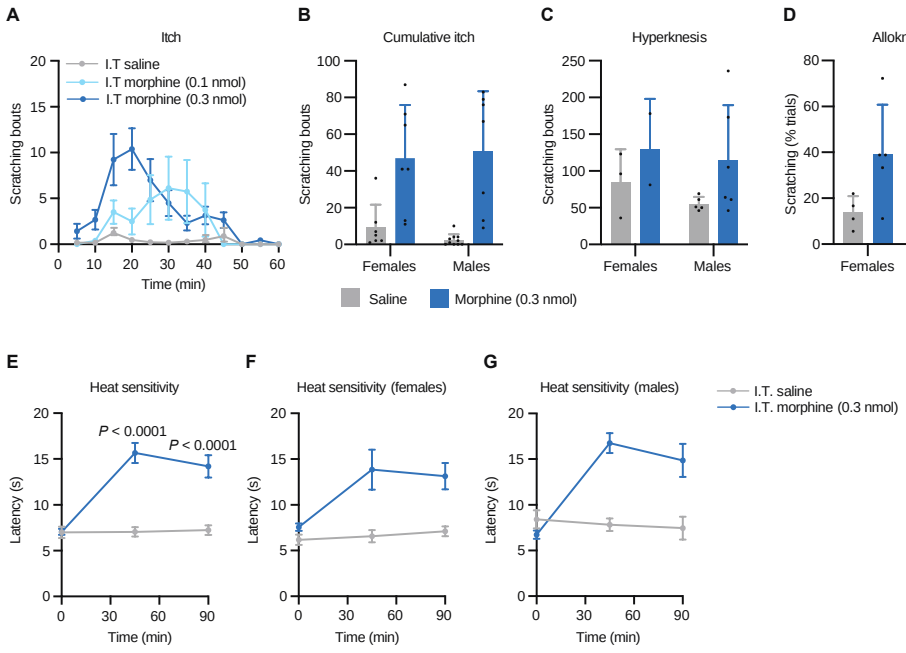

Figure 6. Morphine-induced itch, hyperknesis, and alloknesis in mice.

(A) Time course of itch following I.T. administration of morphine (100 pmol and 300 pmol) and saline. *n* = 7-9 mice per group. **(B** to **D)** Effect of morphine-induced **(B)** itch, **(C)** hyperknesis, and **(D)** alloknesis separated by sex. *n* = 3-4 mice per group. **(E)** Effect of I.T. morphine on heat sensitivity. *n* = 7-9 mice per group, two-way ANOVA with Bonferroni's correction. **(F** and **G)** Effect of morphine on heat sensitivity among **(F)** female **(G)** and male mice. (A and E to G) Data are mean S.E.M. (B to D) Data are mean + S.E.M. with individual dots representing individual mice.

2.4 Discussion

Hyperknesis and alloknesis have been used to characterize the sensitization of itch, such as in setting of atopic dermatitis and eczema (Andersen et al. 2018). Although itch-specific quantitative sensory testing (QST) is used to assess experiences of pruritus (Sikand et al. 2011, 2009), it is less frequently used compared to QST in pain. Particularly, in the context of morphine-induced itch, alloknesis and hyperknesis have only been assessed in anesthetized rats (Moser and Giesler 2013). Here, we uncovered heightened responses to brushing and von Frey stimulation in obstetric patients following spinal morphine, indicative of morphine-induced alloknesis and hyperknesis, respectively. In mice, we found analogous results; morphine-treated mice exhibited alloknesis with von Frey stimulation of the nape of the neck and hyperknesis following the intradermal injection of chloroquine. These results expand on the existing paradigms for assessment of itch dysesthesias in both humans and mice.

3.0 Role of mast cells in morphine-induced itch

3.1 Introduction

First-generation antihistamines, such as diphenhydramine (the active ingredient in Benadryl), are commonly used in many hospitals globally to alleviate morphine-induced itch (Kumar and Singh 2013; Siddik-Sayyid et al. 2010; Millington et al. 2018). The use of antihistamines likely stems from the observation that morphine causes histamine release from mast cells within the skin, and that histamine produces itch (Lansu et al. 2017; Grosman 1981; Hermens et al. 1985). Moreover, clinical data appear to support this idea because numerous studies confirm that antihistamines reduce itch in laboring women who receive morphine (Liao et al. 2011; Horta et al. 2006; Eldor et al. 1994). While antihistamines are widely used to treat morphine-induced itch (Millington et al. 2018), whether this type of itch is indeed a result of peripheral histamine release has never been established and remains controversial (Liu et al. 2011; Ko et al. 2004).

It is widely assumed that histamine release from degranulated mast cells in the skin underlies neuraxial morphine-induced itch (Szarvas, Harmon, and Murphy 2003). When given subcutaneously, morphine, indeed, causes degranulation of peripheral mast cells, which results in itch (Lansu et al. 2017; Grosman 1981; Hermens et al. 1985). However, the evidence for this mechanism is less clear for neuraxial morphine-induced itch; mast cells are not found in the spinal cord and emerging evidence has called the role of mast cells in neuraxial morphine-induced itch into question (Edvinsson et al. 1977; Ko 2015).

3.2 Methods

Mice

The studies were performed in both male and female mice 8-10 weeks of age. All animals were of the C57Bl/6 background. Even numbers of male and female mice were used for all experiments. No sex differences were found and, thus, animals were pooled. Mice were given food and water ad libitum and housed under standard laboratory conditions. $Rosa^{DTA}$ (Jax #009669) mice are available at Jackson Laboratories. $Mcpt5^{Cre}$ mice were a gift from Axel Roers (Dresden University of Technology). The use of animals was approved by the Institutional Animal Care and Use Committee of the University of Pittsburgh.

Pharmacologic agents used in mice

Morphine sulfate (4 mg/ml; Henry Schein Animal Health) and chloroquine diphosphate salt (Sigma) were dissolved in physiological saline. Salvinorin B (SalB; Tocris) was dissolved in DMSO and administered subcutaneously (10 mg/kg). Clozapine-N-oxide (CNO; Tocris) was dissolved in PBS and administered intraperitoneally (5mg/kg). Nalfurafine (Sigma) was dissolved in saline and administered intrathecally. Loratadine (Sigma) and diphenhydramine (Sigma) were prepared in 10% DMSO and given 10 mg/kg I.P. For experiments involving antihistamines, animals were pretreated with vehicle, loratadine, or diphenhydramine 30 minutes prior to recording scratching behavior.

Intrathecal injections

All intrathecal injections were delivered in a total volume of 5 μL using a 30-gauge needle attached to a luer-tip 25 μL Hamilton syringe. The needle was inserted into the tissue at a 45° angle through the fifth intervertebral space (L5 – L6). Solution was injected at a rate of 1 μL/s. The needle was held in position for 10 seconds and removed slowly to avoid any outflow

of the solution. Only mice that exhibited a reflexive flick of the tail following puncture of the dura were included in behavioral analysis. These procedures were performed in awake, restrained mice.

Observation of scratching behavior

Scratching behavior was observed using a previously reported method (Kardon et al. 2014). Mice were individually placed in the observation cage (12 x 9 x 14 cm) to acclimate for 30 minutes. The mice were assigned to dosing conditions in a randomized manner. For dose-dependent subcutaneous morphine-induced itch, animals received either 5 μL morphine (0.3, 3, or 300 pmol) or saline to the nape of the neck. Scratching behavior was videotaped for 60 minutes after administration. For all other experiments, unless otherwise indicated, 300 pmol of morphine was administered (S.C. and I.T.). The total numbers of scratch bouts by the hind paws at various body sites during the first 60 minutes after subcutaneous (morphine or 48/80) intrathecal injection (morphine or 100 pmol GRP) were counted. For subcutaneous injections, only scratch bouts directed to the nape of the neck were counted.

Heat sensitivity assay (Hargreaves testing)

Mice were acclimated on a glass plate held at 30°C (IITC Life Science Inc.). A radiant heat source (activity intensity of 15%) was applied to the hindpaw and latency to paw withdrawal was recorded (Hargreaves et al. 1988). Two trials were conducted on each paw, with at least 5 minutes between testing the opposite paw and at least 10 minutes between testing the same paw. To avoid tissue damage, a cut off latency of 20 seconds was set. Values from both paws were averaged to determine withdrawal latency.

Open field activity

Spontaneous activity in the open field was conducted over 30 minutes in an automated Versamax Legacy open field apparatus for mice (Omnitech Electronics Incorporated, Columbus, OH). Distance traveled (s), ambulatory average velocity (cm/s), and ambulatory time (s) were measured by infrared photobeams located around the perimeter of the arenas interfaced to a computer running Fusion v.6 for Versamax software (Omnitech Electronics Incorporated) which monitored the location and activity of the mouse during testing. Activity plots were generated using the Fusion Locomotor Activity Plotter analyses module (Omnitech Electronics Incorporated). To determine whether antihistamines would modify locomotion, mice were placed into the open field 30 post vehicle, loratadine, or diphenhydramine treatment. For all tests, mice were transferred to the testing room one hour prior to testing.

Quantification of mast cells

For staining of cutaneous mast cells, hair was removed from the nape of the neck two days prior to S.C. injection. S.C. injections for histological analyses were performed in lightly anesthetized (isoflurane) animals to prevent the confounds of scratching on degranulation. Skin and dural samples were collected fresh-frozen, sectioned at 8 μm, and post-fixed in 4% PFA for 60 minutes. Toluidine blue was used to stain mast cells. Images were collected using a TissueGnostics brightfield microscope. Compound 48/80 (100 μg, Sigma) was used as a positive control for mast cell degranulation. Mast cells that contained a nucleus surrounded by granules were considered to be degranulated.

Statistical analysis

All statistical analyses were performed using GraphPad Prism 7. Values are presented as mean SEM. P values were determined by tests indicated in applicable figure legends. Sample sizes were based on pilot data and are similar to those typically used in the field.

3.3 Results

3.3.1 Role of histamine in peripheral and central morphine-induced itch.

Given the contested role of mast cells in morphine-induced itch, we sought to determine their contribution to itch caused by either intrathecal (I.T.) or subcutaneous (S.C.) morphine (Figure 7A). Consistent with previous results (Melo et al. 2018), we found that S.C. morphine caused site-directed scratching in mice in a dose-dependent manner (Figure 8A). In parallel experiments in which mice were given morphine but prevented from scratching, we observed that S.C. morphine (300 pmol) caused the degranulation of cutaneous mast cells that was similar in magnitude to that observed with the mast cell degranulator, compound 48/80 (Figure 7B and Figure 8, B and C). In contrast, the same dose of I.T. morphine, although sufficient for robust analgesia (Figure 6E to G), did not cause peripheral mast cell degranulation (Figure 7B and Figure 8, B and C). Thus, neuraxial morphine for the purpose of analgesia is unlikely to cause the degranulation of mast cells in the periphery.

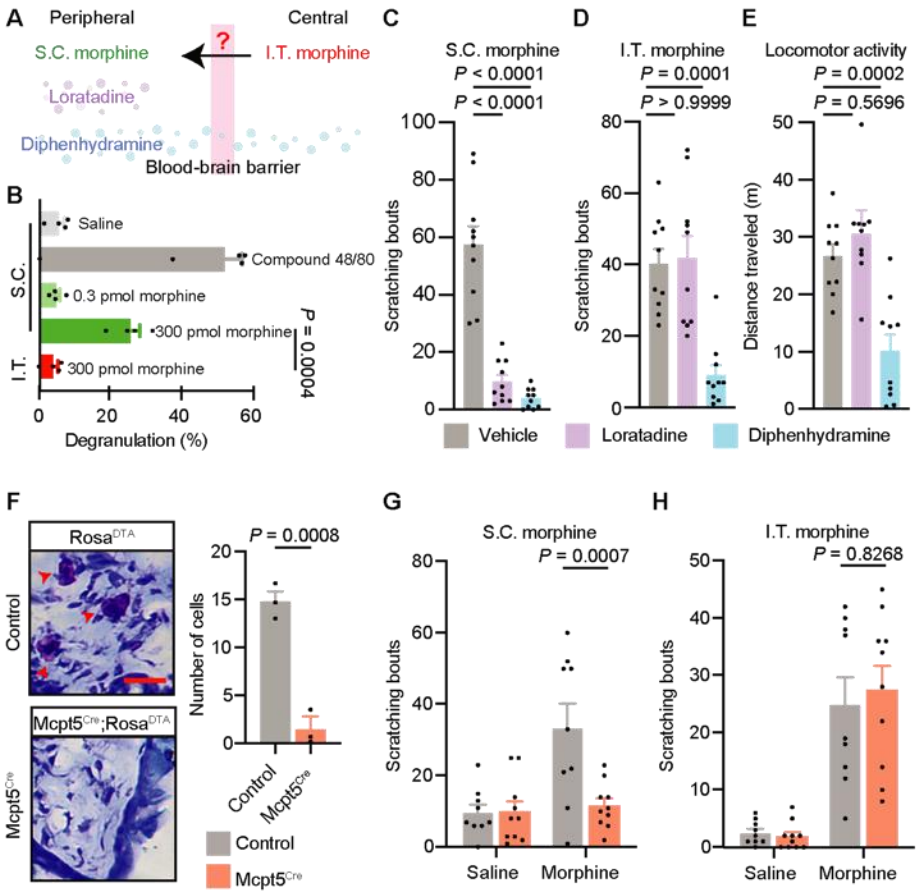

Figure 7. Intrathecal morphine-induced itch is mast-cell independent.

(A) Schematic describing the pharmacological strategy to determine how morphine causes itch. I.T., intrathecal and S.C., subcutaneous. **(B)** Quantification of degranulated mast cells. *n* = 4 mice per group. **(C** to **E)** Effect of antihistamines on **(C)** S.C. morphine-induced itch **(D)** I.T. morphine-induced itch **(E)** and locomotor activity. *n* = 10 mice per group. **(F)** Mast cell deletion and quantification in Mcpt5^{Cre}; Rosa^{DTA} mice. *n* = 3 mice per group. Scale bar = 10 μm. **(G** and **H)** Effect of mast cell depletion on **(G)** S.C. morphine-induced itch **(H)** and I.T. morphine-induced itch. *n* = 9-10 mice per group. *P* value was determined by (B to E) one-way ANOVA, with Bonferroni's correction, (F) two-tailed, unpaired t-test, (G and H) and two-way ANOVA with Bonferroni's correction. (B to H) data are mean + S.E.M with dots representing individual mice.

Diphenhydramine is clinically efficacious for neuraxial morphine-induced itch (Kumar and Singh 2013; Siddik-Sayyid et al. 2010) and is frequently prescribed for its treatment (Kumar and Singh 2013). However, the site at which histamine receptor antagonists exert their effects to reduce itch remains unclear. To address this gap, we compared the effects of two antihistamine

compounds in mice: diphenhydramine, a first-generation histamine receptor (H_1) antagonist that crosses the blood-brain barrier, and loratadine, a second-generation H_1 antagonist that remains peripherally restricted (Figure 7A). As expected, both diphenhydramine and loratadine reduced itch caused by the degranulation of mast cells with compound 48/80 (Figure 8E). Similarly, scratching in response to S.C. morphine was reduced by both types of antihistamines (Figure 7C), consistent with the idea that S.C. morphine causes itch that is mediated by peripheral histamine receptors (Melo et al. 2018). For I.T. morphine-induced itch, diphenhydramine was an effective treatment, just as is observed in humans (Kumar and Singh 2013) (Figure 7D); in contrast, the peripherally restricted H_1 antagonist, loratadine, had no effect (Figure 7D). Analogous findings were observed using I.T. gastrin releasing peptide (GRP) to cause central itch: only diphenhydramine reduced scratching bouts (Figure 8F).

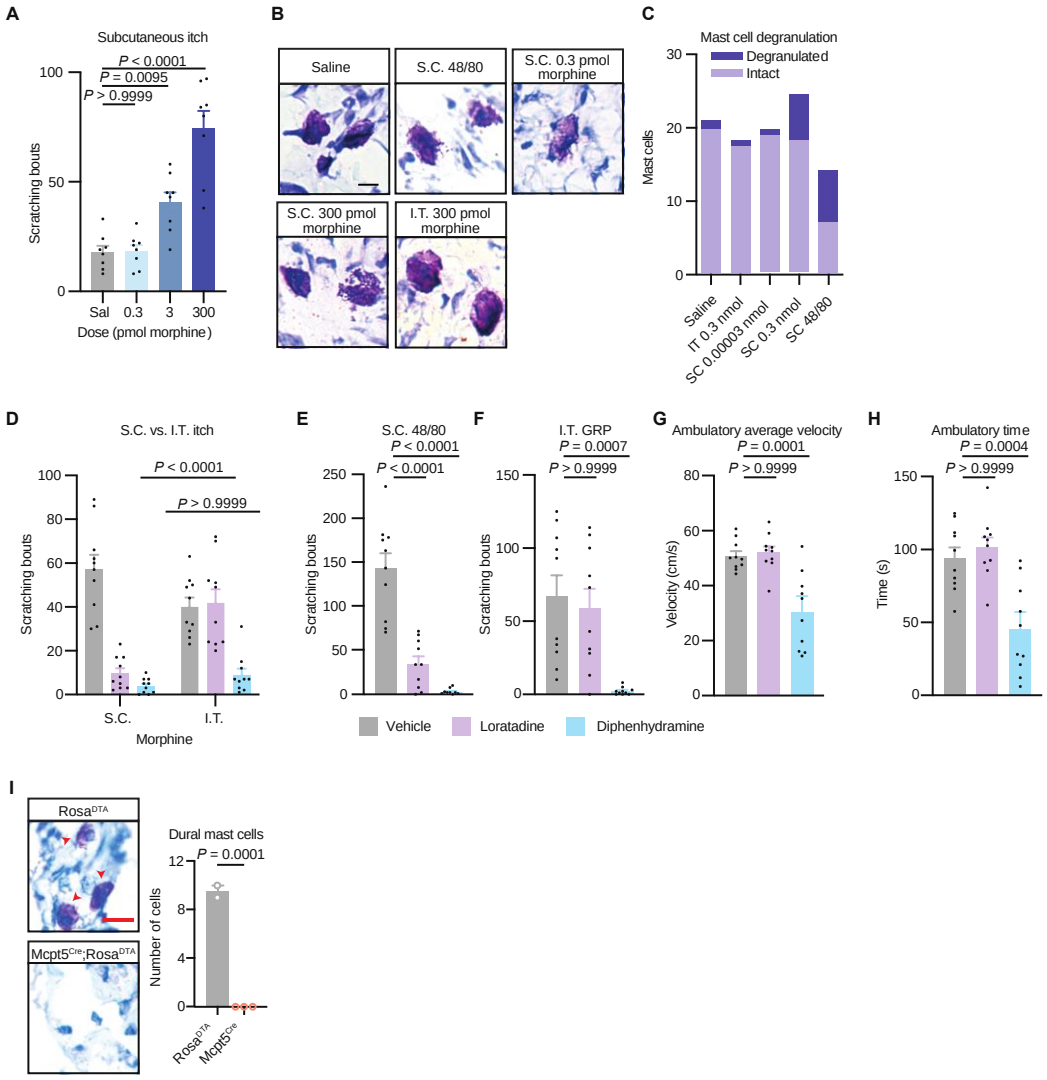

Figure 8. Differential role of mast cells on subcutaneous vs. intrathecal morphine-induced itch.

(A) Itch caused by escalating doses of S.C. morphine. *n* = 8 mice per group. **(B)** Representative images of cutaneous mast cells. Scale bar = 10 μm. **(C)** Quantification of B**.** *n* = 4 mice per group. **(D** to **H)** Comparison of the effects of antihistamines on **(D)** S.C. and I.T. morphine-induced itch, **(E)** S.C. 48/80 induced itch, **(F)** I.T. GRP induced itch, **(G)** ambulatory velocity, **(H)** and ambulatory time. (D to H) *n* = 10 mice per group. (**I)** Validation of dural mast cell deletion in Mcpt5^{Cre}; Rosa^{DTA} mice. *n* = 2-3 mice per group. *P* value was determined by (A and E to H) one-way ANOVA, with Bonferroni's correction, (D) two-way ANOVA, with Bonferroni's correction (I) and two-tailed, unpaired t-test. (A and D to I) Data are mean + S.E.M with dots representing individual mice.

These findings suggest that H_1 antagonists must inhibit centrally-mediated itch through their action on a central target, but the mechanisms remained unclear. In this regard it is

noteworthy that a concentration of diphenhydramine that reduced scratching behavior in mice was also accompanied by a reduction in their locomotor activity (Figure 7D and E and Figure 8D to H). This locomotor effect is in keeping with the idea that drowsiness is a side effect of diphenhydramine in humans (Roth et al. 1987; Ballantyne, Loach, and Carr 1988; Horta et al. 2006). Thus, although diphenhydramine reduces neuraxial-morphine induced scratching behavior, it is possible that this apparent reduction in itch may be secondary to somnolence (Kamei et al. 2005).

3.3.2 Mast cells are dispensable for intrathecal morphine-induced itch.

To directly test whether mast cells are required for morphine-induced itch, we used a mouse model of mast cell depletion. Selective ablation of mast cells was achieved using $Mcpt5^{Cre}$ mice (Scholten et al. 2008) together with Cre-dependent expression of diphtheria toxin ($Rosa^{DTA}$) (Schubert et al. 2018) (Figure 7F and Figure 8I). As expected, mice lacking mast cells no longer exhibited itch upon S.C. delivery of morphine (Figure 7G). However, neuraxial morphine-induced itch was still intact in these mice (Figure 7H). Overall, these findings indicate that mast cells are dispensable for neuraxial morphine-induced itch, and that, insofar as first-generation antihistamines reduce itch, this effect is central.

3.4 Discussion

Diphenhydramine is still frequently prescribed as a first-line treatment for morphine-induced itch (Szarvas, Harmon, and Murphy 2003; Jannuzzi 2016). However, clinicians have

observed that the severe anticholinergic effects of antihistamines have caused patients to verbally deny itch while continuing to scratch, and that patients are itchy in between periods of sleep (Roth et al. 1987; Ballantyne, Loach, and Carr 1988; Horta et al. 2006). Furthermore, the sedating side effects of antihistamines have raised concerns about the safety of antihistamine treatment for neuraxial morphine-induced itch in view of their potential to exacerbate respiratory depression caused by opioids (Anwari and Iqbal 2003; Jannuzzi 2016; Roth et al. 1987).

Our results challenge this practice of using diphenhydramine for neuraxial morphine-induced itch because we show that mast cells are not involved in neuraxial morphine-induced itch. In addition, the finding that diphenhydramine only reduces scratching at a dose that also suppresses locomotor activity further underscores the concept that the use of antihistamines for neuraxial morphine-induced itch may be inappropriate.

4.0 Dynorphin neurons mediate morphine-induced itch

4.1 Introduction

Molecularly-defined inhibitory neurons have been implicated in the modulation of itch. Prior studies have contributed significant advances in our understanding of spinal circuitry; particularly, inhibitory neurons containing dynorphin (Pdyn) and neuropeptide Y (Npy) are critically important for the inhibition of chemical (Kardon et al. 2014; Ross et al. 2010; Huang et al. 2018) and mechanical itch (Acton et al. 2019; Bourane et al. 2015), respectively. Developmental deletion of either Pdyn neurons or Npy neurons results in profound spontaneous scratching behavior suggesting that these populations tonically inhibit itch (Ross et al. 2010; Bourane et al. 2015; Kardon et al. 2014; Huang et al. 2018; Acton et al. 2019).

To begin to address how these neurons could be involved in opioid-induced itch, we considered the canonical view that opioids typically signal through Gαi-coupled G-protein coupled receptors to inhibit neuronal activity (Al-Hasani and Bruchas 2011; Torrecilla et al. 2008). Thus, we tested whether morphine elicits itch through inhibition of inhibitory neurons, or disinhibition.

4.2 Methods

Mice

The studies were performed in both male and female mice 8-10 weeks of age. All animals were of the C57Bl/6 background. Even numbers of male and female mice were used for all experiments. No sex differences were found and, thus, animals were pooled. Mice were given food and water ad libitum and housed under standard laboratory conditions. $Pdyn^{Cre}$, Npy^{Cre}, $Oprm1^{fl/fl}$, and Ai34(RCL-Syp/tdT)-D ($Rosa^{tdt}$) back-crossed into the C57Bl/6 background were bred and raised at the University of Pittsburgh. $Pdyn^{Cre}$ (Jax #027958), Npy^{Cre} (Jax #027851), $Oprm1^{fl/fl}$ (Jax #030074), and $Rosa^{tdt}$ (Jax #012570) mice are available at Jackson Laboratories.

Pharmacologic agents used in mice

Morphine sulfate (4 mg/ml; Henry Schein Animal Health) and chloroquine diphosphate salt (Sigma) were dissolved in physiological saline. Salvinorin B (SalB; Tocris) was dissolved in DMSO and administered subcutaneously (10 mg/kg). Clozapine-N-oxide (CNO; Tocris) was dissolved in PBS and administered intraperitoneally (5mg/kg).

Intradermal and intrathecal injections

For intradermal injection of chloroquine, hair was clipped from the neck or calf of each mouse at least 24 hours before the experiment. Chloroquine (100 μg in 10 μL) was administered into the nape of the neck or calf, which could be subsequently visualized by the formation of a small bubble under the skin. For intrathecal injections, hair was clipped from the back of each mouse at least 24 hours before the experiment. All intrathecal injections were delivered in a total volume of 5 μL using a 30-gauge needle attached to a luer-tip 25 μL Hamilton syringe. The needle was inserted into the tissue at a 45° angle through the fifth intervertebral space (L5 – L6). Solution was injected at a rate of 1 μL/s. The needle was held in position for 10 seconds and

removed slowly to avoid any outflow of the solution. Only mice that exhibited a reflexive flick of the tail following puncture of the dura were included in behavioral analysis. These procedures were performed in awake, restrained mice.

Intraspinal injections

Mice were anesthetized with 100 mg/kg ketamine and 10 mg/kg xylazine. An incision was made at the spinal cord level corresponding to L4-6 dermatome. The intrathecal space was exposed, and two injections of approximately 300 nl of virus (AAV8-DF-KORD-mCitrine, Addgene #65417; AAV2.hSyn.DIO.mCherry Addgene #50459; AAV2.hSyn.DIO.hM4D(Gi)-mCherry, Addgene #44362) were infused 300 mm below the surface of the spinal cord at 5 nL/s via glass pipette through the intrathecal space corresponding to L4-6 of the spinal cord. The glass pipette was left in place for an additional 5 minutes before withdrawal. The incision was closed with 5-0 vicryl suture. Ketofen was delivered I.P. 10 mg/kg and mice were allowed to recover over a heat pad. The injections were validated post-mortem by fluorescent in-situ hybridization of Pdyn and eYFP or mCherry to detect KORD-mCitrine or hM4Di-mCherry, respectively.

All behavioral tests described below were performed in a blinded manner.

Observation of scratching behavior

Scratching behavior was observed using a previously reported method (Kardon et al. 2014). Mice were individually placed in the observation cage (12 x 9 x 14 cm) to acclimate for 30 minutes. The mice were assigned to dosing conditions in a randomized manner. Scratching behavior was videotaped for 60 minutes after administration. 300 pmol of morphine was administered (I.T.). For experiments directed at the calf, the amount of time spent biting the leg was quantified over 60 minutes. Both control and KORD or control and hM4Di treated animals were pretreated with SalB or CNO, respectively, 30 minutes prior to the start of the experiment.

Heat sensitivity assay (Hargreaves testing)

Mice were acclimated on a glass plate held at 30°C (IITC Life Science Inc.). A radiant heat source (activity intensity of 15%) was applied to the hindpaw and latency to paw withdrawal was recorded (Hargreaves et al. 1988). Two trials were conducted on each paw, with at least 5 minutes between testing the opposite paw and at least 10 minutes between testing the same paw. To avoid tissue damage, a cut off latency of 20 seconds was set. Values from both paws were averaged to determine withdrawal latency.

Alloknesis

One hour after the intrathecal injection of morphine, mice were assessed for alloknesis. As previously described (Akiyama et al. 2012), alloknesis was assessed by delivering 3 separate innocuous mechanical stimuli using a von Frey filament (bending force: 0.7 mN; Stoelting, USA) every 5 minutes. Each application of the von Frey filament was reported as 1 trial, yielding a total of 18 trials over 30 minutes.

Hyperknesis

One hour after the intrathecal injection of morphine, mice were assessed for hyperknesis. Chloroquine (100 μg in 10 μL) was injected intradermally into the nape of the neck or calf and scratching behavior was recorded for 30 minutes. The total number of scratch bouts by the hand paws directed to the nape of the neck was counted. For hyperknesis following chemogenetic inhibition, chloroquine (100 μg in 10 μL) was injected intradermally into the calf and biting behavior was recorded for 30 minutes.

RNAscope fluorescent in-situ hybridization

Multiplex fluorescent in-situ hybridization (FISH) was performed according to the manufacturer's instructions (Advanced Cell Diagnostics #320850). Briefly, 16 μm-thick fresh-

frozen sections containing the mouse or human spinal cord were fixed in 4% paraformaldehyde, dehydrated, treated with protease for 15 minutes, and hybridized with gene- and species-specific probes. Probes were used to detect eYFP-C1 (#312131), mCherry-C2 (#431201), Mm-Oprm1-C1 (#315841), Mm-Npy-C2 (#313321-C2), Mm-Pdyn-C2 (#318771-C2), Mm-GRPR-C2 (#317871-C2), Mm-Pvalb-C2 (#421931-C2), Mm-Nos1-C2 (#437651-C2), Mm-Slc32a1-C3 (#319191), Hs-OPRM1-C1 (#410681), Hs-PDYN-C2 (#507161-C2). DAPI (#320858) was used to visualize nuclei. 3-plex positive (#320881) and negative (#320871) control probes were tested.

Immunohistochemistry

Mice were anesthetized with an intraperitoneal injection of urethane, transcardially perfused, and post-fixed at least four hours in 4% paraformaldehyde. 25 μm thick spinal cord or dorsal root ganglion sections were collected on a cryostat and slide-mounted for immunohistochemistry. Sections were blocked at room temperature for two hours in a 5% donkey serum, 0.2% triton, in phosphate buffered saline. Primary antisera was incubated for 14 hours overnight at 4°C with rabbit anti-RFP (1:1K; Cat #600-401-379, Rockland, USA). Sections were subsequently washed and incubated in secondary antibodies (Life Technologies, 1:500) at room temperature for two hours. Sections were then incubated in Hoechst (ThermoFisher, 1:10K) for 1 minute and washed, mounted, and a cover slip was applied.

Image acquisition and quantification

Full-tissue thickness sections were imaged using either an Olympus BX53 fluorescent microscope with UPlanSApo 4x, 10x, or 20x objectives or a Nikon A1R confocal microscope with 20X or 60X objectives. All images were quantified and analyzed using ImageJ. To quantify images in RNAscope in-situ hybridization experiments, confocal images of tissue samples (3-4 dorsal horns per mouse over 3-4 mice or 5-6 images per dorsal horn from two human spinal

cords) were imaged and only cells whose nuclei were clearly visible by DAPI staining and exhibited fluorescent signal were counted.

Electrophysiological recordings

The semi-intact somatosensory preparation was made as previously described (Hachisuka et al. 2016; Hachisuka, Koerber, and Ross 2020). Briefly, young adult mice (5–9 weeks old) were deeply anesthetized and perfused transcardially through the left ventricle with oxygenated (95% O2 and 5% CO2) sucrose-based artificial cerebrospinal fluid (ACSF) (in mM; 234 sucrose, 2.5 KCl, 0.5 CaCl2, 10 MgSO4, 1.25 NaH2PO4, 26 NaHCO3, 11 Glucose) at room temperature. Immediately following perfusion, the skin was incised along the dorsal midline and the spinal cord was quickly exposed via dorsal laminectomy. The right hindlimb and spinal cord (~C2 – S6) were excised, transferred into Sylgard-lined dissection/recording dish, and submerged in the same sucrose-based ACSF, which circulated at 50 ml/min to facilitate superfusion of the cord. The skin innervated by the saphenous nerve and the femoral cutaneous nerve was dissected free of surrounding tissue. L2 and L3 DRG were left on the spine. Pial membrane was carefully removed and the spinal cord was pinned onto the Sylgard chamber with the right dorsal horn facing upward. Following dissection, the chamber was transferred to the rig. Then the preparation was perfused with normal ACSF solution (in mM; 117 NaCl, 3.6 KCl, 2.5 CaCl2, 1.2 MgCl2, 1.2 NaH2PO4, 25 NaHCO3, 11 glucose) saturated with 95% O2 and 5% CO2 at 32 °C. Tissue was rinsed with ACSF for at least 30 min to wash out sucrose. Thereafter, recordings were performed for up to 6 hours post-dissection.

Patch clamp recording from dorsal horn neurons

Neurons were visualized using a fixed stage upright microscope (BX51WI Olympus microscope, Tokyo, Japan) equipped with a 40x water immersion objective lens, a CCD camera

(ORCA-ER Hamamatsu Photonics, Hamamatsu City, Japan) and monitor screen. A narrow beam infrared LED (L850D-06 Marubeni, Tokyo, Japan, emission peak, 850 nm) was positioned outside the solution meniscus, as previously described (Szucs, Pinto, and Safronov 2009; Safronov, Pinto, and Derkach 2007; Hachisuka et al. 2016). $Pdyn^{Cre}$ neurons in lamina I were easily identified by td-Tomato expression. Whole-cell patch-clamp recordings were made with a pipette constructed from thin-walled single-filamented borosilicate glass using a microelectrode puller (PC-10; Narishige International, East Meadow NY). Pipette resistances ranged from 6 to 12 MΩ. Electrodes were filled with an intracellular solution containing the following (in mM): 135 K-gluconate, 5 KCl, 0.5 CaCl2, 5 EGTA, 5 HEPES, 5 MgATP, pH 7.2. Alexa fluor 488 (Invitrogen; 25 µM) was added to confirm recording from the target cell. Signals were acquired with an amplifier (Axopatch 200B, Molecular Devices, Sunnyvale CA). The data were low-pass filtered at 2 kHz and digitized at 10 kHz with an A/D converter (Digidata 1322A, Molecular Devices) and stored using a data acquisition program (Clampex version 10, Molecular Devices). The liquid junction potential was not corrected.

Statistical analysis

All statistical analyses were performed using GraphPad Prism 7. Values are presented as mean SEM. P values were determined by tests indicated in applicable figure legends. Sample sizes were based on pilot data and are similar to those typically used in the field.

4.3 Results

4.3.1 Pdyn neurons are required for neuraxial morphine-induced itch

Given that morphine-induced itch is most commonly seen in humans when morphine is given neuraxially (Ballantyne, Loach, and Carr 1988), we next examined the possible role of spinal neurons. A previous study suggested that neuraxial morphine causes itch through activation of gastrin-releasing peptide receptor (Grpr) neurons in the dorsal horn (Liu et al. 2011), an excitatory population that is involved in mediating itch (Sun and Chen 2007; Pagani et al. 2019). However, when we performed dual fluorescent in-situ hybridization (FISH) for Oprm1 and Grpr in the dorsal horn, we found very limited overlap (Figure 9A).

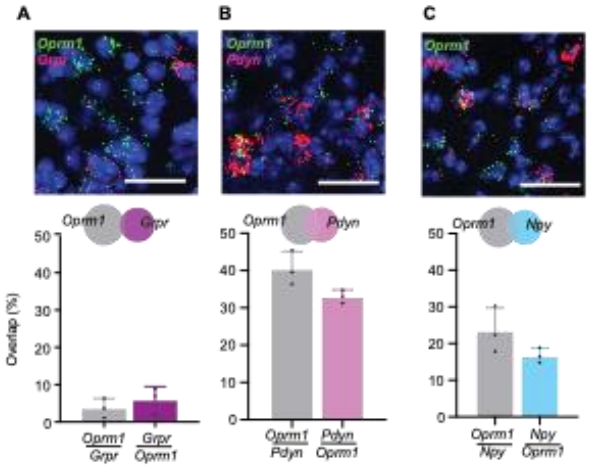

Figure 9. Spinal expression of Oprm1 in Grpr, Pdyn, and Npy neurons.

(A to **C)** Representative image of fluorescent in-situ hybridization in the spinal dorsal horn comparing expression of *Oprm1* to **(A)** *Grpr*, **(B)** *Pdyn*, **(C)** and *Npy*. The overlap is quantified below. Scale bar = 50 μm. *n* = 3 mice. Data are mean + S.E.M with dots representing individual mice.

Because opioids typically signal through Gαi-coupled G-protein coupled receptors to inhibit neuronal activity (Al-Hasani and Bruchas 2011; Torrecilla et al. 2008), we favored the hypothesis that morphine causes itch through disinhibition. Therefore, we examined the expression of Oprm1 across four distinct populations that account for the majority of inhibitory neurons in the dorsal horn (Boyle et al. 2017): Pdyn, Npy, Nos1, and Pvalb. Through multiplex FISH, we found that roughly half of the neurons in the dorsal horn that express Oprm1 are inhibitory neurons, as revealed by co-expression of Slc32a1, the gene encoding Vgat. Among these neurons, we found that Oprm1 is expressed across all four populations, with the highest expression in Pdyn neurons (40.52.7% of Pdyn neurons express Oprm1, representing 33.01.0% of Oprm1-expressing inhibitory neurons in the dorsal horn) followed by Npy neurons (23.53.6% and 18.22.6%, respectively) (Figure 10A and Figure 9B and C).

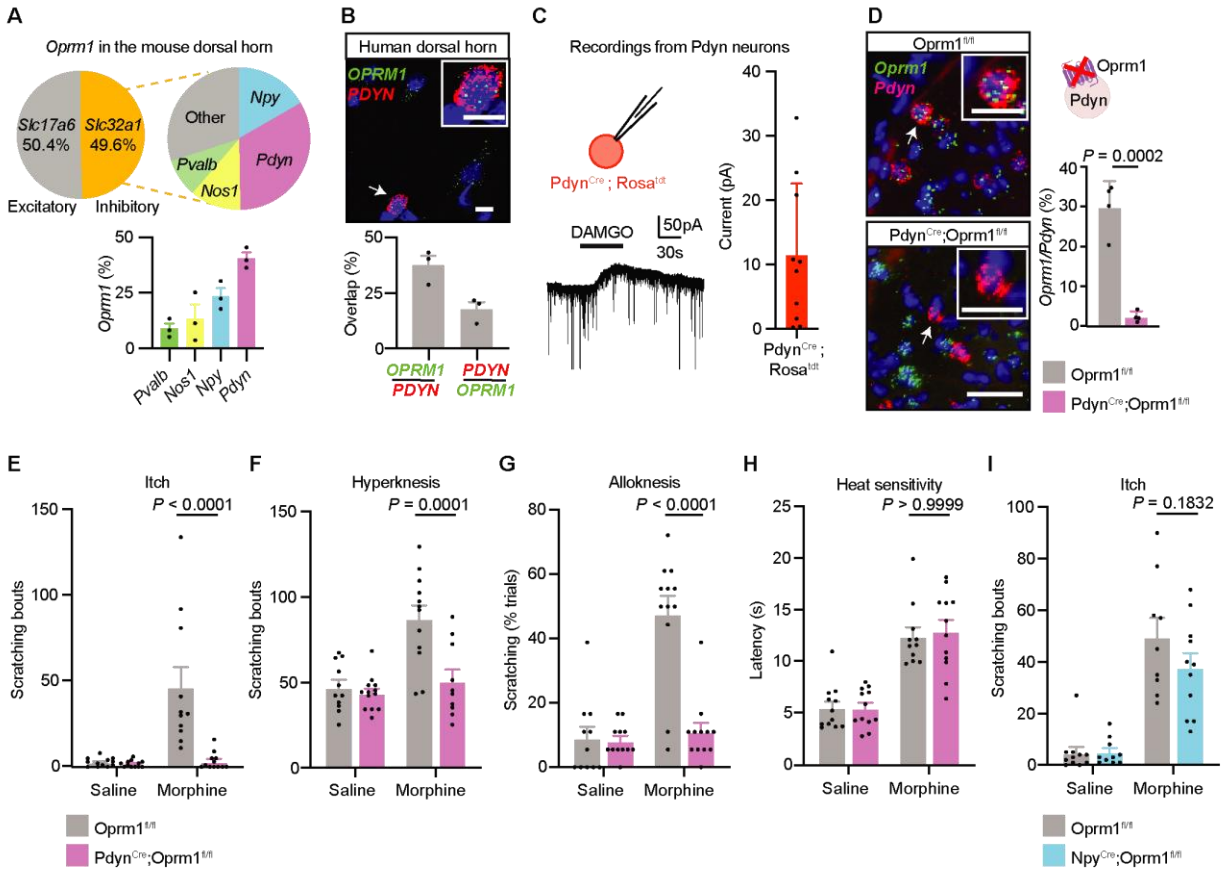

Figure 10. Oprm1 expression in Pdyn neurons is required for morphine-induced itch.

(A) *Oprm1* expression in neurons in the mouse spinal dorsal horn. *n* = 3 mice. **(B)** Fluorescent in-situ hybridization of human spinal dorsal horn depicting the co-expression of *OPRM1* and *PDYN*. *n* = 3 individual dorsal horns. Arrow indicates the cell shown in the inset. Scale bar = 50 µm. **(C)** Electrophysiological recordings of Pdyn^{Cre}; Rosa^{tdt} neurons in the presence of DAMGO. *n* = 10 neurons. **(D)** Deletion of *Oprm1* in *Pdyn* neurons in the spinal dorsal horn of Pdyn^{Cre}; Oprm1$^{fl/fl}$ animals compared to Oprm1$^{fl/fl}$ controls. Arrow indicates the cell shown in the inset. Scale bar = 50 µm, inset = 25 µm. *n* = 4 mice per group. **(E** to **G)** Deletion of *Oprm1* in Pdyn neurons on morphine-induced **(E)** itch **(F)** alloknesis, **(G)** and hyperknesis. **(H)** and heat sensitivity. *n* = 11-13 mice per group. **(I)** *Oprm1* deletion in Npy neurons on morphine-induced itch. *n* = 12 mice per group. *P* value was determined by (D) two-tailed, unpaired t-test., (E to I), two-way ANOVA, with Bonferroni's correction. (A to I) Data are mean + S.E.M. with individual dots representing (A and D to I) individual mice, (B) individual human dorsal horns, (C) and individual neurons.

The Pdyn and Npy inhibitory neurons were particularly intriguing to us because we and others had previously discovered that these two populations inhibit itch (Acton et al. 2019; Bourane et al. 2015; Ross et al. 2010; Kardon et al. 2014). Indeed, when either Pdyn neurons or

Npy neurons are lost during development, mice show spontaneous scratching behavior suggesting that these populations are involved in the tonic inhibition of itch (Ross et al. 2010; Bourane et al. 2015). We therefore investigated these populations in more detail, beginning with Pdyn neurons. Just as in rodents, we found that human PDYN neurons express OPRM1, as revealed by dual FISH of the spinal dorsal horn from post-mortem tissue (Figure 10A and B). Furthermore, recordings from tdTomato-labeled Pdyn neurons (in $Pdyn^{Cre}$; $Rosa^{tdt}$ mice) revealed that ~50% showed outward current in response to the Oprm1 agonist D-Ala^2, N-$MePhe^4$, Gly-ol-enkephalin (DAMGO) (Figure 10C), consistent with the idea that Pdyn cells express functional Oprm1 and that activation of this receptor inhibits the cells.

Based on these findings, we next asked whether expression of Oprm1 in Pdyn neurons was required for morphine-induced itch. Using a conditional deletion strategy, we selectively removed Oprm1 from Pdyn neurons (Figure 10D). Strikingly, this genetic manipulation completely eliminated I.T. morphine-induced itch, alloknesis, and hyperknesis (Figure 10E to G). Importantly, morphine-induced increases in paw withdrawal latency was unaffected in these animals (Figure 10H), indicating that Oprm1 expression on Pdyn neurons is required for morphine-induced itch but not morphine-induced analgesia. Because our data suggested that Npy neurons also express Oprm1 (Figure 10A and Figure 9C) and that these cells are known to inhibit itch, we also examined the contribution of this population. In contrast to Pdyn neurons, conditional deletion of Oprm1 from Npy neurons had no effect on neuraxial morphine-induced itch (Figure 10I and Figure 11A to D). These findings identify Pdyn neurons as the cellular mediator of morphine-induced itch.

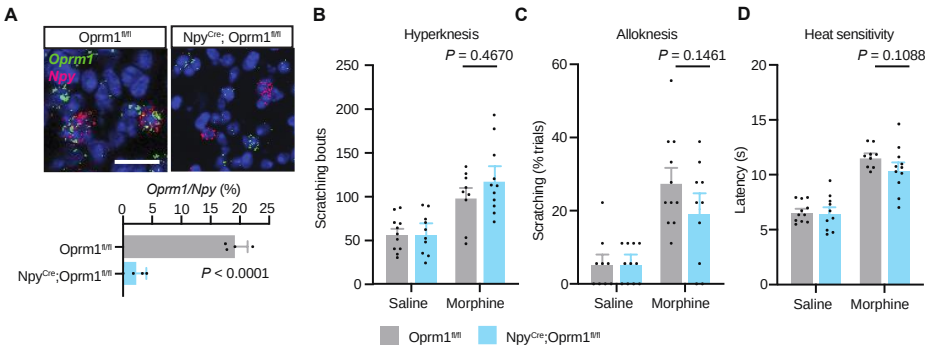

Figure 11. Expression of Oprm1 in Npy neurons is not required for morphine-induced itch.

(A) Fluorescent in-situ hybridization to validate deletion of *Oprm1* in *Npy* neurons in the spinal dorsal horn in Npy^{Cre}; $Oprm1^{fl/fl}$ animals compared to $Oprm1^{fl/fl}$ controls. Scale bar = 50 μm. *n* = 4 mice per group. **(B** to **D)** Deletion of Oprm1 in Npy neurons on morphine-induced **(B)** hyperknesis, **(C)** alloknesis, **(D)** and heat sensitivity. *n* = 12 mice. *P* value was determined by (A) two-tailed, unpaired t-test, (B to D) and two-way ANOVA, with Bonferroni's correction. Data are mean + S.E.M with dots representing individual mice.

4.3.2 Inhibition of Pdyn neurons causes itch

Our loss-of-function experiments implied that morphine causes itch through disinhibition of Pdyn cells. To test this idea directly, we sought to mimic opioid signaling in these cells through chemogenetic manipulation using either KORD or hM4Di, two Gi-coupled designer receptors exclusively activated by designer drugs (DREADDs). In these experiments, we injected Cre-dependent adeno-associated viruses (AAVs) into the lumbar spinal cord of $Pdyn^{Cre}$ mice (Figure 12A and Figure 13A to D). Notably, in both approaches, chemogenetic inhibition of Pdyn neurons elicited spontaneous itch in the form of increased time spent biting the leg (the dermatome segment that corresponded to the site of viral delivery) (Figure 12B and C). We also observed hyperknesis and alloknesis, but no changes to heat sensitivity, upon chemogenetic inhibition of Pdyn neurons (Figure 12D to F). Together, these findings suggest that morphine causes itch through disinhibition of Pdyn neurons.

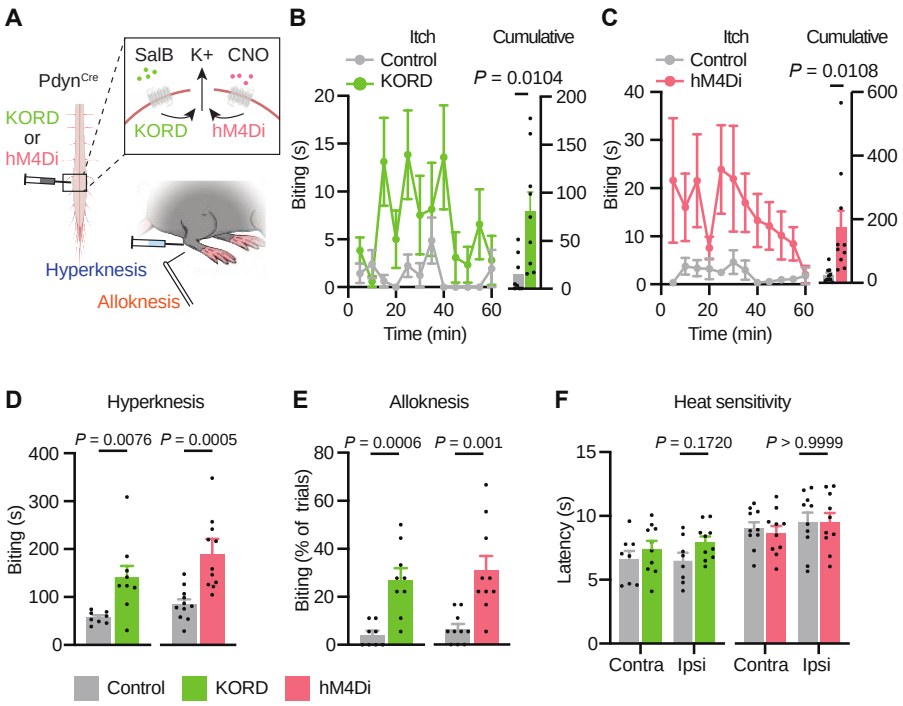

Figure 12. Inhibition of Pdyn neurons is sufficient to evoke itch.

(A) Experimental design. **(B** and **C)** Time course for itch following chemogenetic inhibition of Pdyn neurons with **(B)** KORD **(C)** or hM4Di. **(D** to **F)** Chemogenetic inhibition of Pdyn neurons with KORD (green, left) and hM4Di (red, right) on **(D)** hyperknesis, **(E)**, alloknesis, **(F),** and heat sensitivity. *n* = 7-11 mice per group. *P* value was determined by (B to E) two-tailed, unpaired t-test (F), and two-way ANOVA, with Bonferroni's correction. (B, C) Time course data are mean S.E.M. (B to F) data are mean + S.E.M. with individual dots representing individual mice.

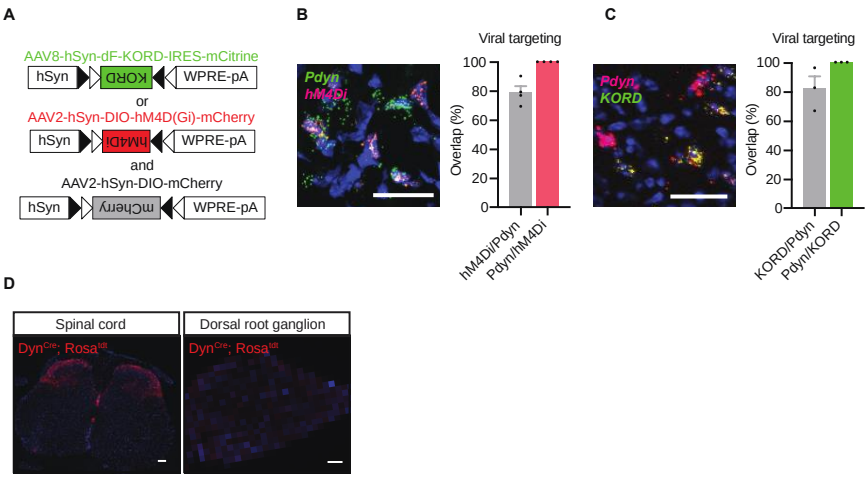

Figure 13. Validation of viral infection of Pdyn neurons.

(A) Cre-dependent viruses used to selectively express KORD and hM4Di DREADDs into the spinal cord of Pdyn^{Cre} mice. **(B** and **C)** Representative image of fluorescent in-situ hybridization (left) and quantification (right) of the dorsal horn in Pdyn-Cre mice injected with **(B)** hM4Di **(C)** and KORD. *n* = 3 mice per group. **(D)** Representative image of a spinal cord and dorsal root ganglion section in Pdyn^{Cre}; Rosa^{tdt} mouse. Scale bar = 50 μm. (B and C) Data are mean + S.E.M with dots representing individual mice.

4.4 Discussion

Our study has uncovered a previously undescribed role for neuronal disinhibition in morphine-induced itch. It was previously suggested that an excitatory population of Grpr^{+} spinal neurons mediates morphine-induced itch through a specific isoform of the mu-opioid receptor, *MOR1D* (Liu et al. 2011). However, we observed very little overlap in the dorsal horn between *Grpr* and *Oprm1* using a probe that targets a region common to all *Oprm1* isoforms, including *MOR1D* (Figure 9A). Instead, we show that deletion of the mu opioid receptor from dynorphin neurons eliminated neuraxial morphine-induced itch. Furthermore, we found that ectopic expression of the opioid receptor on dynorphin neurons was sufficient for itch.

These findings further validate the concept that inhibitory spinal neurons inhibit itch (Ross et al. 2010; Kardon et al. 2014; Wang, Jiang, Yao, Chen, Rahman, Gu, Zhao, et al. 2020) and demonstrate that the dynorphin population of spinal neurons is modulated by mu agonists, such as morphine, to elicit itch. Dynorphin neurons provide a substrate upon which future therapies could be targeted for the management of itch conditions.

5.0 Nalfurafine treats morphine-induced itch in preclinical models

5.1 Introduction

Mixed opioid agonist-antagonists, such as nalbuphine and butorphanol, are frequently used for neuraxial opioid-induced pruritus (Jannuzzi 2016; Cohen et al. 1992; Lee et al. 2007). Compared to pure mu opioid antagonists, mixed agonist-antagonists are often preferred to manage pruritus because they do not reduce morphine's analgesic effects (Cohen et al. 1992). However, one potential limitation of this class of antipruritics is sedation (Kjellberg and Tramèr 2001; Jannuzzi 2016).

Selective kappa opioid receptor agonists, such as nalfurafine, have also been proposed as therapeutic candidates for the treatment of opioid-induced pruritus (Ko 2015). Nalfurafine is frequently used for the treatment of uremic and cholestatic pruritus in Japan (Cowan, Kehner, and Inan 2015), although it is not presently FDA approved for use in the United States. Emerging evidence in preclinical models, involving both mice and non-human primates, support that kappa agonists can reduce morphine-induced itch without affecting morphine-induced analgesia (Ko and Husbands 2009; Akiyama et al. 2015). Thus, we tested whether nalfurafine, a selective kappa agonist, could treat morphine-induced itch in mice and non-human primates.

5.2 Methods

Mice

The studies were performed in both male and female mice 8-10 weeks of age. All animals were of the C57Bl/6 background. Even numbers of male and female mice were used for all experiments. No sex differences were found and, thus, animals were pooled. Mice were given food and water ad libitum and housed under standard laboratory conditions.

Non-human primates

All animal care and experiments in non-human primate study were conducted according to the Guide for the Care and Use of Laboratory Animals by the US National Institutes of Health (Bethesda, MD, USA), reported according to the ARRIVE guidelines (Kilkenny et al. 2010), and approved by the Institutional Animal Care and Use Committee of Wake Forest University (Winston-Salem, NC, USA). Five adult male and female rhesus monkeys (Macaca mulatta), 8–16 years of age, 5.1–12.2 kg, with implanted intrathecal catheters (Ding et al. 2015) were used in this study. The monkeys were housed at an indoor facility accredited by the Association for Assessment and Accreditation of Laboratory Animal Care International (Frederick, MD, USA). The monkeys were individually housed in cages with 6-12 square feet of floor space with ceilings 2.7-5.4 feet high in a temperature-controlled room (21–25 °C, 40–60% relative humidity) with a 12-h light/dark cycle (Light On: 6:30-18:30). The monkeys were provided with water and their diet consisted of approximately 20–30 biscuits (Purina Monkey Chow; Ralston Purina Co., St. Louis, MO, USA) and fresh fruit ad libitum. Primate enrichment devices and small amounts of treats were provided daily.

Drug administration in non-human primates

Morphine sulfate (National Institute on Drug Abuse, Bethesda, MD, USA) and nalfurafine HCl (provided by Dr. Stephen Husbands, University of Bath, Bath, UK) were dissolved in sterile water. For intrathecal administration(Ding et al. 2015), 1 mL of the test compound was administered through the subcutaneous access port, followed by 0.35 mL of saline to flush the dead volume of the port and catheter.

Pharmacologic agents used in mice

Morphine sulfate (4 mg/ml; Henry Schein Animal Health) and chloroquine diphosphate salt (Sigma) were dissolved in physiological saline. Nalfurafine (Sigma) was dissolved in saline and administered intrathecally. Loratadine (Sigma) and diphenhydramine (Sigma) were prepared in 10% DMSO and given 10 mg/kg I.P. For experiments involving antihistamines, animals were pretreated with vehicle, loratadine, or diphenhydramine 30 minutes prior to recording scratching behavior.

Intradermal and intrathecal injections

For intradermal injection of chloroquine, hair was clipped from the neck or calf of each mouse at least 24 hours before the experiment. Chloroquine (100 μg in 10 μL) was administered into the nape of the neck or calf, which could be subsequently visualized by the formation of a small bubble under the skin. For intrathecal injections, hair was clipped from the back of each mouse at least 24 hours before the experiment. All intrathecal injections were delivered in a total volume of 5 μL using a 30-gauge needle attached to a luer-tip 25 μL Hamilton syringe. The needle was inserted into the tissue at a 45° angle through the fifth intervertebral space (L5 – L6). Solution was injected at a rate of 1 μL/s. The needle was held in position for 10 seconds and removed slowly to avoid any outflow of the solution. Only mice that exhibited a reflexive flick

of the tail following puncture of the dura were included in behavioral analysis. These procedures were performed in awake, restrained mice.

Observation of scratching behavior

Scratching behavior was observed using a previously reported method (Kardon et al. 2014). Mice were individually placed in the observation cage (12 x 9 x 14 cm) to acclimate for 30 minutes. The mice were assigned to dosing conditions in a randomized manner. Scratching behavior was videotaped for 60 minutes after administration. 300 pmol of morphine was administered (I.T.). For experiments directed at the calf, the amount of time spent biting the leg was quantified over 60 minutes.

To assess the effect of nalfurafine on intrathecal morphine-induced itch in non-human primates, scratching activity (Ko et al. 2004) was recorded when monkeys were in their home cages. Each 15-minute recording session was conducted at 0.5, 1, 2, 2.5 and 3 hours following intrathecal morphine administration. Nalfurafine (0.1 or 0.3 μg) or vehicle was intrathecally administered at 1.5 hours after intrathecal morphine (10 or 30 μg) administration. A scratch was defined as one brief (<1 second) action of scraping on the skin surface of other body parts using the forepaw or hind paw (Ko et al. 2004). The total number of scratches were counted and summed for each 15-minute period.

Acute thermal nociception

To assess the effect of nalfurafine on intrathecal morphine-induced antinociception in non-human primates, nalfurafine (0.3 μg) or vehicle was intrathecally administered at 1.5 hours after intrathecal morphine (10 μg). The warm water tail-withdrawal assay (Ko et al. 1999) was conducted before and 0.5, 1, 2, 2.5 and 3 hours after intrathecal morphine administration. The lower parts of their shaved tails (~15 cm) were immersed in water maintained at 42, 46, or 50 °C.

The monkeys were assigned to dosing conditions in a randomized manner. Water at 42 or 46 °C was used as a non-noxious stimuli (no tail-withdrawal movement was expected), and water at 50 °C was used as an acute noxious stimulus (2-3 second tail-withdrawal latency). Experimenters measured tail-withdrawal latencies at each temperature by using a computerized timer. If a monkey did not withdraw its tail within 20 seconds (cut-off), the stimulus was removed and a maximum time of 20 seconds was recorded.

Heat sensitivity assay (Hargreaves testing)

Mice were acclimated on a glass plate held at 30°C (IITC Life Science Inc.). A radiant heat source (activity intensity of 15%) was applied to the hindpaw and latency to paw withdrawal was recorded (Hargreaves et al. 1988). Two trials were conducted on each paw, with at least 5 minutes between testing the opposite paw and at least 10 minutes between testing the same paw. To avoid tissue damage, a cut off latency of 20 seconds was set. Values from both paws were averaged to determine withdrawal latency.

Alloknesis

One hour after the intrathecal injection of morphine, mice were assessed for alloknesis. As previously described (Akiyama et al. 2012), alloknesis was assessed by delivering 3 separate innocuous mechanical stimuli using a von Frey filament (bending force: 0.7 mN; Stoelting, USA) every 5 minutes. Each application of the von Frey filament was reported as 1 trial, yielding a total of 18 trials over 30 minutes.

Hyperknesis

One hour after the intrathecal injection of morphine, mice were assessed for hyperknesis. Chloroquine (100 μg in 10 μL) was injected intradermally into the nape of the neck or calf and

scratching behavior was recorded for 30 minutes. The total number of scratch bouts by the hand paws directed to the nape of the neck was counted.

RNAscope fluorescent in-situ hybridization

Multiplex fluorescent in-situ hybridization (FISH) was performed according to the manufacturer's instructions (Advanced Cell Diagnostics #320850). Briefly, 16 μm-thick fresh-frozen sections containing the mouse or human spinal cord were fixed in 4% paraformaldehyde, dehydrated, treated with protease for 15 minutes, and hybridized with gene- and species-specific probes. Probes were used to detect Mm-Oprk1-C1 (#316111), Mm-Slc17a6-C3 (#319171). DAPI (#320858) was used to visualize nuclei. 3-plex positive (#320881) and negative (#320871) control probes were tested.

Image acquisition and quantification

Full-tissue thickness sections were imaged using either an Olympus BX53 fluorescent microscope with UPlanSApo 4x, 10x, or 20x objectives or a Nikon A1R confocal microscope with 20X or 60X objectives. All images were quantified and analyzed using ImageJ. To quantify images in RNAscope in-situ hybridization experiments, confocal images of tissue samples (3-4 dorsal horns per mouse over 3-4 mice or 5-6 images per dorsal horn from two human spinal cords) were imaged and only cells whose nuclei were clearly visible by DAPI staining and exhibited fluorescent signal were counted.

Quantification of Fos

Mice were lightly anesthetized with isoflurane before receiving I.T. morphine or saline. Twenty minutes later, their spinal cords were harvested for FISH. The total number of cells co-expressing Fos, Oprk1, and Slc17a6 were counted and compared to the total number of cells co-expressing Oprk1 and Slc17a6.

Statistical analysis

All statistical analyses were performed using GraphPad Prism 7. Values are presented as mean SEM. P values were determined by tests indicated in applicable figure legends. Sample sizes were based on pilot data and are similar to those typically used in the field.

5.3 Results

5.3.1 Restoration of dynorphin signaling alleviates morphine-induced itch

Next, studies involving the immediate-early gene *Fos* were performed to examine the mechanism through which the inhibition of $Pdyn^+$ neurons by morphine causes itch (Figure 14A). Following I.T. morphine, we found an upregulation of *Fos* expression in neurons that express the kappa opioid receptor (Oprk1), consistent with the idea that inhibition of $Pdyn^+$ neurons results in disinhibition (activation) of $Oprk1^+$ neurons (Figure 14B and C, and Figure 15A). Because $Pdyn^+$ neurons release several inhibitory mediators, including dynorphin and GABA (Sardella et al. 2011; Tiong et al. 2011), we wondered which ones might be involved (Figure 14A). Therefore, we performed occlusion studies using the long-acting Oprk1 antagonist nor-binaltorphimine dihydrochloride (norBNI) to inhibit Oprk1 (Figure 17A and B). Substantial scratching was observed in mice pretreated with I.T. norBNI (Figure 17A), consistent with the idea that ongoing dynorphin tone in the spinal cord inhibits itch, as previously described (Kardon et al. 2014). However, pretreatment with norBNI did not prevent morphine from causing further itch (Figure 17A). This lack of occlusion suggests that morphine-induced itch is not due solely to

the inhibition of dynorphin release, and might therefore involve the disinhibition of Oprk1 neurons through a reduction in the release of both inhibitory transmitters: dynorphin and GABA.

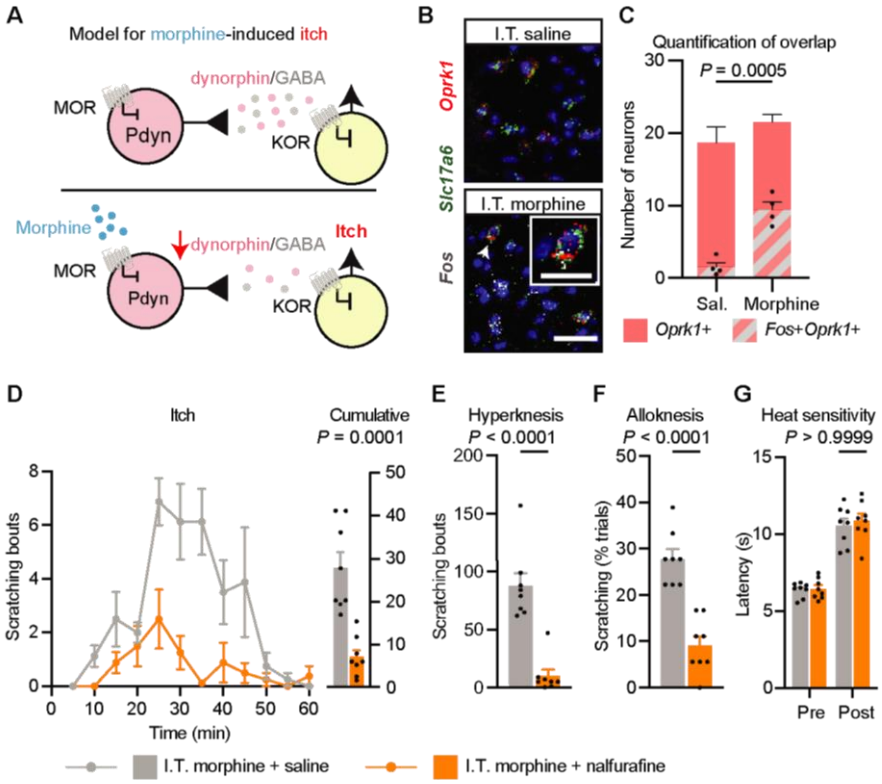

Figure 14. Restoration of dynorphin signaling alleviates morphine-induced itch.

(A) Model for morphine-induced itch. **(B)** Representative image for the expression of *Fos* in excitatory (*Slc17a6* containing) *Oprk1* neurons. Arrow indicates the cell shown in the inset. Scale bar = 50 µm, inset = 25 µm. **(C)** Quantification of B. *n* = 3 mice. **(D** to **G)**, in mice, the effect of nalfurafine (40 ng) on morphine-induced **(D)** itch, **(E)** hyperknesis, **(F)** alloknesis, **(G)** and heat sensitivity. *n* = 8 mice per group. *P* value was determined by (D to F) two-tailed, unpaired t-test and (G) two-way ANOVA, with Bonferroni's correction. (C to G) Data are mean + S.E.M. with dots representing individual mice. (D) Time course data are mean +/- S.E.M.

Our model suggested that inhibition of Oprk1^{+} neurons should alleviate morphine-induced itch. To test this idea, we examined the effect of nalfurafine, a selective Oprk1 agonist (Schattauer et al. 2017). In mice, we found that co-administration of nalfurafine and morphine

(I.T.) reduced morphine-induced itch, hyperknesis, and alloknesis compared to controls (Figure 14D to F and Figure 15B to D). Importantly, the dose of nalfurafine that abrogated morphine-induced itch did not reduce the analgesic efficacy of morphine to thermal sensitivity (Figure 14G and Figure 15E). These findings suggest that inhibition of Oprk1 neurons suppresses morphine-induced itch without reducing morphine's analgesic effects.

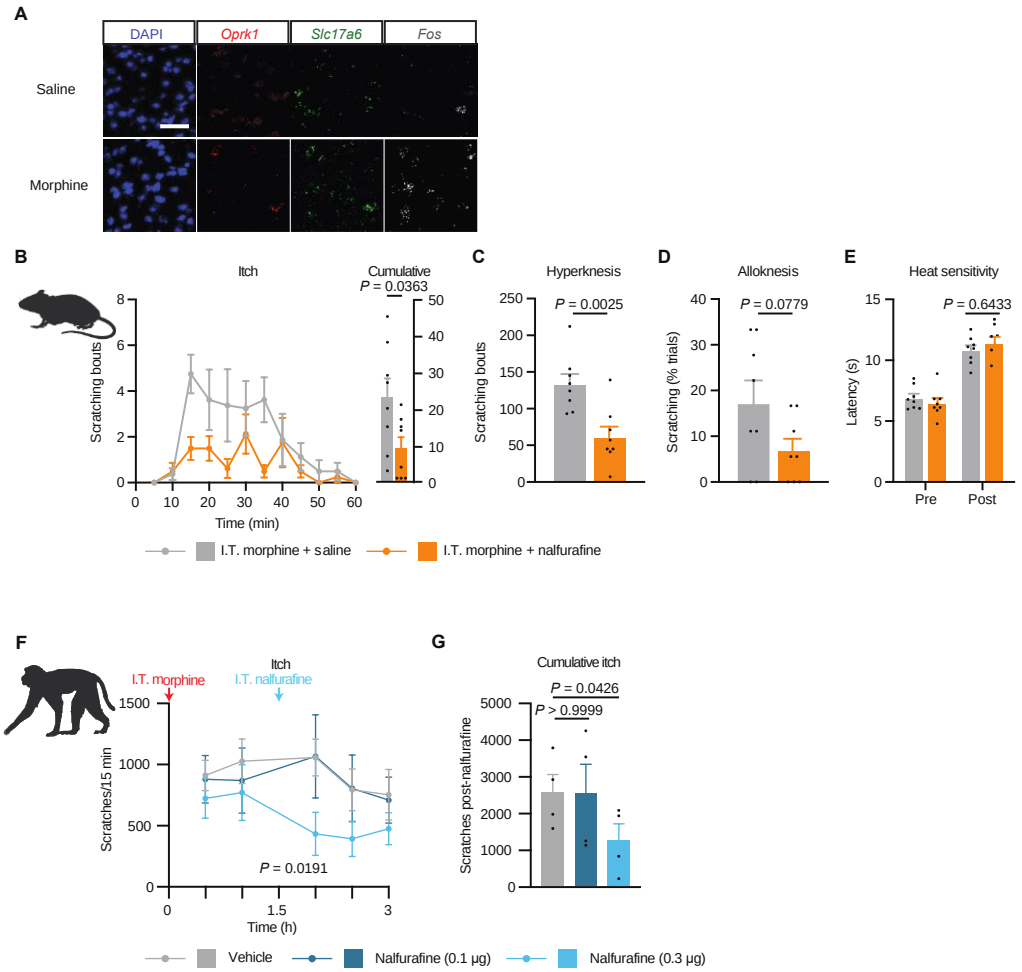

Figure 15. Dose-response analysis of nalfurafine treatment for morphine-induced itch.

(A) Representative image for the expression of *Fos* in *Oprk1* neurons containing *Slc17a6*. These panels are shown merged in the main figure. Scale bar = 50 µm. **(B** to **E)** in mice, the effect of nalfurafine (1.25 ng) on morphine-induced **(B)** itch, **(C)** hyperknesis, **(D)** alloknesis **(E)** and heat sensitivity. *n* = 8 mice per group. **(F** and **G)** in primates, the effect of nalfurafine (10 ug) following I.T. morphine (30 ug) on itch **(F)** as a time course, **(G)** and cumulatively over 60 minutes. *n* = 4 primates per group. *P* value was determined by (B to D) two-tailed, unpaired t-test, (E and F) two-way ANOVA, with Bonferroni's correction, (G) and one-way ANOVA with Bonferroni's correction. (B and F) Time course data are mean S.E.M. (B to E and G) data are mean + S.E.M with dots representing individual (B to E) mice, (G) and primates.

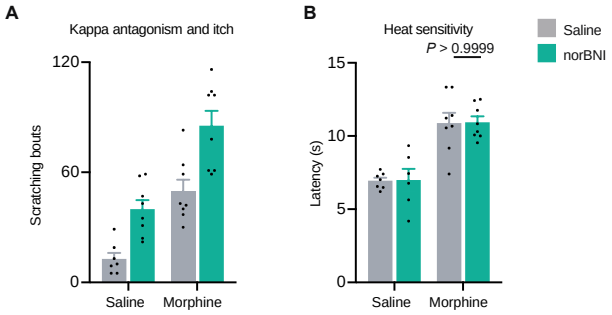

Figure 16. Antagonism of the kappa-opioid receptor evokes itch.

(A) Antagonism of the kappa-opioid receptor with nor-Binaltorphimine dihydrochloride (norBNI, (1 μg) on spontaneous and morphine-induced itch. **(B)** Oprk1 antagonism on morphine-induced analgesia to heat sensitivity. *n* = 6-8 mice per group. *P* value was determined by two-way ANOVA with Bonferroni's correction. Data are mean + S.E.M with dots representing individual mice.

To examine the translational relevance of these findings, we repeated these experiments in non-human primates. Again, I.T. nalfurafine reduced the number of morphine-induced scratches without affecting analgesia to tail withdrawal (Figure 17A and B, and Figure 15F and G). Thus, in both mouse as well as non-human primate models, we observed that treatment with an Oprk1 agonist mitigates morphine-induced itch without affecting morphine-induced analgesia.

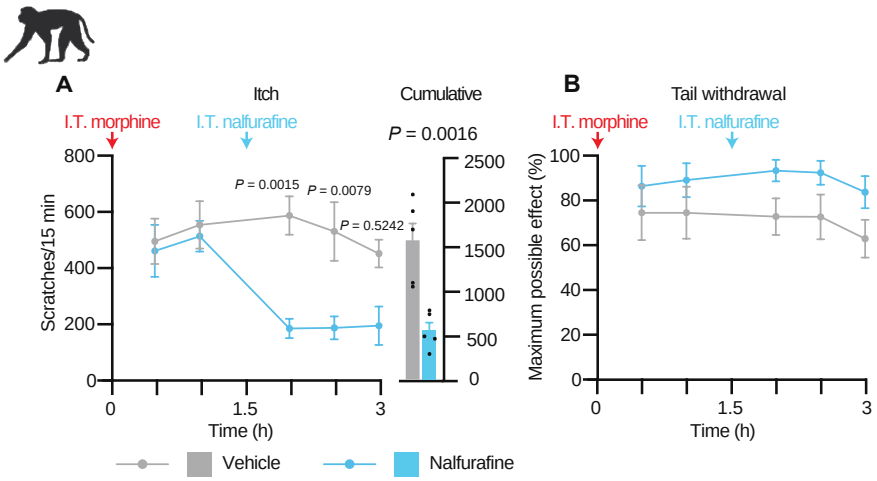

Figure 17. I.T. nalfurafine alleviates morphine-induced itch in non-human primates.

(A) The effect of nalfurafine (0.3 μg) on I.T. morphine-induced itch (10 μg). *P* values were determined by two-way ANOVA, with Bonferroni's correction (left) and two-tailed, unpaired t-test (right). **(B)** Effect of nalfurafine (0.3 μg) on tail-withdrawal. *n* = 5 primates per group. Data are mean + S.E.M. with dots representing individual primates. Time course data are mean S.E.M.

5.4 Discussion: relation to human health

In mice and in non-human primates models, we found that the intrathecal administration of nalfurafine significantly reduces morphine-induced itch. These results help explain the mechanism of action for nalbuphine (a mixed kappa agonist and mu antagonist) (Szarvas, Harmon, and Murphy 2003; Jannuzzi 2016) as a treatment for morphine-induced itch. However, a major limitation of nalbuphine is that it reduces the analgesia provided by morphine (Anwari and Iqbal 2003; Jannuzzi 2016). Unlike nalbuphine, we found that nalfurafine does not affect the therapeutic analgesic effects of morphine, assessed by thermal behaviors (Figure 14G and Figure 17B).

However, one limitation of our study is that we did not perform extensive dose-response investigations to address the specificity of nalfurafine for the inhibition morphine-induced itch.

Although nalfurafine is a selective agonist for the kappa-opioid receptor, it is possible it may also have off-target effects on other receptors, such as the mu-opioid receptor. Furthermore, potential extra-pyramidal effects were not assessed in our models. The dose that was chosen (40 ng IT) was based on a previous study from our group (Kardon et al. 2014) that demonstrated that nalfurafine inhibits various forms of pruritogen-evoked itch in mice. Before nalfurafine can be considered in clinical studies, it will be necessary to evaluate its appropriate dosing regimen and specificity for opioid-induced itch and not opioid-induced analgesia.

Our results provide a mechanistic explanation for how nalbuphine may be useful for morphine-induced itch, our experiments in mice and non-human primates model a circuit upon which a selective Oprk1 agonist, such as nalfurafine, can effectively be used for the treatment of clinical neuraxial morphine-induced itch in humans.

6.0 Conclusion

In this study, we first addressed the long-standing controversy regarding the mechanism through which antihistamines block neuraxial morphine-induced itch by demonstrating that mast cells are not involved. Instead, our studies suggest that the apparent reduction in itch mediated by centrally-acting antihistamines may be secondary to their somnolescent effects. Next, we discovered that *Oprm1* expression in $Pdyn^+$ neurons is required for neuraxial morphine-induced itch and that chemogenetic inhibition of $Pdyn^+$ neurons is sufficient to cause itch. Lastly, we activated Oprk1 signaling using nalfurafine, an Oprk1 agonist, to block morphine-induced itch in mice and non-human primates. Together, these findings reveal a distinct disinhibitory neural circuit for morphine-induced itch, which might have important implications for the clinical management of this condition.

Diphenhydramine is still frequently prescribed as a first-line treatment for morphine-induced itch (Szarvas, Harmon, and Murphy 2003; Jannuzzi 2016). However, clinicians have observed that the sedating effects of antihistamines have caused patients to verbally deny itch while continuing to scratch, and that patients are itchy in between periods of sleep (Roth et al. 1987; Ballantyne, Loach, and Carr 1988; Horta et al. 2006). Histaminergic neurons in the tuberomammillary nucleus of the posterior hypothalamus are thought to promote wakefulness through their activation of H_1R, and antihistamines are thought to cause sedation through the antagonism of these receptors, which are widely distributed in the brainstem (Lin et al. 1996) and cortex (Tashiro et al. 2009; Reiner and Kamondi 1994; Thakkar 2011). Importantly, this unwanted side effect of sedation is particularly undesirable in the context of morphine-induced itch because it raises safety concerns due to the potential of antihistamines to exacerbate

respiratory depression caused by opioids (Anwari and Iqbal 2003; Jannuzzi 2016; Roth et al. 1987).

Our findings support that diphenhydramine reduces morphine-induced itch in mice, but is accompanied by a reduction in locomotor activity, consistent with the clinical observation that diphenhydramine also reduces opioid-induced pruritus and is sedating in patients. We rule out the contribution of mast cells using a mast cell depletion model. However, the possibility that opioids act on descending histamine-producing neurons to elicit itch remains an open question. It is interesting to speculate that the ability to restrict the action of an H_1R antagonist to the spinal cord (to avoid its action on supraspinal targets involved in wakefulness) may also attenuate morphine-induced itch. Future experiments that could separate the possible itch-producing and sleep-producing effects of histamine in the nervous system may help to address the role and appropriateness of using antihistamines for neuraxial opioid-induced itch.

Presently our results suggest that mast cells are not involved in opioid-induced itch. In addition, the finding that diphenhydramine only reduces scratching at a dose that also suppresses locomotor activity further underscores the concept that the use of antihistamines for neuraxial morphine-induced itch may be inappropriate.

In human, non-human primate, and mouse models, we have validated that neuraxial morphine causes itch (Waxler et al. 2005b; Jannuzzi 2016; Ganesh and Maxwell 2007; Szarvas, Harmon, and Murphy 2003; Ballantyne, Loach, and Carr 1988; Sakakihara, Imamachi, and Saito 2016; Liu et al. 2011; Ko and Husbands 2009; Lee et al. 2007; Ko 2015). Intriguingly, although neuraxial morphine elicited itch in all three species, the duration of itch in humans and non-human primates was longer than that observed in mice. This difference in duration of morphine action likely reflects species differences in a variety of factors that influence drug distribution

and half-life, including the relative expression levels of metabolic enzymes, receptor signaling, and trafficking (Yamamoto et al. 2018). Other possible explanations include the ways in which animals (such as rodents and primates) model itch compared to patients. It is possible that mice are sensitized to opioid-induced itch on a more extended timeframe, but this does not result in significant scratching behaviors compared to grooming at later timepoints. In humans, a single rating is typically reported at specific timepoints and this may not completely capture patients' experiences with itch over time. A more interesting comparison may be made using wearable devices that could quantify scratching over time in human subjects. Another possible explanation is that there may be additional, divergent mechanisms that underlie opioid-induced itch in different species. Nevertheless, the finding that nalfurafine reduces morphine-induced itch in both mice and non-human primates suggests a common underlying circuit mechanism, which may also apply to humans.

6.1 Limitations

6.1.1 The mu-opioid receptor is only expressed in a subset of spinal dynorphin neurons

One prior study identified Pdyn excitatory neurons, largely enriched in the medial third of the dorsal horn, and these neurons are presumed to innervate the glabrous skin and modulate mechanical sensitivity (Huang et al. 2018). In our experiments, we only counted the expression of the mu-opioid receptor within Pdyn neurons as a subset of the GABAergic population. Chemogenetic activation was previously found to facilitate mechanical allodynia (Huang et al. 2018), but did not affect thermal thresholds, consistent with our lack of Hargreaves findings. The

finding that chemogenetic activation of Pdyn neurons facilitates mechanical hypersensitivity (Huang et al. 2018) is consistent with the upregulation of dynorphin in models of chronic pain (Luo et al. 2008). Although we did not test animals for mechanical thresholds, in this paradigm, if excitatory Pdyn neurons involved in mechanical sensitivity contain the mu-opioid receptor, then it is plausible that morphine could also inhibit this excitatory population to produce anti-allodynic effects, consistent with its role as an analgesic. However, excitatory Pdyn neurons are unlikely to be involved in the inhibition of itch. Nevertheless, it is interesting to speculate that patients who experience chronic pain may also have elevated levels of dynorphin as well as reduced susceptibility to opioid-induced pruritus. This would be in line with the high incidence of opioid-induced pruritus in healthy patients. Examination of spinal dynorphin levels in the CSF among chronic pain and healthy patients prior to the administration of neuraxial opioid anesthesia and correlation to patients' experiences with pain and itch following neuraxial opioid anesthesia may test this idea further.

Our finding that roughly 40% of Pdyn neurons contain *Oprm1* highlights the possibility that there may exist sub-populations of Pdyn neurons. It is possible that different subsets of these Pdyn cells modulate chemical and mechanical itch as well as mechanical hypersensitivity (Huang et al. 2018). By using the Pdyn-Cre allele, our approach does not allow us to assess the contributions of distinct subpopulations within the dynorphin population; thus, our approach lacks genetic specificity. Advances in intersectional genetic strategies can allow further dissection of individual subpopulation and their contributions to itch and pain.

6.1.2 The role of Oprm1 isoforms

Although several studies have implicated differential contributions of Oprm1 isoforms in opioid-induced pruritus and analgesia (Pasternak 2004; Andoh et al. 2008; Sia et al. 2008), one limitation of our study is that the specific *Oprm1* isoform in $Pdyn^{+}$ neurons that could be responsible for morphine-induced itch was not addressed because our genetic strategy does not distinguish among splice variants. Specific knock-down studies are necessary to differentiate the contributions of specific splice variants to morphine-induced analgesia and pruritus (discussed further in the future directions).

6.1.3 Peptides and transmitters involved in opioid-induced pruritus

Another limitation is that although we found that mu-opioid signaling inhibits dynorphin neurons and although we do not yet know the degree to which this modulation involves dynorphin or GABA release from these cells, our occlusion studies raise the possibility that both may be involved. Interestingly, we found that treatment with a kappa antagonist, norBNI, in the presence of morphine resulted in an enhancement of morphine-induced itch. This implicates the role of GABA in the modulation of opioid-induced itch in mice. In any case, the finding that nalfurafine reverses morphine-induced itch suggests that neurons containing the kappa opioid receptor are the relevant target for inhibition by Pdyn neurons.

6.1.4 Other sources of dynorphin in the spinal cord

Our conditional deletion approach provided genetic specificity and permitted the selective removal of the mu-opioid receptor from dynorphin neurons. However, this approach lacks spatial specificity. Although we speculate that it is the expression of the mu-opioid receptor on inhibitory spinal neurons that make dynorphin that is required for morphine-induced itch, it is unknown what, if any, role other dynorphin neurons expressing the mu-opioid receptor may have on itch. We believe that the intrathecal administration of morphine supports the idea that spinal dynorphin neurons are important, it is possible that the drug may spread rostrally to other possible, mu-sensitive dynorphin neurons. These other targets are not likely to include the dorsal root ganglia (due to a lack of dynorphin expression in primary sensory neurons), but may include descending dynorphin neurons recently identified in the lateral pons that also inhibit itch (Agostinelli 2020). Genetic approaches that allow for the targeting of mu-expressing dynorphin neurons at different sites of the nervous system will provide more clarity on this question.

6.2 Future directions

6.2.1 Modulation of itch and pain by Oprm1 polymorphisms and splice isoforms

Sequencing of the *OPRM1* gene has revealed that certain polymorphisms may be associated with protection against the side effect of pruritus (Tsai et al. 2010; Pettini et al. 2018). For example, genetic association studies have focused on the A118G polymorphism of *OPRM1* (Tsai et al. 2010; Pettini et al. 2018). The recessive G allele in this polymorphism is associated

with lower incidences of pruritus among obstetric patients receiving epidural (4.8%) and spinal (0-50%) morphine (Tsai et al. 2010; Pettini et al. 2018). This variant is further associated with reduced sensitivity to the analgesic effects of opioids (Sia et al. 2008), suggesting that the A118G polymorphism may give rise to a mu-opioid receptor that is less responsive to opioid medications. In mice, distinct splice variants of the mu-opioid receptor, *MOR1D* and *MOR1*, have been shown to differentially modulate morphine-induced itch and morphine-induced analgesia, respectively (Liu et al. 2011).

Nearly 20 splice variants have been identified in humans, which may explain the varied effects of opioid medications on patient outcomes (Pasternak 2010). However, the contributions of these splice variants have not yet been fully characterized in humans. Additional multi-center genetic association studies are necessary to further assess the clinical contributions of genetic variations to acute postoperative pain management and its side effects. Furthermore, knockdown studies of these isoforms in preclinical models, such as in rodents, or in vitro, within specific neuronal populations could further elucidate the differential contributions of these isoforms in pruritus and analgesia. These findings could pave the way for genetic therapies that target specific receptors to improve the clinical management of both itch and pain.

6.2.2 Role of KOR neurons in itch

A similar, contemporary study found that expression of *Oprm1* in GABAergic neurons is required for opioid-induced itch in mice (Wang, Jiang, Yao, Chen, Rahman, Gu, Huh, et al. 2020). It was also found that intrathecal administration of an Npy antagonist also treated opioid-induced itch. In our experiments, we found that deletion of *Oprm1* from Npy neurons did not affect morphine induced-itch (P=0.1832, two-way ANOVA with Bonferroni's correction). We

also observed that morphine-induced alloknesis in mice lacking Oprm1 in Npy neurons was not different from saline-controls (P>0.9999, two-way ANOVA with Bonferroni's correction). Based on these findings, we propose that it is unlikely that Oprm1 in Npy neurons is contributory to morphine-induced alloknesis. This, in some ways, is a departure from previous work implicating Npy neurons in the inhibition of mechanical itch (Bourane et al. 2015; Acton et al. 2019). We propose that unlike Npy neurons, which are not presently thought to be involved in gating chemical itch, Pdyn neurons could be involved in gating both forms of itch.

In particular, from our data, we speculate that both chemical and mechanical itch following morphine exposure, as observed in humans and in mice, could arise from downstream pathways that can be modulated with a kappa-opioid receptor agonist. Our pharmacological management of spontaneous itch, alloknesis, and hyperknesis with nalfurafine suggests that mechanical and chemical itch could converge on neurons containing the kappa opioid receptor.

These results highlight the importance of defining the roles of spinal neurons containing the kappa opioid receptor (KOR) in both chemical and mechanical forms of itch. Pharmacological studies have highlighted the potential roles of KOR neurons in the modulation of pain and itch (Ko and Husbands 2009; Akiyama et al. 2015; Phan et al. 2012). They have also been proposed to overlap with an excitatory population of itch neurons containing GRPR (Munanairi et al. 2018). Thus, given the established role of dynorphin neurons in the inhibition of itch and the efficacy of kappa agonists in the management of itch, it follows that KOR spinal neurons could also function as mediators of itch. It remains unknown whether KOR-expressing spinal neurons comprise a class of interneurons, projection neurons, or both. The development of the KOR-Cre knock-in allele from our laboratory provides an opportunity to begin the investigations (Cai et al. 2016; Snyder et al. 2018). Determination of the locus of dynorphin

neurons within an itch circuit, particularly with respect to downstream neurons that express KOR, could provide a definitive explanation for how chemical itch is spinally-processed, transmitted to the brain, and capable of entering conscious perception.

7.0 Introduction to the role of the rostral ventromedial medulla in descending pain modulation

The rostral ventromedial medulla RVM constitutes one of the major bulbospinal regions that conveys information from the brainstem to the spinal cord (Liang, Watson, and Paxinos 2016; Basbaum and Fields 1984). Through a process known as descending modulation, the RVM has been shown to participate in many critical processes including nociception, arousal, thermoregulation, and feeding (Fields, Malick, and Burstein 1995; De Felice et al. 2011; Mason, Gao, and Genzen 2007; Foo and Mason 2003; Foo, Crabtree, and Mason 2010; Mason 2012).

The RVM has functionally been defined as the midline medullary structure in which electrical stimulation or opioid microinjection is sufficient to evoke behavioral antinociception (Heinricher et al. 2009). It is thought to comprise two major structures: the raphe nuclei, including raphe magnus (RMg) and the nucleus gigantocellularis, alpha (NGCα). Within these structures are diverse populations of neurons, heterogeneous in size and morphology. Furthermore, their molecular identities and functional roles remain to be fully characterized. Understanding the roles of specific RVM neurons is further complicated by the structure's importance in broad functions: from feeding, to thermosensation, nociception, and arousal. This section highlights the role of the RVM in these varied functions, examines the putative cell types involved based on pharmacological studies, and summarizes the recent findings of genetically labeled RVM cell types that have emerged from studies involving genetically-modified mice (Figure 18).

7.1 Descending modulation of pain

In the 1970s, it was discovered that stimulation of the PAG was sufficient to inhibit behavioral responses to noxious stimulation in rats (Reynolds 1969; Mayer and Liebeskind 1974; Mayer et al. 1971). This discovery was further translated and reproduced in humans, whereby neurosurgical electrical stimulation of the PAG produced clinically significant relief for pain (Hosobuchi, Adams, and Linchitz 1977; Baskin et al. 1986). Critically, stimulation of the PAG also inhibited nociceptive dorsal horn neurons, suggesting that analgesia was mediated through sensory, rather than motor, responses (Liebeskind et al. 1973; Budai, Harasawa, and Fields 1998; Peng, Lin, and Willis 1996b, 1996a).

The discovery of an endogenous system for analgesia, together with the expansion of methodology to investigate this system (including pharmacology, anatomical tract tracing, and combined electrophysiology with electrical stimulation) rapidly led to detailed knowledge of the role of the PAG in descending modulation (Millan 2002). Ultimately, it was found that the PAG does not project directly to the spinal cord (Basbaum and Fields 1979), but, instead, modulates nociception through projection projections to the RVM, which can be considered the output of the pain-modulation system (Prieto, Cannon, and Liebeskind 1983; Basbaum and Fields 1979; Gebhart 1982). Thus, the RVM produces endogenous modulation of pain at the spinal level.

The majority of research into the RVM has focused on its role in the descending modulation of pain. Although it may be enticing to ascribe the role of the RVM to an exclusively pain-modulatory hub, RVM functions are highly diverse and complex (Ma and Huang 2016). A few of its other roles are discussed in the following sections.

7.2 Circuitry of RVM neurons in descending modulation

7.2.1 Inputs to the RVM

The most well-studied region projecting to the RVM is the PAG. Lesioning and inactivation of the RVM (with local anesthetics) block the antinociceptive action of PAG (Behbehani and Fields 1979; Prieto, Cannon, and Liebeskind 1983; Gebhart 1982). Therefore, the RVM is a necessary component within the descending modulatory circuit activated by stimulation of the PAG. The PAG receives direct inputs from the hypothalamus and from the limbic system, including the frontal neocortex and several subregions of the amygdala that could pertain to nociception (Tracey and Mantyh 2007). For instance, microinjection of opioids in the basolateral amygdala (BLA) is sufficient to produce antinociception and modulates RVM ON and OFF cells in a manner similar to that seen following systemic or RVM opioid administration (McGaraughty and Heinricher 2002). Whether the effect of the BLA on RVM is direct or is mediated through the PAG as an intermediary region remains unclear (Barbaro, Heinricher, and Fields 1986; Ansah et al. 2009; Helmstetter et al. 1998). Together with these corticolimbic structures, such as the amygdala, the PAG has been implicated in the affective and cognitive aspects of pain (Millan 1999)

Currently, it is thought that the PAG also contains at least two classes of neurons that divergently modulate nociception, not unlike the ON/OFF model in the RVM. In addition to their differences in sensitivity to pharmacological agents (Moreau and Fields 1986; Carstens, Stelzer, and Zimmermann 1988; Behbehani et al. 1990), PAG neurons can also be distinguished by their transmitter. *Vgat*, or inhibitory neurons are thought to be pain facilitating, whereas *Vglut2*, or excitatory neurons are thought to be anti-nociceptive (Samineni et al. 2019, 2017; Aimone and

Gebhart 1986; Jiang and Behbehani 2001). Interestingly, unlike RVM neurons, PAG neurons appear to have modality-specificity and are differentially engaged to modulate pain and itch (Samineni et al. 2019). While there have considerable advances to the understanding of PAG circuitry, such as the discoveries that implicate a disinhibitory model by which inhibitory neurons in the PAG exert tonic inhibition over RVM-projecting, excitatory neurons (Vaughan et al. 1997; Budai and Fields 1998; Heinricher et al. 2009), how these circuits are engaged for distinct somatosensory modalities warrants further investigation.

Another midbrain structure that has also been extensively documented in relaying nociceptive information to the RVM is the PBN. The PBN is thought to be a central "alarm" nucleus, one that synchronizes information that could represent threats to the body (Han et al. 2015; Campos et al. 2018; Carter, Han, and Palmiter 2015). The PBN has also been shown to engage descending pain modulatory systems (Lapirot et al. 2009; Roeder et al. 2016). Optogenetic activation of PBN terminals in the RVM has a net effect of inhibiting OFF cells and activating ON cells, giving rise to pro-nociceptive phenotypes (Chen et al. 2017). However, it is also important to note that in addition to nociceptive information, the PBN also conveys information to the RVM pertaining to autonomic homeostasis, such as thermoregulation (Nakamura et al. 2004; Tupone, Madden, and Morrison 2014; Cano et al. 2003; Shaun F Morrison 2016). Some experiments have been able to dissociate the pain-modulating and autonomic functions of RVM neurons by using pharmacology to selectively block specific classes of neurons (Martenson, Cetas, and Heinricher 2009). However, it remains unknown how nociception and thermoregulation may be encoded at the cellular, molecular, and circuit level.

Research into the hypothalamus has emphasized its role in coordinating autonomic and sensory information, particularly in response to stress (Martenson, Cetas, and Heinricher 2009)

and sleep (Foo and Mason 2003). Further, stimulation of the lateral hypothalamus has also been shown to produce antinociception via the PAG and RVM (Aimone, Bauer, and Gebhart 1988; Dafny et al. 1996; Behbehani, Park, and Clement 1988; Cechetto and Saper 1988; Manning and Franklin 1998), which leads to the descending inhibition of pain. Considering that patients with chronic pain have poor sleep Disturbed Sleep in Patients Complaining of Chronic Pain : The Journal of Nervous and Mental Disease; Drewes et al. 1998; Mahowald et al. 1989; Gudbjörnsson et al. 1993; Drewes et al. 1994), this pathway may represent a promising candidate to help these patients.

Lastly, stimulation of the nucleus tractus solitarius (NTS) can elicit antinociception (Morgan et al. 1989; Aicher and Randich 1990; Lewis, Baldrighi, and Akil 1987) as well as the facilitation of pain through vagal stimulation (Zhuo and Gebhart 1992; Ren, Randich, and Gebhart 1991; Wiertelak et al. 1997). This bi-directional modulation of pain is thought to occur through NTS projections to the RVM (Aicher and Randich 1990; Zhuo and Gebhart 1992, 1997). In addition to these dualistic roles in the descending modulation of pain, the NTS also conveys visceral and autonomic information to the RVM (Pérez and Ruiz 1995). Further research is needed to elucidate these roles.

Although there are many other brain regions that participate in the descending modulation of pain and may exhibit connectivity with the RVM, this section emphasizes the structures that have received recent attention and highlight the role of the RVM in the integration of diverse, autonomic, sensory, and motor behaviors.

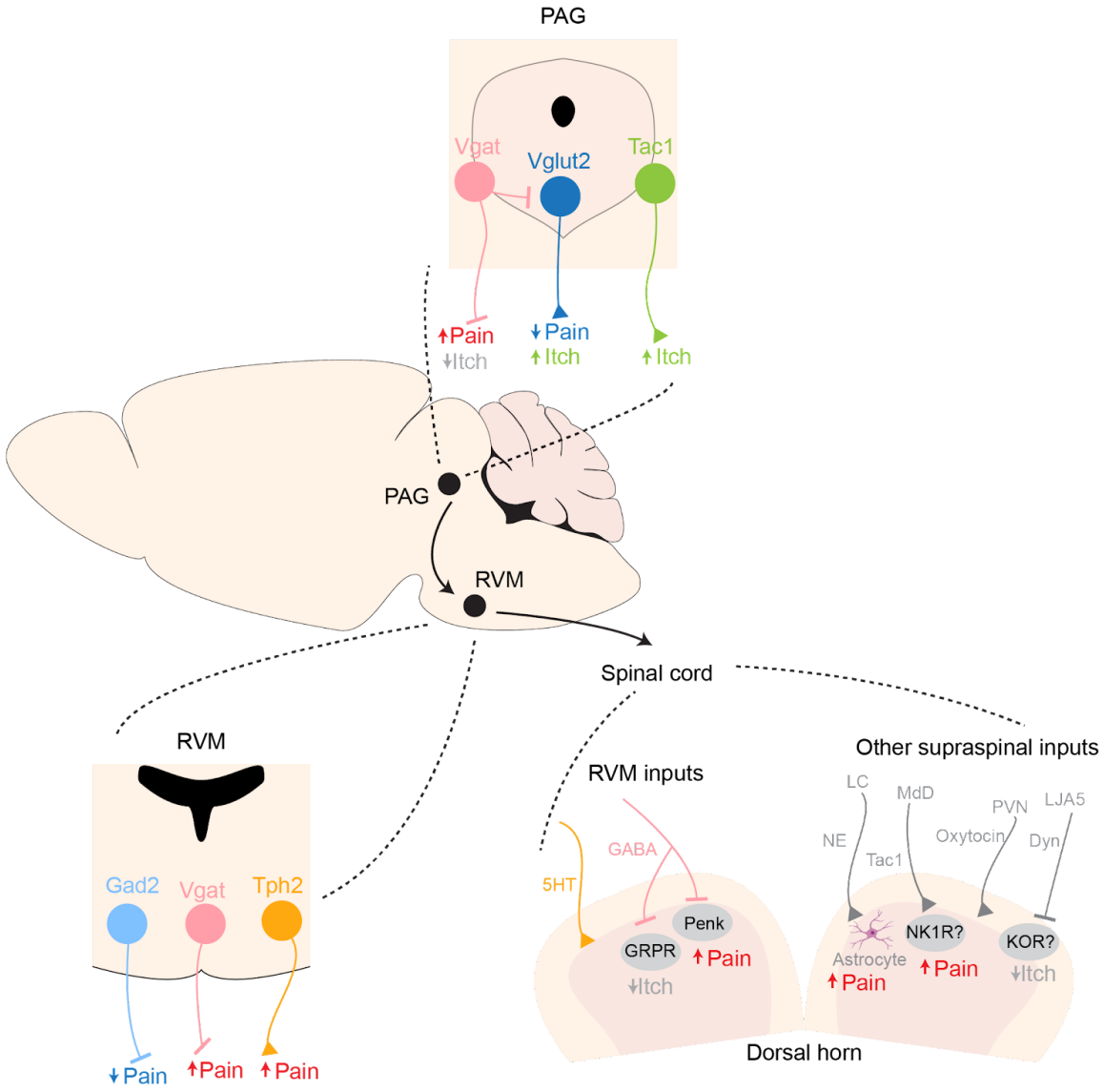

Figure 18. Nodes for descending modulation and identified cell types.

Within the canonical PAG RVM spinal pathway, distinct neuronal populations have been directly manipulated using genetic tools. These molecular populations are shown and their roles in the modulation of itch and pain are denoted. In the spinal cord dorsal horn, RVM and other supraspinal inputs that have been identified using labeled genetic drivers are detailed. PAG, periaqueductal gray; RVM, rostral ventromedial medulla; LC, locus coeruleus; MdD, medullary reticular nucleus; PVN, paraventricular nucleus of hypothalamus; LJA5, lateral pons, juxta A5; Vgat, vesicular GABA transporter; Vglut2, vesicular glutamate transporter 2; Tac1, tachykinin 1; Gad2, glutamate decarboxylase 2; Tph2, tryptophan hydroxylase 2; GRPR, gastrin releasing peptide receptor; Penk, proenkephalin; NE, norepinephrine; NK1R, neurokinin 1 receptor; Dyn, dynorphin; KOR, kappa opioid receptor.

7.2.2 RVM efferent projections

7.2.2.1 Ascending projections

Supraspinal targets of RVM projections have been observed in the brainstem (PAG, NTS, PBN) as well as the midbrain (parafascicular nucleus, lateral hypothalamus, and locus coeruleus) (François et al. 2017; Sim and Joseph 1992; Hammond, Tyce, and Yaksh 1985). It is proposed that RVM projections to the PBN and lateral hypothalamus may be involved in analgesia and hyperalgesia in the setting of acute and chronic stress, respectively (François et al. 2017). However, these efferent pathways arising from the RVM have not been tested directly with respect to pain.

7.2.2.2 Projections to the spinal cord

Input from the RVM to the dorsal horn of the spinal cord has been well-characterized (Fields, Malick, and Burstein 1995; Watkins et al. 1980). The RVM has been shown to project to superficial as well as deep laminae in the spinal cord (Fields, Malick, and Burstein 1995; Martins and Tavares 2017; Millan 2002) via the dorsolateral and ventrolateral funiculi (F Wei, Ren, and Dubner 1998; Jones and Gebhart 1987; Mokha, McMillan, and Iggo 1986; McMahon and Wall 1988).

One recent study used optogenetics to examine RVM inputs to neurons in the spinal cord (François et al. 2017). This study found that GABAergic projections from the RVM provided pro-nociceptive input to enkephalinergic (Penk) neurons in the dorsal horn and that these Penk neurons presynaptically inhibit mechanosensory neurons, thereby reducing mechanical pain (François et al. 2017). The contributions of other RVM neurons, such as the excitatory ones, to

dorsal horn circuits remain unknown. Nevertheless, advances in molecular approaches (François et al. 2017) present exciting opportunities to uncover the complexity of top-down modulation.

There exists a precedent for the direct innervation of primary sensory neurons by the RVM. Inoculation of the DRG with a retrograde virus has resulted in labeling in the RVM, suggesting that RVM neurons could project to primary afferents (Zhang et al. 2015). Axo-axonic synapses between inhibitory RVM to DRG neurons are proposed to modulate heat, but not mechanical pain (Zhang et al. 2015). However, these same inhibitory (Gad2) RVM neurons also project extensively to the dorsal horn, and experiments have not been conducted to differentiate between the contributions of RVM neurons that project directly to spinal neurons or to DRG inputs into spinal neurons. Furthermore, electron microscopy of RVM-spinally projecting neurons have previously revealed that RVM contacts to the dorsal horn are largely axo-somatic in nature (Aicher et al. 2012). Given the paucity of further literature that supports a direct projection from the RVM to primary afferents, it is likely that the labeling detected in the RVM with DRG infection may be nonspecific and that observed behavioral phenotypes are a result of the RVM influence over dorsal horn neurons.

7.2.3 Differential modulation of dermatomal segments by the RVM

The question as to whether somatotopic organization exists within the RVM with respect to descending modulation remains an open one. Previous studies have reported variations in descending modulation between spinally-innervated lumbar segments, and uncovered differential modulation to heat to the tail and foot (Fang and Proudfit 1996). Furthermore, another study in an inflammatory model found that RVM inactivation completely blocked allodynia to the face, but not plantar hind paw (Edelmayer et al. 2009). Recordings of RVM neurons has revealed that

different proportions of ON, OFF, and NEUTRAL cells respond to noxious stimuli directed to different parts of the body, such as pinching of the hind paw, facial skin, intra-TMJ injection of ATP, and capsaicin to the ocular surface (Khasabov et al. 2015). RVM projections to the dorsal horn have also been shown to be more likely to contain GAD67 than those to the trigeminal dorsal horn (Aicher et al. 2012). Given the precedent for divergent modulation of different body parts by the RVM, further studies are necessary to consistently examine the roles of RVM neurons at modulating pain at different dermatomal segments.

7.2.4 RVM interneurons

In addition to ascending and descending projections, RVM neurons have also been shown to participate in local microcircuits (Millan 2002). For example, infusions of KOR agonists into the RVM have uncovered that in addition to the ON and OFF classification scheme (discussed further in the next section), RVM neurons can also be classified as primary and secondary cells (Pan, Tershner, and Fields 1997). In this model, primary cells function similarly to OFF cells, are inhibited by KOR agonists, and receive inhibition from secondary (ON) cells. The ability of primary cells to inhibit spinal pain transmission occurs when they are disinhibited by mu-opioid receptor inhibition of secondary cells (Pan, Tershner, and Fields 1997). This model highlights an opposing relationship between mu- and kappa-opioid receptors in the RVM. In other areas of the CNS, a disruption between mu and kappa signaling has been implicated in pathophysiological processes such as addiction, emotion, and itch (Pfeiffer et al. 1986; Hooke, He, and Lee 1995; Bolanos et al. 1996; Ko 2015). Thus, it is possible that an imbalance in opioidergic signaling within the RVM could also underlie pain.

7.3 Characterizations of RVM neurons

Single unit recordings within the RVM in lightly anesthetized rats have provided significant insight into three types of neurons in the RVM: ON, OFF, NEUTRAL neurons based on their firing activity and responses to noxious stimulation (Fields, Malick, and Burstein 1995; Heinricher et al. 2009; Mason, Gao, and Genzen 2007). ON cells are active during noxious stimulation, inhibited by morphine and proposed to facilitate nociception, whereas OFF cells are inactive or exhibit silent ongoing activity during noxious stimulation, are excited by morphine, and are thought to inhibit nociception (Cleary, Neubert, and Heinricher 2008; Heinricher et al. 2009; Mason 2012; Zhuo and Gebhart 1997). NEUTRAL cells are unaffected by noxious cutaneous stimuli or by exogenous opioids, and their role in nociception is unclear, although they are generally thought to be largely serotonergic (Potrebic, Fields, and Mason 1994) and are believed to participate in autonomic and homeostatic functions (Mason, Gao, and Genzen 2007; Hellman et al. 2009; Foo and Mason 2003; Foo, Crabtree, and Mason 2010; Foo and Mason 2005).

Another proposed model by which to classify RVM neurons has been achieved by assigning them as “primary” or “secondary” cells based on their responsiveness to opioid agonists and roles in the descending modulation of nociception. Under this schema, primary cells are anti-nociceptive and secondary cells are pro-nociceptive. Primary cells are tonically inhibited by secondary cells, but this inhibition is relieved in the presence of mu agonists (Pan, Tershner, and Fields 1997). Primary cells are proposed to be directly inhibited by kappa agonists, but disinhibited by mu agonists (Pan, Tershner, and Fields 1997; Pan, Williams, and Osborne 1990; Pan, Hirakawa, and Fields 2000). However, it is important to note that the sensitivity of RVM neurons to kappa agonists remains contested. Other studies have found that kappa agonists

inhibit excitatory input onto secondary cells as well as produce outward currents in primary cells (Ackley et al. 2001; Meng et al. 2005). Still, the net behavioral effect was antinociception -- freely-behaving rats exhibited elevated withdrawal latencies to Hargreaves' and hot plate tests (Ackley et al. 2001). Although differences in the experimental design, such as performing recordings in anesthetized animals but conducting behavioral assays in freely-behaving ones may underlie these discrepancies, it is more likely that kappa and mu receptors are co-expressed in some neurons (Gutstein et al. 1998), making it challenging to classify RVM neurons as simply primary or secondary cells by this classification scheme.

In addition to opioid agonists, other pharmacological agents have also been infused into the RVM. The results from these pharmacological studies, in combination with neurochemical approaches have also identified putative cell types within the RVM. Based on these studies, a few of these cell types are discussed here:

Tachykinin receptor-1 (NK1R) neurons

Neurons in the RVM containing NK1R are thought to respond to substance P release from Tac1 neurons in the PAG (Lagraize et al. 2010) and have pro-nociceptive effects. Microinjection of NK1R antagonists in the RVM can inhibit and attenuate hypersensitivity to heat and mechanical stimuli following inflammatory injury (Lagraize et al. 2010; Hamity, White, and Hammond 2010; Pacharinsak et al. 2008). Furthermore, pharmacological ablation of NK1R RVM neurons reduces hyperalgesia in both acute and chronic pain models (Khasabov and Simone 2013). More recently, PAG Tac1 neurons have also been shown to facilitate itch (Gao et al. 2019). Neurochemically, NK1R neurons comprise roughly 8% of neurons in the RVM and a proportion of them have been found to overlap with 5HT and Gad67 (Chen et al. 2013). Furthermore, only the Gad67+, NK1R+ neurons are thought to be spinally projecting (Chen et al.

2013). This suggests there are at least two neurochemically distinct NK1R subtypes, but whether they are both pro-nociceptive is unclear.

Neurotensin-R (NTR1) neurons

Neurotensin produces persistent antinociceptive effects in the tail-flick assay following infusion into the RVM (Fang, Moreau, and Fields 1987). NTR1 is expressed by spinally projecting 5HT neurons (Wang et al. 2014) in the RVM and contributes to the descending inhibitory modulation of neurotensin-induced antinociception (Buhler et al. 2005). Interestingly, infusion of high doses of neurotensin into the RVM can evoke anti-nociception, but small doses produce pro-nociception (Urban and Smith 1993, 1994). These opposing actions may be due to the differential expression of the neurotensin receptor in the RVM. Indeed, NTR-2 has also been implicated in mediating the anti-nociceptive effects of neurotensin (Buhler et al. 2005), and 80% of NTR-2 expressing neurons also express NTR-1 (Buhler et al. 2005), further highlighting the diversity of subtypes in the RVM.

Serotonergic (5HT) neurons

The contribution of serotonergic neurons is highly disputed. It was previously thought that serotonergic neurons comprise NEUTRAL cells (Potrebic, Fields, and Mason 1994), engage in autonomic responses (Mason, Gao, and Genzen 2007; Hellman et al. 2009; Foo and Mason 2003; Foo, Crabtree, and Mason 2010; Foo and Mason 2005), or participate in the inhibition of pain when the NTR1 subpopulation is targeted (Buhler et al. 2005), but recent studies suggest they may also be pronociceptive (Cai et al. 2014; Kim et al. 2014; Wei et al. 2010). In addition to this emerging view of 5HT neurons as pain-facilitatory, depletion of serotonin in the RVM has been shown to also be anti-pruritic (Wei et al. 2010). Neurochemical characterizations of serotonergic neurons have revealed their overlap with many other markers including NK1R

(Chen et al. 2013), MOR (Cai et al. 2014), Gad67 (Cai et al. 2014; Wei et al. 2010), and NTR1 (Buhler et al. 2005). Given the highly diverse roles of serotonergic neurons and their heterogeneity, it is clear that serotonin does not label a specific and molecularly distinct RVM population.

Inhibitory (GABAergic) neurons

Expression of the mu opioid receptor (*Oprm1*), which is thought to be a marker for ON or secondary cells (H. Fields 2004), is found in inhibitory GABAergic neurons (François et al. 2017). In one study, selective activation of *Vgat* neurons was found to be allodynic (François et al. 2017). However, in another, Gad2 neurons, which comprise a subpopulation of GABAergic neurons, were found to be important for suppressing heat and mechanical pain (Zhang et al. 2015). Further complicating the classification of these neurons is the expression of Gad1 (Gad67) in kappa opioid receptor-expressing (OFF) and NEUTRAL cells (Winkler et al. 2006). Thus, similar to serotonergic neurons, GABA is found in many RVM neuronal subtypes, making it challenging to ascribe a specific role to RVM neurons based solely on their expression of this marker.

Excitatory (glutamatergic) neurons

Although most spinally-projecting RVM neurons are GABAergic (Aicher et al. 2012; François et al. 2017; Y. Zhang et al. 2015; Millhorn et al. 1987), and it remains unclear what role, if any, the sparsely labeled glutamatergic neurons may have in descending modulation (François et al. 2017). Whether glutamatergic RVM neurons participate in cortical, local, or in descending spinal circuits also remains unknown.

Cholecystokinin receptor

The neuropeptide cholecystokinin (CCK), arising from CCK-expressing neurons in the dorsomedial hypothalamus is thought to act in the RVM to enhance nociception (Wagner et al. 2013). It is proposed that this is one pathway by which chronic stress can lead to hyperalgesia (Wagner et al. 2013). Indeed, several pharmacological studies have shown that CCK infusion into the RVM can activate the descending pain facilitatory system (Xie et al. 2005; Heinricher and Neubert 2004; Zhang et al. 2009; Heinricher, McGaraughty, and Tortorici 2001). CCK produces its pro-nociceptive actions at CCK2, Gαs-coupled receptors in the RVM (Ghilardi et al. 1992; Zhang et al. 2009; Xie et al. 2005). Conversely, CCK antagonists can augment the antinociceptive effects of opioid administration (Faris et al. 1983; Dourish et al. 1990). Lastly, CCK2 receptors are expressed on neurons with mu opioid receptors, further implicating that they may be on pro-nociceptive cells (Zhang et al. 2009).

Nitric oxide synthase (nNOS) neurons

The role of neurons that produce nitric oxide in the RVM is presently thought to be important for antinociception, based on studies that have inhibited the NO synthase enzyme (Ohgami et al. 2009). Nos1 neurons have been shown to overlap with Gad67 (Buhler et al. 2018) and possibly 5HT (Lu et al. 2010), though this is debated (Buhler et al. 2018). Interestingly, however, nNOS neurons are not spinally-projecting and are thought to instead mediate their antinociceptive effects through local RVM circuits or to cortical and subcortical areas (Buhler et al. 2018; Lu et al. 2010).

Given the extensive overlap among various markers, the neurochemical identities for pro- and anti- nociceptive RVM cells remain unclear. Advances in sequencing, neurochemical, tracing, and behavioral methods may one day elucidate and define specific RVM cell types.

7.4 Manipulations of cell types using mouse genetics

Recent advances in molecular techniques have enabled researchers to use genetically-modified mouse lines to target unique subsets of RVM neurons expressing specific receptors and molecular markers. These studies allow for genetic manipulations of distinct subpopulations of neurons for targeted anatomical, molecular, and functional dissection.

Still, one limitation of these manipulations is that while researchers may have tight control over neurons based on their expression of a particular marker, conclusions made from the targeting of individual alleles ignores the heterogeneity within the RVM. For example, expression of the mu opioid receptor (*Oprm1*), which is thought to be a marker for ON cells (H. Fields 2004), is found in inhibitory neurons. In one study, *Vgat* neurons were found to facilitate mechanical hypersensitivity (François et al. 2017). However, in another study, *Gad2* neurons, which comprise a subpopulation of *Vgat* neurons, were found to be important for suppressing thermal and mechanical nociception (Zhang et al. 2015).

Furthermore, it has been widely presumed that serotonergic neurons are NEUTRAL cells, but when neurons containing *Tph*, the enzyme necessary for serotonin synthesis, were optogenetically manipulated, they were found to drive mechanical and thermal hypersensitivity (Cai et al. 2014). It is interesting to note that serotonergic neurons have previously been shown to co-express *Oprm1* (Marinelli et al. 2002; Wang and Wessendorf 1999), an indication that there may be some overlap between putative ON and NEUTRAL cells. One may be able to speculate that the global activation of *Tph* neurons exerts a dominant effect over the NEUTRAL phenotype, which gives rise to a pro-nociceptive one (Cai et al. 2014). Another possibility is that the genetic tool, the Tph-Cre allele, may not capture 5HT-expressing neurons in the adult mouse with high fidelity which may explain discordant findings from single unit recordings of

classically-defined NEUTRAL cells. Reconciling these studies that have directly manipulated RVM neurons using individual alleles, it is likely that a reasonable population of *Oprm1+*, *Vgat+* neurons are pro-nociceptive (François et al. 2017), and that not all inhibitory neurons in the RVM are pro-nociceptive (Zhang et al. 2015). The role of serotonergic, GABA-expressing neurons that do not contain the mu-opioid receptor still remains unclear.

In addition to the molecular complexity in the RVM illuminated by these discoveries, it is interesting that Cre-dependent manipulations of these neuronal populations gave rise to specificity with respect to modality (such as the finding that *Vgat* and *Gad2* neurons are important for mechanical and heat pain, respectively) (François et al. 2017; Zhang et al. 2015). These results contrast with single unit recordings of RVM neurons, which have shown their responsiveness to different sensory stimuli - from itch to innocuous and noxious mechanical and thermal stimuli (Follansbee et al. 2018; Young and Dawson 1987; Fields and Anderson 1978). The variety of stimuli that can elicit a response in an individual RVM neuron suggests that these cells may not be tuned to the processing of distinct modalities of sensory input. Additional work is needed, and recordings in freely-behaving mice with genetic manipulations could someday clarify this discrepancy.

Thus, while it is possible to use genetic tools to discern unique properties among neurons within a subset, it is important to consider that they may not represent truly unique populations *per se*. Advances in molecular techniques, such as the ability to use intersectional recombinant strategies, through viral delivery or genetic breeding (François et al. 2017; Plummer et al. 2015), will permit access to neurons expressing multiple markers and will provide further, important insight into RVM function.

7.5 The role of the RVM beyond descending modulation of pain

7.5.1 Thermoregulation

The rRPA, which constitutes more rostral segments of the RMg, has been consistently targeted following retrograde tracing of brown adipose tissue using pseudorabies virus and analysis of tissue samples at short time points following inoculation (Cano et al. 2003; Yoshida et al. 2003, 2002). Through this approach, experimenters have highlighted a connection between the rRPA and sympathetic preganglionic neurons in the intermediolateral cell column (IML). In addition to the labeling observed in the rRPA following infection of the IML and BAT, viral retrograde labeling of cardiac as well as skeletal muscle result in dense labeling of the rRPA (Ter Horst et al. 1996; Kerman et al. 2003). Changes in heart rate, heart contractility, and muscle contractions (such as shivering) that promote thermogenesis may also be mediated by the rRPA, implicating its diverse and important roles on several aspects of the sympathetic response to generate heat.

Other lines of evidence highlighting the crucial role of the rRPA on thermogenesis include fos induction studies and microinjections of pharmacologic agents into this region. In the studies involving viral retrograde labeling of BAT, fos, an immediate early gene used to infer neuronal activity, localized with BAT-innervating rRPA neurons following cold exposure (Cano et al. 2003).

Physiologically, microinjections of bicuculline into the rRPA, which leads to blockade of GABA-A receptors, caused significant increases in BAT thermogenesis (Morrison, Sved, and Passerin 1999; Cao and Morrison 2003). This would suggest that the rRPA could promote thermogenesis under conditions of disinhibition. Conversely, microinjections of glycine into the

rRPA profoundly reversed BAT thermogenesis, heart rate, metabolism, resulting in dramatic reductions in heat production (Nakamura et al. 2004; Cao and Morrison 2003; Zaretsky, Zaretskaia, and DiMicco 2003; Zaretsky et al. 2006). Given its role as the primary bulbospinal pathway from the brain to sympathetic preganglionic neurons, the rRPA is, thus, critically important for the regulation of thermogenesis. Still the lack of specificity of infusing bicuculline or glycine, which may affect fibers of passage, as well as act on undetermined local circuits within the rRPA highlights the further investigation necessary to determine the role of inhibition in rRPA-mediated thermogenesis.

7.5.2 Behavioral arousal, wakefulness, and sexual climax

Neurons within the reticular formation, which shares overlapping boundaries with the RVM, participate in the reticular activating system (RAS), an ascending arousal system that is involved with regulating wakefulness, arousal, and sleep (Arguinchona and Tadi 2020; de Lecea, Carter, and Adamantidis 2012; Scammell, Arrigoni, and Lipton 2017). The reticular formation comprises many regions and nuclei and the specific role of the structures that are confined to the boundaries of the RVM have begun to be explored (Moruzzi and Magoun 1949; Satpute et al. 2019; S. Gao et al. 2019). One recent study found that optogenetic stimulation or pharmacological disinhibition of neurons in the NGCa was sufficient to elicit autonomic, cortical, and behavioral arousal in mice and rats under deep anesthesia (Gao et al. 2019). Similarly, in another study, chemogenetic activation of the medullary neurons evoked wakefulness and reduced REM sleep (Chen et al. 2017). Conversely, optogenetic activation of Vgat-expressing (GABAergic) neurons produced opposite findings to the global, chemogenetic activation of all neurons; selective stimulation of inhibitory neurons induced REM sleep episodes

and prolonged their durations (Weber et al. 2015). It was also found that optogenetic inhibition of the inhibitory neurons produced behaviors consistent with wakefulness (Weber et al. 2015). These reports suggest that there are at least two types of neurons that bi-directionally modulate wakefulness, not unlike the ON/OFF/NEUTRAL model for the descending modulation of pain.

Indeed, a considerable amount of work has been conducted to examine how the RVM could contribute to the state-dependence of somatosensation, including nociception (Mason 2001; Mason, Gao, and Genzen 2007; Mason et al. 2001; Leung and Mason 1999; Foo and Mason 2003; Hellman and Mason 2012). Recordings from OFF cells revealed that they are tonically active during SWS and intermittently active during waking, but ON cells show bursts of activity during waking and exhibit low activity during SWS (Foo, Crabtree, and Mason 2010; Hellman and Mason 2012). Interestingly, however, although arousal to aversive stimuli are dampened during sleep (Foo, Crabtree, and Mason 2010), reflexive responses to noxious stimuli are similar in magnitude during both waking and sleep (Mason et al. 2001). Recordings from serotonergic neurons in cats within the RMg revealed a correlation between their discharge rates and wakefulness - highest rates were observed during active waking, whereas the neurons were nearly silent during REM sleep (Fornal, Auerbach, and Jacobs 1985). Based on the differential firing pattern of 5HT neurons at different stages of wakefulness, it has been proposed that ON/OFF cells augment and inhibit alertness to painful stimuli, respectively, and that NEUTRAL cells may modulate reflexive responses to these painful stimuli (Foo and Mason 2003).

Furthermore, there is evidence for the role of the RVM in coordination of complex arousal states such as feeding and sexual climax. The activity of ON/OFF neurons in the context of feeding appears to parallel their activity during wakefulness; during feeding, ON cells are quiet and OFF cells are excited. Although feeding reduced animals' responses to painful stimuli,

priming animals with an innocuous air puff suppressed feeding behavior and facilitated nocifensive responses to noxious stimuli (Foo and Mason 2005). Similar findings were reproduced when the RVM was inactivated with muscimol, suggesting that RVM neurons suppress responses to painful stimuli during feeding (Foo and Mason 2005).

In the context of sexual climax, pseudorabies viral injections into the penis label serotonergic neurons in the RVM (Marson and McKenna 1996; Marson, Platt, and McKenna 1993). Furthermore, it has been shown that intrathecal administration of a serotonin neurotoxin can lead to a disinhibition of the urethrogenital reflex. Conversely, intrathecal serotonin raises the threshold needed to evoke an urethrogenital reflex (Marson and McKenna 1992). Thus, there is evidence for the role of serotonergic neurons in the RVM to contribute to the modulation of sexual climax, but this connection needs to be tested directly.

7.5.3 RVM and motor control

There is evidence that neurons in the RVM participate in somatic motor control, but given the broad functions of the RVM, it seems unlikely that a specific role for these neurons in motor control will emerge. In a tract-tracing study, researchers found that inoculation of shoulder and arm muscles with pseudorabies virus led to the detection of labeling in the ventral raphe nuclei, the NGCα, and reticular formation (Rubelowski et al. 2013). When brain tissues are collected at earlier time points, labeling in the RVM is not detected, and signal is detectable only in the superior colliculus (Rubelowski et al. 2013). Stimulation of the superior colliculus has been shown to be sufficient for voluntary motor control (Stuphorn, Bauswein, and Hoffmann 2000; Werner, Dannenberg, and Hoffmann 1997; Werner 1993). These findings suggest that RVM neurons may innervate neurons in the superior colliculus to modulate motor activity within

arm and shoulder muscles. Given that RVM neurons are situated to coordinate autonomic motor activity, it is conceivable they may also modulate axial motor functions to properly maintain and harmonize sensory, motor, and homeostatic control critical for survival. Currently, these findings are, at best, correlative. With the labeling approach used, it is difficult to determine whether these projections are motor-specific because all neurons that innervate the superior colliculus are labeled. Still, functional studies to directly test the contribution of RVM neurons are necessary.

A group of excitatory neurons within the gigantocellular nucleus, defined by their expression of Chx10 (named V2a neurons) have been shown to be involved in the inhibition of ongoing locomotion (Bouvier et al. 2015). Optogenetic activation of these glutamatergic neurons was sufficient to arrest ongoing motor activity. Interestingly, mini-endoscopic imaging of V2a neurons in freely-behaving mice uncovered that although many of these neurons are active during locomotion arrest, several are activated by other movements, such as grooming (Schwenkgrub et al. 2020). This suggests that much like the ON/OFF cell model for nociception, there also exists distinct subsets of V2a neurons that could be differentially engaged for diverse motor behaviors. Given that RVM neurons are situated to coordinate autonomic motor activity, it is conceivable they may also modulate axial motor functions to properly maintain and harmonize sensory, motor, and homeostatic control critical for survival.

These diverse sensory, autonomic, and homeostatic roles of the RVM underscore its myriad contributions to integrating and coordinating ascending and descending pathways crucial for survival. The functions described are by no means exhaustive, but provide an overview on the scope of research that has been conducted to elucidate RVM functions (Figure 19.

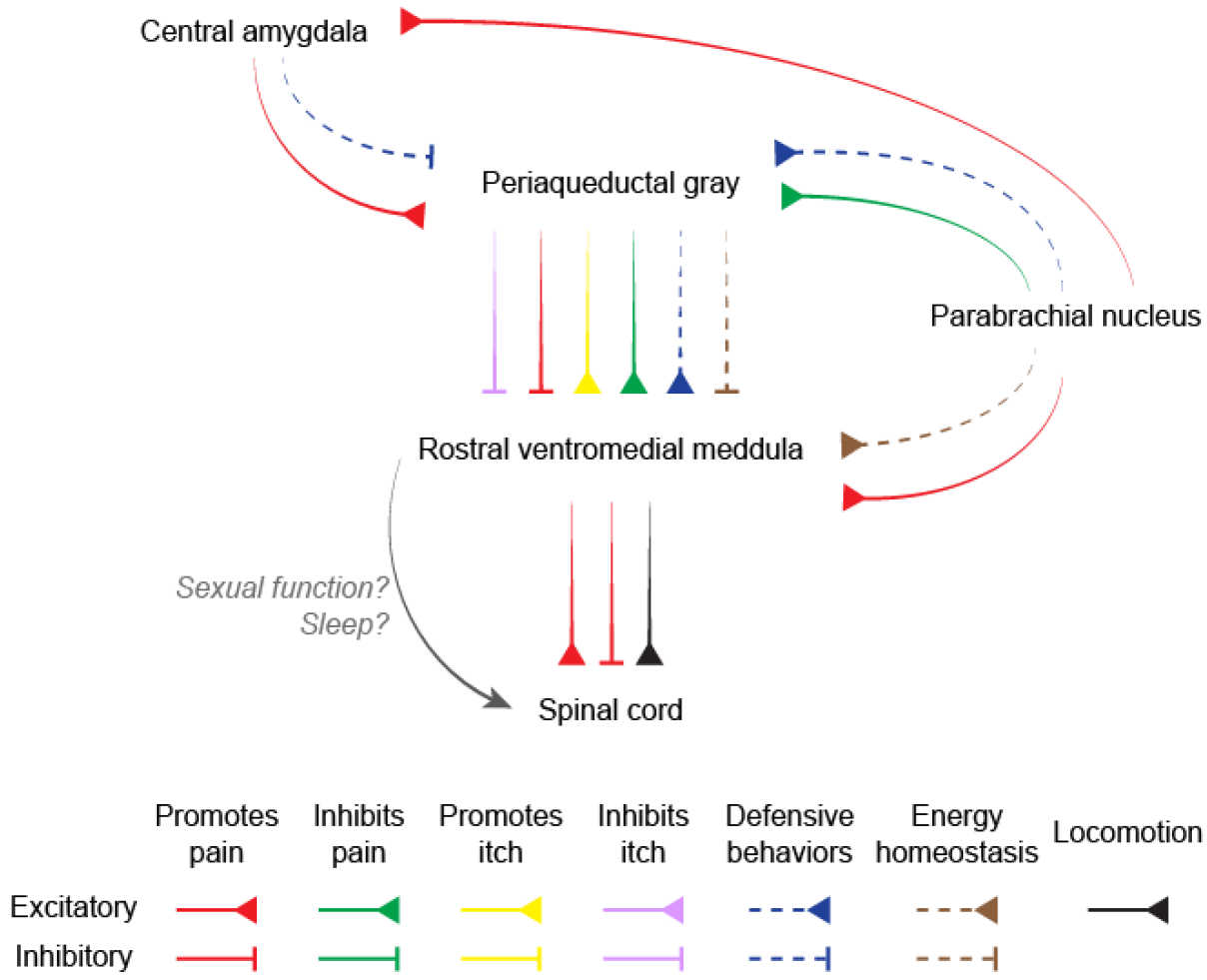

Figure 19. Descending circuits for diverse functions.

The regions discussed in this review have primarily been thought to be important for nociception. However, these structures modulate diverse homeostatic, motor, and defensive functions. A few excitatory and inhibitory pathways are illustrated.

7.6 Summary

This section examines the role of the RVM as a conduit between the brain and spinal cord and focuses on its powerful control over the descending modulation of pain. Given the myriad roles of the RVM and the heterogeneity of cell types within it, it has been a challenge to precisely define the molecules, cells, and circuits that participate in specific aspects of descending modulation. Although the evidence for the bidirectional role of the RVM in descending modulation has been reproduced across numerous studies, the identities of the pro- and anti-nociceptive cells remain elusive. The use of optogenetics and chemogenetics, combined with advances in molecular techniques such as sequencing and intersectional strategies, will continue to develop a more comprehensive and precise study of the integrative role and the specificity of the intricate circuits of the RVM.

8.0 Identification of RVM populations involved in descending modulation

8.1 Introduction

The brain exerts powerful control over nociceptive processing at the level of the spinal cord. This occurs through a process known as the descending modulation of pain (Liang, Watson, and Paxinos 2016; Basbaum and Fields 1984). Critically, the rostral ventromedial medulla (RVM), represents the final common node within the brain that directly modulates the activity of spinal neurons involved in pain transmission (Heinricher et al. 2009). Placebo and stress can alter the perception of pain through the descending endogenous opioidergic and adrenergic pain modulatory system, centered upon the RVM (Eippert et al. 2009; Shamsizadeh et al. 2014; Wiedenmayer and Barr 2000; Bellgowan and Helmstetter 1998; Pertovaara 2006). Elucidating how neurons within the RVM can modulate pain presents unique opportunities to harness the brain's natural pain-inhibitory system to potentially treat chronic pain disorders, which can avoid the unwanted and deadly side effects of existing pharmacological approaches.

Through extensive pharmacological studies involving microinjection of various agents into the RVM, which comprises the nucleus raphe magnus and gigantocellularis, pars alpha (Heinricher et al. 2009), several interesting neuronal cell types have been implicated in the descending modulation of pain. Single unit recordings within the RVM in lightly anesthetized rats have provided significant insight into three types of neurons in the RVM: ON, OFF, NEUTRAL neurons based on their firing activity and responses to noxious stimulation (Fields, Malick, and Burstein 1995; Heinricher et al. 2009; Mason, Gao, and Genzen 2007). ON cells are active during noxious stimulation, inhibited by morphine and proposed to facilitate nociception,

whereas OFF cells are inactive or exhibit silent ongoing activity during noxious stimulation, are excited by morphine, and are thought to inhibit nociception (Cleary, Neubert, and Heinricher 2008; Heinricher et al. 2009; Mason 2012; Zhuo and Gebhart 1997). However, until recently, there lacked molecular tools with which to directly manipulate these unique cell types and assess their contributions to pain behaviors in vivo.

Previous work has highlighted the existence of OFF neurons in the RVM that robustly inhibit pain (Cleary, Neubert, and Heinricher 2008; Heinricher et al. 2009; Mason 2012; Zhuo and Gebhart 1997) yet distinct cell types have not been identified due to technical challenges that precluded experimentation in awake, freely behaving animals. To discover OFF cells, we acquired Cre lines to test the serotonin (Fev), Gad65 (Gad2), nNOS, tachykinin 1 (Tac1) and kappa opioid receptor (KOR) populations. Immunohistochemical, pharmacologic, electrophysiological, and behavioral studies have implicated that these neurons could participate in the descending modulation of pain (Cai et al. 2014; Kim et al. 2014; Wei et al. 2010; Zhang et al. 2015; François et al. 2017; Buhler et al. 2018; Lu et al. 2010; Maduka et al. 2016; Pan, Tershner, and Fields 1997; Pan, Williams, and Osborne 1990; Pan, Hirakawa, and Fields 2000).

8.2 Methods

Mice

The studies were performed in both male and female mice 8-10 weeks of age. All animals were of the C57Bl/6 background. Fev-Cre (Jax #012712), Gad2-Cre (Jax #010802), Nos1-Cre (Jax #014541), Tac1-Cre (Jax #021877), and KOR-Cre mice were used. Even numbers of male and female mice were used for all experiments. Mice were given free access to food and water

and housed under standard laboratory conditions. The use of animals was approved by the Institutional Animal Care and Use Committee of the University of Pittsburgh.

Pharmacologic agents

Clozapine-N-oxide (Tocris) was dissolved in PBS and administered intraperitoneally (5mg/kg). Chloroquine diphosphate salt (Sigma) was dissolved in physiological saline (100μg in 10μL) and administered intradermally.

Intradermal injections

For intradermal injection of chloroquine, hair was removed at least 24 hours before the experiment. Chloroquine (100μg in 10μL) was administered into the nape of the neck or calf, which could be subsequently visualized by the formation of a small bubble under the skin. These procedures were performed in awake mice.

Stereotaxic injections

Animals were anesthetized with 2% isoflurane and placed in a stereotaxic head frame. A drill bit (MA Ford, #87) was used to create a burr hole and custom-made metal needle (33 gauge) loaded with virus was subsequently inserted through the hole to the injection site. Virus was infused at a rate of 100nL/min using a Hamilton syringe with a microsyringe pump (World Precision Instruments). Mice received 250-500 nL of virus (AAV2.hSyn.DIO.mCherry Addgene #50459; AAV2.hSyn.DIO.hM3D(Gq)-mCherry, Addgene #44361). The injection needle was left in place for an additional 15 min and then slowly withdrawn over another 15 min. Injections were performed at the following coordinates for each brain region: RVM: AP -5.80 mm, ML 0.00 mm, DV -6.00. The incision was closed using Vetbond and animals were given ketofen (IP 10 mg/kg) and allowed to recover over a heat pad. Mice were given 4 weeks to recover prior to experimentation.

Behavior

All assays were performed in the Pittsburgh Phenotyping Core and scored by an experimenter blind to treatment.

Observation of scratching behavior

All tests were performed in a blinded manner. Scratching behavior was observed using a previously reported method (Kardon et al. 2014). On the testing day, the mice were individually placed in the observation cage (12x9x14 cm) to permit acclimation for 30 minutes. Scratching behavior was videotaped for 30 minutes after administration of chloroquine. The temporal and total numbers of scratch bouts by the hind paws at various body sites during the first 30 minutes after intrathecal injection were counted.

Hargreaves testing

Animals were acclimated on a glass plate held at 30°C (Model 390 Series 8, IITC Life Science Inc.). A radiant heat source was applied to the hindpaw and latency to paw withdrawal was recorded (Hargreaves et al. 1988). 2 trials were conducted on each paw, with at least 5 min between testing the opposite paw and at least 10 min between testing the same paw. To avoid tissue damage, a cut off latency of 20 sec was set. Values from both paws were averaged to determine withdrawal latency.

Von Frey testing

Mechanical sensitivity was measured using the Chaplan up-down method of the von Frey test (Chaplan et al. 1994). Calibrated von Frey filaments (North Coast Medical Inc.) were applied to the plantar surface of the hindpaw. Lifting, shaking, and licking were scored as positive responses to von Frey stimulation. Average responses were obtained from each hindpaw, with 3 min between trials on opposite paws, and 5 min between trials on the same paw.

Cold plantar assay

Paw withdrawal to cold sensitivity was measured as previously described (Brenner et al. 2015; Brenner, Golden, and Gereau 2012). Briefly, animals were acclimated to a 1/4" glass plate and crushed dry ice was packed into a modified 3 mL syringe and used as a probe. The dry ice probe was applied to the glass beneath the plantar hindpaw and the latency to withdrawal was recorded. Two trials were conducted on each hindpaw, with 3 min between trials on opposite paws, and 5 min between trials on the same paw. A cut off latency of 20 s was used to prevent tissue damage. Withdrawal latencies for each paw were determined by averaging values across 2 trials per paw.

Tail immersion test

Mice were habituated to mice restraints 15 minutes for 3 days before testing. Tails were immersed 3 cm into a water bath at 48°C, and the latency to tail flick was measured three times with a 1 minute interval between trials.

Rotarod

Coordination and balance were determined using an accelerating rotarod. A session involving 120 s on a non-accelerating rotarod was prior to experimentation. Five consecutive trials were performed while the rotarod accelerated from 4 to 40 rpm in 30 s increments. The latency to fall off (s) was recorded for each trial.

Open field activity

Spontaneous activity in the open field was conducted over 30 minutes in an automated Versamax Legacy open field apparatus for mice (Omnitech Electronics Incorporated, Columbus, OH). Distance traveled (s), ambulatory average velocity (cm/s), and ambulatory time (s) were measured by infrared photobeams located around the perimeter of the arenas interfaced to a

computer running Fusion v.6 for Versamax software (Omnitech Electronics Incorporated) which monitored the location and activity of the mouse during testing. Activity plots were generated using the Fusion Locomotor Activity Plotter analyses module (Omnitech Electronics Incorporated). Mice were placed into the open field 30 post CNO injection. For all tests, mice were transferred to the testing room one hour prior to testing.

Acoustic startle

Prepulse inhibition of acoustic startle was measured by placing mice into a soundproof chamber (Kinder Scientific Startle Monitor). After 5 min of white noise acclimation, mice were exposed to randomized trials of 500 ms exposures to 65 or 115 decibel sound pressure level (dB SPL) with a 500 ms intertrial interval. Trials were repeated between seven and eight times for each mouse in a randomized order. Startle was measured as the maximum force in Newtons (N) and the average response across the trial repetitions for each mouse was used for data analysis.

RNAscope in situ hybridization

Multiplex fluorescent in situ hybridization was performed according to the manufacturer's instructions (Advanced Cell Diagnostics #320850). Briefly, 16 um-thick fresh-frozen sections containing the RVM were fixed in 4% paraformaldehyde, dehydrated, treated with protease for 15 minutes, and hybridized with gene-specific probes to mouse. Probes were used to detect Mm-Oprm1-C1 (#315841), Mm-Oprk1-C1 (#316111), Mm-Nos1-C2 (#437651-C2), Mm-Tac1-C1 (#517971), Mm-Tph2-C2 (#318691-C2), Mm-Slc32a1-C3 (#319191), and Mm-Slc17a6-C3 (#319171). DAPI (#320858) was used to visualize nuclei. 3-plex positive (#320881) and negative (#320871) control probes were tested. Three to four z-stacked sections were quantified for a given mouse, and 3-4 mice were used per experiment.

Immunohistochemistry

Mice were anesthetized with an intraperitoneal injection of urethane, transcardially perfused, and post-fixed at least four hours in 4% paraformaldehyde. 40um and 25um thick RVM and spinal cord sections were collected on a cryostat and slide-mounted for immunohistochemistry. Sections were blocked at room temperature for two hours in a 5% donkey serum, 0.2% triton, in phosphate buffered saline. Primary antisera was incubated for 14 hours overnight at 4°C: rabbit anti-RFP (1:1K). Sections were subsequently washed three times for 20 minutes in wash buffer (0.2% triton, in PBS) and incubated in secondary antibodies (Life Technologies, 1:500) at room temperature for two hours. Sections were then incubated in Hoechst (ThermoFisher, 1:10K) for 1 minute and washed 3 times for 15 minutes in wash buffer, mounted and cover slipped.

Image acquisition and quantification

Full-tissue thickness sections were imaged using either an Olympus BX53 fluorescent microscope with UPlanSApo 4x, 10x, or 20x objectives or a Nikon A1R confocal microscope with 20X or 60X objectives. All images were quantified and analyzed using ImageJ. To quantify images in RNAscope in situ hybridization experiments, confocal images of tissue samples (3-4 sections per mouse over 3-4 mice) were imaged and only cells whose nuclei were clearly visible by DAPI staining and exhibited fluorescent signal were counted.

Statistical analysis

All statistical analyses were performed using GraphPad Prism 8. Values are presented as mean +/- SEM. Statistical significance was assessed using tests indicated in applicable figure legends. Significance was indicated by $p < 0.05$. Sample sizes were based on pilot data and are similar to those typically used in the field.

8.3 Results

As a starting point, we examined the expression of these putative neuronal cell types using multiplex fluorescent in situ hybridization (Figure 20A) and found that most neurons in the RVM are GABAergic (based on their expression of Slc32a1) and expressed a combination of Tph2, Nos1, Tac1, and Oprk1. Using commercially-available Cre-alleles and Cre-dependent viral vectors, we sought to selectively label and manipulate distinct RVM neuronal cell types using fluorescent tracers and chemogenetically activate them with AAV2-hSyn-DIO-hM3Dq-mCherry (Figure 20B, Figure 21A, B).

When we chemogenetically activated these neurons and assessed animals using a variety of somatosensory tests for cold, thermal, pruritic, mechanical stimuli and tail flick, we found, strikingly, that the chemogenetic activation of KOR-RVM neurons in the KOR-Cre allele robustly inhibited responses to cold and thermal sensitivities, chloroquine-evoked itch, but not responses to von Frey testing and tail flick assay (Figure 20C-G).

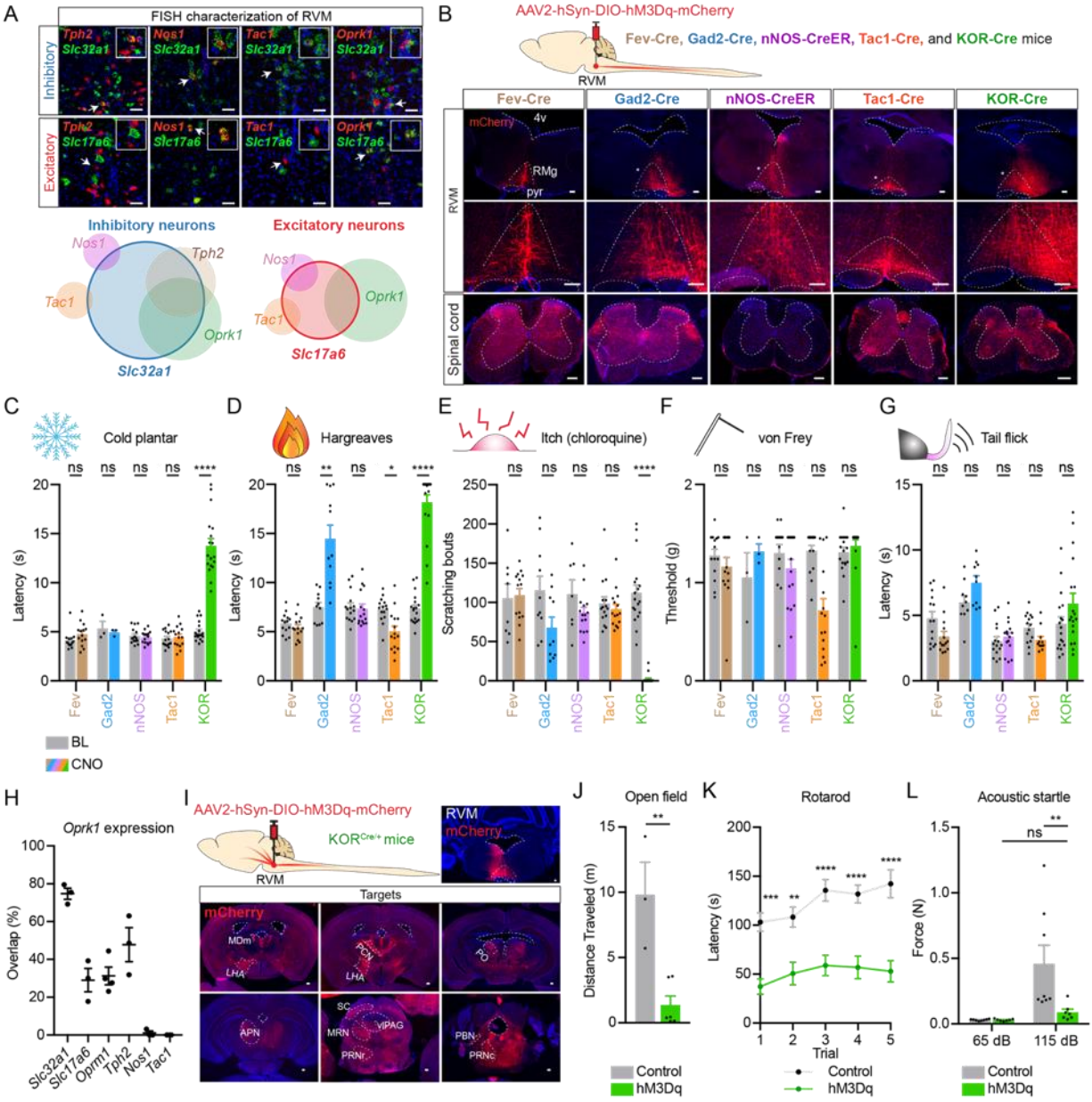

Figure 20. Identification and manipulation of diverse RVM neuronal cell types.

(A) Characterization of neuronal populations in the RVM using fluorescent in-situ hybridization. Intersecting venn diagrams indicate the relative abundance of neurons expressing particular markers and their relative overlap.

(B) Experimental approach to deliver Cre-dependent hM3Dq-mCherry to visualize labeled RVM neurons and their spinal projections across Fev, Gad2, nNos, Tac1, and KOR-Cre alleles. 4v: fourth ventricle, RMg: raphe magnus, pyr: pyramidal tract. Scale bar = 100 μm.

(C) Chemogenetic activation of Fev, Gad2, nNos, Tac1, and KOR-Cre neurons on the latency to respond to the cold plantar assay. Data are mean + SEM with dots representing individual mice. Fev (n=14), Gad2 (n=3), nNos (n=15),

Tac1 (n=15), KOR (n=18) mice. Asterisks indicate the results of paired t-tests, corrected for multiple comparisons (ns $p>0.05$, **** $p<0.0001$).

(D) Chemogenetic activation of Fev, Gad2, nNos, Tac1, and KOR-Cre neurons on the latency to respond to the hargreaves assay. Data are mean + SEM with dots representing individual mice. Fev (n=14), Gad2 (n=11), nNos (n=15), Tac1 (n=15), KOR (n=18) mice. Asterisks indicate the results of paired t-tests, corrected for multiple comparisons (ns $p>0.05$, * $p<0.05$, ** $p<0.01$, **** $p<0.0001$).

(E) Chemogenetic activation of Fev, Gad2, nNos, Tac1, and KOR-Cre neurons in chloroquine-evoked itch. Data are mean + SEM with dots representing individual mice. Fev (n=8), Gad2 (n=10), nNos (n=7), Tac1 (n=15), KOR (n=18) mice. Asterisks indicate the results of paired t-tests, corrected for multiple comparisons (ns $p>0.05$, **** $p<0.0001$).

(F) Chemogenetic activation of Fev, Gad2, nNos, Tac1, and KOR-Cre neurons in mechanical thresholds in the von Frey assay. Data are mean + SEM with dots representing individual mice. Fev (n=14), Gad2 (n=3), nNos (n=15), Tac1 (n=15), KOR (n=18) mice. Asterisks indicate the results of paired t-tests, corrected for multiple comparisons (ns $p>0.05$).

(G) Chemogenetic activation of Fev, Gad2, nNos, Tac1, and KOR-Cre neurons in the tail-flick assay. Data are mean + SEM with dots representing individual mice. Fev (n=14), Gad2 (n=10), nNos (n=15), Tac1 (n=15), KOR (n=18) mice. Asterisks indicate the results of paired t-tests, corrected for multiple comparisons (ns $p>0.05$).

(H) FISH characterization of Oprk1-expressing neurons in the RVM relative to other markers of interest. Data are mean +/- SEM with dots representing individual mice (n=3-4 mice per group).

(I) Experimental approach to deliver Cre-dependent hM3Dq-mCherry to KOR-Cre mice to visualize labeled RVM neurons and their supraspinal projections. MDm: mediodorsal nucleus of the thalamus, medial part, LHA: lateral hypothalamic area, PCN: paracentral nucleus, PO: posterior complex of the thalamus, APN: anterior pretectal nucleus, SC: superior colliculus, vlPAG: ventrolateral periaqueductal gray, MRN: midbrain reticular nucleus, PRNr: pontine reticular nucleus, PBN: parabrachial nucleus, PPNc: pontine reticular nucleus, caudal part. Scale bar = 50 μm.

(J) Activation of KOR-RVM neurons suppresses locomotor activity measured in an open field test. Data are mean + SEM with dots representing individual mice (n=3 controls, n=6 hM3Dq mice). Asterisks indicate the results of unpaired t-test (** $p<0.01$).

(K) Activation of KOR-RVM neurons reduces the latency to fall on a rotarod test. Data are mean +/- SEM (n=8 controls, n=14 hM3Dq mice). Asterisks indicate the results of two-way ANOVA with Bonferroni's correction (** $p<0.01$, *** $p<0.001$, **** $p<0.0001$).

(L) Activation of KOR-RVM neurons suppresses responses to the acoustic startle test. Data are mean + SEM with dots representing individual mice (n=8 controls, n=7 hM3Dq mice). Asterisks indicate the results of two-way repeated measures ANOVA with Bonferroni's correction (ns $p>0.05$, ** $p<0.01$).

Strikingly, we also observed that KOR-RVM neurons comprised a significant number of neurons in the brainstem that were molecularly diverse (Figure 20H, Figure 22A) and provided

inputs to many structures through the brainstem (Figure 20I). In agreement with prior reports (Gutstein et al. 1998; Winkler et al. 2006), many Oprk1 neurons co-expressed Slc32a1 and Oprm1 (Figure 20H). Beyond the observed reductions in pain and itch responses with chemogenetic activation (Figure 20C-E), we also found that chemogenetic activation of these neurons suppressed animals' locomotor behaviors on an open field and rotarod (Figure 20J, K). Moreover, in the acoustic startle assay, activation of KOR-RVM neurons also reduced animals' responses to a 115 decibels noise burst (Figure 20L). These remarkable motor and arousal responses could have confounded our significant behavioral findings (Figure 20C-G); thus, we attempted to isolate the somatosensory deficits from the motor and arousal ones by restricting the amount of virus delivered to the RVM using a very dilute titer (Figure 222B). This approach allowed us to sparsely label KOR-RVM neurons (Figure 22B). Using very dilute titers, we found that animals in which spinally-projecting KOR-RVM neurons were infected exhibited robust inhibition of itch with chemogenetic activation (Figure 22C, D). In contrast, animals in which the spinally-projecting KOR-RVM neurons were not captured did not exhibit a reduction in chloroquine-evoked itch and behaved similarly to controls (Figure 21C, D). We chose the chloroquine-induced itch assay due to its robust and consistent effects on itch behaviors, allow us to efficiently screen animals for a sensory response with chemogenetic activation. Although we did not assess whether motor behaviors or startle were affected in our serial dilution studies, we determined that at dilute titers, chemogenetic activation of RVM-KOR neurons depressed itch, but not locomotor behaviors, suggesting that our approach was selective for sensory, but not motor responses.

Lastly, we used a modified iDISCO clearing approach to compare labeling of KOR-RVM projections throughout the brain and spinal cords of animals receiving viral titers with and

without dilution (Figure 22E). Thus, we determined that only a small number of KOR-RVM neurons, and only those projecting to the spinal cord, could be sufficient to drive the descending modulation of itch.

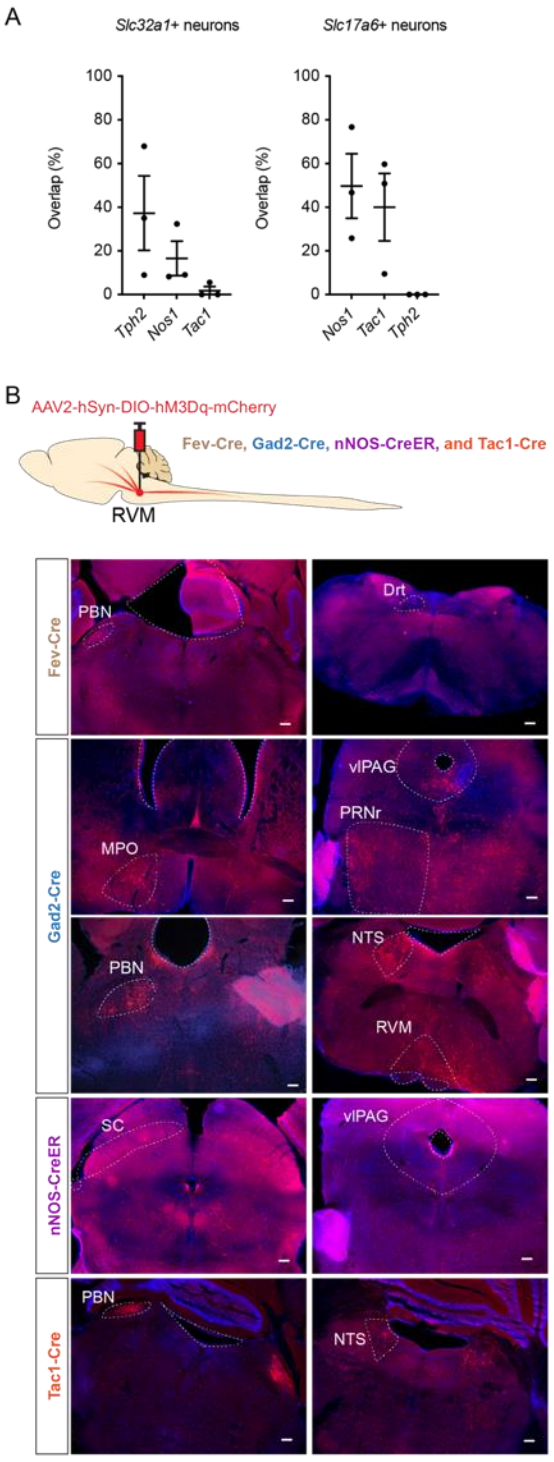

Figure 21. Tracing of RVM cell types to supraspinal structures.

(A) FISH characterization of *Tph2, Tac1,* and *Nos1* RVM neurons and their overlap with inhibitory (*Slc32a1)* and excitatory (*Slc17a6)* markers.

(B) Experimental approach to deliver Cre-dependent hM3Dq-mCherry to visualize labeled RVM neurons and their supraspinal projections across Fev, Gad2, nNos, Tac1, and KOR-Cre alleles. Representative supraspinal targets of Fev-Cre, Gad2-Cre, nNOS-CreER, and Tac1-Cre labeled RVM neurons are shown. PBN: parabrachial nucleus, Drt: doral reticular nucleus, MPO: medial preoptic area, vlPAG: ventrolateral periaqueductal gray, PRNr: pontine reticular nucleus, NTS: nucleus solitary tract, RVM: rostralventromedial medulla, and SC: superior colliculus. Scale bar = 50 μm.

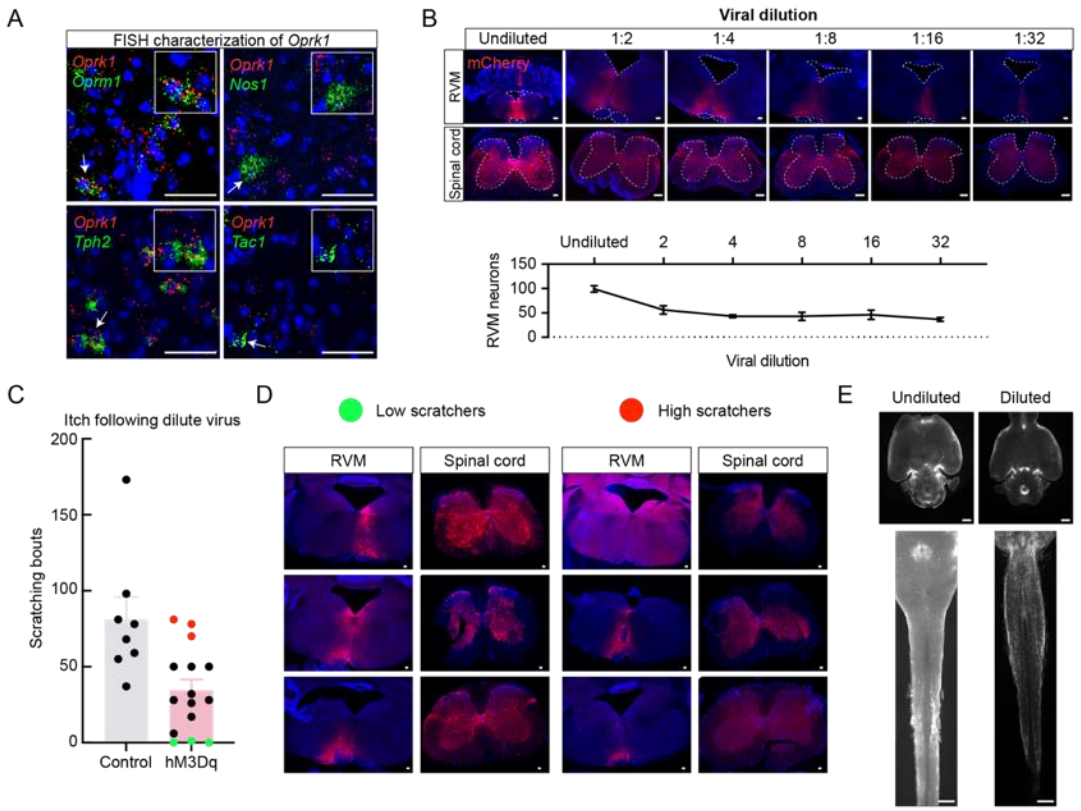

Figure 22. Restricted targeting of KOR-RVM spinally-projecting neurons reveals their contribution to somatosensation.

(A) Representative images of FISH characterization of KOR-RVM neurons for the quantifications shown in Figure 20H. Scale bar = 50 μm.

(B) Serial dilutions of the hM3Dq-mCherry virus (originaly titer 8.6x10^10) captures smaller populations of KOR-RVM neurons. Scale bar = 50 μm.

(C) A separation in the distribution of animals receiving 32x diluted hM3Dq reveals animals that behave comparably to controls (red) and animals with abolished itch responses to chloroquine (light blue).

(D) Representative RVM and spinal cord images of animals highlighted in (C). Scale bar = 50 μm.

(E) iDISCO cleared brain and brainstem-spinal samples in animals receiving viral injections into the RVM with and without dilution. Scale bar = 1 mm

8.4 Discussion

In perilous and stressful situations, the ability to suppress pain can be critical for survival. The rostral ventromedial medulla (RVM) contains neurons that can robustly inhibit pain processing in the spinal cord through a top-down modulatory pathway. Although much is known about the role of the RVM in the inhibition of pain, the precise identities and mechanisms of pain-inhibitory neurons in the RVM have never been identified. In this chapter, we tested a battery of known genetic markers of RVM neurons and found that among the five populations tested, by far the most promising candidate were neurons expressing KOR. We found that across all assays, chemogenetic activation of this population robustly inhibited nociception to cold and thermal plantar testing and itch. However, activation of RVM-KOR neurons did not elevated mechanical thresholds above baseline, likely due to a ceiling effect and did not reduce sensitivity to the tail-flick assay. The divergent findings with respect to thermal nociception between the plantar (Hargreaves) and tail-flick test suggest that different circuits are involved in the modulating these different responses. Tail-flick is thought to reflect a spinal, reflexive response, whereas a more coordinated behavioral sequence underlies the withdrawal to plantar testing. Our results indicate that RVM-KOR neurons do not participate in the inhibition of the tail-withdrawal reflex.

Interestingly, however, we also observed that these neurons may also modulate motor and arousal behaviors, which we ascribe to the non-spinally-projecting KOR brainstem neurons. By diluting the DREADD virus, we determined a strong correlation between animals displaying anti-pruritic behaviors and the presence of spinally-projecting fibers, providing us a basis upon which to directly test the contributions of spinally-projecting KOR-RVM neurons to the descending modulation of pain and itch.

9.0 KOR RVM neurons are anti-nociceptive

9.1 Introduction

Previous studies have implicated the role of neurons expressing the kappa opioid receptor (KOR) as OFF cells (Pan, Tershner, and Fields 1997; Pan, Williams, and Osborne 1990; Pan, Hirakawa, and Fields 2000), but this has been controversial (Ackley et al. 2001; Meng et al. 2005). Previously, experiments investigating KOR-RVM neurons were conducted in unconscious animals and relied on reflexive behaviors, making it challenging to definitively prescribe the functions of these neurons in awake, freely-behaving systems. Thus, the exact identity of cells that could inhibit pain were never molecularly identified and directly manipulated.

Given the finding that KOR-RVM neurons inhibit itch, even with the diluted viral titer used, we wanted to test whether KOR-RVM neurons may more broadly inhibit pain and itch. Among neurons in the RVM that are thought to express the kappa opioid receptor, evidence from pharmacological studies remains controversial. OFF cells are proposed to be directly inhibited by kappa agonists, but disinhibited by mu agonists (Pan, Tershner, and Fields 1997; Pan, Williams, and Osborne 1990; Pan, Hirakawa, and Fields 2000). However, other studies suggest that kappa agonists inhibit excitatory input onto secondary cells to produce anti-nociception (Ackley et al. 2001; Meng et al. 2005). Using the KOR-Cre allele developed by our lab, we were able to directly test the roles of KOR-RVM neurons in descending modulation.

9.2 Methods

Mice

The studies were performed in both male and female mice 8-10 weeks of age. All animals were of the C57Bl/6 background. KOR-Cre mice were used. Even numbers of male and female mice were used for all experiments. Mice were given free access to food and water and housed under standard laboratory conditions. The use of animals was approved by the Institutional Animal Care and Use Committee of the University of Pittsburgh.

Pharmacologic agents

Clozapine-N-oxide (Tocris) was dissolved in PBS and administered intraperitoneally (5mg/kg), IT (50ug/kg), or locally via cannula injection (1mmol in 300nl). Morphine sulfate (Henry Schein; 1ug in 0.25ul) was diluted in sterile saline and microinjected into the RVM. Capsaicin (0.1%) in 10% EtOH in PBS was injected 10ul into the plantar hindpaw. Chloroquine diphosphate salt (Sigma) was dissolved in physiological saline (100μg in 10μL) and administered intradermally.

Intradermal and intrathecal injections

For intradermal injection of chloroquine, hair was removed at least 24 hours before the experiment. Chloroquine (100μg in 10μL) was administered into the nape of the neck or calf, which could be subsequently visualized by the formation of a small bubble under the skin. For intrathecal injections, hair was clipped from the back of each mouse at least 24 hours before the experiment. All intrathecal injections were delivered in a total volume of 10 μL using a 30-gauge needle attached to a luer-tip 25 μL Hamilton syringe. The needle was inserted into the tissue at a 45° angle and through the fifth intervertebral space (L5 – L6). Solution was injected at a rate of 1 μL/s. The needle was held in position for 10 s and removed slowly to avoid any outflow of the

solution. Only mice that exhibited a reflexive flick of the tail following puncture of the dura were included in our behavioral analysis. These procedures were performed in awake mice.

Intraspinal injections

Mice were anesthetized with 100mg/kg ketamine and 10 mg/kg xylazine. An incision was made at the spinal cord level corresponding to L4-6 dermatome. The intrathecal space was exposed, and two injections of approximately 300nl of virus was infused 300 mm below the surface of the spinal cord at 5nL/s via glass pipette through the intrathecal space corresponding to L4-6 of the spinal cord (AAVr.EF1a.DIOhChR2(H134R).eyfp-wpre-hghpa, Addgene 20298; AAVr-hSyn-DIO-hM3D(Gq)-mCherry, Addgene 44361; AAVr-FLEX-tdTomato, Addgene 28306). For experiments examining RVM innervation of the cervical spinal cord, the same approach was used to target thoracic cord (T6-8). The glass pipette was left in place for an additional 5 minutes before withdrawal. The incision was closed with 5-0 vicryl suture. Ketofen was delivered (IP 10mg/kg) and mice were allowed to recover over a heat pad.

Stereotaxic injections and cannula implantation

Animals were anesthetized with 2% isoflurane and placed in a stereotaxic head frame. A drill bit (MA Ford, #87) was used to create a burr hole and custom-made metal needle (33 gauge) loaded with virus was subsequently inserted through the hole to the injection site. Virus was infused at a rate of 100nL/min using a Hamilton syringe with a microsyringe pump (World Precision Instruments). Mice received 250-500 nL of virus (AAV2.hSyn.DIO.mCherry Addgene #50459; AAV2.hSyn.DIO.hM3D(Gq)-mCherry, Addgene #44361). The injection needle was left in place for an additional 15 min and then slowly withdrawn over another 15 min. Injections and cannula implantations were performed at the following coordinates for each brain region: RVM: AP -5.80 mm, ML 0.00 mm, DV -6.00. For implantation of guide cannulas (P1 Technologies),

implants were slowly lowered 0.300-0.500 mm above the site of injection and secured to the skull with a thin layer of Vetbond (3M) and dental cement. The incision was closed using Vetbond and animals were given ketofen (IP 10 mg/kg) and allowed to recover over a heat pad. Mice were given 4 weeks to recover prior to experimentation.

Spared nerve injury

For spared nerve injury surgery (SNI), the sural and superficial peroneal branches of the sciatic nerve were ligated (size 6.0 suture thread) and transected, leaving the tibial nerve intact. The muscle tissue overlying the injury was gently placed back together and the skin sutured. Animals were tested 3 weeks post-injury.

Behavior

All assays were performed in the Pittsburgh Phenotyping Core and scored by an experimenter blind to treatment.

Observation of scratching behavior

All tests were performed in a blinded manner. Scratching behavior was observed using a previously reported method (Kardon et al. 2014). On the testing day, the mice were individually placed in the observation cage (12x9x14 cm) to permit acclimation for 30 minutes. Scratching behavior was videotaped for 30 minutes after administration of chloroquine. The temporal and total numbers of scratch bouts by the hind paws at various body sites during the first 30 minutes after intrathecal injection were counted.

Hargreaves testing

Animals were acclimated on a glass plate held at 30°C (Model 390 Series 8, IITC Life Science Inc.). A radiant heat source was applied to the hindpaw and latency to paw withdrawal was recorded (Hargreaves et al. 1988). 2 trials were conducted on each paw, with at least 5 min

between testing the opposite paw and at least 10 min between testing the same paw. To avoid tissue damage, a cut off latency of 20 sec was set. Values from both paws were averaged to determine withdrawal latency.

Von Frey testing

Mechanical sensitivity was measured using the Chaplan up-down method of the von Frey test (Chaplan et al. 1994). Calibrated von Frey filaments (North Coast Medical Inc.) were applied to the plantar surface of the hindpaw. Lifting, shaking, and licking were scored as positive responses to von Frey stimulation. Average responses were obtained from each hindpaw, with 3 min between trials on opposite paws, and 5 min between trials on the same paw.

Cold plantar assay

Paw withdrawal to cold sensitivity was measured as previously described (Brenner et al. 2015; Brenner, Golden, and Gereau 2012). Briefly, animals were acclimated to a 1/4" glass plate and crushed dry ice was packed into a modified 3 mL syringe and used as a probe. The dry ice probe was applied to the glass beneath the plantar hindpaw and the latency to withdrawal was recorded. Two trials were conducted on each hindpaw, with 3 min between trials on opposite paws, and 5 min between trials on the same paw. A cut off latency of 20 s was used to prevent tissue damage. Withdrawal latencies for each paw were determined by averaging values across 2 trials per paw.

Tail immersion test

Mice were habituated to mice restraints 15 minutes for 3 days before testing. Tails were immersed 3 cm into a water bath at 48°C, and the latency to tail flick was measured three times with a 1 minute interval between trials.

RNAscope in situ hybridization

Multiplex fluorescent in situ hybridization was performed according to the manufacturer's instructions (Advanced Cell Diagnostics #320850). Briefly, 16 um-thick fresh-frozen sections containing the RVM were fixed in 4% paraformaldehyde, dehydrated, treated with protease for 15 minutes, and hybridized with gene-specific probes to mouse. Probes were used to detect tdTomato-C2 (#317041-C2), mCherry-C2 (#431201), Mm-Oprm1-C1 (#315841), Mm-Oprk1-C1 (#316111), Mm-Nos1-C2 (#437651-C2), Mm-Tac1-C1 (#517971), Mm-Tph2-C2 (#318691-C2), Mm-Fos-C3 (#498401-C3), Mm-Slc32a1-C3 (#319191), and Mm-Slc17a6-C3 (#319171). DAPI (#320858) was used to visualize nuclei. 3-plex positive (#320881) and negative (#320871) control probes were tested. Three to four z-stacked sections were quantified for a given mouse, and 3-4 mice were used per experiment.

Immunohistochemistry

Mice were anesthetized with an intraperitoneal injection of urethane, transcardially perfused, and post-fixed at least four hours in 4% paraformaldehyde. 40um and 25um thick RVM and spinal cord sections were collected on a cryostat and slide-mounted for immunohistochemistry. Sections were blocked at room temperature for two hours in a 5% donkey serum, 0.2% triton, in phosphate buffered saline. Primary antisera was incubated for 14 hours overnight at 4°C: rabbit anti-RFP (1:1K), chicken anti-GFP (1:1K), and mouse anti-NeuN (1:500). Sections were subsequently washed three times for 20 minutes in wash buffer (0.2% triton, in PBS) and incubated in secondary antibodies (Life Technologies, 1:500) at room temperature for two hours. Sections were then incubated in Hoechst (ThermoFisher, 1:10K) for 1 minute and washed 3 times for 15 minutes in wash buffer, mounted and cover slipped.

Fos experiments

Morphine sulfate (1ug in 0.25ul) was microinjected into the RVM. Twenty minutes thereafter, brain samples were collected and processed for FISH. Spinal cords were harvested 20 minutes and 90 minutes following CNO administration for FISH and immunohistochemistry, respectively.

Image acquisition and quantification

Full-tissue thickness sections were imaged using either an Olympus BX53 fluorescent microscope with UPlanSApo 4x, 10x, or 20x objectives or a Nikon A1R confocal microscope with 20X or 60X objectives. All images were quantified and analyzed using ImageJ. To quantify images in RNAscope in situ hybridization experiments, confocal images of tissue samples (3-4 sections per mouse over 3-4 mice) were imaged and only cells whose nuclei were clearly visible by DAPI staining and exhibited fluorescent signal were counted.

Statistical analysis

All statistical analyses were performed using GraphPad Prism 8. Values are presented as mean +/- SEM. Statistical significance was assessed using tests indicated in applicable figure legends. Significance was indicated by $p < 0.05$. Sample sizes were based on pilot data and are similar to those typically used in the field.

9.3 Results

In our experiments, we found that microinjection of morphine into the RVM increased in response latencies to Hargreaves (Figure 23A) and led to the upregulation of fos expression in Oprk1 neurons (Figure 23B, Figure 24A). When we recorded from spinally-projecting KOR-

RVM neurons by injecting AAVr-FLEX-tdtomato into the spinal cord of KOR-Cre mice, we found that DAMGO resulted a reduction of presynaptic IPSCs (Figure 23C). Thus, our findings are in agreement with the idea that morphine enhances the activity of KOR-RVM neurons to produce analgesia, implicating KOR-RVM neurons as OFF cells.

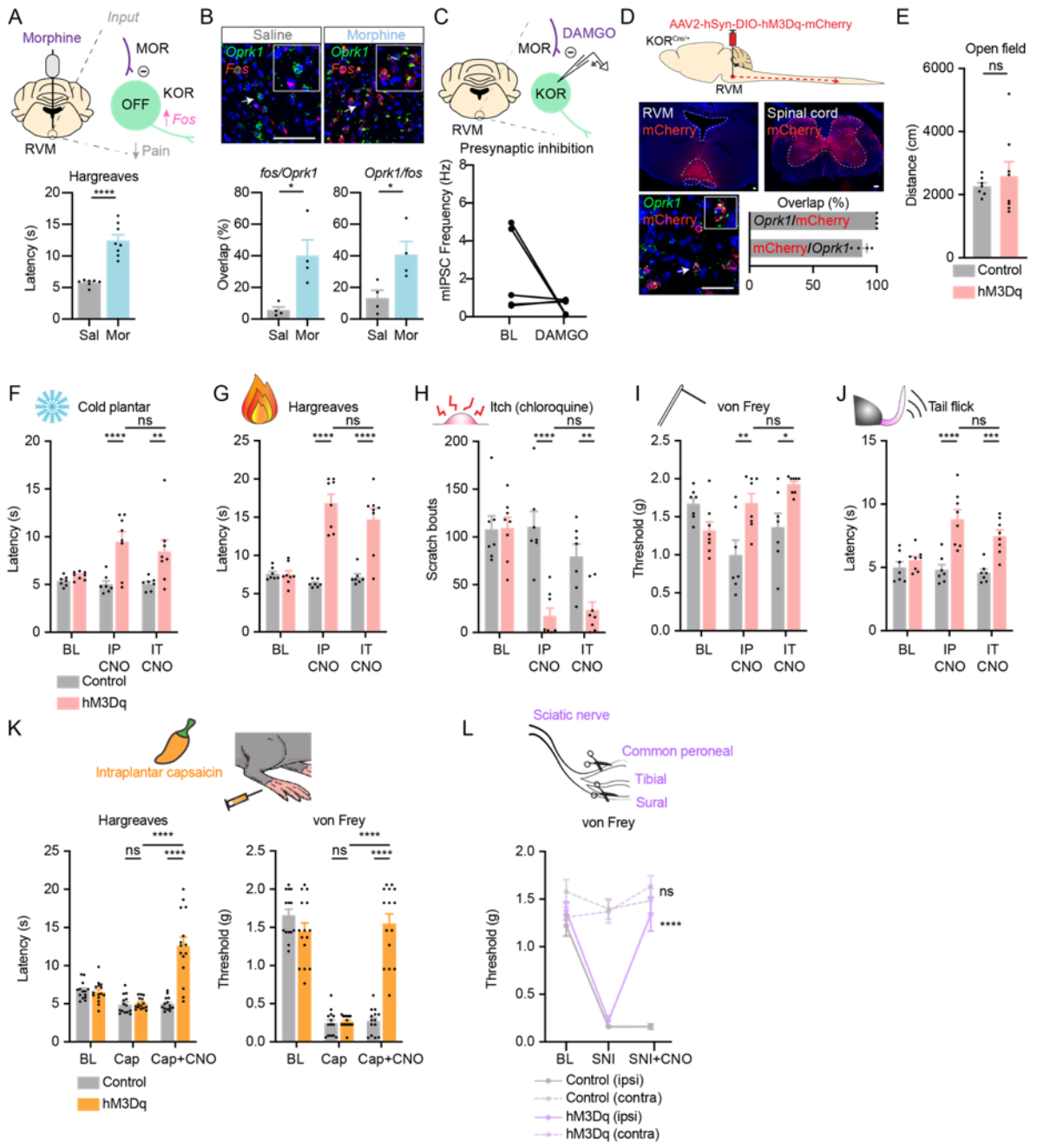

Figure 23. Activation of KOR-RVM neurons is analgesic.

(A) Model to test whether KOR-RVM neurons are OFF cells by examining if microinjection of opioids can disinhibit KOR-RVM neurons to produce analgesia. Microinjection of morphine into the RVM increased latencies to the hargreaves assay. Data are mean + SEM with dots representing individual mice (n=7 saline, n=8 morphine treated animals). Asterisks indicate the results of unpaired t-test (**** $p<0.0001$).

(B) Fos expression is enriched in Oprk1 neurons following microinjection of morphine into the RVM. Data are mean + SEM with dots representing individual mice (n=4 saline, n=4 morphine treated animals). Scale bar = 50 μm.

Asterisks indicate the results of unpaired t-test (* $p<0.05$).

(C) Recordings of labeled spinally-projecting KOR-RVM neurons revealed a reduction in presynaptic IPSCs in the presence of DAMGO (10 nM).

(D) Validation of the diluted viral approach to target KOR-RVM neurons using FISH. Data are mean + SEM with dots representing individual mice (n=4). Scale bar = 50 μm.

(E) Infection of KOR-RVM with a diluted virus does not affect locomotor activity in an open field test. Data are mean + SEM with dots representing individual mice (n=7 controls, n=8 hM3Dq mice). NS indicates the results of unpaired t-test (ns $p>0.05$).

(F to J) Chemogenetic activation of KOR-RVM neurons with IP (intraperitoneal) and IT (intrathecal) CNO reduces naive responses to (F) cold plantar assay, (G) hargreaves assay, (H) chloroquine-evoked itch, (I) von Frey assay, and (J) tail-flick assay. Data are mean + SEM with dots representing individual mice (n=7 controls, n=8 hM3Dq). Asterisks indicate the results of two-way repeated measures ANOVA with Bonferroni's correction (ns $p>0.05$, * $p<0.05$, ** $p<0.01$, *** $p<0.001$, **** $p<0.0001$).

(K) Chemogenetic activation of KOR-RVM inhibits thermal and mechanical responses following intraplantar capsaicin-induced injury. Data are mean + SEM with dots representing individual mice(n=14 controls, n=15 hM3Dq). Asterisks indicate the results of two-way repeated measures ANOVA with Bonferroni's correction (ns $p>0.05$, **** $p<0.0001$).

(L) Chemogenetic activation of KOR-RVM inhibits mechanical hypersensitivity following spared nerve injury. Data are mean +/- SEM (n=14 controls, n=15 hM3Dq). Asterisks indicate the results of two-way repeated measures ANOVA with Bonferroni's correction (ns $p>0.05$, **** $p<0.0001$).

To more directly manipulate KOR-RVM neurons and assess their contributions to the inhibition of pain, we used a diluted viral titer, which we confirmed allowed us to more sparsely infect KOR-RVM neurons with hM3Dq (Figure 22B). Within the RVM, we found that mCherry-expressing neurons comprised 88.6 +/-3.6% of *Oprk1* neurons and that these neurons were 100% specific to the *Oprk1* population (Figure 23D). Moreover, we confirmed that activation of these neurons did not affect locomotor responses in an open field test (Figure 23E), an indication that the use of a dilute viral titer allowed us to manipulate KOR-RVM neurons that do not affect motor behaviors upon activation.

9.3.1 KOR-RVM neurons inhibit itch and acute and chronic pain

Next, we tested the effect of chemogenetically activating KOR-RVM neurons in cold plantar, hargreaves, itch, mechanical, and tail flick assays. We found that for all assays, chemogenetic activation of KOR-RVM neurons with intraperitoneal (IP) CNO produced anti-nociceptive and anti-pruritic effects (Figure 23F-J). Moreover, because we had previous concerns that KOR-RVM neurons may also produce non-specific effects through their non-spinal targets, we also administered intrathecal (IT) CNO, which allowed us to spatially restrict the activation of KOR-RVM neurons that project to the spinal cord. With this manipulation, we also found that chemogenetic activation of KOR-RVM neurons with IT CNO also inhibited pain and itch responses in a manner that was similar to the IP administration of CNO (Figure 23F-J). Additionally, we found that activation of these neurons also reversed thermal responses to Hargreaves and von Frey assays following acute injury with intraplantar capsaicin (Figure 23K). Thus, activation of KOR-RVM neurons seemed to be sufficient to protect against the development of capsaicin-induced thermal and mechanical hyperalgesia (Figure 23K, Figure 24A, B). Finally, we tested animals in a model of persistent pain, and performed spared nerve injury (SNI), in which the common peroneal and sural branches are ligated and transected, sparing the tibial nerve. We found that following SNI, both control and hM3dq groups exhibited pronounced mechanical allodynia, but found that chemogenetic activation of KOR-RVM neurons reversed mechanical hypersensitivity (Figure 23L). Together, these data suggest that KOR-RVM neurons are sufficient for the inhibition of nociception, itch, and the reversal of pain induced by acute (capsaicin) and chronic (SNI) injury. Interestingly, activation of KOR-RVM neurons led to a reduction in thermal sensitivity that was more dramatic than observed with morphine microinjection. This suggests that the disinhibitory effects of morphine are less

efficient (either due to insufficient spread to presynaptic mu-sensitive fibers or due to a sub-therapeutic dose of morphine administered) than the direct activation of neurons containing the kappa-opioid receptor with a viral approach.

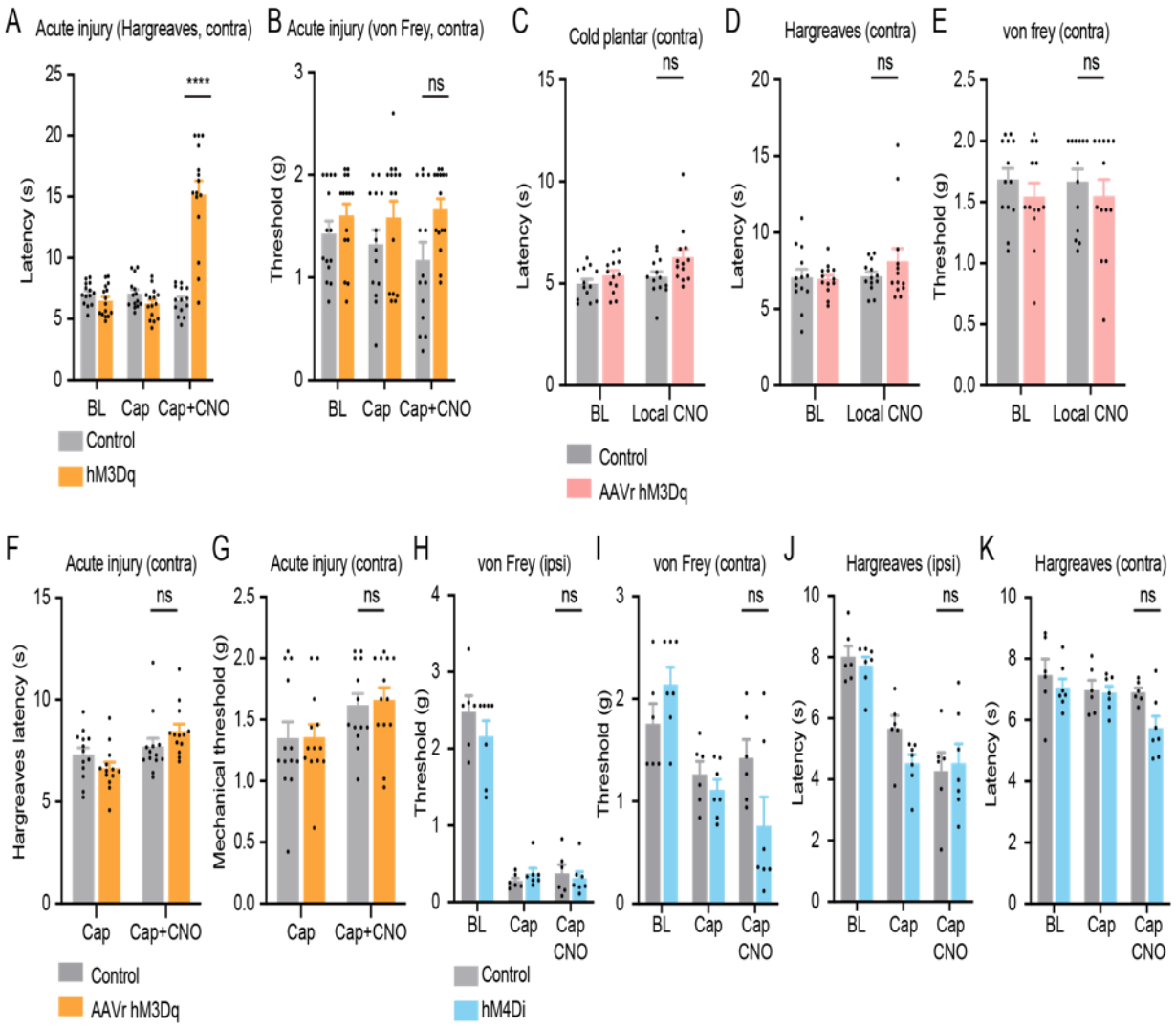

Figure 24. Combined supplementary behavioral data for Figures 23, 25, and 27.

(A-B) Effect of chemogenetic activation of KOR-RVM on (A) thermal and (B) mechanical responses following intraplantar capsaicin-induced injury. Data are mean + SEM with dots representing individual mice (n=14 controls, n=15 hM3Dq). Asterisks indicate the results of two-way repeated measures ANOVA with Bonferroni's correction (* $p<0.05$, **** $p<0.0001$).

(C-E) Effect of chemogenetic activation of spinally-projecting KOR-RVM neurons on (C) cold plantar assay, (D) hargreaves assay, and (E) von Frey assay. Data are mean + SEM with dots representing individual mice (n=13 controls, n=13 hM3Dq). NS indicates the results of two-way repeated measures ANOVA with Bonferroni's correction (ns $p>0.05$).

(F-G) Effect of chemogenetic activation of spinally-projecting KOR-RVM on (F) thermal and (G) mechanical responses following intraplantar capsaicin-induced injury. Data are mean + SEM with dots representing individual

mice (n=13 controls, n=13 hM3Dq). NS indicates the results of two-way repeated measures ANOVA with Bonferroni's correction (ns $p>0.05$).

(H-K) Effect of chemogenetic inhibition of KOR-RVM neurons on (H-I) mechanical and (J-K) thermal responses following intraplantar capsaicin-induced injury. Data are mean + SEM with dots representing individual mice (n=6 control, n=7 hM4Di). NS indicates the results of two-way repeated measures ANOVA with Bonferroni's correction (ns $p>0.05$).

9.3.2 Spinally-projecting KOR-RVM neurons inhibit itch and pain

Given the robust innervation of the spinal cord of KOR-RVM neurons (Figure 20B, Figure 21B, Figure 23D), and the role of the RVM in the descending modulation of pain, we sought to characterize the organization of KOR-RVM neurons that project to the spinal cord. Previous studies have reported variations in descending modulation between spinally-innervated lumbar segments, and uncovered differential modulation to heat in the tail and foot (Fang and Proudfit 1996). Furthermore, another study in an inflammatory model found that RVM inactivation completely blocked allodynia to the face, but not plantar hind paw (Edelmayer et al. 2009). RVM projections to the dorsal horn have also been shown to be more likely to contain GAD67 than those to the trigeminal dorsal horn (Aicher et al. 2012). However, more recent recordings of RVM neurons in the presence of noxious stimuli have not replicated these findings and challenge the idea of somatotopic organization in the RVM (Carlson 2007). Given these conflicting views, we sought to examine whether KOR-RVM neurons could modulate pain at different dermatomal segments. We used multi-color tracers including AAVr-Ef1a-DIO-eYFP, AAVr-hSyn-DIO-mCherry, and CTB-647 to examine whether these neurons exhibited somatotopy and what fraction of all spinally-projecting RVM neurons are KOR+ (Figure 25A). We found a lack of somatotopic organization; KOR-RVM neurons were frequently infected by both eYFP and mCherry, suggesting that the same KOR-RVM neurons innervate both the

cervical and lumbar spinal segments, respectively and that these neurons comprised 44.9 +/- 1.5% of spinally-projecting RVM neurons (Figure 25A).

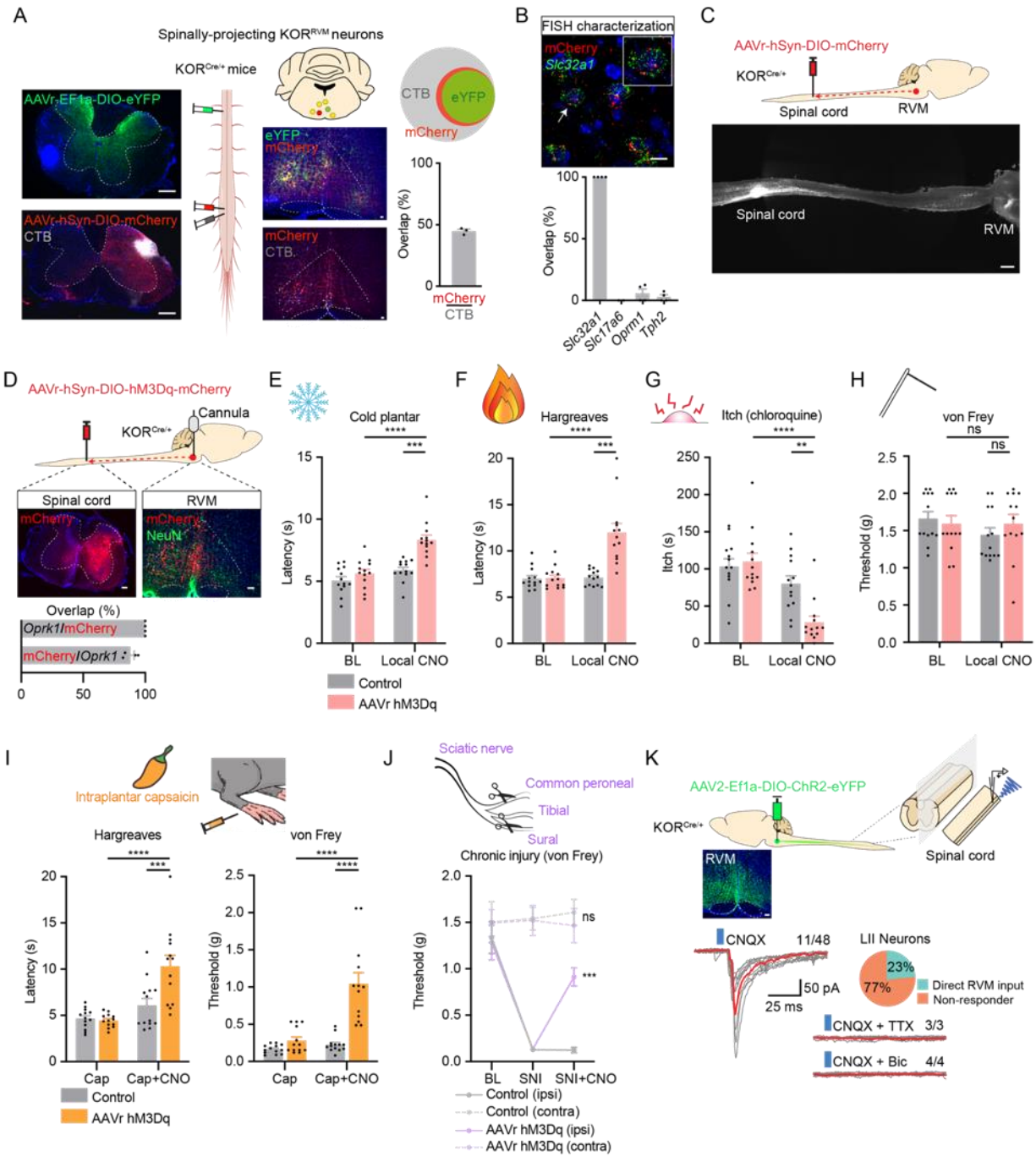

Figure 25. Selective activation of KOR-RVM neurons that project to the spinal cord produces analgesia.

(A) Labeling of spinally-projecting KOR-RVM neurons using AAVr introduced to the lumbar and cervical spinal cords reveals that KOR-RVM neurons indiscriminately innervate all levels of the spinal cord. Scale bar = 50 μm. (B) FISH characterization of spinally-projecting KOR-RVM neurons reveals that they comprise a molecularly distinct GABAergic subset of neurons. Data are mean + SEM with dots representing individual mice (n=4). Scale bar = 50 μm.

(C) iDISCO clearing of brainstem-spinal cord specimen following intraspinal injection of AAVr-FLEX-tdtomato. Scale bar = 1 mm

(D) Approach to selectively activate spinally-projecting KOR-RVM neurons using AAVr-hM3Dq, and local microinjection of CNO to the RVM and validation of the approach. Data are mean + SEM with dots representing individual mice (n=4).

Scale bar = 50 μm.

(E to H) Chemogenetic activation of spinally-projecting KOR-RVM neurons reduces naive responses to (E) cold plantar assay, (F) hargreaves assay, (G) chloroquine-evoked itch, with no effect on (H) von Frey assay. Data are mean + SEM with dots representing individual mice (n=13 controls, n=13 hM3Dq). Asterisks indicate the results of two-way repeated measures ANOVA with Bonferroni's correction (ns $p>0.05$, * $p<0.05$, ** $p<0.01$, *** $p<0.001$, **** $p<0.0001$).

(I) Chemogenetic activation of spinally-projecting KOR-RVM inhibits thermal and mechanical responses following intraplantar capsaicin-induced injury. Data are mean + SEM with dots representing individual mice (n=13 controls, n=13 hM3Dq). Asterisks indicate the results of two-way repeated measures ANOVA with Bonferroni's correction (**** $p<0.0001$).

(J) Chemogenetic activation of spinally-projecting KOR-RVM inhibits mechanical hypersensitivity following spared nerve injury. Data are mean +/- SEM (n=7 controls, n=8 hM3Dq). Asterisks indicate the results of two-way repeated measures ANOVA with Bonferroni's correction (ns $p>0.05$, *** $p<0.001$).

(K) Electrophysiological recordings of spinal cord slices in KOR-RVM neurons containing channelrhodopsin. Representative traces are shown. 11/48 cells in lamina II received direct input from KOR-RVM neurons following optogenetic activation and these responses are abolished in the presence of TTX and bicuculline.

Furthermore, we were able to characterize these spinally-projecting KOR-RVM neurons and found that they were GABAergic (based on their exclusive overlap with *Slc32a1*) and exhibited limited overlap with other markers of RVM neurons (Figure 25B). This is in striking contrast with KOR-RVM neurons as a heterogenous group (Figure 20H), suggesting that spinally-projecting KOR-RVM neurons comprise a molecularly distinct population. Furthermore, we performed whole-tissue clearing of intact brainstem-spinal cord specimens in which descending KOR-RVM neurons are labeled by AAVr-FLEX-tdtomato into the spinal cord to visualize this pathway (Figure 25C).

Using a similar approach to that used to molecularly and anatomically characterize spinally-projecting KOR-RVM neurons, we injected AAVr-hSyn-DIO-hM3Dq-mcherry into the lumbar spinal cord of KOR-Cre mice and implanted guide cannulas over the RVM, allowing us to infuse local CNO into the RVM. This strategy enabled us to selectively activate only the spinally-projecting KOR-RVM using a chemogenetics (Figure 25D). Using this approach, we were able to capture 88.1 +/- 3.1% of *Oprk1* neurons in the RVM with 100% specificity (Figure 25D). When we infused CNO into the cannulas of these KOR-Cre mice receiving AAVr-hSyn-DIO-hM3Dq-mcherry, we found that chemogenetic activation of KOR-RVM inhibited responses to cold plantar testing, hargreaves assay, and chloroquine-evoked itch (Figure 25E-G, Figure 24C, D), but did not affect mechanical thresholds to von Frey testing (Figure 25H, Figure 24E). Furthermore, activation of these neurons reversed capsaicin-induced thermal and mechanical hypersensitivities (Figure 25I, Figure 24F, G) as well as mechanical allodynia following chronic injury with spared-nerve injury (Figure 25J). We conducted slice recordings in the spinal cords of KOR-Cre animals receiving AAV-hSyn-DIO-ChR2-eYFP in the RVM (Figure 25K). We found that nearly a quarter of lamina II neurons received direct inputs from KOR-RVM neurons following optogenetic activation of these terminals in the spinal cord and that this input was inhibitory (Figure 25KFigure 26A-E). Together, we found that selective activation of spinally-projecting KOR-RVM neurons is sufficient to drive anti-nociception and analgesia in both acute and chronic pain states.

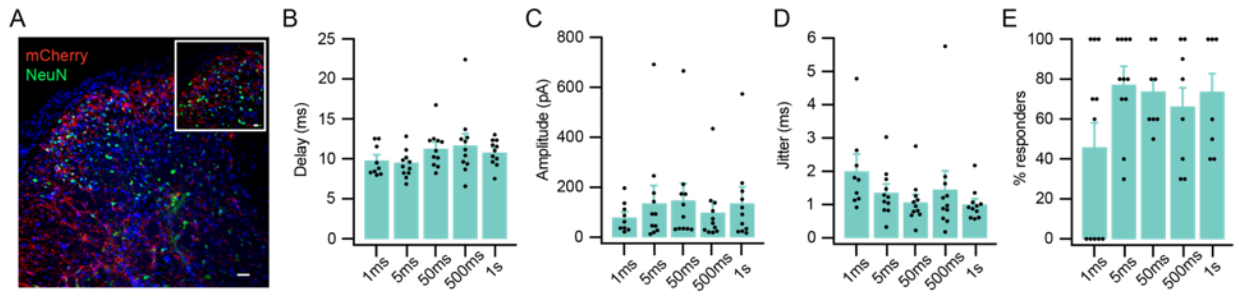

Figure 26. Supplementary spinal electrophysiology data.

(A) Representative image of fibers originating from labeled KOR-RVM neurons in the spinal cord. Scale bar = 50 μm.

(B) Delay between the optical activation of ChR2-expressing fibers in the spinal cord and responsiveness of lamina II neurons at different durations of laser stimulation. (n = 11 cells from 8 animals).

(C) Amplitude of response of lamina II neurons at different durations of laser stimulation. (n = 11 cells from 8 animals).

(D) Response jitter of lamina II neurons at different durations of laser stimulation. (n = 11 cells from 8 animals).

(E) Percentage of cells responding under different durations of laser stimulation.

9.4 Discussion

Our findings support the idea that KOR-RVM neurons are OFF cells. Consistent with the idea that OFF cells are inhibited by ON cells, we found that microinjection of morphine into the RVM led to robust fos expression in KOR neurons and produced anti-nociception to thermal sensitivity. This suggests that KOR-RVM neurons are disinhibited to promote analgesia in the presence of mu agonists, such as morphine.

We also found that activation of KOR-RVM neurons produced strong anti-nociceptive effects on cold, thermal, and mechanical thresholds. Furthermore, activation of these neurons inhibited the expression of acute pain (in an intraplantar capsaicin model) and mechanical allodynia following spared nerve injury. Together, these data suggest that KOR neurons are OFF

cells and activation of this population is sufficient for the inhibition of nociception, itch, and the reversal of pain induced by acute (capsaicin) and chronic (SNI) injury.

Using retrograde tracers, we identified of a unique population of GABAergic KOR-RVM neurons that broadly and dramatically inhibit itch and pain (in both acute and chronic injury models). By retrogradely labeling from KOR-RVM neurons that innervate the spinal cord, we were able to characterize this distinct subset of KOR-RVM neurons and found that they were exclusively GABAergic and lacked overlap with other markers of RVM neurons. In contrast to the general population of KOR-RVM neurons that represent a heterogeneous group, the spinally-projecting population is likely to be molecularly distinct.

Using a combination of fluorescent tracers, we also determined that spinally-projecting KOR-RVM neurons are not somatotopically organized, highlighting their ability to simultaneously modulate pain and itch at different dermatomal segments. This is unsurprising because the lack of somatotopy could allow these neurons to integrate appropriate behavioral responses to noxious stimuli at different spinal levels.

Finally, in this chapter, we build on the previous by explicitly testing the role of spinally-projecting KOR-RVM neurons in the modulation of itch and pain. Using a targeted chemogenetic approach and the local delivery of CNO, we determined that activation of descending KOR-RVM neurons inhibits evoked itch as well as acute and chronic pain.

10.0 Inhibition of KOR neurons facilitates nociception and abolishes stress-induced analgesia

10.1 Introduction

Microinjection of a kappa agonist, U69,593, into the RVM has previously been shown to be block the analgesia driven by mu-agonists within other sites of the CNS (Pan, Tershner, and Fields 1997; Meng et al. 2005) and can precipitate mechanical allodynia following spinal nerve ligation (De Felice et al. 2011). This suggests that KOR-RVM neurons may tonically signal to inhibit pain. However, it is important to note that the sensitivity of RVM neurons to kappa agonists remains controversial. Other work suggests that kappa agonism of KOR-RVM neurons pre-synaptically reduces excitatory input onto secondary cells (ON cells) and leads to inhibition of primary cells (OFF cells) (Ackley et al. 2001; Meng et al. 2005), thereby leading to anti-nociception. Freely-behaving rats exhibited elevated withdrawal latencies to Hargreaves and hot plate tests (Ackley et al. 2001) following the microinjection of U69,593 into the RVM, suggesting that KOR-RVM neurons may exhibit characteristics similar to ON cells. Although differences in the experimental design, such as performing recordings in anesthetized animals but conducting behavioral assays in freely-behaving ones may underlie these discrepancies, it has been a challenge to classify RVM neurons as simply primary or secondary cells. In prior chapters, we establish that chemogenetic activation of RVM-KOR neurons gives rise to behaviors consistent with an OFF cell phenotype. In this section, we weigh in on how U69,593 affects mouse behavior when microinjected into the RVM and use chemogenetic approaches to inhibit RVM-KOR neurons.

Furthermore, we sought to test the role of RVM-KOR neurons in mediating stress-induced analgesia. Acutely, stress inhibits pain (Yilmaz et al. 2010) and stress-induced analgesia is thought to be mediated by the RVM because microinjection of naloxone into the RVM blocks stress-induced analgesia (Shamsizadeh et al. 2014). However, many of these previous studies were conducted in male rodents, which reduces the generalizability of past findings. This is an important limitation because sex differences have been shown to underlie stress-induced analgesia (Vendruscolo 2004). Furthermore, kappa agonists locally administered to the RVM have previously been shown to modulate nociception in a sexually-dimorphic manner (Tershner 2000). Given the profound role of RVM-KOR neurons in the inhibition of itch and pain, we wanted to test whether stress-induced analgesia could also be mediated through these neurons using both male and female mice.

10.2 Methods

Mice

The studies were performed in both male and female mice 8-10 weeks of age. All animals were of the C57Bl/6 background. KOR-Cre mice were used. Even numbers of male and female mice were used for all experiments. Mice were given free access to food and water and housed under standard laboratory conditions. The use of animals was approved by the Institutional Animal Care and Use Committee of the University of Pittsburgh.

Pharmacologic agents

Clozapine-N-oxide (Tocris) was dissolved in PBS and administered intraperitoneally (5mg/kg). Salvinorin B (SalB; Tocris) was dissolved in DMSO and administered subcutaneously

(10 mg/kg). U69,593 (Sigma; 40ng in 0.25ul) was dissolved in 45% (2-Hydroxypropyl)-β-cyclodextrin (HBC; Sigma). Capsaicin (0.1%) in 10% EtOH in PBS was injected 10ul into the plantar hindpaw. Chloroquine diphosphate salt (Sigma) was dissolved in physiological saline (100μg in 10μL) and administered intradermally.

Intradermal injections

For intradermal injection of chloroquine, hair was removed at least 24 hours before the experiment. Chloroquine (100μg in 10μL) was administered into the nape of the neck or calf, which could be subsequently visualized by the formation of a small bubble under the skin. These procedures were performed in awake mice.

Stereotaxic injections

Animals were anesthetized with 2% isoflurane and placed in a stereotaxic head frame. A drill bit (MA Ford, #87) was used to create a burr hole and custom-made metal needle (33 gauge) loaded with virus was subsequently inserted through the hole to the injection site. Virus was infused at a rate of 100nL/min using a Hamilton syringe with a microsyringe pump (World Precision Instruments). Mice received 250-500 nL of virus (AAV8-DF-KORD-mCitrine, Addgene #65417; AAV2.hSyn.DIO.hM4D(Gi)-mCherry, Addgene #44362; AAV2.hSyn.DIO.hM3D(Gq)-mCherry, Addgene #44361; AAV2.hSyn.DIO.mCherry Addgene #50459). The injection needle was left in place for an additional 15 min and then slowly withdrawn over another 15 min. Injections were performed at the following coordinates for each brain region: RVM: AP -5.80 mm, ML 0.00 mm, DV -6.00. The incision was closed using Vetbond and animals were given ketofen (IP 10 mg/kg) and allowed to recover over a heat pad. Mice were given 4 weeks to recover prior to experimentation.

Behavior

All assays were performed in the Pittsburgh Phenotyping Core and scored by an experimenter blind to treatment.

Observation of Scratching Behavior

All tests were performed in a blinded manner. Scratching behavior was observed using a previously reported method (Kardon et al. 2014). On the testing day, the mice were individually placed in the observation cage (12x9x14 cm) to permit acclimation for 30 minutes. Scratching behavior was videotaped for 30 minutes after administration of chloroquine. The temporal and total numbers of scratch bouts by the hind paws at various body sites during the first 30 minutes after intrathecal injection were counted.

Hargreaves testing

Animals were acclimated on a glass plate held at 30°C (Model 390 Series 8, IITC Life Science Inc.). A radiant heat source was applied to the hindpaw and latency to paw withdrawal was recorded(Hargreaves et al. 1988). 2 trials were conducted on each paw, with at least 5 min between testing the opposite paw and at least 10 min between testing the same paw. To avoid tissue damage, a cut off latency of 20 sec was set. Values from both paws were averaged to determine withdrawal latency.

Stress-induced analgesia

Mice were placed in a water bath maintained at 30C and forced to swim for 3 minutes. After the swim, mice were returned to their home cages and tested 30 minutes later for stress-induced analgesia (Ibironke and Rasak 2013) to hotplate and capsaicin (described further in the methods section).

Hotplate

Twenty minutes after the forced-swim test, mice were placed on a 55C hotplate. The latency to first nocifensive response (lick or jump) and total number of licks over a 60s period were measured. Values were averaged across two trials for each mouse.

Von Frey testing

Mechanical sensitivity was measured using the Chaplan up-down method of the von Frey test (Chaplan et al. 1994). Calibrated von Frey filaments (North Coast Medical Inc.) were applied to the plantar surface of the hindpaw. Lifting, shaking, and licking were scored as positive responses to von Frey stimulation. Average responses were obtained from each hindpaw, with 3 min between trials on opposite paws, and 5 min between trials on the same paw.

Cold plantar assay

Paw withdrawal to cold sensitivity was measured as previously described (Brenner et al. 2015; Brenner, Golden, and Gereau 2012). Briefly, animals were acclimated to a 1/4" glass plate and crushed dry ice was packed into a modified 3 mL syringe and used as a probe. The dry ice probe was applied to the glass beneath the plantar hindpaw and the latency to withdrawal was recorded. Two trials were conducted on each hindpaw, with 3 min between trials on opposite paws, and 5 min between trials on the same paw. A cut off latency of 20 s was used to prevent tissue damage. Withdrawal latencies for each paw were determined by averaging values across 2 trials per paw.

Tail immersion test

Mice were habituated to mice restraints 15 minutes for 3 days before testing. Tails were immersed 3 cm into a water bath at 48°C, and the latency to tail flick was measured three times with a 1 minute interval between trials.

Immunohistochemistry

Mice were anesthetized with an intraperitoneal injection of urethane, transcardially perfused, and post-fixed at least four hours in 4% paraformaldehyde. 40um and 25um thick RVM and spinal cord sections were collected on a cryostat and slide-mounted for immunohistochemistry. Sections were blocked at room temperature for two hours in a 5% donkey serum, 0.2% triton, in phosphate buffered saline. Primary antisera was incubated for 14 hours overnight at 4°C: rabbit anti-RFP (1:1K), chicken anti-GFP (1:1K), and mouse anti-NeuN (1:500). Sections were subsequently washed three times for 20 minutes in wash buffer (0.2% triton, in PBS) and incubated in secondary antibodies (Life Technologies, 1:500) at room temperature for two hours. Sections were then incubated in Hoechst (ThermoFisher, 1:10K) for 1 minute and washed 3 times for 15 minutes in wash buffer, mounted and cover slipped.

Image acquisition and quantification

Full-tissue thickness sections were imaged using either an Olympus BX53 fluorescent microscope with UPlanSApo 4x, 10x, or 20x objectives or a Nikon A1R confocal microscope with 20X or 60X objectives. All images were quantified and analyzed using ImageJ. To quantify images in RNAscope in situ hybridization experiments, confocal images of tissue samples (3-4 sections per mouse over 3-4 mice) were imaged and only cells whose nuclei were clearly visible by DAPI staining and exhibited fluorescent signal were counted.

Statistical analysis

All statistical analyses were performed using GraphPad Prism 8. Values are presented as mean +/- SEM. Statistical significance was assessed using tests indicated in applicable figure legends. Significance was indicated by $p < 0.05$. Sample sizes were based on pilot data and are similar to those typically used in the field.

10.3 Results

We tested whether microinjection of a kappa agonist, U69,593, could affect naive responses to nociceptive stimuli (Figure 27A). We found that U69,593 had a pro-nociceptive effect when microinjected into the RVM, leading to a reduction in the latencies to respond to cold and thermal stimuli (Figure 27B, C) as well as a reduction in mechanical thresholds (Figure 27D). Consistent with previous experiments (Pan, Tershner, and Fields 1997), we found that microinjection of the kappa agonist did not affect latencies in response to tail flick (Figure 27E). These data support that, at least for some stimuli, kappa-sensitive neurons in the RVM tonically suppress responses to pain that can be potentiated with their temporary pharmacological inhibition.

10.3.1 Chemogenetic inhibition of RVM-KOR neurons elicits nociception

To follow up on this observation, we sought to chemogenetically inhibit RVM-KOR neurons using both hM4Di and KORD DREADDs (Figure 27F). We found that chemogenetic inhibition of RVM-KOR neurons with both hM4Di and KORD enhanced sensitivities to cold,

thermal, and mechanical stimuli, but not chloroquine-evoked itch (Figure 27G-J). In the tail flick assay, only chemogenetic inhibition with hM4Di, but not KORD, reduced latencies (Figure 27K). Chemeogenetic inhibition of RVM-KOR neurons did not exacerbate hyperalgesia in an acute injury model with intraplantar capsaicin (Figure 24H-K) and had no effect on locomotor activity (Figure 24L). In agreement with our pharmacological inhibition of RVM-KOR neurons (Figure 27B-D), these experiments involving chemogenetics suggest that RVM-KOR neurons are required for the descending inhibition of nociception, and their inhibition exposes a pro-nociceptive state.

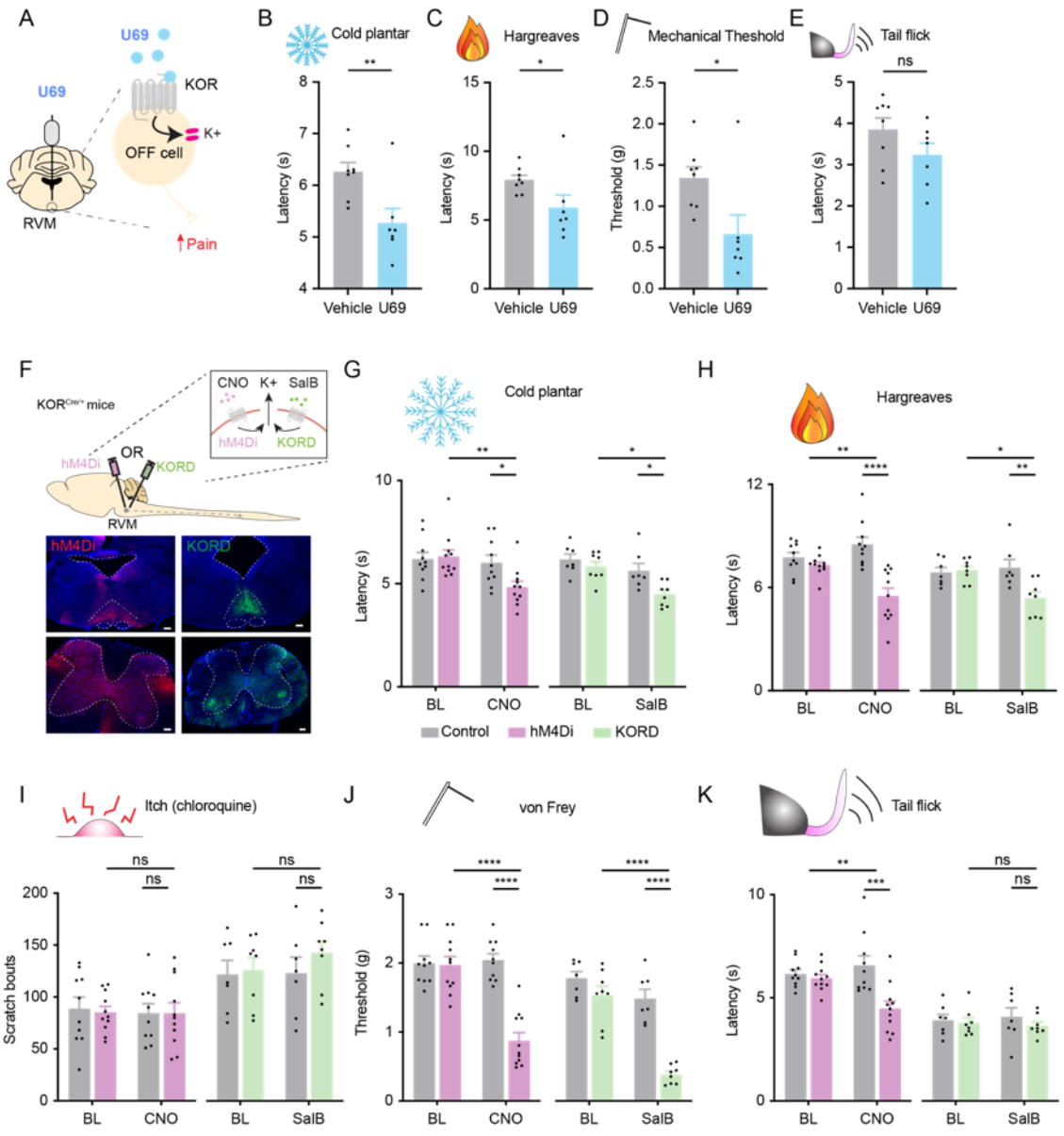

Figure 27. Pharmacological and chemogenetic inhibition of RVM-KOR neurons facilitates nociception.

(A) Model to test whether microinjection of a kappa agonist could inhibit RVM-KOR neurons to facilitate nociception.

(B-E) Microinjection of U69,593 into the RVM increased sensitivities to (B) cold plantar assay, (C) hargreaves assay, (D) von Frey assay, but with no effect on (E) tail flick assay. Data are mean + SEM with dots representing individual mice (n=8 saline, n=7 U69,593 treated animals). Asterisks indicate the results of unpaired t-test (ns $p>0.05$, * $p<0.05$, ** $p<0.01$).

(F) Model for how a chemogenetic strategy using both hM4Di (pink) and KORD (green) DREADDs could mimic the effects of pharmacological inhibition of RVM-KOR neurons. Representative images of the RVM and spinal cords following infection are shown. Scale bar = 50 μm.

(G-K) Chemogenetic inhibition of RVM-KOR neurons with hM4Di (pink, left) and KORD (green, right) on (G) cold plantar assay, (H) hargreaves, (I) chloroquine-evoked itch, (J) von Frey assay, and (K) tail flick assay. Data are mean + SEM with dots representing individual mice (n=10 hM4Di control, n=11 hM4Di, n=7 KORD control, n=8 KORD mice). Asterisks indicate the results of two-way repeated measures ANOVA with Bonferroni's correction (ns $p>0.05$, * $p<0.05$, ** $p<0.01$, *** $p<0.001$, **** $p<0.0001$).

10.3.2 RVM-KOR neurons are required for stress-induced analgesia

To further test the roles of RVM-KOR neurons in the tonic inhibition of pain, next wanted to test their contributions to stress-induced analgesia. We used the forced swim model of stress-induced analgesia (Mogil 1995; Ibironke and Rasak 2013) and tested the contributions of RVM-KOR neurons to stress-induced analgesia to hotplate and intraplantar capsaicin (Figure 28A). With chemogenetic activation of RVM-KOR neurons, we found that naive animals receiving hM3Dq and CNO exhibited similar total licking behaviors and latencies to hotplate that resembled control animals following forced swim test (Figure 28B, C). Furthermore, when we inhibited RVM-KOR with hM4Di and CNO, we found that mice no longer exhibited stress-induced analgesia to intraplantar capsaicin and hotplate (Figure 28D-F). Together, these results suggest that RVM-KOR neurons are required for stress-induced analgesia.

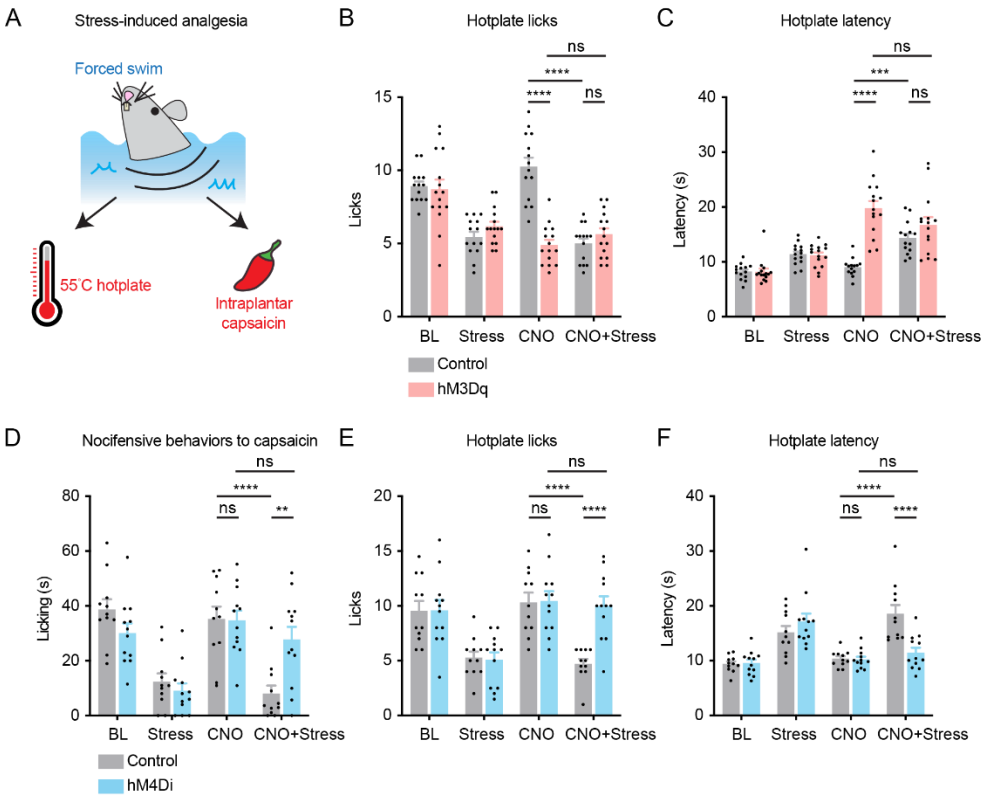

Figure 28. RVM-KOR neurons are required for stress-induced analgesia.

(A) Model to test stress-induced analgesia. Mice were forced to swim for 3 minutes and later tested on a hotplate or their responses to intraplantar capsaicin were quantified.

(B-C) Chemogenetic activation of RVM-KOR neurons produces responses similar to stress-induced analgesia as measured by hotplate (B) total licks and (C) latencies. Data are mean + SEM with dots representing individual mice (n=14 control, n=15 hM3Dq mice). Asterisks indicate the results of two-way repeated measures ANOVA with Bonferroni's correction (ns $p>0.05$, *** $p<0.001$, **** $p<0.0001$).

(D-F) Chemogenetic inhibition of RVM-KOR neurons abolishes stress-induced analgesia as measured by (D) nocifensive responses to capsaicin, hotplate (E) total licks, and (F) latencies. Data are mean + SEM with dots representing individual mice (n=11 control, n=12 hMDi mice). Asterisks indicate the results of two-way repeated measures ANOVA with Bonferroni's correction (ns $p>0.05$, ** $p<0.01$, **** $p<0.0001$).

10.4 Discussion

In our pharmacological experiments, we found that microinjection of the kappa agonist, U69,593, into the RVM, resulted in an increase in sensitivities to cold and thermal stimuli. This is consistent with previous studies that found that microinjection of U69,593 (at a similar dose and volume, scaled down to by weight from rat to mouse) reversed morphine-induced analgesia (Pan, Tershner, and Fields 1997; Meng et al. 2005) and precipitated mechanical allodynia in a chronic injury model (De Felice et al. 2011). These data support that RVM-KOR neurons tonically suppress nociception, which is facilitated with their temporary pharmacological inhibition.

Notably, this is in contrast with another study which found that microinjection of the same kappa agonist into the RVM promoted anti-nociception to thermal stimuli in freely-behaving rats (Ackley et al. 2001). The differences observed in our study may be attributed to two main factors: first, most of the prior literature pertaining to the descending modulation of pain centered upon studies in rats, whereas our studies were conducted in mice. There are important considerations regarding the physiological, behavioral, anatomical, and biochemical differences between rats and mice. Such differences may have contributed to our divergent findings. Secondly, the concentration and volume of the injection is important because, as we found in prior chapters, many RVM neurons express KOR, including those containing MOR. It is possible that kappa agonism in previous work may have inhibited the dual MOR/KOR-expressing ON cells, thereby eliciting responses consistent with analgesia. In our experiments, we did not observe analgesia, suggesting that our agonism of KOR preferentially targeted OFF cells, but it may account for the differences observed in our study. In support of this possibility, it has been shown that U69,593 inhibits the ON cell burst (Meng et al. 2005), suggesting that

some ON cells also express the kappa opioid receptor. Still, it remains unknown how these mixed ON cells could modulate the activity of GABAergic, spinally-projecting RVM-KOR OFF cells.

Extensive pharmacological studies into endogenous analgesic pathways have established that the CNS has the capacity to provide relief to chronic pain patients when engaged by alternative methods such as the placebo effect, stress, mindfulness, fear or pleasure (Fechir et al. 2012; Kut et al. 2011; Sharon et al. 2016; Eippert et al. 2009). Our findings suggest that RVM-KOR neurons participate in the state-dependence of pain modulation. In particular, we found that RVM-KOR neurons are required for the behavioral expression of stress-induced analgesia. Thus these neurons may provide a key entry-point into the body's powerful endogenous pain-modulatory system. RVM-KOR neurons may represent a target for the treatment of pain disorders.

11.0 Dynorphin input from the PAG modulates pain and itch

11.1 Introduction

In this section, we investigated potential inputs to RVM-KOR neurons. In particular, we test the contributions of dynorphin-PAG neurons in pain and itch as a possible pre-synaptic pathway to RVM-KOR neurons. This is due to two reasons: first, dynorphin is the endogenous peptide for the kappa opioid receptor (Kardon et al. 2014). Furthermore, the most well-studied region projecting to the RVM is the PAG. Lesioning and inactivation of the RVM (with local anesthetics) block the antinociceptive action of PAG (Behbehani and Fields 1979; Prieto, Cannon, and Liebeskind 1983; Gebhart 1982). Thus, the RVM is a necessary component within the descending modulatory circuit activated by stimulation of the PAG. On this basis, we wanted to test the contributions of possible dynorphinergic inputs from the PAG to the RVM.

11.2 Methods

Mice

The studies were performed in both male and female mice 8-10 weeks of age. All animals were of the C57Bl/6 background. KOR-Cre and Pdyn-Cre (Jax #027598) mice were used. Even numbers of male and female mice were used for all experiments. Mice were given free access to food and water and housed under standard laboratory conditions. The use of animals was approved by the Institutional Animal Care and Use Committee of the University of Pittsburgh.

Pharmacologic agents

Clozapine-N-oxide (Tocris) was dissolved in PBS and administered intraperitoneally (5mg/kg) or locally via cannula injection (1mmol in 300nl). nor-Binaltorphimine dihydrochloride (norBNI; Sigma, 100ng in 250nl) was dissolved in sterile saline and microinjected into the RVM. Chloroquine diphosphate salt (Sigma) was dissolved in physiological saline (100µg in 10µL) and administered intradermally.

Intradermal injections

For intradermal injection of chloroquine, hair was removed at least 24 hours before the experiment. Chloroquine (100µg in 10µL) was administered into the nape of the neck or calf, which could be subsequently visualized by the formation of a small bubble under the skin. These procedures were performed in awake mice.

Stereotaxic injections and cannula implantation

Animals were anesthetized with 2% isoflurane and placed in a stereotaxic head frame. A drill bit (MA Ford, #87) was used to create a burr hole and custom-made metal needle (33 gauge) loaded with virus was subsequently inserted through the hole to the injection site. Virus was infused at a rate of 100nL/min using a Hamilton syringe with a microsyringe pump (World Precision Instruments). Mice received 250-500 nL of virus (AAV2.hSyn.DIO.mCherry Addgene #50459; AAV2.hSyn.DIO.hM3D(Gq)-mCherry, Addgene #44361; AAVr.EF1a.DIOhChR2(H134R).eyfp-wpre-hghpa, Addgene 20298; AAVr-FLEX-tdTomato, Addgene 28306). The injection needle was left in place for an additional 15 min and then slowly withdrawn over another 15 min. Injections and cannula implantations were performed at the following coordinates for each brain region: RVM: AP -5.80 mm, ML 0.00 mm, DV -6.00 and vlPAG: AP -4.70 mm, ML ± 0.74 mm, DV: -2.75. For implantation of guide cannulas (P1

Technologies), implants were slowly lowered 0.300-0.500 mm above the site of injection and secured to the skull with a thin layer of Vetbond (3M) and dental cement. The incision was closed using Vetbond and animals were given ketofen (IP 10 mg/kg) and allowed to recover over a heat pad. Mice were given 4 weeks to recover prior to experimentation.

Behavior

All assays were performed in the Pittsburgh Phenotyping Core and scored by an experimenter blind to treatment.

Observation of scratching behavior

All tests were performed in a blinded manner. Scratching behavior was observed using a previously reported method (Kardon et al. 2014). On the testing day, the mice were individually placed in the observation cage (12x9x14 cm) to permit acclimation for 30 minutes. Scratching behavior was videotaped for 30 minutes after administration of chloroquine. The temporal and total numbers of scratch bouts by the hind paws at various body sites during the first 30 minutes after intrathecal injection were counted.

Hargreaves testing

Animals were acclimated on a glass plate held at 30°C (Model 390 Series 8, IITC Life Science Inc.). A radiant heat source was applied to the hindpaw and latency to paw withdrawal was recorded (Hargreaves et al. 1988). 2 trials were conducted on each paw, with at least 5 min between testing the opposite paw and at least 10 min between testing the same paw. To avoid tissue damage, a cut off latency of 20 sec was set. Values from both paws were averaged to determine withdrawal latency.

Von Frey testing

Mechanical sensitivity was measured using the Chaplan up-down method of the von Frey test (Chaplan et al. 1994). Calibrated von Frey filaments (North Coast Medical Inc.) were applied to the plantar surface of the hindpaw. Lifting, shaking, and licking were scored as positive responses to von Frey stimulation. Average responses were obtained from each hindpaw, with 3 min between trials on opposite paws, and 5 min between trials on the same paw.

Cold plantar assay

Paw withdrawal to cold sensitivity was measured as previously described (Brenner et al. 2015; Brenner, Golden, and Gereau 2012). Briefly, animals were acclimated to a 1/4" glass plate and crushed dry ice was packed into a modified 3 mL syringe and used as a probe. The dry ice probe was applied to the glass beneath the plantar hindpaw and the latency to withdrawal was recorded. Two trials were conducted on each hindpaw, with 3 min between trials on opposite paws, and 5 min between trials on the same paw. A cut off latency of 20 s was used to prevent tissue damage. Withdrawal latencies for each paw were determined by averaging values across 2 trials per paw.

Tail immersion test

Mice were habituated to mice restraints 15 minutes for 3 days before testing. Tails were immersed 3 cm into a water bath at 48°C, and the latency to tail flick was measured three times with a 1 minute interval between trials.

RNAscope in situ hybridization

Multiplex fluorescent in situ hybridization was performed according to the manufacturer's instructions (Advanced Cell Diagnostics #320850). Briefly, 16 um-thick fresh-frozen sections containing the RVM were fixed in 4% paraformaldehyde, dehydrated, treated

with protease for 15 minutes, and hybridized with gene-specific probes to mouse. Probes were used to detect tdTomato-C2 (#317041-C2), mCherry-C2 (#431201), Mm-Pdyn-C2 (#31877), Mm-Slc32a1-C3 (#319191), and Mm-Slc17a6-C3 (#319171). DAPI (#320858) was used to visualize nuclei. 3-plex positive (#320881) and negative (#320871) control probes were tested. Three to four z-stacked sections were quantified for a given mouse, and 3-4 mice were used per experiment.

Immunohistochemistry

Mice were anesthetized with an intraperitoneal injection of urethane, transcardially perfused, and post-fixed at least four hours in 4% paraformaldehyde. 40um and 25um thick RVM and spinal cord sections were collected on a cryostat and slide-mounted for immunohistochemistry. Sections were blocked at room temperature for two hours in a 5% donkey serum, 0.2% triton, in phosphate buffered saline. Primary antisera was incubated for 14 hours overnight at 4°C: rabbit anti-RFP (1:1K), chicken anti-GFP (1:1K), and mouse anti-NeuN (1:500). Sections were subsequently washed three times for 20 minutes in wash buffer (0.2% triton, in PBS) and incubated in secondary antibodies (Life Technologies, 1:500) at room temperature for two hours. Sections were then incubated in Hoechst (ThermoFisher, 1:10K) for 1 minute and washed 3 times for 15 minutes in wash buffer, mounted and cover slipped.

Image acquisition and quantification

Full-tissue thickness sections were imaged using either an Olympus BX53 fluorescent microscope with UPlanSApo 4x, 10x, or 20x objectives or a Nikon A1R confocal microscope with 20X or 60X objectives. All images were quantified and analyzed using ImageJ. To quantify images in RNAscope in situ hybridization experiments, confocal images of tissue samples (3-4

sections per mouse over 3-4 mice) were imaged and only cells whose nuclei were clearly visible by DAPI staining and exhibited fluorescent signal were counted.

Statistical analysis

All statistical analyses were performed using GraphPad Prism 8. Values are presented as mean +/- SEM. Statistical significance was assessed using tests indicated in applicable figure legends. Significance was indicated by $p < 0.05$. Sample sizes were based on pilot data and are similar to those typically used in the field.

11.3 Results

We injected Cre-dependent retrograde viral tracers into the RVM in Dyn-Cre mice to identify areas that could provide dynorphinergic inputs to the RVM (Figure 29A). We found robust labeling in many areas, including the parabrachial nucleus (PBN), dorsal reticular nucleus (Drt), and the agranular insular area (AIp); however, the most robust labeling was observed in the ventrolateral periaqueductal gray (vlPAG) (Figure 29A).

We characterized RVM-projecting Dyn-PAG neurons using CTB and AAVr-DIO-tdt (Figure 29B) and found that 10.4 +/- 4.0% Dyn-PAG neurons project to the RVM. Using a complementary approach involving retrograde viral labeling and FISH, we found that this population represented 32.3 +/- 2.1% of RVM-projecting Dyn-PAG neurons. We found that these Slc17a6-expressing (glutamatergic) neurons comprised 99.3 +/- 0.7% of all RVM-projecting PAG neurons (Figure 29C). We also found that Dyn-PAG neurons represented a population that was molecularly distinct from a recently described population of Tac1-PAG neurons (Gao et al. 2019) (Figure 30A-C).

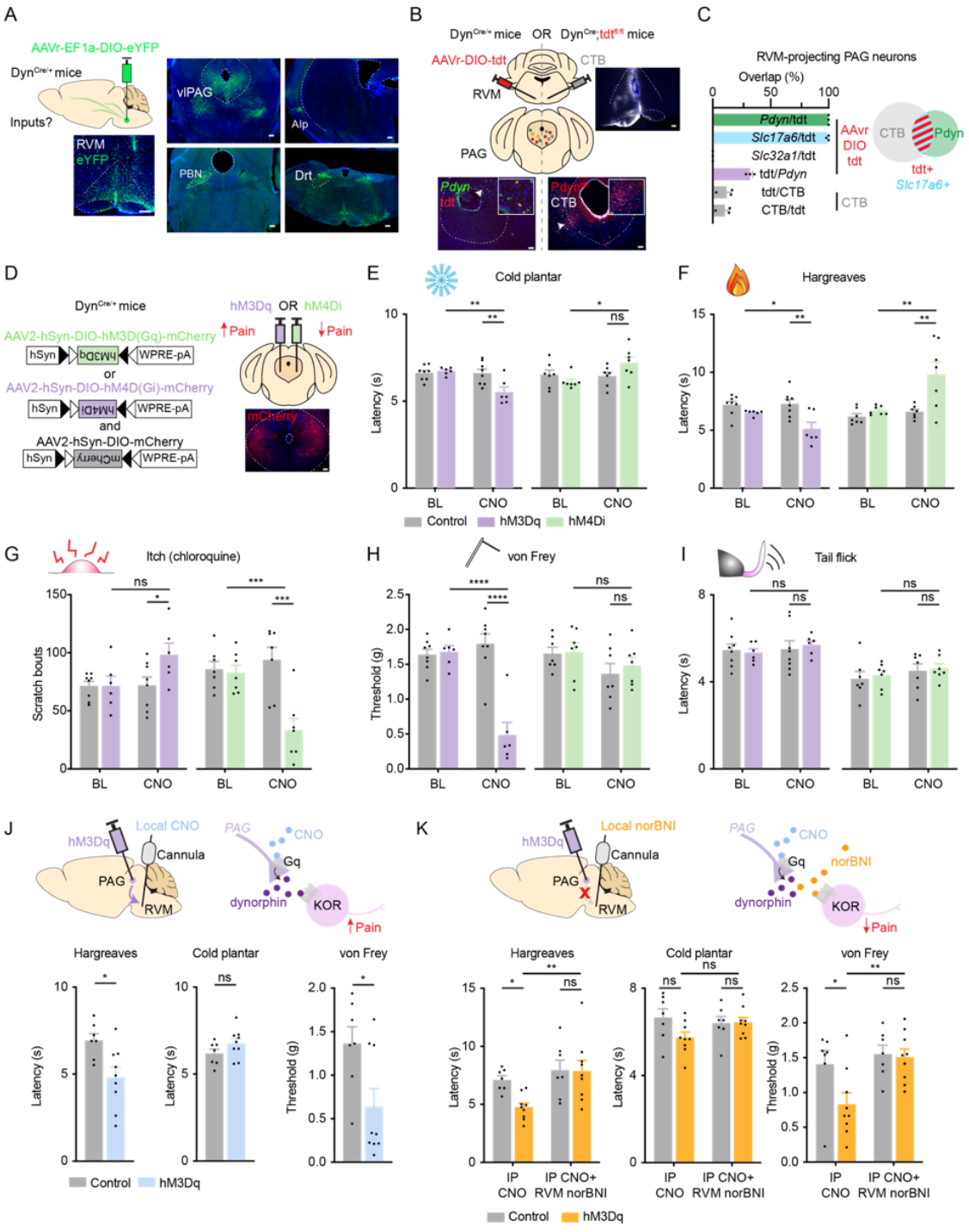

Figure 29. Pdyn-PAG neurons provide input to the RVM and bidirectionally modulate pain.

(A) Experimental strategy to trace dynorphinergic inputs to the RVM. Robust labeling was observed in the vlPAG of Dyn-Cre mice receiving AAVr-Ef1a-DIO-eYFP to the RVM. vlPAG: ventrolateral periaqueductal gray, PBN: parabrachial nucleus, AIp: agranular insular area, Drt: dorsal reticular nucleus. Scale bar = 50 μm.

(B) Approach to characterize dynorphin neurons projecting to the RVM. In one experiment, mice Dyn-Cre mice receiving Cre-dependent AAVr-DIO-tdt in the RVM and RVM-projecting neurons were further characterized using FISH. In a separate experiment, Dyn-Cre;tdt mice received CTB and back labeled CTB neurons were quantified. Scale bar = 50 μm.

(C) Summary of RVM-projecting dynorphin-PAG neurons characterization. Data are mean + SEM with dots representing individual mice.

(D) Experimental strategy to bidirectionally modulate pain behaviors following chemogenetic activation (purple) and inhibition (green) of Dyn-PAG neurons. Scale bar = 50 μm.

(E-I) Chemogenetic activation with hM3Dq (purple, left) and inhibition with hM4Di (green, right) on (E) cold plantar assay, (F) hargreaves assay, (G) chloroquine-evoked itch, (H) von Frey assay, and (I) tail flick assay. Data are mean + SEM with dots representing individual mice (n=8 hM3Dq control, n=6 hM3Dq, n=7 hM4Di control, n=7 hM4Di mice). Asterisks indicate the results of two-way repeated measures ANOVA with Bonferroni's correction (ns $p>0.05$, * $p<0.05$, ** $p<0.01$, *** $p<0.001$, **** $p<0.0001$).

(J) Experimental approach to selectively activate Dyn-PAG neurons containing hM3Dq by delivery of local CNO to the RVM. Chemogenetic activation facilitates responses to thermal and mechanical, but not cold testing. Data are mean + SEM with dots representing individual mice (n=7 control, n=9 hM3Dq mice). Asterisks indicate the results of unpaired t-test (ns $p>0.05$, * $p<0.05$).

(K) Experimental approach to block input from Dyn-PAG neurons containing hM3Dq by delivery of local norBNI to the RVM. Pharmacological blockade of Dyn-PAG activation reverses thermal and mechanical, but not cold testing. Data are mean + SEM with dots representing individual mice (n=7 control, n=9 hM3Dq mice). Asterisks indicate the results of two-way repeated measures ANOVA with Bonferroni's correction (ns $p>0.05$, * $p<0.05$, ** $p<0.01$, *** $p<0.001$, **** $p<0.0001$).

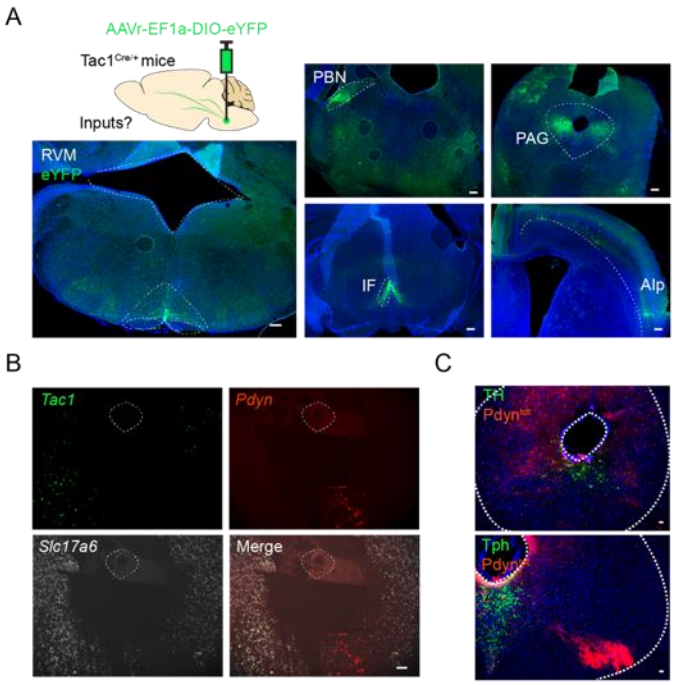

Figure 30. Further characterization of PAG neuronal cell types.

(A) Experimental strategy to trace Tac1 inputs to the RVM. vlPAG: ventrolateral periaqueductal gray, PBN: parabrachial nucleus, AIp: agranular insular area, IF: interfascicular nucleus. Scale bar = 50 μm.
(B) FISH characterization of Pdyn, Tac1, and Slc32a1 expression in the PAG. Scale bar = 50 μm.
(C) Immunohistochemical characterization of Dyn;tdt neurons and TH (tyrosine hydroxylase) and Tph (tryptophan hydroxylase). Scale bar = 50 μm.

11.3.1 Dynorphin-PAG neurons modulate itch and pain

Recent work has revealed that specific manipulation of glutamatergic and GABAergic PAG neurons can bidirectionally modulate pain and itch (Samineni et al. 2017, 2019). We used chemogenetics to bidirectionally modulate the dynorphin population of PAG neurons using Cre-dependent hM3Dq and hM4di in Dyn-Cre mice to activate and inhibit these neurons, respectively (Figure 29D). Mice received either AAV2-hSyn-DIO-hM3Dq-mCherry or AAV2-hSyn-DIO-hM4Di-mCherry. We found that chemogenetic activation and inhibition with IP CNO bidirectionally modulated thresholds to cold plantar and hargreaves testing (Figure 29E, F) and

chloroquine-evoked itch (Figure 29G). Although chemogenetic activation reduced mechanical thresholds (Figure 29H), inhibition did not elevate thresholds above baseline (Figure 29H). Neither activation nor inhibition of Dyn-PAG neurons affected latencies to tail flick (Figure 29I). Overall, we found that activation of Dyn-PAG neurons facilitated pain, whereas inhibition of these neurons reduced sensitivities to cold, thermal, and itch responses.

We confirmed that Dyn-PAG neurons facilitated pain through their input to the RVM by implanting cannulas in the RVM for the local delivery of CNO (Figure 29J). This allowed us to selectively activate RVM-projecting PAG neurons. We found that the selective chemogenetic activation of this pathway generally recapitulated our findings following IP CNO (Figure 29F, H) and facilitated sensitivity to thermal and mechanical testing (Figure 29J).

11.3.2 Dynorphinergic pathways from the PAG to RVM modulates nociception

To test more directly whether Dyn-PAG neurons could exert their effects through dynorphin signaling in the RVM, we used a pharmacological approach to block dynorphin input to the RVM following activation of Dyn-PAG neurons (Figure 29K). We found that IP CNO reduced latencies to hargreaves testing and mechanical thresholds in the von Frey assay. However, microinjection of norBNI prior to the administration of IP CNO blocked the development of thermal and mechanical hypersensitivity (Figure 29K). Thus, these data suggest that Dyn-PAG neurons facilitate pain through dynorphin signaling in the RVM.

11.4 Discussion

Recent studies into the PAG using Cre drivers targeting Vgat (GABAergic) and Vglut2 (glutamatergic) neurons have revealed that these two classes of neurons divergently modulate nociception. Through careful chemogenetic and optogenetic studies, Vgat neurons have been shown to be pain facilitating, whereas Vglut2 are anti-nociceptive (Samineni et al. 2019, 2017). Interestingly, these two populations of PAG neurons exhibit modality-specificity and are differentially engaged to modulate pain and itch: Vgat and Vglut2 neurons inhibit and facilitate itch, respectively (Samineni et al. 2019). Another cell type that has recently been examined using genetic approaches are Tac1-PAG neurons. Glutamatergic PAG neurons containing Tac1 have recently been shown to be involved in the facilitation of itch (Gao et al. 2019). Calcium imaging of this population found them to be active during itch behaviors. Chemogenetic activation and inhibition of Tac1 neurons identified that they are both sufficient and necessary for itch and their behavioral effects were mediated through glutamate signaling in the RVM. Interestingly, these neurons were not found to be involved in nociception (Gao et al. 2019).

Here, we tested the role of dynorphin-PAG neurons in the modulation of pain and itch. In contrast to other recent work, we found that dynorphin neurons participate in the modulation of both itch and pain. Chemogenetic activation of these neurons facilitated both itch and pain, representing a departure from studies of Vgat/Vglut2 populations, which were found to differentially modulate itch and pain (Samineni et al. 2019, 2017). We also found that RVM-projecting dynorphin-PAG neurons are overwhelmingly glutamatergic, which is consistent with previous investigations into Vglut2 and Tac1-PAG populations and their roles in facilitating itch. Lastly, our pharmacological blockade of dynorphinergic-PAG signaling to the RVM using

norBNI expands on prior work by demonstrating that the PAG functionally provides inputs to the RVM and provides the primary source of dynorphin to the RVM to facilitate pain.

12.0 Conclusion

Our study identifies the role of RVM-KOR neurons in the inhibition of pain and itch. Previous work has also implicated the role of RVM-KOR neurons as OFF cells (Pan, Tershner, and Fields 1997; Pan, Williams, and Osborne 1990; Pan, Hirakawa, and Fields 2000). However, depending on the assay tested and whether the animals were lightly anesthetized (Pan, Tershner, and Fields 1997; Pan, Williams, and Osborne 1990; Pan, Hirakawa, and Fields 2000) or awake (Ackley et al. 2001; Meng et al. 2005), there was controversy as to whether RVM neurons responsive to kappa agonists could be pro- or anti-nociceptive. Indeed, our neurochemical characterization of RVM-KOR neurons reveals that they comprise a heterogeneous population; yet our ability to capture and manipulate spinally-projecting RVM-KOR neurons identifies them as a unique and molecularly distinct subgroup of all RVM-KOR neurons. We found that the targeting of a small number of RVM-KOR neurons that project to the spinal cord was sufficient to produce anti-nociception and revealed that RVM-KOR neurons are required for stress-induced analgesia.

A considerable amount of work has been conducted to examine how the RVM could contribute to the state-dependence of somatosensation, including nociception (Mason 2001; Mason, Gao, and Genzen 2007; Mason et al. 2001; Leung and Mason 1999; Foo and Mason 2003; Hellman and Mason 2012). In support of this view, in our loss-of-function experiments, we found that RVM-KOR neurons are required for stress-induced analgesia. Our findings suggest that in addition to the inhibition of nociception, acute, and chronic pain, these RVM-KOR neurons are also engaged in a state of stress. Such a protective mechanism may explain, for example, how firefighters are able perform their heroic duties, despite hazardous and extreme

conditions. Curiously, our experiments also uncovered the possible role of other KOR neurons in the brainstem that could drive profound and diverse functions in movement and arousal whose precise identities and roles remain to be further elucidated.

Dynorphin signaling within the brain has been shown to be involved in myriad behaviors, including stress, addiction, analgesia (Chavkin 2011; Bruchas, Land, and Chavkin 2010). We found that the selective activation and inhibition of dynorphin neurons in the PAG facilitates and inhibits nociception, respectively. Using pharmacological approaches, we determined that these PAG neurons influence nociception through their release of dynorphin within the RVM. This finding, together with the observation that we and others have made that RVM neurons are sensitive to kappa agonism and antagonism, suggest that the descending modulation of pain is influenced by dynorphin signaling between the PAG and RVM. Identification of this dynorphinergic pathway may provide opportunities to take advantage of the body's endogenous opioid system to manage pain. Approaches that make use of the powerful endogenous pain-modulatory system can reduce the need for pharmacological treatments, such as opioids, with fewer side effects and improved outcomes for the treatment of pain disorders.

12.1 Limitations

12.1.1 A simplistic view of inputs to KOR RVM neurons

We tested the contributions of dynorphin-PAG neurons in pain and itch as a possible pre-synaptic pathway to RVM-KOR neurons because 1) dynorphin is the endogenous peptide for the kappa opioid receptor (Kardon et al. 2014) and 2) the PAG is a well-established source of input

to the RVM. We identified a dynorphinergic pathway from the PAG that modulates itch and pain, which we hypothesize directly engages RVM-KOR neurons. In our tracing studies, however, we also observed robust labeling of possible dynorphin inputs from other brain regions including the PBN and dorsal reticular nucleus. Our group has recently uncovered the role of dynorphin PBN neurons as a source for conveying nociceptive information between distinct subnuclei within the PBN (Chiang et al. 2020). Furthermore, activation of PBN terminals in the RVM has been found to inhibit OFF cells and activate ON cells, giving rise to pro-nociceptive phenotypes (Chen et al. 2017). Here, we also provide evidence that dynorphin neurons from several areas including the PAG, PBN, and dorsal reticular areas project to the RVM. Whether these represent distinct subpopulations of dynorphin neurons is not yet known, but given the importance of the PBN as the target of ascending nociceptive inputs, it is conceivable that these neurons may coordinate appropriate nocifensive responses through an RVM-dependent circuit. However, this possibility was not tested in our study. Analogous approaches that were used in our study to determine inputs from the PAG could also be used to characterize and manipulate a dynorphinergic PBN to RVM circuit in the future.

We examined the role of dynorphin inputs because dynorphin is the endogenous peptide for the kappa opioid receptor. However, RVM neurons have been found to respond to numerous pharmacological agents, reflective of their receptor heterogeneity. Thus, RVM-KOR neurons may also receive inputs from other peptide ligands as well as fast transmitters, such as GABA and glutamate, which were not explicitly tested in our study. KOR and MOR have been shown, for instance, to overlap in the RVM (Gutstein et al. 1998). However, our FISH characterization revealed that spinally-projecting KOR neurons do not express MOR, suggesting that, at least among the descending neurons, these receptors mark distinct subpopulations. The use of

retrograde tracers, such as rabies virus, and Cre-dependent AAV helpers will more comprehensively reveal additional inputs to RVM-KOR neurons. Combined with neurochemical and electrophysiological approaches, these studies will reveal the nature of the cell types and transmitters involved in RVM-KOR signaling.

Another limitation of our focus on dynorphin PAG neurons is the observation that these neurons are exclusively glutamatergic, whereas dynorphin activation of the kappa opioid receptor generally leads to the inhibition of KOR-expressing cells through Gai signaling. Although the PAG to RVM projection has been suggested to be excitatory, it has also been proposed that inhibitory output from the PAG helps maintain the GABA tone at the level of the RVM (Behbehani and Fields 1979; Morgan et al. 2008). However, most of the current evidence supports the hypothesis of local GABAergic tone in the PAG which regulates excitatory projections to the RVM (Reichling and Basbaum 1990; Cho and Basbaum 1991; Morgan et al. 2008). Presently, it is unclear how these excitatory dynorphin neurons could modulate the activity of RVM-KOR cells. Our pharmacological blockade of dynorphin inputs to the RVM with norBNI, combined with the observation that chemogenetic manipulation of dynorphin-PAG neurons produces the opposite effect of RVM-KOR manipulation suggests that dynorphin-PAG neurons use dynorphin as their primary transmitter to inhibit RVM-KOR cells. Future electrophysiological recordings of RVM-KOR neurons with simultaneous manipulation of dynorphin-PAG neurons may further elucidate the nature of this circuit.

Lastly, we did not examine the roles of dynorphin-PAG neurons beyond itch and pain. The PAG functions as a hub for many other aspects of physiology and behavior, including autonomic function, motivated behaviors, as well as nociception, which warrant further investigation (Silva and McNaughton 2019; Behbehani 1995; Koutsikou et al. 2015; Morgan and

Clayton 2005; Comoli, Ribeiro-Barbosa, and Canteras 2003; Dampney et al. 2013; Li et al. 2018).

12.1.2 Confounding motor and arousal findings

In our study, we emphasize the role of spinally-projecting RVM-KOR neurons in the inhibition of itch and pain. However, considerable efforts have been conducted to characterize the roles of RVM neurons in myriad behaviors, including sleep, feeding, thermoregulation, sexual climax, movement, and behavioral arousal (discussed further in the future directions) (Mason 2001; Mason, Gao, and Genzen 2007; Mason et al. 2001; Leung and Mason 1999; Foo and Mason 2003; Hellman and Mason 2012) . In accordance with this idea, we also observed in our experiments that the non-specific activation of either local RVM-KOR interneurons and/or non-spinally-projecting RVM-KOR neurons appear to be involved in both locomotion (as determined using rotarod and openfield assays) and arousal (as determined by the lack of acoustic startle to loud sounds).

Given the robust motor and arousal phenotypes, we were required to consider the possibility that either or both of these confounds could affect the interpretation of our somatosensory findings; for instance, because the mice were not moving in the openfield, one could conclude that they lacked the motor coordination to perform withdrawal reflexes and because mice were unresponsive to 115 dB presentations, then perhaps they would not scratch in response to intradermal chloroquine. These confounds necessitated the serial dilution of the viral titer used to capture fewer and fewer neurons with the goal of separating these variables. Because of technical limitations, and the apparent intermingling of these heterogeneous KOR-expressing cell types by FISH, it was not possible to simply restrict our viral targeting to sub-nuclei of the

RVM. Although there may be some organization (our very dilute titer was more circumscribed to the RMg and NGCa), only with the very dilute virus were we able to prevent the non-specific infection of other KOR-expressing brainstem neurons during needle reflux. Furthermore, given that nearly six cohorts of animals were generated by these dilutions, we were unable to perform motor, arousal, and somatosensory assays on all cohorts and only tested animals for pruritogen-evoked scratching when we observed the loss of spinal innervation in the animals receiving very dilute titers. Due to these limitations, it is possible that even with the diluted titers used, we may have captured some neurons that modulate movement and arousal. Nevertheless, our complementary approach using a retrogradely-labeled virus, which allowed us to selectively manipulate only the spinally-projecting RVM-KOR neurons, yielded highly consistent results with respect to the inhibition of itch and pain behaviors.

12.1.3 Molecular heterogeneity of KOR RVM neurons

Our initial FISH characterization of RVM-KOR neurons using several genetic markers revealed that they constituted a diverse population. Although we were able to directly manipulate spinally-projecting RVM-KOR neurons and found that this population is exclusively GABAergic, it remains an open question the functions of the non-spinally-projecting KOR RVM neurons as well as the GABAergic spinally-projecting neurons that do not contain KOR.

The role of inhibitory neurons, as a collective population, is still hotly contested; one study, using very similar approaches to those used in our study, uncovered the role of Vgat-RVM neurons in the facilitation of mechanical, but not heat pain; however, another study found Gad2-RVM neurons (which comprise a subpopulation of Vgat neurons) to be involved in the inhibition of mechanical and theraml pain. Our manipulation of Gad2-RVM neurons is in agreement with

the latter group, where activation of these cells was also anti-nociceptive. We also found that the spinally-projecting RVM-KOR neurons are exclusively GABAergic and broadly inhibit pain and itch. Thus, it is likely that GABAergic neurons in the RVM span several functional subgroups and differences in behavioral findings may reflect the relative subpopulations that are captured with viral approach used. Nevertheless, technological advances involving intersectional genetic approaches provide several advantages that can allow us to continue to identify and directly manipulate unique RVM subpopulations in freely-behaving mice.

12.1.4 Targeting of KOR RVM neurons

We also did not report the injection or implantation site of every mouse that received a viral injection or a cannula surgery. Over four hundred animals, across six different Cre alleles, were used in this study and efficiency was prioritized over validation. Although this is an important limitation to the study, we will, in future experiments, validate the expression of fos within RVM-KOR neurons mice that received an anterograde hM3Dq virus in the RVM as well as in animals receiving AAV-retro into the spinal cord with cannula implantation in the RVM. We also used a high dose of CNO in most experiments (5 mg/kg IP and 0.3 nmol intracranial) and did not perform a dose-response analysis to determine the specificity of the agonist to the behaviors observed. However, some of the concerns of off-target effects of CNO (or its back-metabolite, clozapine) are mitigated due to the use of control animals that received a control viral vector and were exposed to the same doses of IT, intracranial, and IP CNO.

12.2 Future Directions

12.2.1 Role of KOR neurons beyond nociception

In our study, we were surprised to find that the chemogenetic activation of KOR-expressing RVM neurons affected motor and arousal states. Although the use of the KOR-Cre allele allowed us to selectively target KOR-expressing neurons in the brainstem, we found that many brainstem neurons expressed KOR and that these neurons, identified with FISH, represented a heterogenous group. Although we were able to selectively manipulate only the spinally-projecting RVM-KOR neurons and assess their contributions to itch and pain, it remains unknown the other functions of KOR-expressing brainstem neurons. Given the striking behavioral phenotypes, including the suppression of acoustic startle and locomotor deficits, we hypothesize that the non-spinally projecting RVM-KOR neurons may be involved in other homeostatic, motor, and arousal functions. Further dissection of RVM-KOR neurons, which may include a combination of optogenetics or retrograde targeting to isolate distinct pathways arising from the RVM may help to disentangle these complex functions. We found robust labeling within the reticular formation, the superior colliculus, the nucleus of the solitary tract, thalamic, and hypothalamic structures. It is possible that some, or a combination, of these targets could mediate the effects observed. Given the role of medullar neurons in the autonomic regulation, movement, and behavioral arousal (discussed in the introduction of this section), the use of additional assays may allow for the assessment of the contribution of RVM-KOR neurons in functions beyond pain.

12.2.2 Spinal circuits influenced by descending modulation

The spinal cord represents the final target of the pain descending modulatory system. Electrical stimulation of the PAG and RVM induce analgesia that is spinally-mediated; this form of analgesia can be blocked by spinal cord delivery of agents such as lidocaine or modulating monoamine or adrenergic systems, hinting at an interaction between descending circuits and the spinal cord (Sandkühler, Fu, and Zimmermann 1987; Carstens et al. 1981; Rydenhag and Andersson 1981; Camarata and Yaksh 1985; Jensen and Yaksh 1984). Moreover, both the PAG and RVM have been reported to modulate spinal cord circuitry in a fiber-specific fashion. It has been shown that spinal cord neurons receiving C-type fiber inputs are preferentially suppressed during PAG or RVM stimulation (Heinricher et al. 2009; Hentall and Fields 1979; Waters and Lumb 2008; Koutsikou et al. 2007). These observations support that descending pathways target specific spinal neurons to modulate pain.

Recent efforts have begun to elucidate the precise identities of spinal neurons that receive input from the RVM in the context of somatosensation. Optogenetic and chemogenetic manipulations of Vgat-Cre RVM neurons have suggested that GABAergic RVM neurons descend to presynaptically inhibit mechanosensory input onto spinal inhibitory enkephalinergic (Penk) interneurons (François et al. 2017). Thus, this model posits that descending GABAergic neurons could facilitate mechanical nociception through the process of disinhibition of Penk neurons in the dorsal horn. Alternatively, combined optogenetic and electrophysiological experiments in spinal cord slices have suggested that GABAergic RVM-spinal projection neurons inhibit GRPR-expressing neurons in the spinal cord (Liu et al. 2019), a population that has been heavily implicated in driving itch (Sun and Chen 2007). Together, these reports suggest

that GABAergic RVM neurons could facilitate pain through inhibition of Penk spinal neurons, and inhibit itch through inhibition of excitatory GRPR neurons.

Given our finding that activation of GABAergic RVM-KOR neurons inhibits itch and pain, it is unlikely that Penk neurons are downstream of our circuit. However, we speculate that RVM-KOR neurons may inhibit itch through the inhibition of GRPR neurons. Nevertheless, we speculate that RVM-KOR neurons may engage many more subpopulations of spinal neurons due to their extensive innervation of many laminae of the spinal cord. Although we attribute our behavioral findings to an RVM-spinal circuit, it is unclear where in the spinal cord RVM-KOR neurons exert their influence; further work is necessary to determine precisely where and how RVM-KOR neurons elicit their antipruritic and anti-nociceptive effects.

12.2.3 Plasticity of RVM pathways in the transition from acute to chronic pain

Acutely, stress inhibits pain (Yilmaz et al. 2010) and stress-induced analgesia is thought to be mediated by the RVM (Shamsizadeh et al. 2014). Our findings support the idea that RVM neurons are required for stress-induced analgesia. Interestingly, chronic stress-induced hyperalgesia is also thought to be RVM-dependent (Jennings et al. 2014). Recent rodent work suggests that stress enhances the activity of GABAergic RVM neurons to inhibit the activity of spinal neurons producing enkephalins (François et al. 2017), thereby driving hyperalgesia. Still, it remains unclear how structural and functional changes occur within the RVM in the setting of chronic stress; characterization of plasticity in descending neural circuits could facilitate the development of improved, targeted therapies for chronic pain. Although we did not test this transition in our studies (and only examined stress-induced analgesia acutely), it would be interesting to determine which neurons may be differentially involved in the expression of

chronic stress-induced hyperalgesia, which may now be detected using in vivo microendoscopy in a chronic stress model.

Appendix introduction

The following appendix contains additional information pertaining to other major projects and studies that I have worked on throughout my graduate studies. Appendix A features experiments to reveal the molecular identities of PBN neurons and the effect of general inhibition of PBN neurons that I conducted as a contributing author as part of a larger body of work examining PBN circuits for nocifensive behaviors. Appendix B highlights experiments aimed at characterizing a possible tool to understand RVM neurons that express the mu-opioid receptor. Appendix C features experiments that examine the role of delta-opioid receptor signaling in itch behaviors. Appendix D contains neurochemical studies of the kappa-opioid receptor in the spinal cord dorsal horn. Appendix E evaluates the role of NK1R neurons in the descending modulation of itch and pain. Lastly, Appendix F assesses the functional role of neurons in the periaqueductal gray containing the mu-opioid receptor.

These, as well as additional projects, can be found in the following PubMed link: https://www.ncbi.nlm.nih.gov/myncbi/1-_4iDHumLdAx/bibliography/public/

Appendix A Neurochemical characterization of the PBN neurons and its role in nocifensive behaviors

Appendix A.1 Introduction

The lateral parabrachial nucleus (lPBN) participates in numerous homeostatic and nociceptive functions (Palmiter 2018; Carter et al. 2013; Carter et al. 2015; Han et al. 2015). Underlying its ability to coordinate physiological and behavioral changes are the diverse neuronal subpopulations within the PBN. Although a few of these populations have been ascribed to distinct functions, how well these markers define unique populations remains contested. As a part of my contribution to a larger study (Chiang et al. 2020), we used chemogenetics to globally inhibit PBN neurons to determine the role of the PBN in a variety of nociceptive assays. Furthermore, we performed fluorescent in situ hybridization of the PBN to evaluate the overlap among various markers of putative neuronal subpopulations.

Appendix A.2 Methods

RNAscope in situ hybridization

Multiplex fluorescent in situ hybridization was performed according to the manufacturer's instructions (Advanced Cell Diagnostics#320850). Briefly, 18mm-thick fresh-frozen sections containing the parabrachial nucleus were fixed in 4% paraformaldehyde, dehydrated, treated with protease for 15 minutes, and hybridized with gene-specific probes to

mouse Pdyn(#318771), Calca(#417961), Tac1(#410351), Fos(#316921), Slc32a1(#319191), and Slc17a6(#319171). DAPI (#320858) was used to visualize nuclei. 3-plex positive (#320881) and negative (#320871) control probes were tested. Two to three full-thickness z stacked sections were quantified for a given mouse, and 2 - 4 mice were used per experiment.

Behavioral tests described below were performed in a blinded manner.

Conditioned place aversion

Mice were placed in a two-chamber plexiglass box for 20 minutes and allowed to freely roam between one of two sides differentiated by visual cues (spots versus stripes). For two conditioning days, mice were restricted to one of two sides and received either no stimulation or CNO for 20-minute periods in the morning and afternoon. On the test day, mice were placed back into the box and allowed to freely explore either chamber. The behavior was recorded and post hoc analysis performed to determine body position using the open source software Optimouse as described in RTPA. For Formalin-induced CPA, mice were conditioned to 2% 10mL solution of formalin injected into either one hindpaw on the first day of conditioning and the contralateral hindpaw on the second day of conditioning. Control mice received no hindpaw injections. In experiments involving hM4D, mice were pretreated with CNO (5 mg/kg) 30 min prior to conditioning with formalin.

Tail immersion test

Mice were habituated to mice restraints 15 minutes for 5 days before testing. Tails were immersed 3 cm into a water bath at 48C or 55C, and the latency to tail flick was measured three times per temperature with a one-minute interval between trials. For optogenetic testing, mice were photostimulated for 10 s prior to tail immersion testing.

Appendix A.3 Results

Transient inhibition of the lPBN significantly reduced jumping behaviors, the inhibition of the tail flick response, and conditioned place aversion to a noxious stimulus **(Figures 1G-K)**. Collectively, these data suggest that activity in the lPBN is important to help an organism escape from a noxious stimulus and to learn avoidance. Fluorescent in-situ hybridization of the PBN confirmed that many of the previously identified neuronal populations (Palmiter 2018; Barik et al. 2018; Gao et al. 2019) are excitatory (based on expression of *Vglut2*) **(Figure 2A-D, G, and H)**. Furthermore, we found that the neurons that expressed *fos* in response to an aversive stimulus were also excitatory **(Figure 1E)**. Finally, we ablated Pdyn neurons and found a reduction in the expression of *fos* in *Pdyn* and *CGRP*, but not *Tac1* neurons **(Figure 3D-I)**, suggesting there may be some overlap and connectivity between the Pdyn and CGRP populations.

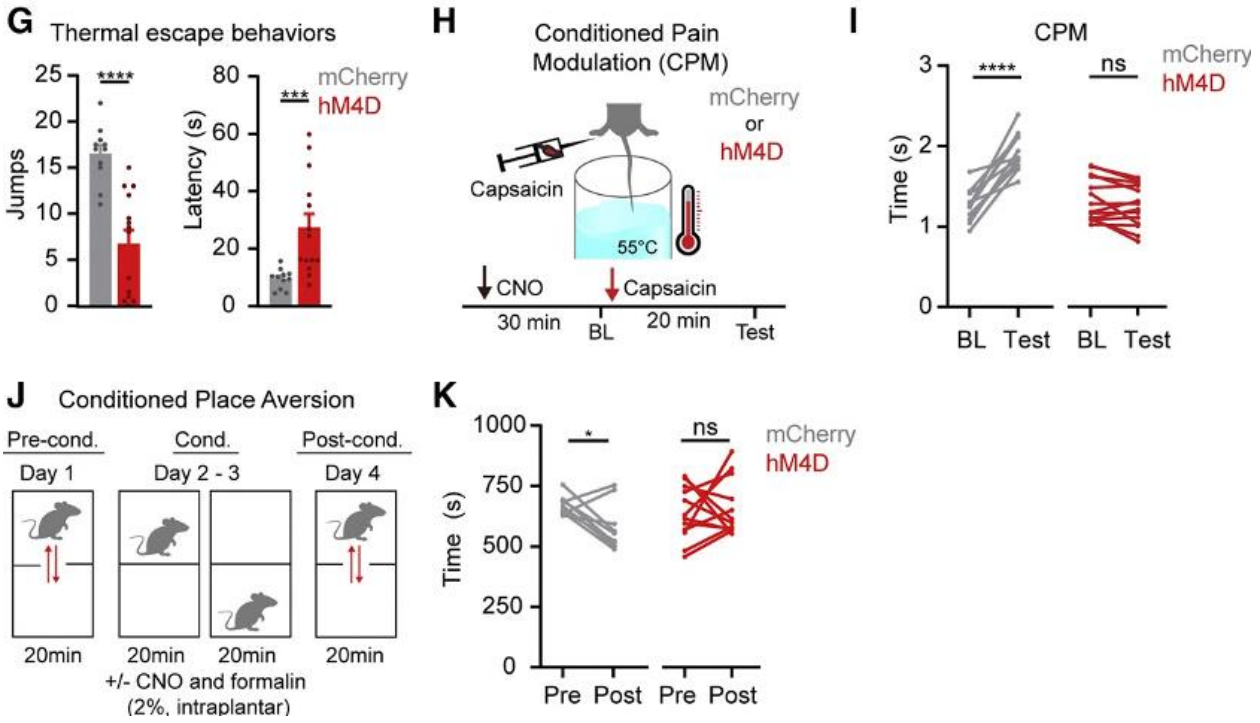

Appendix A Figure 1. lPBN Is Required for Numerous Behavioral Responses to Noxious Stimuli

D) Strategy to inhibit the lPBN through inhibition of excitatory neurons. (E) The PWT was significantly increased following intraperitoneal (i.p.) injection of CNO (orange bar) in hM4D mice compared with mCherry controls in a model of capsaicin-induced mechanical hypersensitivity. Data are mean ± SEM (n = 10–11 mice per group). Two-way RM ANOVA followed by Holm-Sidak post hoc test, ∗∗∗p < 0.001. (F) The PWT was significantly increased following i.p. injection of CNO (orange bar) in hM4D mice compared with mCherry controls in a model of CFA-induced mechanical hypersensitivity. Testing was performed 7 days post-CFA treatment. Data are mean ± SEM (n = 10–11 mice per group). Two-way RM ANOVA followed by Holm-Sidak post hoc test, ∗p < 0.05. (G) Escape behaviors from a 55°C plate increased significantly following i.p. injection of CNO in hM4D mice (red bars) compared with mCherry controls (gray bars). Data are mean ± SEM (n = 11–14 mice per group); ∗∗∗p < 0.001, ∗∗∗∗p < 0.001 (Student's t test). (H) Strategy to test for conditioned pain modulation (CPM) using intraplantar capsaicin (0.03%). (I) CPM was observed in mCherry control mice but not hM4D mice (n = 11–14 mice per group). ∗∗∗∗p < 0.0001; not significant (ns), p > 0.05 (paired Student's t test). (J) Protocol for conditioned place aversion (CPA). CNO was given 30 min prior to 2% intraplantar formalin on days 2 and 3, which was paired with one side of a two-chambered box differentiated by visual cues. (K) Formalin-induced CPA is observed in control mice but not in those expressing hM4D (n = 11–14 mice per group). ∗∗∗∗p < 0.0001); ns, p > 0.05 (paired Student's t test).

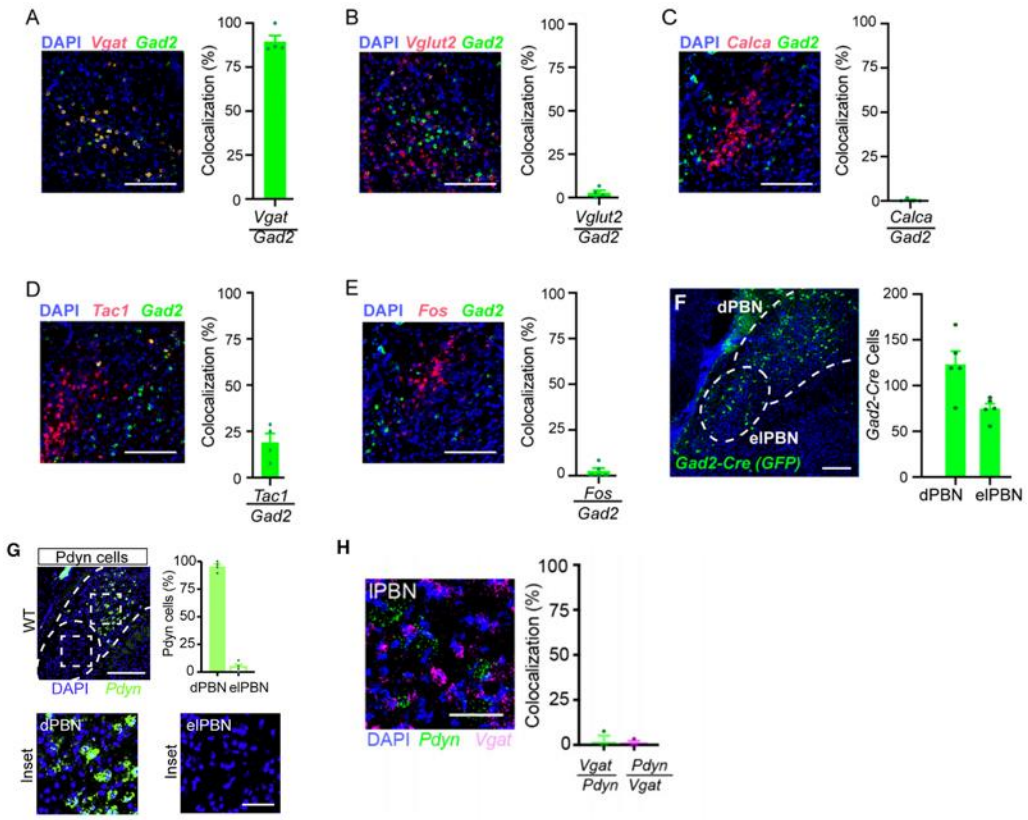

Appendix A Figure 2. Characterization of PBN neurons by fluorescent in-situ hybridization

(A – E) FISH was performed to characterize the neurochemical properties of Gad2 neurons for (A) Vgat, (B) Vglut2, (C) Calca, (D) Tac1, or (E) Fos following intraplantar capsaicin injection (0.03%; 10 µl; unilateral; tissue was collected 20 m after stimulation). (F) Visualization and quantification eYFP expression in dPBN and elPBN following stereotactic injection of Cre-dependent AAV encoding eYFP into GadCre mice. Data are mean and dots represent data points from individual animals (n = 4 - 5 mice). Scale bar = 100 µm. (G) Representative image and quantification of PdynCre-expressing neurons in the dPBN and elPBN as visualized by FISH (n = 4 mice). Scale bars, 100 µm; inset, 25 µm. (H) Representative image (left) and quantification (right) of the lPBN using dual FISH with probes targeting Pdyn and Vgat. Data are mean and dots represent data points from individual animals (n = 3 mice). Scale bar = 100 µm.

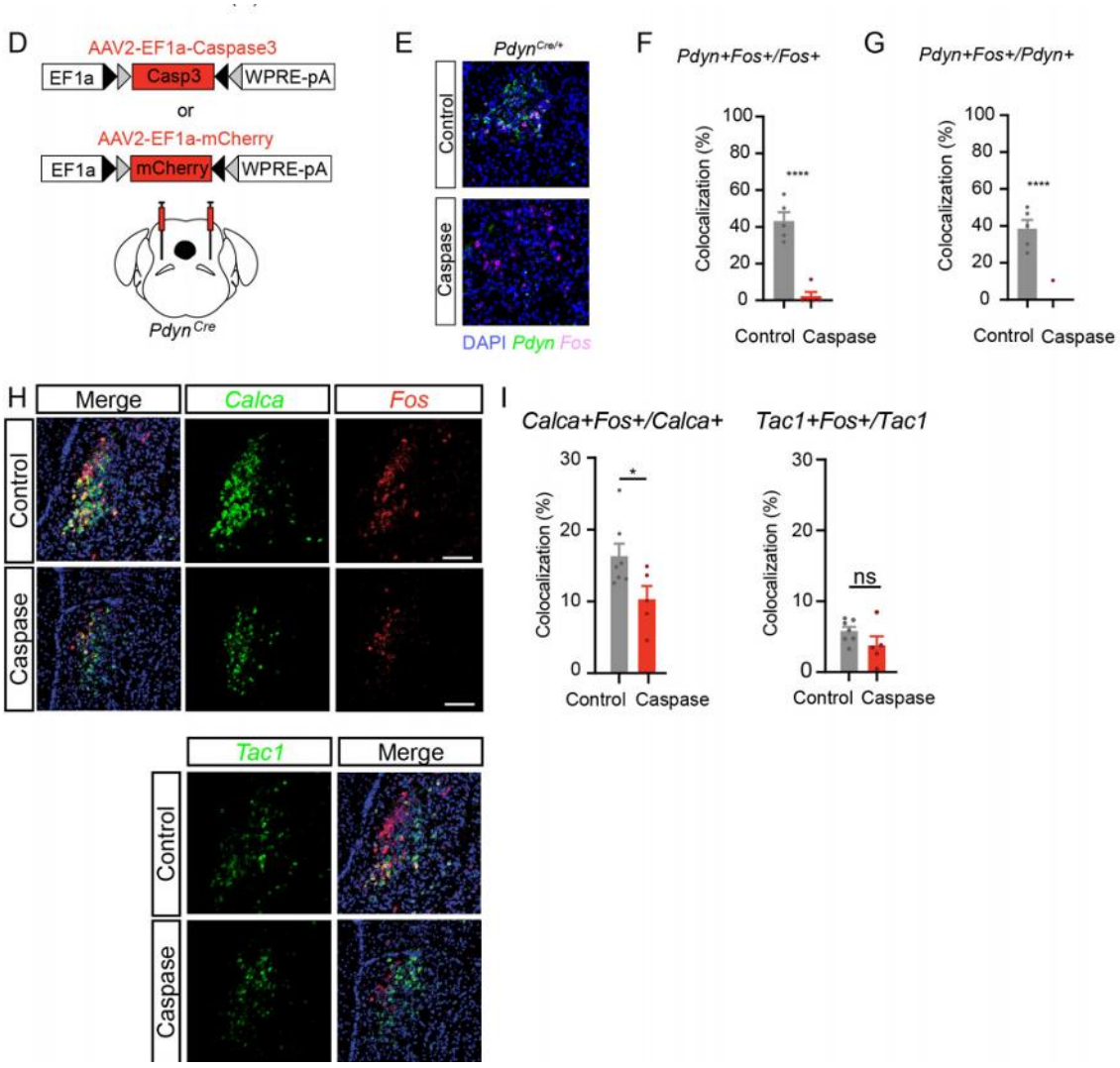

Appendix A Figure 3. Deletion of PBN-Pdyn neurons reduces activity in response to painful stimuli

(D) Strategy to ablate PdynCre lPBN neurons. (E) Representative images of co-localization of PdynCre and Fos in lPBN neurons following intraplantar capsaicin injection. (F) The proportion of Fos+ neurons that co-localized with PdynCre was significantly reduced in mice treated with capsaicin compared to control-treated mice (n = 5 mice per group). **** indicates $p < 0.0001$ (unpaired Student's t-test). (G) The proportion of PdynCre neurons that co-localized with Fos was reduced in mice treated with capsaicin compared to controltreated mice (unable to compare statistics as a result of complete or near complete loss of PdynCre neurons). (H) Representative images from multiplex FISH experiments for Fos (red), Calca (green, top) and Tac1 (pseudocolored green, bottom) between control vs. caspase-injected mice. (I) Ablation of PdynCre neurons in dPBN reduces the number of Fos expressing-Calca neurons in elPBN following intraplantar injection of capsaicin. Data are mean with dots representing individual animals (n = 5 – 7 mice) * indicates $p < 0.05$; n.s. indicates $p > 0.05$ (unpaired Student's t-test).

Appendix A.4 Discussion

Overall, these experiments helped to contextualize the role of Pdyn neurons within the PBN and validate prior suspicions that transiently inhibiting the PBN would have robust effects on nocifensive behaviors.

Appendix A.5 Bibliography

Barik, Arnab, James Hunter Thompson, Mathew Seltzer, Nima Ghitani, and Alexander T Chesler. 2018. "A Brainstem-Spinal Circuit Controlling Nocifensive Behavior." *Neuron* 100 (6): 1491-1503.e3.

Carter, Matthew E, Sung Han, and Richard D Palmiter. 2015. "Parabrachial Calcitonin Gene-Related Peptide Neurons Mediate Conditioned Taste Aversion." *The Journal of Neuroscience* 35 (11): 4582–86.

Carter, Matthew E, Marta E Soden, Larry S Zweifel, and Richard D Palmiter. 2013. "Genetic Identification of a Neural Circuit That Suppresses Appetite." *Nature* 503 (7474): 111–14.

Chiang, Michael C, Eileen K Nguyen, Martha Canto-Bustos, Andrew E Papale, Anne-Marie M Oswald, and Sarah E Ross. 2020. "Divergent Neural Pathways Emanating from the Lateral Parabrachial Nucleus Mediate Distinct Components of the Pain Response." *Neuron*, April.

Han, Sung, Matthew T Soleiman, Marta E Soden, Larry S Zweifel, and Richard D Palmiter. 2015. "Elucidating an Affective Pain Circuit That Creates a Threat Memory." *Cell* 162 (2): 363–74.

Palmiter, Richard D. 2018. "The Parabrachial Nucleus: CGRP Neurons Function as a General Alarm." *Trends in Neurosciences* 41 (5): 280–93.

Appendix B Validation of Oprm1-Cre in RVM

Appendix B.1 Introduction

Previous reports have provided strong evidence for the existence of morphine-sensitive, Oprm1-expressing neurons in the RVM that could facilitate pain (Heinricher et al. 2009; Cleary et al. 2008; Skinner et al. 1997; Basbaum and Fields 1984). These neurons have been termed ON-cells. However, these pharmacological manipulations may have off-target effects, given that Oprm1 is expressed in many RVM neuronal subpopulations (Pedersen et al. 2011; Cai et al. 2014; François et al. 2017). Thus, prior studies have been unable to tease apart the underlying circuitry by which MOR+ spinal projections facilitate pain. With the development of viral and genetic tools to selectively visualize and manipulate the activity of Oprm1 RVM neurons, we sought to address new questions about the descending circuitry which facilitates pain.

Appendix B.2 Methods

RNAscope in situ hybridization

Multiplex fluorescent in situ hybridization was performed according to the manufacturer's instructions (Advanced Cell Diagnostics #320850). Briefly, 16 um-thick fresh-frozen sections containing the RVM were fixed in 4% paraformaldehyde, dehydrated, treated with protease for 15 minutes, and hybridized with gene-specific probes to mouse. Probes were used to detect Mm-tdt-C2 (#431201), Mm-Oprm1-C1 (#315841), and Mm-Slc17a6-C3

(#319171). DAPI (#320858) was used to visualize nuclei. 3-plex positive (#320881) and negative (#320871) control probes were tested. Three to four 16um z-stacked sections were quantified for a given mouse, and 3-4 mice were used per experiment.

Immunohistochemistry

Mice were anesthetized with an intraperitoneal injection of urethane, transcardially perfused, and post-fixed at least four hours in 4% paraformaldehyde. 40um and 25um thick RVM and spinal cord sections were collected on a cryostat and slide-mounted for immunohistochemistry. Sections were blocked at room temperature for two hours in a 5% donkey serum, 0.2% triton, in phosphate buffered saline. Primary antisera was incubated for 14 hours overnight at 4°C: rabbit anti-RFP (1:1K). Sections were subsequently washed three times for 20 minutes in wash buffer (0.2% triton, in PBS) and incubated in secondary antibodies (Life Technologies, 1:500) at room temperature for two hours. Sections were then washed 3 times for 15 minutes in wash buffer, mounted and cover slipped.

Image acquisition and quantification

Full-tissue thickness sections were imaged using either an Olympus BX53 fluorescent microscope with UPlanSApo 4x, 10x, or 20x objectives or a Nikon A1R confocal microscope with 20X or 60X objectives. All images were quantified and analyzed using ImageJ. To quantify images in RNAscope in situ hybridization experiments, confocal images of tissue samples (3-4 sections per mouse over 3-4 mice) were imagined and only cells whose nuclei were clearly visible by DAPI staining and exhibited fluorescent signal were counted.

Appendix B.3 Results

Using the recently developed Oprm1-Cre mouse (a gift from Dr. Richard Palmiter), I tested the potential of using this allele to target Oprm1 RVM neurons. I used fluorescent in-situ hybridization to validate this Cre allele **(Figure 1)** and a Cre-dependent virus to infect Oprm1 neurons in the RVM **(Figure 2)**.

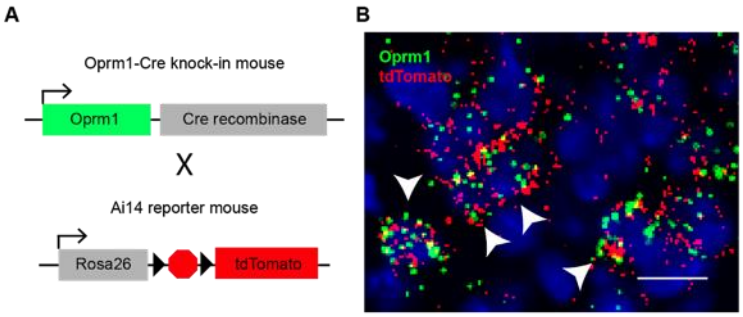

Appendix B Figure 1 Validation of Oprm1-Cre mice.

(A) Oprm1-Cre crossed to a tdtTomato reporter. **(B)** Fluorescent in-situ hybridization of *Oprm1* (green) and *tdTomato* (red). Arrows indicate neurons positive for both markers. Scale bar = 50 µm

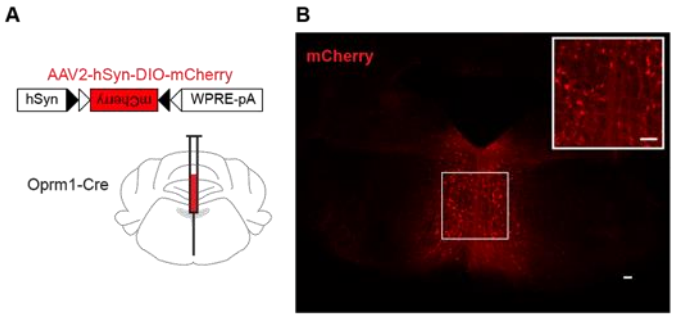

Appendix B Figure 2. Viral approach to target Oprm1 neurons in the RVM.

(A) Strategy to infect the RVM. **(B)** Immunohistochemistry of infected RVM neurons. Scale bar = 50 µm.

Appendix B.4 Discussion

The neurochemical characterization of the Oprm1-Cre allele suggests that it may be a promising tool to study the role of Oprm1 neurons in RVM signaling.

Appendix B.5 Bibliography

Basbaum, A I, and H L Fields. 1984. "Endogenous Pain Control Systems: Brainstem Spinal Pathways and Endorphin Circuitry." *Annual Review of Neuroscience* 7: 309–38.

Cai, You-Qing, Wei Wang, Yuan-Yuan Hou, and Zhizhong Z Pan. 2014. "Optogenetic Activation of Brainstem Serotonergic Neurons Induces Persistent Pain Sensitization." *Molecular Pain* 10 (November): 70.

Cleary, D R, M J Neubert, and M M Heinricher. 2008. "Are Opioid-Sensitive Neurons in the Rostral Ventromedial Medulla Inhibitory Interneurons?" *Neuroscience* 151 (2): 564–71.

François, Amaury, Sarah A Low, Elizabeth I Sypek, Amelia J Christensen, Chaudy Sotoudeh, Kevin T Beier, Charu Ramakrishnan, et al. 2017. "A Brainstem-Spinal Cord Inhibitory Circuit for Mechanical Pain Modulation by GABA and Enkephalins." *Neuron* 93 (4): 822-839.e6.

Heinricher, M M, I Tavares, J L Leith, and B M Lumb. 2009. "Descending Control of Nociception: Specificity, Recruitment and Plasticity." *Brain Research Reviews* 60 (1): 214–25.

Pedersen, Nigel P, Christopher W Vaughan, and MacDonald J Christie. 2011. "Opioid Receptor Modulation of GABAergic and Serotonergic Spinally Projecting Neurons of the Rostral Ventromedial Medulla in Mice." *Journal of Neurophysiology* 106 (2): 731–40.

Skinner, K, H L Fields, A I Basbaum, and P Mason. 1997. "GABA-Immunoreactive Boutons Contact Identified OFF and ON Cells in the Nucleus Raphe Magnus." *The Journal of Comparative Neurology* 378 (2): 196–204.

Appendix C Bi-directional modulation of delta signaling in itch

Appendix C.1 Introduction

Opioid peptides and their receptors are widely expressed throughout the peripheral and central nervous systems. Due to its role in regulating nociception, the opioid system has been the target of the most widely used analgesics. The four characterized opioid receptors subtypes include the mu, kappa, delta, orphanin receptors (Al-Hasani and Bruchas 2011). All four are G-protein coupled receptors and exert their influence on inhibitory G-proteins (Dhawan et al. 1996).

Mu opioid receptor agonists, such as morphine, act on the mu opioid receptor (MOR) to inhibit pain signaling (Matthes et al. 1996) but it has also been documented in human as well as non-human models that MOR agonists are associated with itch (Ko 2015; Liu et al. 2011; Sukhtankar and Ko 2013; Ding et al. 2015; Thomas et al. 1992). Numerous prior studies have investigated MOR and KOR signaling using pharmacology. For instance, mu-opioid receptor (MOR) agonists have been shown to cause itch that is reversible with mu antagonists (Ko and Naughton 2000). Furthermore, it has previously been shown that kappa opioid receptor (KOR) agonists, when given systemically, can also mitigate pruritus induced by MOR signaling (Somrat et al. 1999; Charuluxananan et al. 2003; Ben-David et al. 2002).

However, the role of delta opioid receptors (DORs) and their peptides in the modulation of itch is less clear. Indeed, delta opioid signaling has been shown to be a promising target for the treatment of pain (Custodio-Patsey et al. 2020; Vicente-Sanchez et al. 2016; Abdallah and Gendron 2018; Wang et al. 2018). Given the precedence that other opioid receptors modulate

itch as well as pain transmission, the role of delta signaling in itch, in particular, warrants further investigation.

Previously, it was found that DOR agonists do not cause itch, and, conversely, DOR antagonists do not reverse itch (Ko et al. 2003; Thomas et al. 1992). However, the inverse of these experiments have never been tested. Given that KOR agonists inhibit itch, whereas KOR antagonists exacerbate itch (Kardon et al. 2014), we tested whether DOR signaling may work in a similar manner. That is, we performed experiments to test whether a DOR antagonist (naltrindole) could evoke spontaneous itch and whether a DOR agonist (SNC-80) could suppress itch caused by a pruritogen (chloroquine).

Appendix C.2 Methods

Mice

The studies were performed in both male and female mice 8-10 weeks of age. All animals were of the C57Bl/6 wild-type mice acquired from Charles River (Strain #027). Even numbers of male and female mice were used for all experiments. Mice were given food and water ad libitum and housed under standard laboratory conditions. The use of animals was approved by the Institutional Animal Care and Use Committee of the University of Pittsburgh.

Pharmacologic agents used in mice

Naltrindole (Sigma #111469-81-9), SNC-80 (Tocris #0764), and chloroquine diphosphate salt (Sigma) were dissolved in physiological saline immediately prior to administration.

Intradermal and intrathecal Injections

For intradermal injection of chloroquine, hair was clipped from the neck or calf of each mouse at least 24 hours before the experiment. Chloroquine (100 μg in 10 μL) was administered into the nape of the neck or calf, which could be subsequently visualized by the formation of a small bubble under the skin. For intrathecal injections, hair was clipped from the back of each mouse at least 24 hours before the experiment. All intrathecal injections were delivered (naltrindole, 15 pmol; SNC-80, 500 pmol) in a total volume of 5 μL using a 30-gauge needle attached to a luer-tip 25 μL Hamilton syringe. The needle was inserted into the tissue at a 45° angle through the fifth intervertebral space (L5 – L6). Solution was injected at a rate of 1 μL/s. The needle was held in position for 10 seconds and removed slowly to avoid any outflow of the solution. Only mice that exhibited a reflexive flick of the tail following puncture of the dura were included in behavioral analysis. These procedures were performed in awake, restrained mice.

All behavioral tests described below were performed in a blinded manner.

Observation of scratching behavior

Scratching behavior was observed using a previously reported method(Kardon et al. 2014). Mice were individually placed in the observation cage (12 x 9 x 14 cm) to acclimate for 30 minutes. The mice were assigned to dosing conditions in a randomized manner. Scratching behavior was videotaped for 60 minutes after administration of naltrindole. For assessment of SNC-80 inhibition of itch SNC-80 was intrathecally administered 20 minutes prior to the intradermal chloroquine injection. In these experiments, only scratch bouts directed to the nape of the neck were counted over 30 minutes. The total numbers of scratch bouts by the hind paws were binned every minute and tallied cumulatively. The latency to the first scratch and the total time spent scratching were also quantified.

RNAscope in situ hybridization

Multiplex fluorescent in situ hybridization was performed according to the manufacturer's instructions (Advanced Cell Diagnostics #320850). Briefly, 16 um-thick fresh-frozen sections containing the RVM were fixed in 4% paraformaldehyde, dehydrated, treated with protease for 15 minutes, and hybridized with gene-specific probes to mouse. Probes were used to detect Mm-Npy-C2 (#313321-C2), Mm-Penk-C1 (#318761), Mm-Slc32a1-C3 (#319191-C3), Mm-Oprd1-C2 (#427371-C2) and Mm-Oprk1-C1 (#31611). DAPI (#320858) was used to visualize nuclei. 3-plex positive (#320881) and negative (#320871) control probes were tested. Three to four 16um z-stacked sections were quantified for a given mouse, and 3-4 mice were used per experiment.

Image acquisition and quantification

Full-tissue thickness sections were imaged using either an Olympus BX53 fluorescent microscope with UPlanSApo 4x, 10x, or 20x objectives or a Nikon A1R confocal microscope with 20X or 60X objectives. All images were quantified and analyzed using ImageJ. To quantify images in RNAscope in situ hybridization experiments, confocal images of tissue samples (3-4 sections per mouse over 3-4 mice) were imagined and only cells whose nuclei were clearly visible by DAPI staining and exhibited fluorescent signal were counted.

Statistical analysis

All statistical analyses were performed using GraphPad Prism 8. Values are presented as mean $\pm$ SEM. *P* values were determined by tests indicated in applicable figure legends. Sample sizes were based on pilot data and are similar to those typically used in the field.

Appendix C.3 Results

We found that a low dose of naltrindole compared to doses commonly used in the field (Scherrer et al. 2009) was sufficient to cause itch behaviors **(Figure 1A-E)**. The effect of DOR antagonism caused itch that was sustained **(Figure 1A, B-D)**, and also decreased animals' latency to scratch following an intrathecal injection of naltrindole (15 pmol) compared to controls **(Figure 1E)**. When we pre-treated animals with intradermal chloroquine, we found that DOR agonism with SNC-80 (500 pmol) reduced the total number of scratch bouts over 30 minutes and increased animals' latencies to scratch **(Figure 2A, B).** These effects were also confirmed to occur dose-dependently **(Figure 3D-F)**. Consistent with previous work (Scherrer et al. 2009), we also found that DOR agonism suppressed capsaicin-induced mechanical hypersensitivity **(Figure 3G).**

When we examined the overlap of *Penk*, encoding for proenkephalin, the endogenous peptide for the delta-opioid receptor, we founde extensive overlap with *Npy*, a population of inhibitory spinal neurons implicated in the inhibition of itch (Bourane et al. 2015). We also found that *Oprd1*, encoding for the delta-opioid receptor, overlapped with *Oprk1*, the kappa-opioid receptor, which has also been implicated in modulating itch at the spinal level **(Figure 4).**

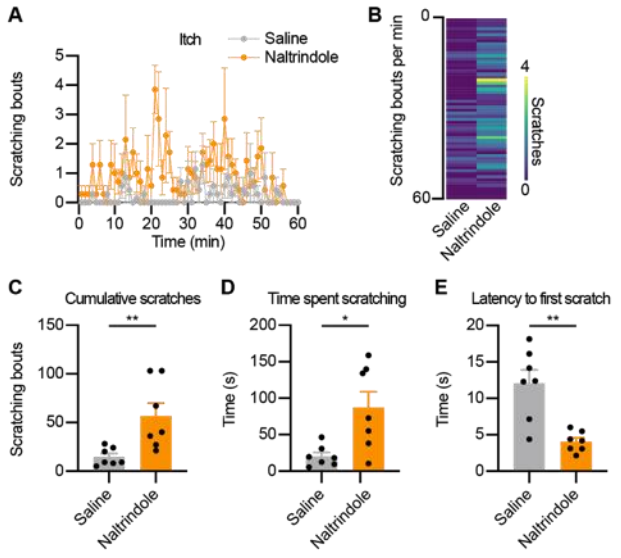

Appendix C Figure 1. Antagonism of DOR causes itch.

A, Effect of naltrindole (15 pmol) on itch as a time course B, and shown as a heat map. C, The number of scratch bouts D, and time spent scratching summated over a 60 minute period. E, Effect of naltrindole on the latency to the first observed scratch bout. Asterisks indicate the results of a two-tailed, unpaired t-test. * $p < 0.05$, ** $p < 0.01$. N = 7 mice per group, with dots representing individual mice.

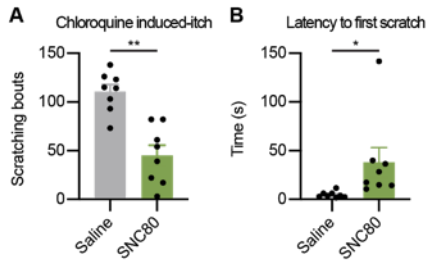

Appendix C Figure 2. Agonism of DOR suppresses itch.

A, Effect of SNC-80 (500 pmol) on suppressing chloroquine-induced itch totaled over a 30 minute period B, and on the latency to the first observed scratch bout. Asterisks indicate the results of a two-tailed, unpaired t-test. * $p < 0.05$, ** $p < 0.01$. N = 7 mice per group, with dots representing individual mice.

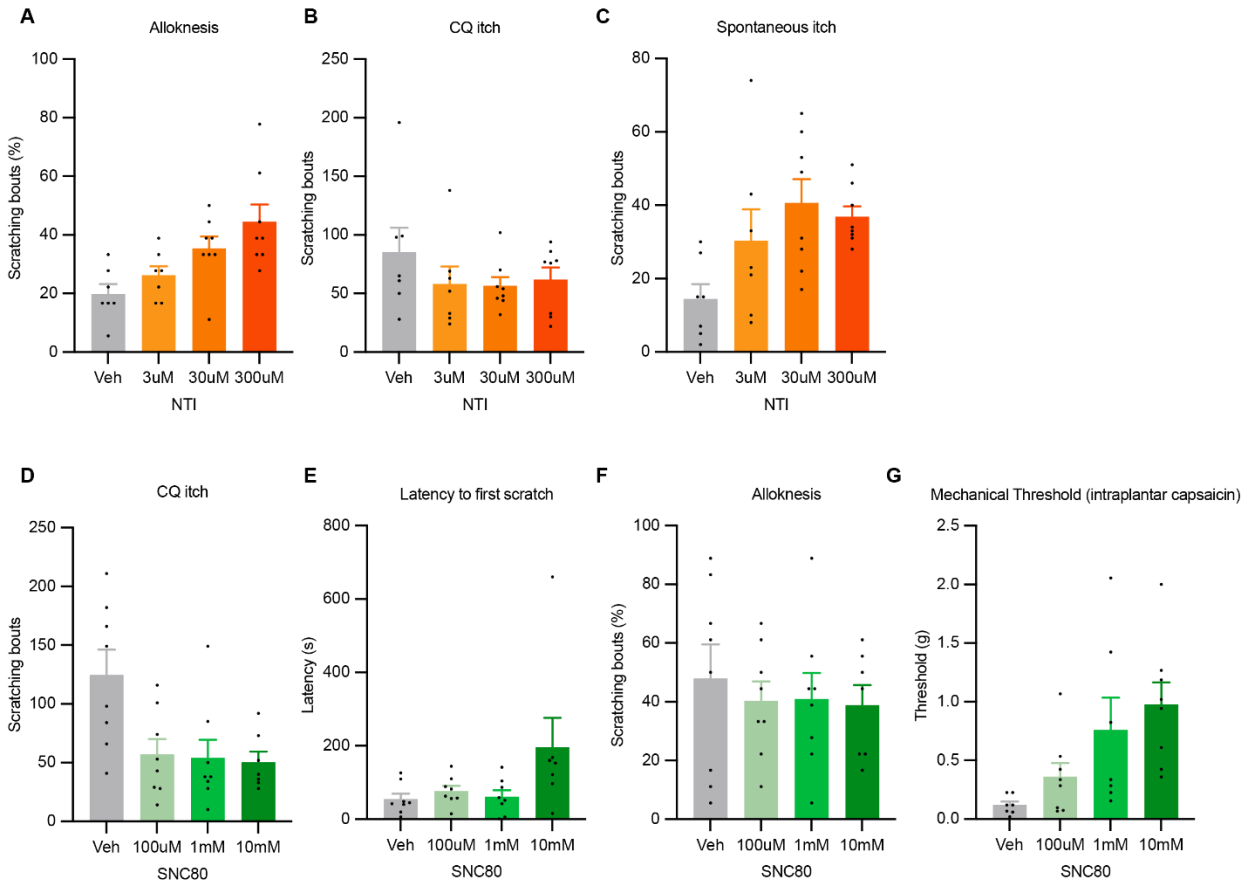

Appendix C Figure 3. Dose-response effects of DOR agonism and antagonism on itch and mechanical hypersensitivity.

A, Effect of naltrindole on alloknesis, B, chloqoruine-induced itch, C, and spontaneous itch. D, Effect of SNC-80 on chloroquine-induced itch, E, the latency to the first observed scratch bout, F, alloknesis, G, and mechanical thersholds following capsaicin-induced injury. N = 8 mice per group, with dots representing individual mice.

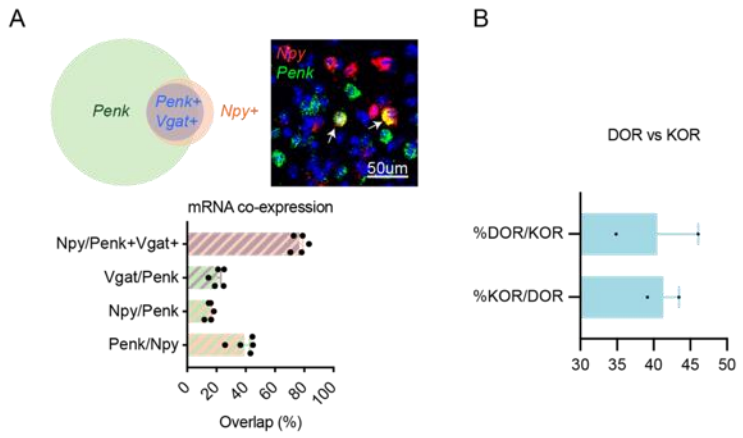

Appendix C Figure 4. RNAscope analysis of Penk and DOR.

A, neurons expressing *Penk* co-localize with *Npy*. B, *Oprd1* overlaps with *Oprk1*. N = 2-4 mice, with dots representing individual mice.

Appendix C.4 Discussion

Much like the previously established roles for MOR and KOR in itch, these results with bidirectional modulation of DOR-expression neurons in the neuraxis suggest now that DOR signaling could also be important for gating itch. Our pharmacological studies reveal that delta agonists inhibit chemical and possible mechanical itch, whereas delta antagonists elicit spontaneous as well as chemical and mechanical-evoked itch. Based on our RNAscope analysis, we speculate that *Npy* neurons that co-release proenkephalin may inhibit itch through downstream neurons containing the delta-opioid receptor. Given the overlap with the kappa-opioid receptor, these neurons may be situated to modulate both mechanical and chemical itch through both the delta and kappa-opioid receptors.

Appendix C.5 Bibliography

Abdallah, Khaled, and Louis Gendron. 2018. “The Delta Opioid Receptor in Pain Control.” *Handbook of Experimental Pharmacology* 247: 147–77.

Al-Hasani, Ream, and Michael R Bruchas. 2011. “Molecular Mechanisms of Opioid Receptor-Dependent Signaling and Behavior.” *Anesthesiology* 115 (6): 1363–81.

Ben-David, Bruce, Patrick J DeMeo, Christen Lucyk, and David Solosko. 2002. “Minidose Lidocaine-Fentanyl Spinal Anesthesia in Ambulatory Surgery: Prophylactic Nalbuphine versus Nalbuphine plus Droperidol.” *Anesthesia and Analgesia* 95 (6): 1596–1600.

Bourane, Steeve, Bo Duan, Stephanie C Koch, Antoine Dalet, Olivier Britz, Lidia Garcia Campmany, Euiseok Kim, et al. 2015. “Gate Control of Mechanical Itch by a Subpopulation of Spinal Cord Interneurons.” *Science* 350 (6260): 550–54.

Charuluxananan, Somrat, Oranuch Kyokong, Wanna Somboonviboon, Arunchai Narasethakamol, and Pissamai Promlok. 2003. “Nalbuphine versus Ondansetron for Prevention of Intrathecal Morphine-Induced Pruritus after Cesarean Delivery.” *Anesthesia and Analgesia* 96 (6): 1789–93, table of contents.

Custodio-Patsey, Lilian, Renée R Donahue, Weisi Fu, Joshua Lambert, Bret N Smith, and Bradley K Taylor. 2020. “Sex Differences in Kappa Opioid Receptor Inhibition of Latent Postoperative Pain Sensitization in Dorsal Horn.” *Neuropharmacology* 163: 107726.

Dhawan, B N, F Cesselin, R Raghubir, T Reisine, P B Bradley, P S Portoghese, and M Hamon. 1996. “International Union of Pharmacology. XII. Classification of Opioid Receptors.” *Pharmacological Reviews* 48 (4): 567–92.

Ding, H, K Hayashida, T Suto, D D Sukhtankar, M Kimura, V Mendenhall, and M C Ko. 2015. “Supraspinal Actions of Nociceptin/Orphanin FQ, Morphine and Substance P in Regulating Pain and Itch in Non-Human Primates.” *British Journal of Pharmacology* 172 (13): 3302–12.

Kardon, Adam P, Erika Polgár, Junichi Hachisuka, Lindsey M Snyder, Darren Cameron, Sinead Savage, Xiaoyun Cai, et al. 2014. “Dynorphin Acts as a Neuromodulator to Inhibit Itch in the Dorsal Horn of the Spinal Cord.” *Neuron* 82 (3): 573–86.

Ko, Mei-Chuan. 2015. “Neuraxial Opioid-Induced Itch and Its Pharmacological Antagonism.” *Handbook of Experimental Pharmacology* 226: 315–35.

Ko, M C H, H Lee, C Harrison, M J Clark, H F Song, N N Naughton, J H Woods, and J R Traynor. 2003. “Studies of Micro-, Kappa-, and Delta-Opioid Receptor Density and G Protein Activation in the Cortex and Thalamus of Monkeys.” *The Journal of Pharmacology and*

Experimental Therapeutics 306 (1): 179–86.

Ko, M C, and N N Naughton. 2000. “An Experimental Itch Model in Monkeys: Characterization of Intrathecal Morphine-Induced Scratching and Antinociception.” *Anesthesiology* 92 (3): 795–805.

Liu, Xian-Yu, Zhong-Chun Liu, Yan-Gang Sun, Michael Ross, Seungil Kim, Feng-Fang Tsai, Qi-Fang Li, et al. 2011. “Unidirectional Cross-Activation of GRPR by MOR1D Uncouples Itch and Analgesia Induced by Opioids.” *Cell* 147 (2): 447–58.

Matthes, H W, R Maldonado, F Simonin, O Valverde, S Slowe, I Kitchen, K Befort, et al. 1996. “Loss of Morphine-Induced Analgesia, Reward Effect and Withdrawal Symptoms in Mice Lacking the Mu-Opioid-Receptor Gene.” *Nature* 383 (6603): 819–23.

Scherrer, Grégory, Noritaka Imamachi, Yu-Qing Cao, Candice Contet, Françoise Mennicken, Dajan O’Donnell, Brigitte L Kieffer, and Allan I Basbaum. 2009. “Dissociation of the Opioid Receptor Mechanisms That Control Mechanical and Heat Pain.” *Cell* 137 (6): 1148–59.

Somrat, C, K Oranuch, U Ketchada, S Siriprapa, and R Thipawan. 1999. “Optimal Dose of Nalbuphine for Treatment of Intrathecal-Morphine Induced Pruritus after Caesarean Section.” *The Journal of Obstetrics and Gynaecology Research* 25 (3): 209–13.

Sukhtankar, Devki D, and Mei-Chuan Ko. 2013. “Physiological Function of Gastrin-Releasing Peptide and Neuromedin B Receptors in Regulating Itch Scratching Behavior in the Spinal Cord of Mice.” *Plos One* 8 (6): e67422.

Thomas, D A, G M Williams, K Iwata, D R Kenshalo, and R Dubner. 1992. “Effects of Central Administration of Opioids on Facial Scratching in Monkeys.” *Brain Research* 585 (1–2): 315–17.

Vicente-Sanchez, Ana, Laura Segura, and Amynah A Pradhan. 2016. “The Delta Opioid Receptor Tool Box.” *Neuroscience* 338 (December): 145–59.

Wang, Dong, Vivianne L Tawfik, Gregory Corder, Sarah A Low, Amaury François, Allan I Basbaum, and Grégory Scherrer. 2018. “Functional Divergence of Delta and Mu Opioid Receptor Organization in CNS Pain Circuits.” *Neuron* 98 (1): 90-108.e5.

Appendix D Neurochemical characterization of KOR spinal neurons

Appendix D.1 Introduction

Our lab has previously identified the role for spinal dynorphin signaling in itch (Snyder et al. 2018; Ross et al. 2010; Kardon et al. 2014). Dynorphin is the precursor peptide for dynorphin, a kappa opioid receptor (KOR) agonist (Kardon et al. 2014). KOR agonists, such as nalfurafine, nalbuphine, and butorphanol, have also been used for the therapeutic treatment of various forms of itch in humans (Phan et al. 2012; Lawhorn et al. 1991; Cowan et al. 2015; Kumagai et al. 2010). Despite the clear roles for both dynorphin and other KOR agonists in the management of itch, KOR spinal circuitry remains poorly understood.

Appendix D.2 Methods

RNAscope in situ hybridization

Multiplex fluorescent in situ hybridization was performed according to the manufacturer's instructions (Advanced Cell Diagnostics #320850). Briefly, 16 um-thick fresh-frozen sections containing the RVM were fixed in 4% paraformaldehyde, dehydrated, treated with protease for 15 minutes, and hybridized with mouse-gene-specific probes. Probes were used to detect Mm-Oprm1-C1 (#315841), Mm-Oprk1-C1 (#316111), Mm-Npy-C2 (#313321-C2), Mm-Pdyn-C2 (#318771-C2), Mm-Pvalb-C2 (#421931-C2), Mm-Nos1-C2 (#437651-C2), Mm-Slc31a1-C3 (#319191), Mm-Slc17a6-C3 (#319171). DAPI (#320858) was used to visualize

nuclei. 3-plex positive (#320881) and negative (#320871) control probes were tested. Three to four 16um z-stacked sections were quantified for a given mouse.

Image acquisition and quantification

Full-tissue thickness sections were imaged using either an Olympus BX53 fluorescent microscope with UPlanSApo 4x, 10x, or 20x objectives or a Nikon A1R confocal microscope with 20X or 60X objectives. All images were quantified and analyzed using ImageJ. To quantify images in RNAscope in situ hybridization experiments, confocal images of tissue samples (3-4 sections per mouse over 3-4 mice) were imagined and only cells whose nuclei were clearly visible by DAPI staining and exhibited fluorescent signal were counted.

Appendix D.3 Results

To begin to understand KOR circuitry, we sought to neurochemically characterize KOR (*Oprk1-expressing)* neurons in the dorsal horn. Using fluorescent in-situ hybridization, we found, surprisingly, that a majority of KOR neurons expressed *Slc32a1*, the gene encoding Vgat, indicating that they are inhibitory neurons **(Figure 1A-D)**. Among the inhibitory subset, nearly a third of these neurons also contained *Pdyn* (dynorphin) **(Figure 1B, D)**. Further characterization of *Oprk1* neurons also revealed that they did not co-express *Oprm1* (mu opioid receptor) **(Figure 2A, B)**.

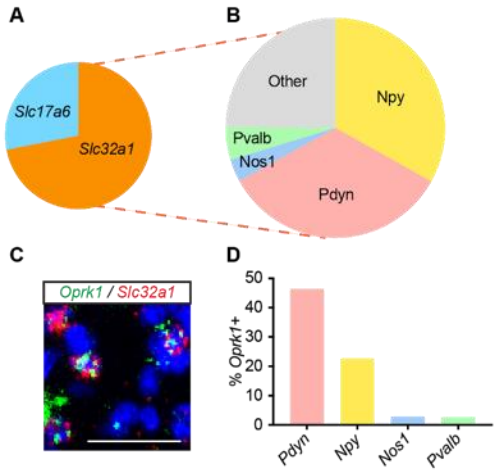

Appendix D Figure 1. RNAscope characterization of *Oprk1* in the dorsal horn.

(A) Relative proportions of Oprk1 neurons and their expression of Slc17a6 (Vglut2) and Slc31a1 (Vgat). **(B)** Among *Oprk1+*, *Slc32a1+* neurons, the relative proportions of other markers of inhibitory spina neurons; *Pvalb:* parvalbumin, *Nos1:* nNos, *Pdyn:* dynorphin, *Npy:* NPY. **(C)** A representative image of overlap between *Oprk1* and *Slc32a1*. Scale bar = 50 μm. **(D)** Relative expression of the various inhibitory markers and *Oprk1*.

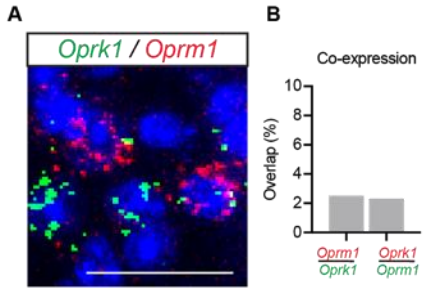

Appendix D Figure 2. Overlap between *Oprk1* and *Oprm1*.

(A) Representative image of staining for *Oprk1 and Oprm1*. Scale bar = 50 μm. **(B)** Quantification A.

Appendix D.4 Discussion

These intriguing findings suggest that the majority of KOR neurons in the dorsal horn are not glutamatergic, which casts doubt on prior models for how KOR signaling produces itch (Munanairi et al. 2018). Additionally, many KOR neurons co-expressed *Pdyn*, the peptide that

binds to KOR, suggesting a possible mechanism for auto-regulation. These data shed light on the complexity of itch spinal circuitry and further experimentation is necessary to better understand the role of KOR in itch.

Appendix D.5 Bibliography

Cowan, Alan, George B Kehner, and Saadet Inan. 2015. "Targeting Itch with Ligands Selective for κ Opioid Receptors." *Handbook of Experimental Pharmacology* 226: 291–314.

Kardon, Adam P, Erika Polgár, Junichi Hachisuka, Lindsey M Snyder, Darren Cameron, Sinead Savage, Xiaoyun Cai, et al. 2014. "Dynorphin Acts as a Neuromodulator to Inhibit Itch in the Dorsal Horn of the Spinal Cord." *Neuron* 82 (3): 573–86.

Kumagai, Hiroo, Toshiya Ebata, Kenji Takamori, Taro Muramatsu, Hidetomo Nakamoto, and Hiromichi Suzuki. 2010. "Effect of a Novel Kappa-Receptor Agonist, Nalfurafine Hydrochloride, on Severe Itch in 337 Haemodialysis Patients: A Phase III, Randomized, Double-Blind, Placebo-Controlled Study." *Nephrology, Dialysis, Transplantation* 25 (4): 1251–57.

Lawhorn, C D, J D McNitt, E E Fibuch, J T Joyce, and R J Leadley. 1991. "Epidural Morphine with Butorphanol for Postoperative Analgesia after Cesarean Delivery." *Anesthesia and Analgesia* 72 (1): 53–57.

Munanairi, Admire, Xian-Yu Liu, Devin M Barry, Qianyi Yang, Jun-Bin Yin, Hua Jin, Hui Li, et al. 2018. "Non-Canonical Opioid Signaling Inhibits Itch Transmission in the Spinal Cord of Mice." *Cell Reports* 23 (3): 866–77.

Phan, Ngoc Quan, Tobias Lotts, Attila Antal, Jeffrey D Bernhard, and Sonja Ständer. 2012. "Systemic Kappa Opioid Receptor Agonists in the Treatment of Chronic Pruritus: A Literature Review." *Acta Dermato-Venereologica* 92 (5): 555–60.

Ross, Sarah E, Alan R Mardinly, Alejandra E McCord, Jonathan Zurawski, Sonia Cohen, Cynthia Jung, Linda Hu, et al. 2010. "Loss of Inhibitory Interneurons in the Dorsal Spinal Cord and Elevated Itch in Bhlhb5 Mutant Mice." *Neuron* 65 (6): 886–98.

Snyder, Lindsey M, Michael C Chiang, Emanuel Loeza-Alcocer, Yu Omori, Junichi Hachisuka, Tayler D Sheahan, Jenna R Gale, et al. 2018. "Kappa Opioid Receptor Distribution and Function in Primary Afferents." *Neuron* 99 (6): 1274-1288.e6.

Appendix E NK1R RVM neurons in modulation of itch

Appendix E.1 Introduction

Pharmacological manipulations of neurons in the RVM containing NK1R have suggested that these neurons may respond to substance P release from SP (tachykinin) neurons in the PAG (Lagraize et al. 2010)). Microinjection of substance P into the RVM has been shown to have pro-nociceptive effects. Conversely, infusion of NK1R antagonists in the RVM has been found to inhibit thermal thresholds and attenuate hypersensitivity to heat and mechanical stimuli following inflammatory injury (Lagraize et al. 2010; Hamity, White, and Hammond 2010; Pacharinsak et al. 2008).

Pharmacological ablation of NK1R RVM neurons reduces hyperalgesia in both acute and chronic pain models (S G Khasabov and Simone 2013). However, the contributions of these neurons to itch has not been examined. Recently, PAG Tac1 neurons were found to facilitate itch through an RVM-spinal pathway (Gao et al. 2019). Neurochemically, NK1R neurons comprise roughly 8% of neurons in the RVM and have been found to overlap with Gad67, suggesting that they may be inhibitory neurons (T. Chen et al. 2013). Furthermore, only the Gad67+, NK1R+ neurons are thought to be spinally projecting (T. Chen et al. 2013). This suggests there are at least two neurochemically distinct NK1R subtypes, and whether these distinct subpopulations are pro-nociceptive is unclear. Lastly, given the precedent that Tac1-PAG neurons participate in the facilitation of itch, we wanted to test the role of NK1R-CreER RVM neurons in itch behaviors.

Appendix E.2 Methods

Mice

NK1R-CreER mice used were generated as previously described (Huang et al. 2016). The studies were performed in both male and female mice 8-10 weeks of age. All animals were of the C57Bl/6 background. Even numbers of male and female mice were used for all experiments. Mice were given free access to food and water and housed under standard laboratory conditions. The use of animals was approved by the Institutional Animal Care and Use Committee of the University of Pittsburgh.

Pharmacologic agents

Clozapine-N-oxide (Tocris) was dissolved in PBS and administered intraperitoneally (5mg/kg) or IT (50ug/kg). In CNO treated mice, experiments were conducted 30 minutes following the administration of CNO. Chloroquine diphosphate salt (Sigma) was dissolved in physiological saline (100μg in 10μL) and administered intradermally.

Intradermal and Intrathecal Injections

For intradermal injection of chloroquine, hair was removed at least 24 hours before the experiment. Chloroquine (100μg in 10μL) was administered into the nape of the neck, which could be subsequently visualized by the formation of a small bubble under the skin. Injections were delivered in a total volume of 10 μL using a 30-gauge needle attached to a luer-tip 25 μL Hamilton syringe. These procedures were performed in awake mice.

Stereotaxic injections

Animals were anesthetized with 2% isoflurane and placed in a stereotaxic head frame. A drill bit (MA Ford, #87) was used to create a burr hole and custom-made metal needle (33 gauge) loaded with virus was subsequently inserted through the hole to the injection site. Virus was

infused at a rate of 100nL/min using a Hamilton syringe with a microsyringe pump (World Precision Instruments). Mice received 250-500 nL of virus. The injection needle was left in place for an additional 15 min and then slowly withdrawn over another 15 min. Injections were performed at the following coordinates for the RVM: AP -5.80 mm, ML 0.00 mm, DV -6.00. The incision was closed using Vetbond and animals were given ketofen (IP 10 mg/kg) and allowed to recover over a heat pad. Mice were given 4 weeks to recover prior to experimentation.

Behavior

All assays were performed in the Pittsburgh Phenotyping Core and scored by an experimenter blind to treatment (infection with Cre-dependent hM3Dq or the control, mCherry, virus).

Observation of Scratching Behavior

All tests were performed in a blinded manner. Scratching behavior was observed using a previously reported method (Kardon et al. 2014). On the testing day, the mice were individually placed in the observation cage (12x9x14 cm) to permit acclimation for 30 minutes. Spontaneous behavior was videotaped for 60 minutes following habituation, the total numbers of scratch bouts by the hind paws at various body sites were counted. Scratching behavior was videotaped for 30 minutes after administration of chloroquine. The total numbers of scratch bouts by the hind paws directed at the site of injection (nape of the neck) during the first 30 minutes after chloroquine injection were counted.

Hargreaves testing

Animals were acclimated on a glass plate held at 30°C (Model 390 Series 8, IITC Life Science Inc.). A radiant heat source was applied to the hindpaw and latency to paw withdrawal was recorded (Hargreaves et al. 1988). 2 trials were conducted on each paw, with at least 5 min

between testing the opposite paw and at least 10 min between testing the same paw. To avoid tissue damage, a cut off latency of 20 sec was set. Values from both paws were averaged to determine withdrawal latency.

Von Frey testing

Mechanical sensitivity was measured using the Chaplan up-down method of the von Frey test (Chaplan et al. 1994). Calibrated von Frey filaments (North Coast Medical Inc.) were applied to the plantar surface of the hindpaw. Lifting, shaking, and licking were scored as positive responses to von Frey stimulation. Average responses were obtained from each hindpaw, with 3 min between trials on opposite paws, and 5 min between trials on the same paw.

RNAscope in situ hybridization

Multiplex fluorescent in situ hybridization was performed according to the manufacturer's instructions (Advanced Cell Diagnostics #320850). Briefly, 16 um-thick fresh-frozen sections containing the RVM were fixed in 4% paraformaldehyde, dehydrated, treated with protease for 15 minutes, and hybridized with gene-specific probes to mouse. Probes were used to detect Mm-TacR1-C1 (#428781) and Mm-Slc32a1-C3 (#319191). DAPI (#320858) was used to visualize nuclei. 3-plex positive (#320881) and negative (#320871) control probes were tested. Three to four z-stacked sections were quantified for a given mouse, and 3-4 mice were used per experiment.

Immunohistochemistry

Mice were anesthetized with an intraperitoneal injection of urethane, transcardially perfused, and post-fixed at least four hours in 4% paraformaldehyde. 40um and 25um thick RVM and spinal cord sections were collected on a cryostat and slide-mounted for immunohistochemistry. Sections were blocked at room temperature for two hours in a 5%

donkey serum, 0.2% triton, in phosphate buffered saline. Primary antisera was incubated for 14 hours overnight at 4°C: rabbit anti-RFP (1:1K). Sections were subsequently washed three times for 20 minutes in wash buffer (0.2% triton, in PBS) and incubated in secondary antibodies (Life Technologies, 1:500) at room temperature for two hours. Sections were then incubated in Hoechst (ThermoFisher, 1:10K) for 1 minute and washed 3 times for 15 minutes in wash buffer, mounted and cover slipped.

Image acquisition and quantification

Full-tissue thickness sections were imaged using either an Olympus BX53 fluorescent microscope with UPlanSApo 4x or 10x objectives. All images were quantified and analyzed using ImageJ. To quantify images in RNAscope in situ hybridization experiments, images of tissue samples (3-4 sections per mouse over 3 mice) were imaged and only cells whose nuclei were clearly visible by DAPI staining and exhibited fluorescent signal were counted.

Statistical analysis

All statistical analyses were performed using GraphPad Prism 8. Values are presented as mean +/- SEM. Statistical significance was assessed using a two-way, repeated measures ANOVA with Bonferroni's correction. Significance was indicated by $p < 0.05$. Sample sizes were based on pilot data and are similar to those typically used in the field.

Appendix E.3 Results

Using fluorescent in situ hybridization, we found that 75.6 +/- 4.9 of Tacr1-expressing neurons co-expressed Slc32a1, the gene for Vgat, indicating that a majority of NK1R neurons are GABAergic, and thus, inhibitory. Following viral infection with the Cre-dependent DREADD

(AAV2.hSyn.DIO.hM3Dq.mCherry), we chemogenetically activated NK1R-CreER neurons and tested mice for pain and itch-related behaviors. In mice receiving the hM3Dq DREADD virus, chemogenetic activation using CNO significantly reduced chloroquine evoked scratch bouts **(Figure 1A)** and spontaneous scratching behavior **(Figure 1B)**, and also significantly reduced the von Frey mechanical withdrawal threshold **(Figure 1C)** with no effect on thermal withdrawal latency **(Figure 1D)**. CNO had no effect in the control mice. We also observed mCherry expression in the RVM of virally-injected neurons **(Figure 1E)** and their descending innervation of the spinal cord dorsal horn **(Figure 1F)**.

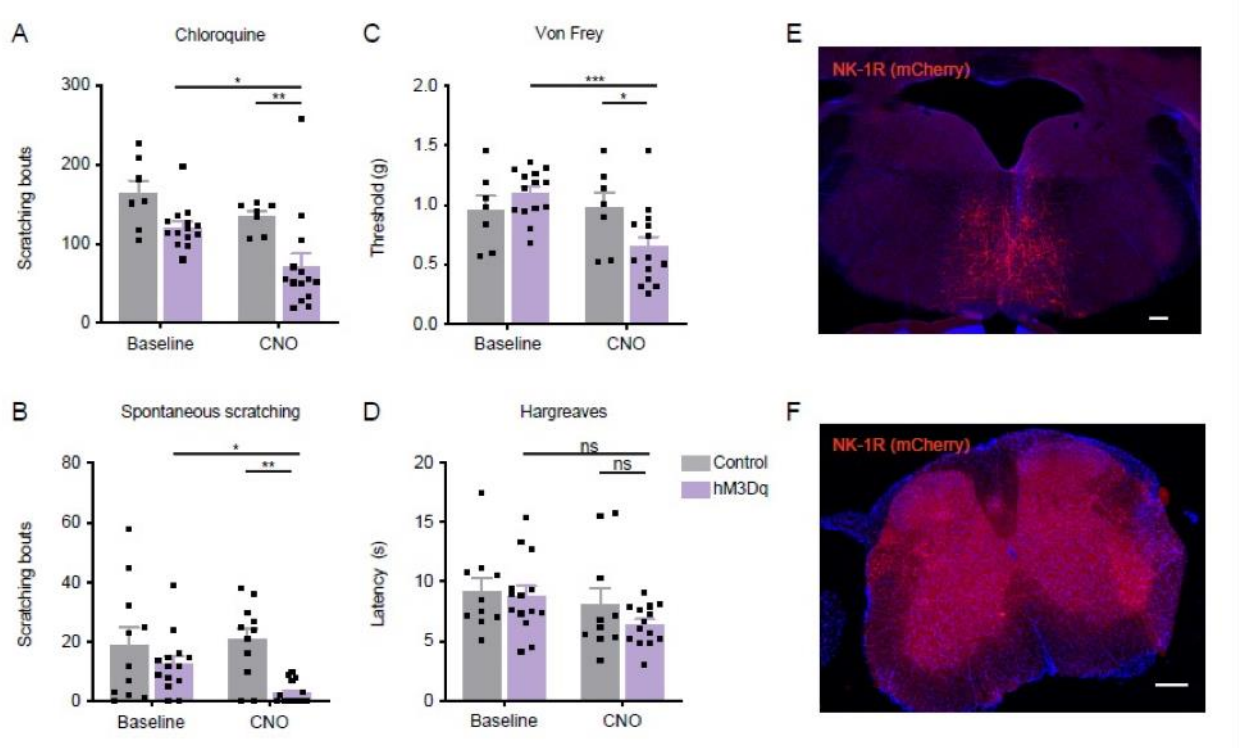

Appendix E Figure 1. Chemogenetic activation of RVM NK-1R expressing neurons inhibits itch related behavior.

(A) CNO administration significantly reduced chloroquine evoked scratch bouts in DREADDs but not control vector mice (n = 5-7 males, 5-7 females). (B) CNO reduced spontaneous scratching in mice receiving DREADDs (n = 5 males, 5 females). (C) CNO administration significantly reduced mechanical withdrawal thresholds in DREADDs but not control vector mice (n = 5-7 males, 5-7 females). (D) CNO did not affect thermal withdrawal latency in any group (n = 5-7 males, 5-7 females). (E) mCherry expression (red) was robust at the site of injection in the RVM. (F) mCherry expression was observed in axonal projections in the dorsolateral funiculus. Scale bar = 100 um.

Appendix E.4 Discussion

Previous work has established a possible pronociceptive role for substance P on NK1R-RVM neurons (S G Khasabov and Simone 2013), and their descending spinal input has previously been identified (T. Chen et al. 2013). We establish for the first time that activation of NK1R-RVM neurons inhibits spontaneous grooming and pruritogen-evoked itch. In this study, we also found that chemogenetic activation of NK1R-expressing RVM neurons facilitates mechanical nociception, consistent with previous work. However, we found that activation of these neurons had no effect on thermal nociception. Our results support the idea that NK1R-RVM neurons modulate both itch and mechanical, but not heat pain. Nevertheless, whether these neurons are preferentially tuned to modulate pain or itch warrants further investigation.

Appendix E.5 Bibliography

Assessment of Tactile Allodynia in the Rat Paw." *Journal of Neuroscience Methods* 53 (1): 55–63.

Hargreaves, K, R Dubner, F Brown, C Flores, and J Joris. 1988. "A New and Sensitive Method for Measuring Thermal Nociception in Cutaneous Hyperalgesia." *Pain* 32 (1): 77–88.

Huang, Huizhen, Marissa S Kuzirian, Xiaoyun Cai, Lindsey M Snyder, Jonathan Cohen, Daniel H Kaplan, and Sarah E Ross. 2016. "Generation of a NK1R-CreER Knockin Mouse Strain to Study Cells Involved in Neurokinin 1 Receptor Signaling." *Genesis* 54 (11): 593–601.

Kardon, Adam P, Erika Polgár, Junichi Hachisuka, Lindsey M Snyder, Darren Cameron, Sinead Savage, Xiaoyun Cai, et al. 2014. "Dynorphin Acts as a Neuromodulator to Inhibit Itch in the Dorsal Horn of the Spinal Cord." *Neuron* 82 (3): 573–86.

Appendix F Neurons in the PAG expressing the mu-opioid receptor

Appendix F.1 Introduction

Supraspinal structures including the midbrain periaqueductal gray (PAG) represent highly organized anatomical systems for the inhibition and facilitation of pain. The PAG has been shown to modulate pain behaviors through a descending pathway involving the rostral ventromedial medulla (RVM) and spinal cord and is also a major component of the endogenous opioid analgesic system (Basbaum and Fields 1978).

Pharmacological manipulations of the PAG have provided critical insight into the types of receptors that participate in the descending modulation of pain. For example, the injection of an mu-opioid receptor (MOR) agonist into the PAG results in elevation of sensory thresholds and analgesia (Lewis and Gebhart 1977; Carstens et al. 1990; Loyd, Wang, and Murphy 2008; Loyd, Morgan, and Murphy 2008; Yaksh 1997). Local microinjections of the mu-antagonist, naloxone, into the PAG or lesioning of the PAG have blocked the analgesic effects of systemic morphine (Vigouret et al. 1973; Tsou and Jang 1964; Zhang et al. 1998; Loyd, Wang, and Murphy 2008), underscoring the role of the PAG as a crucial site of action for the analgesic effects of systemically-administered opioids.

Despite the clear role for opioidergic signaling within the PAG, the molecular and anatomical characterizations of neurons containing the mu-opioid receptor remain elusive. It has been proposed that inhibitory cells within the PAG express the mu-opioid receptor (Vaughan et al. 1997; Osborne et al. 1996), which implies that mu agonists may produce analgesia through the disinhibition of PAG output (Vaughan et al. 1997; Budai and Fields 1998; Heinricher et al.

2009). In support of this model, MOR-expressing PAG neurons have also been shown through immunohistochemistry to comprise a subset of GABAergic neurons, but do not appear to be those that project to the RVM (Commons et al. 2000; Reichling and Basbaum 1990; Kalyuzhny and Wessendorf 1998). Nevertheless, PAG neurons containing the mu-opioid receptor comprise over half of RVM-projecting cells (Commons et al. 2000), and these neurons are also presumed to be GABAergic. Presently, the effects of opioid microinjections within the PAG are thought to induce analgesia through inhibition of both local interneurons within the PAG as well as the inhibition of RVM-projecting PAG neurons. Thus, although there have been considerable advances to the understanding of opioidergic circuits in the PAG, how the direct manipulation of these circuits affects distinct somatosensory modalities warrants further investigation. The expansion of cell type-specific drivers, fluorescent tracers, and behavioral paradigms may now permit the detailed understanding of molecularly-defined PAG neurons and ascertain their precise contributions to somatosensation.

Using combinatorial anatomical, optogenetic, and chemogenetic approaches, we delineate a supraspinal pathway for the modulation of pain and itch behaviors. We found that optogenetic activation of PBN projections to the PAG inhibits response to noxious thermal stimuli and activation of PAG-MOR afferents in the RVM facilitates jumping on the hotplate assay. Chemogenetic manipulations of PAG-MOR neurons unveiled surprising results; whereas activation of these neurons facilitated responses to noxious stimuli and jumping behaviors on the hotplate assay, opposing patterns were observed with respect to reflexive responses to sensory testing. These dichotomous findings across distinct types of sensory testing emphasize the contextual behavioral expression of nociception using reflexive and noxious paradigms. Lastly,

we uncovered the role for PBN projections in the PAG that modulate pain in an uninjured, post-surgical state of latent sensitization.

Appendix F.2 Methods

Mice

All animals were of the C57BL/6J background. The studies were performed in both male and female mice 8-10 weeks of age. Even numbers of male and female mice were used for all experiments and no clear sex differences were observed so data were pooled. Mice were given free access to food and water and housed under standard laboratory conditions. The use of animals was approved by the Institutional Animal Care and Use Committee of the University of Pittsburgh.

Viral vectors

All viruses are commercially available from UNC Vector Core and Addgene. AAV2.hSyn.DIO.hM4D(Gi)-mCherry, AAV2-hsyn-DIO-mCherry, AAV2-hsyn-DIO-hM3D(Gq)-mCherry, AAV2/EF1a-DIO-hChR2(H134R)-eYFP, AAV2.EF1a.DIO.eYFP, pENN.AAV.hSyn.HI.eGFP-Cre.WPRE.SV40, and AAVr-hsyn-DIO-mCherry.

Stereotaxic injections and optical fiber implantation

Animals were anesthetized with 2% isoflurane and placed in a stereotaxic head frame. A drill bit (MA Ford, #87) was used to create a burr hole and a custom-made metal needle (33 gauge) loaded with virus was subsequently inserted through the hole to the injection site. Virus was infused at a rate of 100 nL/min using a Hamilton syringe with a microsyringe pump (World Precision Instruments). Mice received 250-500 nL of virus. The injection needle was left in place

for an additional 5 min and then slowly withdrawn over another 5 min. Injections and cannula implantations were performed at the following coordinates for each brain region: RVM: AP -5.80 mm, ML 0.00 mm, DV -6.00, PAG: AP -4.70 mm, ML ± 0.74 mm, DV: -2.75 at a 4° angle, and PBN: AP -5.11 mm, ML ± 1.25 mm, DV: -3.25. For implantation of optical fibers (Thor Labs: 1.25 mm ceramic ferrule 230 mm diameter), implants were slowly lowered 0.3 - 0.5 mm above the site of injection and secured to the skull with a thin layer of Vetbond (3M) and dental cement. The incision was closed using Vetbond, and animals were provided analgesics (ketofen, i.p. 10 mg/kg; buprenorphine, subcutaneous, 0.3mg/kg) and allowed to recover over a heat pad. Mice were given 4 weeks to recover prior to experimentation.

Pharmacologic agents

Clozapine-N-oxide (Tocris) was dissolved in PBS and administered intraperitoneally (5 mg/kg). Capsaicin (0.1%) in 10% EtOH in PBS was injected 10 μL into the plantar hindpaw. Chloroquine diphosphate salt (Sigma) was dissolved in physiological saline (100 μg in 10 μL) and administered intradermally. Formalin (Sigma; 2% w/v) in saline was injected 10 μL into the plantar hindpaw.

RNAscope in situ hybridization

Multiplex fluorescent in situ hybridization (FISH) was performed according to the manufacturer's instructions (Advanced Cell Diagnostics #320850). Briefly, 14 um-thick fresh-frozen sections containing the RVM were fixed in 4% paraformaldehyde, dehydrated, treated with protease for 15 min, and hybridized with gene-specific probes to mouse. Probes were used to detect eYFP, Th, tdTomato-C2 (#317041-C2), mCherry-C2 (#431201), Mm-Oprm1-C1 (#315841), Mm-Tac1-C1 (#517971), Mm-Tph2-C2 (#318691-C2), Mm-Fos-C3 (#498401-C3), Mm-Pdyn-C2 (#31877), Mm-Slc32a1-C3 (#319191), and Mm-Slc17a6-C3 (#319171). DAPI

(#320858) was used to visualize nuclei. 3-plex positive (#320881) and negative (#320871) control probes were tested. Three to four z-stacked sections were quantified for a given mouse, and 3-4 mice were used per experiment.

Immunohistochemistry

Mice were anesthetized with an intraperitoneal injection of urethane, transcardially perfused, and post-fixed at least 4 h in 4% paraformaldehyde. 40 μm and 25 μm thick brain sections were collected on a cryostat and slide-mounted for immunohistochemistry. Sections were blocked at room temperature for 2 h in a 5% donkey serum, 0.2% triton, in phosphate buffered saline. Primary antisera was incubated for 14 h overnight at 4° C: rabbit anti-RFP (1:1K), chicken anti-GFP (1:1K), and mouse anti-NeuN (1:500). Sections were subsequently washed three times for 20 min in wash buffer (0.2% triton, in PBS) and incubated in secondary antibodies (Life Technologies, 1:500) at room temperature for 2 h. Sections were then incubated in Hoechst (ThermoFisher, 1:10K) for 1 min and washed 3 times for 15 min in wash buffer, mounted and cover slipped.

Fos experiments

Mice received either optical stimulation or CNO as described for behavioral testing. Brain tissues were harvested 90 min after for immunohistochemistry. For optogenetically-induced fos expression, mice were photostimulated for 20 minutes at a 3 s on, 2 s off stimulation pattern and subsequently perfused 90 minutes after the initial onset of photostimulation as noted for immunohistochemistry.

Image acquisition and quantification

Full-tissue thickness sections were imaged using either an Olympus BX53 fluorescent microscope with UPlanSApo 4x, 10x, or 20x objectives or a Nikon A1R confocal microscope

with 20X or 60X objectives. All images were quantified and analyzed using ImageJ. To quantify images in RNAscope in situ hybridization experiments, confocal images of tissue samples (3-4 sections per mouse over 3-4 mice) were imaged and only cells whose nuclei were clearly visible by DAPI staining and exhibited fluorescent signal were counted.

Behavior

All assays were performed in the Pittsburgh Phenotyping Core and scored by an experimenter blind to treatment. For all chemogenetic behavioral experiments, CNO was administered (5 mg/kg IP) 30 minutes prior to the start of behavioral testing. Mice that were optogenetically tested were photostimulated with the following parameters: 10 mW laser power, 20Hz stimulation frequency, and 5ms pulse duration.

Observation of scratching behavior

Scratching behavior was observed using a previously reported method (Kardon et al. 2014). On the testing day, the mice were individually placed in the observation cage (12x9x14 cm) to permit acclimation for 30 min. Scratching behavior was videotaped for 30 min after administration of chloroquine. The temporal and total numbers of scratch bouts by the hind paws at various body sites during this period were counted. For the experiments targeting the lumbar spinal cord, the amount of time spent biting following intradermal chloroquine was summated.

Hargreaves testing

Animals were acclimated on a glass plate held at 30°C (Model 390 Series 8, IITC Life Science Inc.). A radiant heat source was applied to the hindpaw and latency to paw withdrawal was recorded (Hargreaves et al. 1988). Two trials were conducted on each paw, with at least 5 min between testing the opposite paw and at least 10 min between testing the same paw. To

avoid tissue damage, a cut off latency of 20 sec was set. Values from both paws were averaged to determine withdrawal latency.

Tail-flick assay

Mice were placed in custom-made mouse restraints and allowed to habituate 15 minutes before testing. Tails were immersed 3 cm into a water bath at 48° and 55° C, and the latency to tail-flick was measured three times with a 1 min interval between trials. For optogenetic testing, mice were photostimulated for 10 s prior to testing. Cut-offs times were implemented at 25 s (48°) and 5 s (55°C) to prevent tissue damage.

Hotplate

Mice were placed on a 55°C hotplate, and the latency to first nocifensive response (jump) and total number of jumps were measured over a 60 s period. Values were averaged across two trials for each mouse spaced several minutes apart. For optogenetic testing, mice were photostimulated for 10 s prior to testing.

Openfield

Spontaneous activity in the open field was conducted over 30 min in an automated Versamax Legacy open field apparatus for mice (Omnitech Electronics Incorporated, Columbus, OH). Distance traveled was measured by infrared photobeams located around the perimeter of the arenas interfaced to a computer running Fusion v.6 for Versamax software (Omnitech Electronics Incorporated) which monitored the location and activity of the mouse during testing. Activity plots were generated using the Fusion Locomotor Activity Plotter analyses module (Omnitech Electronics Incorporated). Mice were placed into the open field 30 min post CNO injection.

Acute injury models

For formalin-induced injury, 10 μL of 2% formalin was injected into the intraplantar hindpaw. Mice were video recorded for 1 hr after formalin injection and time spent licking and lifting the paw was scored in 5-min bins. For capsaicin-induced injury, animals received 10 μL of intraplantar capsaicin (0.1% w/v in 10% ethanol diluted in saline) and the total time spent licking the injured paw was quantified over 20 minutes. Hargreaves and von Frey testing following capsaicin-induced injury occurred 20 min and 1 h after intraplantar injection.

Statistical analysis

Statistical analyses were performed using GraphPad Prism 8. Values are presented as mean +/- SEM. Statistical significance was assessed using tests indicated in applicable figure legends. Significance was indicated by $p < 0.05$. Sample sizes were based on pilot data and are similar to those typically used in the field.

Appendix F.3 Results

Activation of a descending circuit inhibits nociception

Midbrain and brainstem structures, centered upon the PAG, have been shown to modulate nociception. In particular, we focused on inputs to the PAG from the PBN, which has been extensively documented in relaying nociceptive information from the spinal cord to supraspinal targets. The PBN has also been shown to engage descending pain modulatory systems (Lapirot et al. 2009; Roeder et al. 2016). Given the role of the PBN in integrating nociceptive information from the spinal cord, we sought to determine whether it could directly modulate nociception through a descending pathway. Consistent with previous reports, when we injected the retrograde

tracer, cholera toxin B (CTB) into the PAG, we identified extensive labeling of cell bodies within the PBN, highlighting that PBN neurons directly project to the PAG (Figure 1A). To follow up on this observation, we sought to neurochemically characterize PBN neurons that project to the PAG using a combination of retrograde tracing and multiplex fluorescent in situ hybridization (FISH). We injected AAVretro-hSyn-eGFP into the PAG of wild type mice and subsequently stained PBN sections containing eYFP and analyzed their expression of known markers of PBN populations that have previously been implicated in modulating pain behaviors including Tac1, Pdyn, and Penk. We identified that among the PBN neurons that project to the PAG, there was considerable overlap with Tac1 (19.4+/-3.5), but minimal overlap with Pdyn (1.6+/-1.6) and Penk (1.8+/-1.4) (Figure 1B).

We next functionally assessed the role of PBN projections within the PAG using optogenetics. We introduced AAV2-EF1a-DIO-hChR2-eYFP into the PBN and implanted optical fibers within the PAG to directly stimulate PBN projections within the PAG (Figure 1C). Consistent with our previous findings, photostimulation of this pathway robustly inhibited reflexive responses in the tail flick assay (Figure 1D). This observation supports the role of the PBN in the central modulation of pain through a direct connection to the PAG.

Direct projections by the PAG to the spinal cord are sparse (Basbaum and Fields 1979), but, instead, the PAG modulates nociception through projections to the RVM, which is generally considered the primary output of the pain-modulation system (Prieto, Cannon, and Liebeskind 1983; Basbaum and Fields 1979; Gebhart 1982). Therefore, we then assessed the functional connection between the PAG and RVM using the same optogenetic approach in MOR-Cre mice. The optogenetic activation of PAG-MOR fibers in the RVM resulted in the robust induction of fos-expressing neurons in animals receiving channelrhodopsin compared to controls (Figure 1E).

Behaviorally, photostimulation of PAG-MOR fibers within the RVM resulted in heightened jumping responses on the hotplate test (Figure 1F).

Molecular and anatomical characterization of PAG-MOR neurons

Immunohistochemical and combined electrophysiological and pharmacological studies have highlighted the existence of neurons containing the mu-opioid receptor within the PAG [36,37,49,50]. For instance, microinjections of mu agonists such as morphine [51] and DAMGO [52] into the RVM inhibits withdrawal reflexes to noxious heat [51] and acts directly on PAG neurons containing the mu-opioid receptor.

The circuitry and molecular identities of mu-sensitive PAG neurons remains unclear. Although it is thought that morphine may inhibit local GABAergic PAG neurons containing the mu-opioid receptor to mediate anti-nociception [50], a significant number of PAG neurons immunoreactive for the mu-opioid receptor have been shown to project directly to the RVM [36]. Furthermore, it also remains unknown whether these opioid-sensitive neurons comprise glutamatergic or GABAergic subpopulations of PAG neurons. We performed tracing analysis of PAG-MOR neurons using a Cre-dependent fluorescent reporter (Figure 2A). We identified projection targets in numerous structures throughout the forebrain and brainstem such as the anterior hypothalamus, ventral tegmental area, and RVM (Figure 2A). Given the important role of the PAG in the descending modulation of pain and its significant projections to the RVM, we focused on this particular pathway (Figure 2B). When we stained Oprm1-expressing neurons in the PAG, we found that these neurons extensively overlapped with both Slc32a1 (Vgat) and Slc17a6 (Vglut2) (Figure 2C). This observation supports the idea that PAG-MOR neurons comprise a heterogeneous population and that the glutamatergic and GABAergic subpopulations may contribute distinct roles in nociception. To characterize PAG-MOR neurons projecting to

the RVM, we injected complementary Cre-dependent and Cre-independent retrograde tracers in the RVM of MOR-Cre and wild type mice, respectively (Figure 2D). We then used FISH to characterize back labeled neurons in the PAG. In contrast to Oprm1 neurons within the PAG that expressed either Slc32a1 or Slc17a6, PAG-MOR neurons that project to the RVM were found to be exclusively glutamatergic by their expression of Slc17a6 and limited expression of Slc32a1 (Figure 2E). On the basis of these findings, we propose that inhibitory PAG-MOR neurons may participate in the modulation of local circuitry within the PAG whereas excitatory PAG-MOR neurons project to other structures including the RVM (Figure 2F).

PAG-MOR neurons modulate complex somatosensory behaviors

Given the dramatic effects of pharmacological application of mu agonists within the PAG, we sought to test the contributions of PAG-MOR neurons directly. We used a chemogenetic approach to activate and inhibit PAG-MOR neurons by injection of AAV2.hSyn.DIO.hM3Dq-mCherry and AAV2.hSyn.DIO.hM4Di-mCherry, respectively, into the PAG of MOR-Cre mice. As a validation of these chemogenetic actuators, the chemogenetic activation of PAG-MOR neurons resulted in the induction of fos expression in the PAG (Figure 3A). Consistent with our optogenetic activation of the population, the chemogenetic activation of PAG-MOR neurons also activated neurons in the RVM, as determined by fos expression (Figure 3B). Neither activation nor inhibition of PAG-MOR neurons affected locomotor activity in an open field assay (Figure 3C), suggesting that the manipulation of these neurons does not influence locomotion. To examine the contribution of PAG-MOR neurons to nocifensive behaviors, we tested mice in several noxious pain assays, including hotplate (55 C) and injury models using intraplantar formalin and capsaicin. On the hotplate assay, the chemogenetic activation of PAG-MOR neurons facilitated jumping in naive animals (Figure 3D) and

chemogenetic inhibition attenuated jumping in capsaicin-injured animals (Figure 3E). However, neither chemogenetic activation nor inhibition influenced licking behaviors in an acute capsaicin-induced injury model (using 0.1% w/v capsaicin dissolved in 10% ethanol and saline) (Figure 3F). To assess the contribution of PAG-MOR neurons to a more persistent injury model, we injected mice with intraplantar formalin (2% w/v in saline) and quantified their licking behaviors targeted to the injured paw. We found that activation of PAG-MOR neurons modestly enhanced cumulative licking responses over the second phase of the formalin assay, although this trend was not found to be statistically significant (Figure 3H). In contrast, the inhibition of PAG-MOR neurons inclined toward a reduction in formalin-induced licking, yet this was also not found to be statistically significant. Together, our chemogenetic manipulations of PAG-MOR neurons robustly modulated jumping behaviors on a noxious hotplate, but did not significantly affect licking responses in acute injury models.

Upon assessment of reflexive nociceptive behaviors, the chemogenetic manipulations of PAG-MOR neurons revealed striking complexity in contrast to the behaviors observed on the hotplate assay and with formalin and capsaicin-induced licking. For example, with intradermal injection of chloroquine into the nape of the neck, chemogenetic activation of PAG-MOR neurons with CNO robustly attenuated scratching responses compared to baseline (Figure 4A). In the von frey assay, chemogenetic activation and inhibition of PAG-MOR neurons bidirectionally modulated mechanical thresholds (Figure 4B). In both the von Frey and Hargreaves assays, activation of PAG-MOR neurons consistently inhibited thresholds (Figure 4B, C), in contrast to its facilitation of responses to noxious stimuli, such as hotplate (Figure 3D). However, tail flick responses were not affected by either chemogenetic activation or inhibition of PAG-MOR neurons (Figure 4D, E). Curiously, for assays involving noxious stimulation,

activation of PAG-MOR neurons generally facilitated nocifensive responses (such as licking and jumping), however for reflexive nociceptive assays such as the von frey and Hargreaves test, chemogenetic excitation inhibited responses. The activation of PAG-MOR neurons also robustly attenuated chloroquine-induced scratching, representing a divergence from its facilitation of licking responses following capsaicin and formalin-induced injury.

Modulation of latent sensitization by a brainstem circuit

Endogenous opioid signaling has been shown to mask the behavioral expression of pain in a variety of chronic and inflammatory models of pain in a process known as latent sensitization of pain (Le Roy et al. 2011; Li, Angst, and Clark 2001; Corder et al. 2013). Following a noxious injury, animals exhibit a hyperalgesic state that is later masked by the upregulation of opioid signaling (Taylor and Corder 2014). However, the masking of hyperalgesia has been shown to be reversed following the application of opioid receptor antagonists, such as naloxone (Corder et al. 2013). We sought to test the contribution of the PAG in the latent sensitization of pain (Figure 5A). Consistent with previous findings, we established that the systemic administration of naloxone (10 mg/kg IP) in naive animals did not affect jumping behaviors (either latency to jump or total jumps) on the hotplate assay compared to saline (Figure B). In our optogenetic experiments, however, the administration of naloxone facilitated jumping behaviors in control mice compared to baseline (Figure 5C). Naloxone decreased control animals' latency to jump and increased their total jumping behaviors (Figure 5C). However, optogenetic photostimulation of PBN fibers within the PAG blocks the hyperalgesic effects of naloxone and results in the elevation of latencies to jump and reduces total jumps on the hotplate test (Figure 5C). The robust effects of naloxone in control animals in the absence of a prior injury (beyond the intracranial viral injection and implant) highlight the

role of compensatory endogenous opioids mechanisms that are engaged following cranial surgery. The striking attenuation of latent sensitization by optical stimulation of PBN terminals within the PAG suggests that this particular circuit is important for the modulation of opioidergic transmission in latent sensitization.

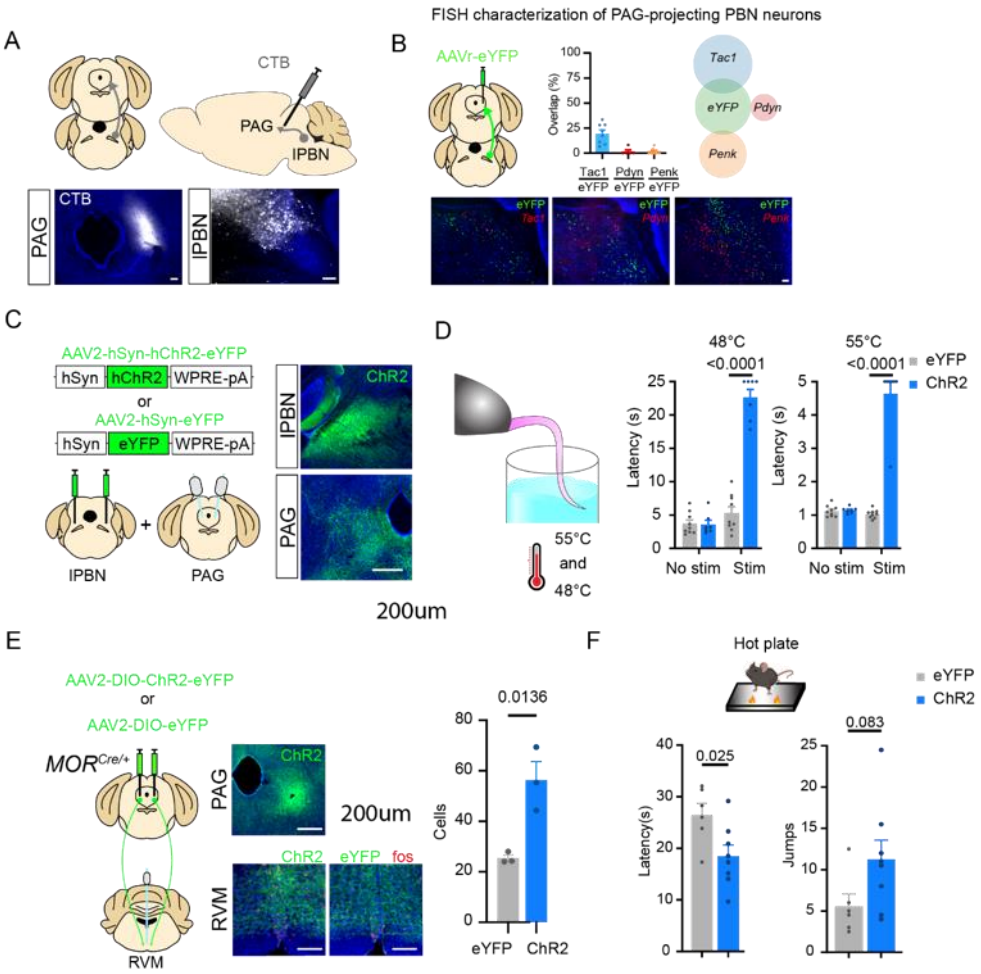

Appendix F Figure 1. A polysynaptic brainstem circuit for descending modulation

Stereotaxic delivery of CTB in the PAG and back labeled cell bodies in the PBN. Representative images are shown. Scale bars = 50 um.

Characterization of PBN neurons that project to the PAG using a retrogradely-labeled reporter (AAVr-eYFP) and FISH. Representative images are shown. Percentages of eYFP-expressing PBN neurons expressing *Tac1* (19.4+/-3.5), *Pdyn* (1.6+/-1.6), and *Penk* (1.8+/-1.4) and their relative overlap are shown. Data are mean + SEM with dots representing 5-8 PBN sections from 2-3 mice. Scale bars =

Strategy to optogenetically activate PBN projections within the PAG. Scale bars = 200 um.

The effect of optogenetically activating PBN projections to the PAG on the tail-flick assay at 48 C and 55 C. Data are mean + SEM with dots representing individual mice (n=7 control, n=9 ChR2 mice). *P* values indicate the results of 2-way repeated measures ANOVA with Holm-Sidak's multiple comparisons test.

Approach to optogenetically activate PAG projections within the RVM. The activation of this pathway induces the expression of *fos* in the RVM. Data are mean + SEM with dots representing individual mice (3 sections are averaged

for each animal). *P* value represents the result of two-tailed, unpaired t-test. Representative images from control and ChR2 mice. Scale bars = 200 um.

The effect of optogenetic activation of PAG projections in the RVM on jumping behaviors on the hotplate assay (total jumps and latency to jump). Data are mean + SEM with dots representing individual mice. *P* value represents the result of two-tailed, unpaired t-test.

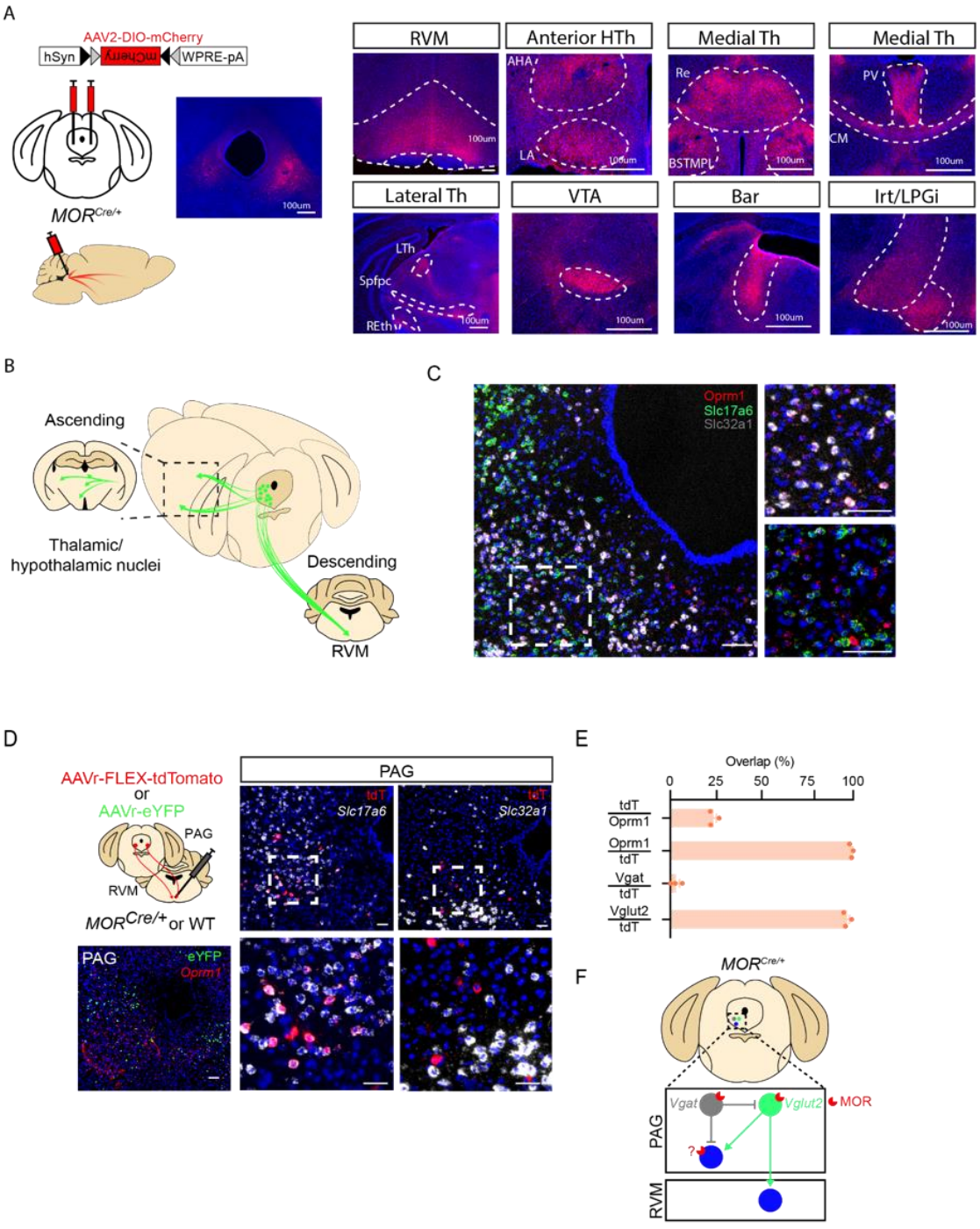

Appendix F Figure 2. Molecular and anatomic characterization of MOR neurons in the PAG.

(A) Approach to visualize projections from PAG-MOR neurons using Cre-dependent tracers introduced into the PAG. Major downstream targets of PAG-MOR neurons throughout the brain and brainstem. Representative images are shown. Re: reuniens thalamic nucleus, BSTMPL: bed nucleus stria terminalis, medial posterolateral, PV:

paraventricular thalamic nucleus, CM: centromedial thalamic nucleus, Spfpc: subparafascicular thalamus, REth: retroethmoid intramedullar thalamic area, PR: prerubral thalamic area, RVM: rostral ventromedial medulla, AHA: anterior hypothalamic area, LA: lateroanterior nuclei, Bar: Barrington's nucleus, Irt: intermediate reticular nucleus, LPGi: lateral paragigantocellular nucleus, VTA: ventral tegmental area, RRF: retrorubral field. Scale bar = 100 um.

(B) Cartoon representation of PAG-MOR ascending and descending projections throughout the brain.

(C) FISH characterization of *Oprm1* PAG neurons with respect to excitatory (*Slc17a6)* and inhibitory (*Slc32a1)* markers. Scale bars = 100 um.

(D) Cartoon depiction of two complementary approaches used to characterize descending projections of PAG-MOR neurons to the RVM. Retrograde tracers are introduced into the RVM of MOR-Cre or WT mice and labeled cell bodies in the PAG are characterized (using *Oprm1, Slc17a6,* and *Slc32a1)* using FISH. Representative images of PAG sections are shown. Scale bar = 50 um.

(E) Quantification of (D). Data are mean + SEM with dots representing individual mice (n=3 mice, with an average of 3-4 sections per mouse).

(F) Model for how divergent excitatory and inhibitory PAG neurons containing the mu-opioid receptor (MOR) modulate pain behaviors.

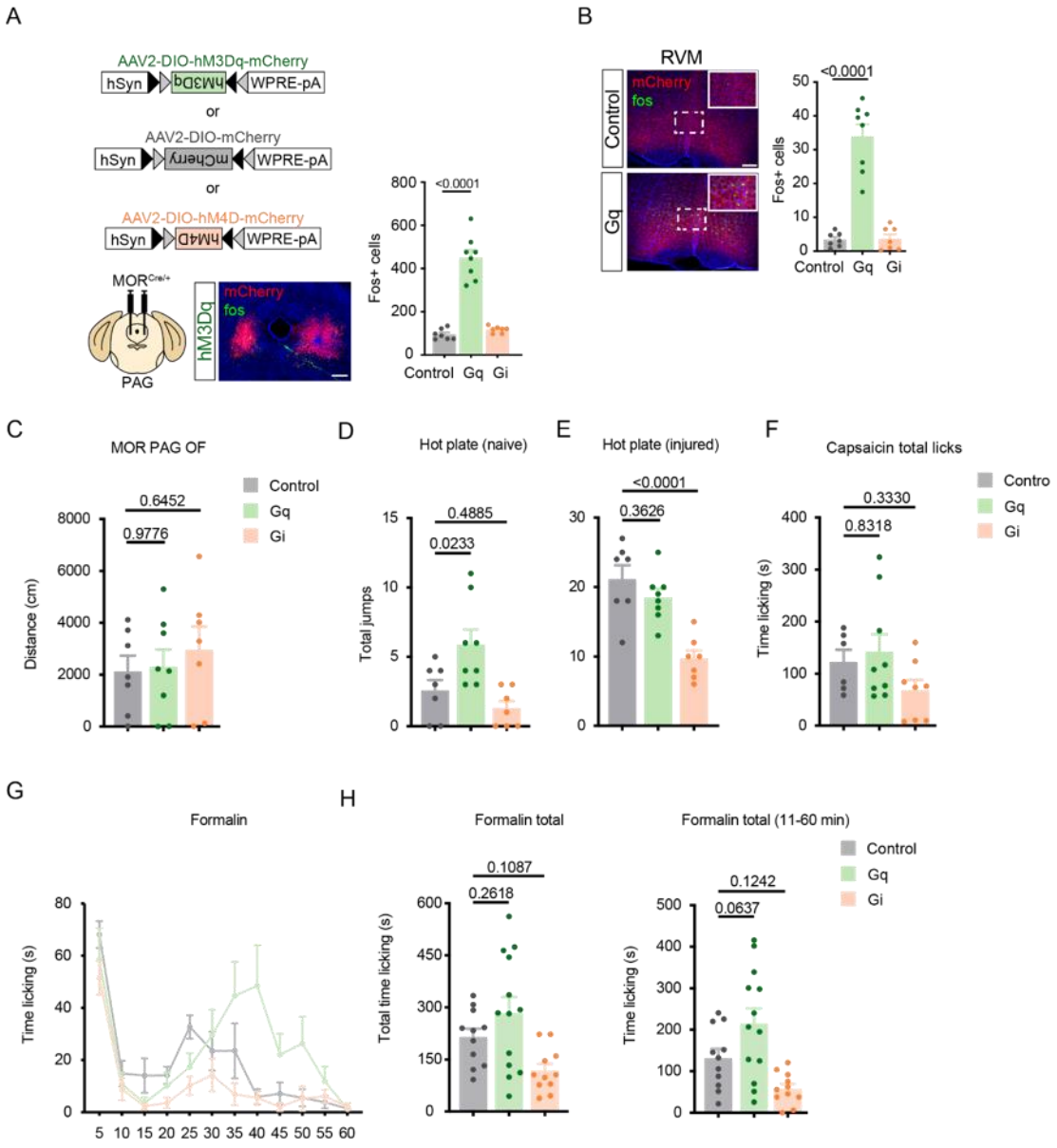

Appendix F Figure 3. PAG-MOR neurons modulate nocifensive behaviors.

(A) Approach to chemogenetically activate and inhibit PAG-MOR neurons involving the injection of Cre-dependent hM3Dq and hM4Di, respectively to the PAG. A representative image is shown. Scale bar = 50 um.

(B) Induction of fos expression within the RVM following chemogenetic manipulation of PAG-MOR neurons. Representative images of RVM sections are shown. Scale bar = 50 um. Comparison of fos expression in the RVM. Data are mean + SEM with dots representing individual mice (n=7-8 mice per group, averaging 4 sections per mouse). *P* values indicate the results of one-way ANOVA with Dunnett's multiple corrections test.

(C-F) Effect of chemogenetic activation and inhibition on the (C) openfield, (D-E) hotplate test (D) without and (E) with capsaicin-induced injury, and (F) nocifensive licking behaviors following intraplantar capsaicin-induced injury.

Data are mean + SEM with dots representing individual mice (Control: 6-11, hM3Dq: 7-13, and hM4Di: 7-11 mice per group). *P* values indicate the results of one-way ANOVA with Dunnett's multiple corrections test.

(G-H) Effect of chemogenetic manipulations of PAG-MOR neurons on licking responses following intraplantar formalin. (G) Time course of licking responses binned every 5 min over 1 h. Data are (G) mean +/- SEM and (H) mean + SEM with dots representing individual mice (n=11-13 mice per group. *P* values indicate the results of one-way ANOVA with Dunnett's multiple corrections test.

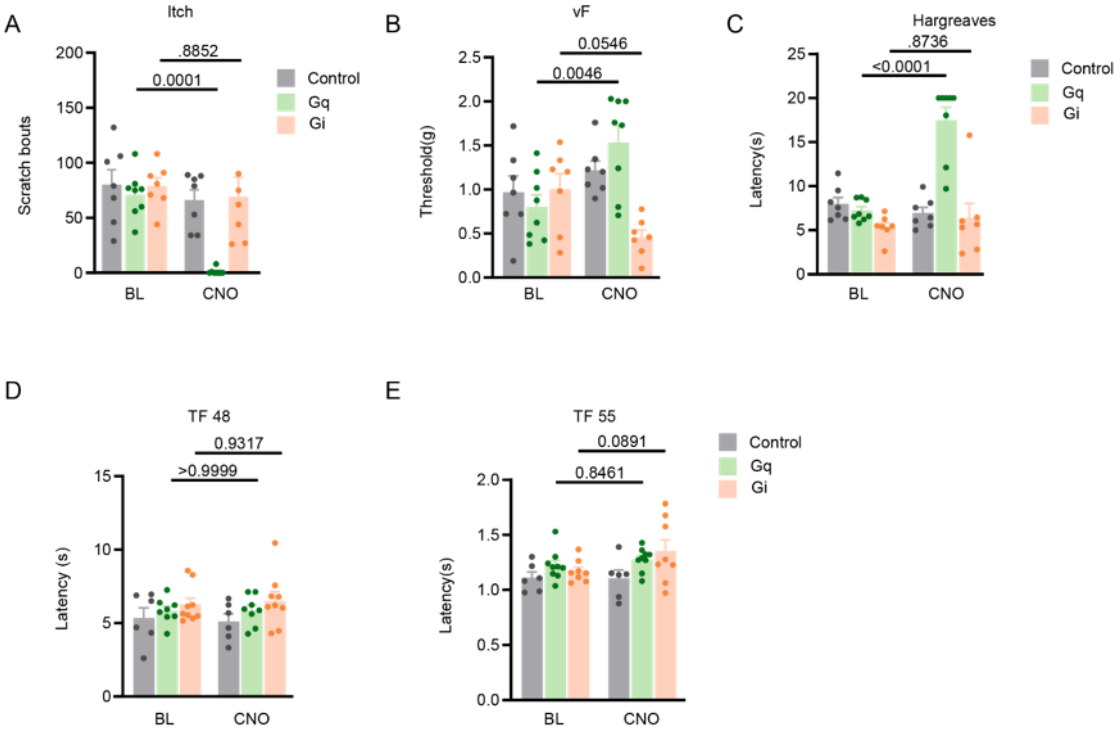

Appendix F Figure 4. PAG-MOR neurons modulate itch and reflexive pain behaviors.

(A-E) Effect of chemogenetic manipulations of PAG-MOR neurons on (A) chloroquine-induced itch, (B) von Frey assay, (C) Hargreaves assay, and (D-E) tail flick assay at (D) 48 C (E) and 55 C. Data are mean + SEM with dots representing individual mice (Control: 6-7, hM3Dq: 8-9, and hM4Di: 7-8 mice per group). *P* values indicate the results of two-way repeated measures ANOVA with Sidak's multiple corrections test.

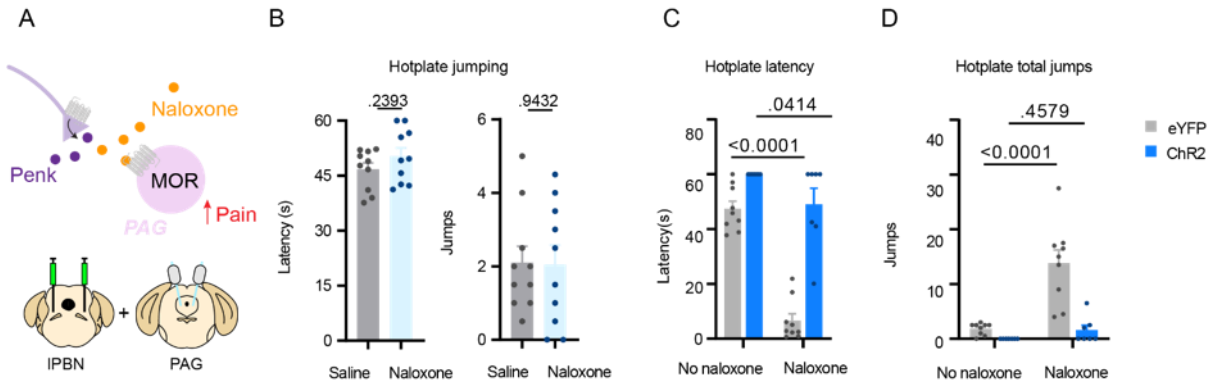

Appendix F Figure 5. Latent sensitization of pain is modulated by a PBN → PAG pathway

(A) Model for compensatory endogenous opioid signaling between the PBN and PAG following injury.

(B) Jumping behaviors among naive animals receiving saline or naloxone. Latency to jump and total jumps on a hotplate were quantified. Data are mean + SEM with dots representing individual mice (n=10 mice per group). P values indicate the results of two-tailed unpaired t-test.

(C-D) Effect of optogenetic stimulation of PBN projections in the PAG in the presence of naloxone on hotplate jumping behaviors including (C) latency to jump and (D) total jumps. Data are mean + SEM with dots representing individual mice (n=7-9 mice per group). *P* values indicate the results of two-way repeated measures ANOVA with Holm-Sidak's multiple comparisons test.

Appendix F.4 Discussion

It has recently been shown that the PAG contains at least two classes of neurons that divergently modulate nociception. In addition to their differences in sensitivity to pharmacological agents (Moreau and Fields 1986; Carstens, Stelzer, and Zimmermann 1988; Behbehani et al. 1990), PAG neurons can also be distinguished by their transmitter. GABAergic (Vgat), or inhibitory, neurons are thought to be pain facilitating, whereas glutamatergic (Vglut2), or excitatory, neurons are thought to be anti-nociceptive (Samineni et al. 2019, 2017; Aimone and Gebhart 1986; M. Jiang and Behbehani 2001). Interestingly, PAG neurons have recently

been shown to exhibit modality-specificity and are differentially engaged to modulate pain and itch (Samineni et al. 2019).

Appendix F.5 Bibliography

Aimone, L D, and G F Gebhart. 1986. “Stimulation-Produced Spinal Inhibition from the Midbrain in the Rat Is Mediated by an Excitatory Amino Acid Neurotransmitter in the Medial Medulla.” *The Journal of Neuroscience* 6 (6): 1803–13.

Basbaum, A I, and H L Fields. 1978. “Endogenous Pain Control Mechanisms: Review and Hypothesis.” *Annals of Neurology* 4 (5): 451–62.

Behbehani, M M, M R Jiang, S D Chandler, and M Ennis. 1990. “The Effect of GABA and Its Antagonists on Midbrain Periaqueductal Gray Neurons in the Rat.” *Pain* 40 (2): 195–204.

Budai, D, and H L Fields. 1998. “Endogenous Opioid Peptides Acting at Mu-Opioid Receptors in the Dorsal Horn Contribute to Midbrain Modulation of Spinal Nociceptive Neurons.” *Journal of Neurophysiology* 79 (2): 677–87.

Carstens, E, M Hartung, B Stelzer, and M Zimmermann. 1990. “Suppression of a Hind Limb Flexion Withdrawal Reflex by Microinjection of Glutamate or Morphine into the Periaqueductal Gray in the Rat.” *Pain* 43 (1): 105–12.

Carstens, E, B Stelzer, and M Zimmermann. 1988. “Microinjections of Glutamate or Morphine at Coincident Midbrain Sites Have Different Effects on Nociceptive Dorsal Horn Neurons in the Rat.” *Neuroscience Letters* 95 (1–3): 185–91.

Commons, K G, S A Aicher, L M Kow, and D W Pfaff. 2000. “Presynaptic and Postsynaptic Relations of Mu-Opioid Receptors to Gamma-Aminobutyric Acid-Immunoreactive and Medullary-Projecting Periaqueductal Gray Neurons.” *The Journal of Comparative Neurology* 419 (4): 532–42.

Corder, G, S Doolen, R R Donahue, M K Winter, B L Jutras, Y He, X Hu, et al. 2013. “Constitutive μ-Opioid Receptor Activity Leads to Long-Term Endogenous Analgesia and Dependence.” *Science* 341 (6152): 1394–99. https://doi.org/10.1126/science.1239403.

Gebhart, G F. 1982. “Opiate and Opioid Peptide Effects on Brain Stem Neurons: Relevance to Nociception and Antinociceptive Mechanisms.” *Pain* 12 (2): 93–140.

Hargreaves, K, R Dubner, F Brown, C Flores, and J Joris. 1988. “A New and Sensitive Method for Measuring Thermal Nociception in Cutaneous Hyperalgesia.” *Pain* 32 (1): 77–88.

Heinricher, M M, I Tavares, J L Leith, and B M Lumb. 2009. “Descending Control of Nociception: Specificity, Recruitment and Plasticity.” *Brain Research Reviews* 60 (1): 214–25.

Jiang, M, and M M Behbehani. 2001. “Physiological Characteristics of the Projection Pathway from the Medial Preoptic to the Nucleus Raphe Magnus of the Rat and Its Modulation by the Periaqueductal Gray.” *Pain* 94 (2): 139–47.

Kalyuzhny, A E, and M W Wessendorf. 1998. “Relationship of Mu- and Delta-Opioid Receptors to GABAergic Neurons in the Central Nervous System, Including Antinociceptive Brainstem Circuits.” *The Journal of Comparative Neurology* 392 (4): 528–47.

Kardon, Adam P, Erika Polgár, Junichi Hachisuka, Lindsey M Snyder, Darren Cameron, Sinead Savage, Xiaoyun Cai, et al. 2014. “Dynorphin Acts as a Neuromodulator to Inhibit Itch in the Dorsal Horn of the Spinal Cord.” *Neuron* 82 (3): 573–86.

Lapirot, Olivier, Raja Chebbi, Lénaic Monconduit, Alain Artola, Radhouane Dallel, and Philippe Luccarini. 2009. “NK1 Receptor-Expressing Spinoparabrachial Neurons Trigger Diffuse Noxious Inhibitory Controls through Lateral Parabrachial Activation in the Male Rat.” *Pain* 142 (3): 245–54.

Le Roy, Chloé, Emilie Laboureyras, Stéphanie Gavello-Baudy, Jérémy Chateauraynaud, Jean-Paul Laulin, and Guy Simonnet. 2011. “Endogenous Opioids Released during Non-Nociceptive Environmental Stress Induce Latent Pain Sensitization Via a NMDA-Dependent Process.” *The Journal of Pain* 12 (10): 1069–79.

Lewis, V A, and G F Gebhart. 1977. “Evaluation of the Periaqueductal Central Gray (PAG) as a Morphine-Specific Locus of Action and Examination of Morphine-Induced and Stimulation-Produced Analgesia at Coincident PAG Loci.” *Brain Research* 124 (2): 283–303.

Li, X, M S Angst, and J D Clark. 2001. “Opioid-Induced Hyperalgesia and Incisional Pain.” *Anesthesia and Analgesia* 93 (1): 204–9.

Loyd, Dayna R, Michael M Morgan, and Anne Z Murphy. 2008. “Sexually Dimorphic Activation of the Periaqueductal Gray-Rostral Ventromedial Medullary Circuit during the Development of Tolerance to Morphine in the Rat.” *The European Journal of Neuroscience* 27 (6): 1517–24.

Loyd, Dayna R, Xioaya Wang, and Anne Z Murphy. 2008. “Sex Differences in Micro-Opioid Receptor Expression in the Rat Midbrain Periaqueductal Gray Are Essential for Eliciting

Sex Differences in Morphine Analgesia." *The Journal of Neuroscience* 28 (52): 14007–17.

Moreau, J L, and H L Fields. 1986. "Evidence for GABA Involvement in Midbrain Control of Medullary Neurons That Modulate Nociceptive Transmission." *Brain Research* 397 (1): 37–46.

Osborne, P B, C W Vaughan, H I Wilson, and M J Christie. 1996. "Opioid Inhibition of Rat Periaqueductal Grey Neurones with Identified Projections to Rostral Ventromedial Medulla in Vitro." *The Journal of Physiology* 490 (Pt 2) (January): 383–89.

Prieto, G J, J T Cannon, and J C Liebeskind. 1983. "N. Raphe Magnus Lesions Disrupt Stimulation-Produced Analgesia from Ventral but Not Dorsal Midbrain Areas in the Rat." *Brain Research* 261 (1): 53–57.

Reichling, D B, and A I Basbaum. 1990. "Contribution of Brainstem GABAergic Circuitry to Descending Antinociceptive Controls: I. GABA-Immunoreactive Projection Neurons in the Periaqueductal Gray and Nucleus Raphe Magnus." *The Journal of Comparative Neurology* 302 (2): 370–77.

Roeder, Zachary, QiLiang Chen, Sophia Davis, Jonathan D Carlson, Domenico Tupone, and Mary M Heinricher. 2016. "Parabrachial Complex Links Pain Transmission to Descending Pain Modulation." *Pain* 157 (12): 2697–2708.

Samineni, Vijay K, Jose G Grajales-Reyes, Bryan A Copits, Daniel E O'Brien, Sarah L Trigg, Adrian M Gomez, Michael R Bruchas, and Robert W Gereau. 2017. "Divergent Modulation of Nociception by Glutamatergic and Gabaergic Neuronal Subpopulations in the Periaqueductal Gray." *ENeuro* 4 (2).

Samineni, Vijay K, Jose G Grajales-Reyes, Saranya S Sundaram, Judy J Yoo, and Robert W Gereau. 2019. "Cell Type-Specific Modulation of Sensory and Affective Components of Itch in the Periaqueductal Gray." *Nature Communications* 10 (1): 4356.

Taylor, Bradley K, and Gregory Corder. 2014. "Endogenous Analgesia, Dependence, and Latent Pain Sensitization." *Current Topics in Behavioral Neurosciences* 20: 283–325.

Tsou, K, and C S Jang. 1964. "Studies on the Site of Analgesic Action of Morphine by Intracerebral Micro-Injection." *Scientia Sinica* 13 (July): 1099–1109.

Vaughan, C W, S L Ingram, M A Connor, and M J Christie. 1997. "How Opioids Inhibit GABA-Mediated Neurotransmission." *Nature* 390 (6660): 611–14.

Vigouret, J, H Teschemacher, K Albus, and A Herz. 1973. "Differentiation between Spinal and Supraspinal Sites of Action of Morphine When Inhibiting the Hindleg Flexor Reflex in

Rabbits.” *Neuropharmacology* 12 (2): 111–21.

Yaksh, T L. 1997. “Pharmacology and Mechanisms of Opioid Analgesic Activity.” *Acta Anaesthesiologica Scandinavica* 41 (1 Pt 2): 94–111.

Zhang, Y, L N Du, G C Wu, and X D Cao. 1998. “Modulation of Intrathecal Morphine-Induced Immunosuppression by Microinjection of Naloxone into Periaqueductal Gray.” *Zhongguo Yao Li Xue Bao = Acta Pharmacologica Sinica* 19 (6): 519–22.

Bibliography

"European Medicines Agency. Assessment Report: Winfuran. European Medicines Agency. Committee for Medicinal Products for Human Use; 2013."

Ackley, M A, R W Hurley, D E Virnich, and D L Hammond. 2001. "A Cellular Mechanism for the Antinociceptive Effect of a Kappa Opioid Receptor Agonist." *Pain* 91 (3): 377–88.

Acton, David, Xiangyu Ren, Stefania Di Costanzo, Antoine Dalet, Steeve Bourane, Ilaria Bertocchi, Carola Eva, and Martyn Goulding. 2019. "Spinal Neuropeptide Y1 Receptor-Expressing Neurons Form an Essential Excitatory Pathway for Mechanical Itch." *Cell Reports* 28 (3): 625-639.e6.

Aicher, S A, and A Randich. 1990. "Antinociception and Cardiovascular Responses Produced by Electrical Stimulation in the Nucleus Tractus Solitarius, Nucleus Reticularis Ventralis, and the Caudal Medulla." *Pain* 42 (1): 103–19.

Aicher, Sue A, Sam M Hermes, Kelsey L Whittier, and Deborah M Hegarty. 2012. "Descending Projections from the Rostral Ventromedial Medulla (RVM) to Trigeminal and Spinal Dorsal Horns Are Morphologically and Neurochemically Distinct." *Journal of Chemical Neuroanatomy* 43 (2): 103–11.

Aimone, L D, and G F Gebhart. 1986. "Stimulation-Produced Spinal Inhibition from the Midbrain in the Rat Is Mediated by an Excitatory Amino Acid Neurotransmitter in the Medial Medulla." *The Journal of Neuroscience* 6 (6): 1803–13.

Aimone, L D, C A Bauer, and G F Gebhart. 1988. "Brain-Stem Relays Mediating Stimulation-Produced Antinociception from the Lateral Hypothalamus in the Rat." *The Journal of Neuroscience* 8 (7): 2652–63.

Akhan, Ayse, Ferhunde Dilek Subasi, Gulsen Bosna, Osman Ekinci, Hakan Pamuk, Siddika Batan, Rezzan Yagmur Ateser, and Gulden Turan. 2016. "Comparison of Mirtazapine, Gabapentin and Ondansetron to Prevent Intrathecal Morphine-Induced Pruritus." *Northern Clinics of Istanbul* 3 (1): 53–59.

Akiyama, Tasuku, Mirela Iodi Carstens, Akihiko Ikoma, Ferda Cevikbas, Martin Steinhoff, and Earl Carstens. 2012. "Mouse Model of Touch-Evoked Itch (Alloknesis)." *The Journal of Investigative Dermatology* 132 (7): 1886–91.

Akiyama, Tasuku, Mirela Iodi Carstens, Dorothea Piecha, Sonja Steppan, and Earl Carstens. 2015. "Nalfurafine Suppresses Pruritogen- and Touch-Evoked Scratching Behavior in Models of Acute and Chronic Itch in Mice." *Acta Dermato-Venereologica* 95 (2): 147–50.

Al-Hasani, Ream, and Michael R Bruchas. 2011. “Molecular Mechanisms of Opioid Receptor-Dependent Signaling and Behavior.” *Anesthesiology* 115 (6): 1363–81.

Alam, Asim, and David N Juurlink. 2016. “The Prescription Opioid Epidemic: An Overview for Anesthesiologists.” *Canadian Journal of Anaesthesia* 63 (1): 61–68.

Alran, Séverine, Olivier Sibony, Jean-François Oury, Dominique Luton, and Philippe Blot. 2002. “Differences in Management and Results in Term-Delivery in Nine European Referral Hospitals: Descriptive Study.” *European Journal of Obstetrics, Gynecology, and Reproductive Biology* 103 (1): 4–13.

Anand, Sheeba. 2013. “Gabapentin for Pruritus in Palliative Care.” *The American Journal of Hospice & Palliative Care* 30 (2): 192–96.

Andersen, Hjalte Holm, Tasuku Akiyama, Leigh Ann Nattkemper, Antoinette van Laarhoven, Jesper Elberling, Gil Yosipovitch, and Lars Arendt-Nielsen. 2018. “Alloknesis and Hyperknesis-Mechanisms, Assessment Methodology, and Clinical Implications of Itch Sensitization.” *Pain* 159 (7): 1185–97.

Andoh, Tsugunobu, Yuichi Yageta, Mitsuhiro Konno, Tomomi Yamaguchi-Miyamoto, Hiroki Takahata, Hiroshi Nojima, Hideo Nemoto, and Yasushi Kuraishi. 2008. “Evidence for Separate Involvement of Different Mu-Opioid Receptor Subtypes in Itch and Analgesia Induced by Supraspinal Action of Opioids.” *Journal of Pharmacological Sciences* 106 (4): 667–70.

Ansah, Osei B, Leonor Gonçalves, Armando Almeida, and Antti Pertovaara. 2009. “Enhanced Pronociception by Amygdaloid Group I Metabotropic Glutamate Receptors in Nerve-Injured Animals.” *Experimental Neurology* 216 (1): 66–74.

Anwari, J S, and S Iqbal. 2003. “Antihistamines and Potentiation of Opioid Induced Sedation and Respiratory Depression.” *Anaesthesia* 58 (5): 494–95.

Arendt, Katherine, and Scott Segal. 2008. “Why Epidurals Do Not Always Work.” *Reviews in Obstetrics and Gynecology* 1 (2): 49–55.

Arguinchona, Joseph H., and Prasanna Tadi. 2020. “Neuroanatomy, Reticular Activating System.” In *StatPearls*. Treasure Island (FL): StatPearls Publishing.

Asokumar, B, L M Newman, R J McCarthy, A D Ivankovich, and K J Tuman. 1998. “Intrathecal Bupivacaine Reduces Pruritus and Prolongs Duration of Fentanyl Analgesia during Labor: A Prospective, Randomized Controlled Trial.” *Anesthesia and Analgesia* 87 (6): 1309–15.

Bailey, A G, R D Valley, E B Freid, and P Calhoun. 1994. “Epidural Morphine Combined with Epidural or Intravenous Butorphanol for Postoperative Analgesia in Pediatric Patients.” *Anesthesia and Analgesia* 79 (2): 340–44.

Baldini, Angee, Michael Von Korff, and Elizabeth H B Lin. 2012. “A Review of Potential Adverse Effects of Long-Term Opioid Therapy: A Practitioner’s Guide.” *The Primary Care*

Companion for CNS Disorders 14 (3).

Baldo, B A, and N H Pham. 2012. “Histamine-Releasing and Allergenic Properties of Opioid Analgesic Drugs: Resolving the Two.” *Anaesthesia and Intensive Care* 40 (2): 216–35.

Ballantyne, J C, A B Loach, and D B Carr. 1988. “Itching after Epidural and Spinal Opiates.” *Pain* 33 (2): 149–60.

Barbaro, N M, M M Heinricher, and H L Fields. 1986. “Putative Pain Modulating Neurons in the Rostral Ventral Medulla: Reflex-Related Activity Predicts Effects of Morphine.” *Brain Research* 366 (1–2): 203–10.

Basbaum, A I, and H L Fields. 1979. “The Origin of Descending Pathways in the Dorsolateral Funiculus of the Spinal Cord of the Cat and Rat: Further Studies on the Anatomy of Pain Modulation.” *The Journal of Comparative Neurology* 187 (3): 513–31.

Baskin, D S, W R Mehler, Y Hosobuchi, D E Richardson, J E Adams, and M A Flitter. 1986. “Autopsy Analysis of the Safety, Efficacy and Cartography of Electrical Stimulation of the Central Gray in Humans.” *Brain Research* 371 (2): 231–36.

Behbehani, M M, and H L Fields. 1979. “Evidence That an Excitatory Connection between the Periaqueductal Gray and Nucleus Raphe Magnus Mediates Stimulation Produced Analgesia.” *Brain Research* 170 (1): 85–93.

Behbehani, M M, M R Jiang, S D Chandler, and M Ennis. 1990. “The Effect of GABA and Its Antagonists on Midbrain Periaqueductal Gray Neurons in the Rat.” *Pain* 40 (2): 195–204.

Behbehani, M M, M R Park, and M E Clement. 1988. “Interactions between the Lateral Hypothalamus and the Periaqueductal Gray.” *The Journal of Neuroscience* 8 (8): 2780–87.

Behbehani, M M. 1995. “Functional Characteristics of the Midbrain Periaqueductal Gray.” *Progress in Neurobiology* 46 (6): 575–605.

Bellgowan, P S, and F J Helmstetter. 1998. “The Role of Mu and Kappa Opioid Receptors within the Periaqueductal Gray in the Expression of Conditional Hypoalgesia.” *Brain Research* 791 (1–2): 83–89.

Bernards, Christopher M., Danny D. Shen, Emily S. Sterling, Jason E. Adkins, Linda Risler, Brian Phillips, and Wolfgang Ummenhofer. 2003. “Epidural, Cerebrospinal Fluid, and Plasma Pharmacokinetics of Epidural Opioids (Part 1).” *Anesthesiology* 99 (2): 455–65.

Blunk, James A, Martin Schmelz, Susanne Zeck, Per Skov, Rudolf Likar, and Wolfgang Koppert. 2004. “Opioid-Induced Mast Cell Activation and Vascular Responses Is Not Mediated by Mu-Opioid Receptors: An in Vivo Microdialysis Study in Human Skin.” *Anesthesia and Analgesia* 98 (2): 364–70.

Bolanos, C A, G M Garmsen, M A Clair, and S A McDougall. 1996. “Effects of the Kappa-Opioid Receptor Agonist U-50,488 on Morphine-Induced Place Preference Conditioning in

the Developing Rat." *European Journal of Pharmacology* 317 (1): 1–8.

Bonnet, M P, E Marret, J Josserand, and F J Mercier. 2008. "Effect of Prophylactic 5-HT3 Receptor Antagonists on Pruritus Induced by Neuraxial Opioids: A Quantitative Systematic Review." *British Journal of Anaesthesia* 101 (3): 311–19.

Borgeat, A, O H Wilder-Smith, M Saiah, and K Rifat. 1992. "Subhypnotic Doses of Propofol Relieve Pruritus Induced by Epidural and Intrathecal Morphine." *Anesthesiology* 76 (4): 510–12.

Bourane, Steeve, Bo Duan, Stephanie C Koch, Antoine Dalet, Olivier Britz, Lidia Garcia-Campmany, Euiseok Kim, et al. 2015. "Gate Control of Mechanical Itch by a Subpopulation of Spinal Cord Interneurons." *Science* 350 (6260): 550–54.

Bouvier, Julien, Vittorio Caggiano, Roberto Leiras, Vanessa Caldeira, Carmelo Bellardita, Kira Balueva, Andrea Fuchs, and Ole Kiehn. 2015. "Descending Command Neurons in the Brainstem That Halt Locomotion." *Cell* 163 (5): 1191–1203.

Boyle, Kieran A, Maria Gutierrez-Mecinas, Erika Polgár, Nicole Mooney, Emily O'Connor, Takahiro Furuta, Masahiko Watanabe, and Andrew J Todd. 2017. "A Quantitative Study of Neurochemically Defined Populations of Inhibitory Interneurons in the Superficial Dorsal Horn of the Mouse Spinal Cord." *Neuroscience* 363 (November): 120–33.

Brenner, Daniel S, Judith P Golden, and Robert W Gereau. 2012. "A Novel Behavioral Assay for Measuring Cold Sensation in Mice." *Plos One* 7 (6): e39765.

Brenner, Daniel S, Judith P Golden, Sherri K Vogt, and Robert W Gereau. 2015. "A Simple and Inexpensive Method for Determining Cold Sensitivity and Adaptation in Mice." *Journal of Visualized Experiments*, no. 97 (March).

Bromage, P R. 1981. "The Price of Intraspinal Narcotic Analgesia: Basic Constraints." *Anesthesia and Analgesia* 60 (7): 461–63.

Bruchas, M R, B B Land, and C Chavkin. 2010. "The Dynorphin/Kappa Opioid System as a Modulator of Stress-Induced and pro-Addictive Behaviors." *Brain Research* 1314 (February): 44–55.

Brust, Tarsis F, Jenny Morgenweck, Susy A Kim, Jamie H Rose, Jason L Locke, Cullen L Schmid, Lei Zhou, et al. 2016. "Biased Agonists of the Kappa Opioid Receptor Suppress Pain and Itch without Causing Sedation or Dysphoria." *Science Signaling* 9 (456): ra117.

Budai, D, and H L Fields. 1998. "Endogenous Opioid Peptides Acting at Mu-Opioid Receptors in the Dorsal Horn Contribute to Midbrain Modulation of Spinal Nociceptive Neurons." *Journal of Neurophysiology* 79 (2): 677–87.

Budai, D, I Harasawa, and H L Fields. 1998. "Midbrain Periaqueductal Gray (PAG) Inhibits Nociceptive Inputs to Sacral Dorsal Horn Nociceptive Neurons through Alpha2-Adrenergic Receptors." *Journal of Neurophysiology* 80 (5): 2244–54.

Buhler, A V, J Choi, H K Proudfit, and G F Gebhart. 2005. “Neurotensin Activation of the NTR1 on Spinally-Projecting Serotonergic Neurons in the Rostral Ventromedial Medulla Is Antinociceptive.” *Pain* 114 (1–2): 285–94.

Buhler, Amber V K, Sean Tachibana, Yangmiao Zhang, and Raymond M Quock. 2018. “NNOS Immunoreactivity Co-Localizes with GABAergic and Cholinergic Neurons, and Associates with β-Endorphinergic and Met-Enkephalinergic Opioidergic Fibers in Rostral Ventromedial Medulla and A5 of the Mouse.” *Brain Research* 1698 (November): 170–78.

Bujedo, Borja Mugabure. 2014. “Current Evidence for Spinal Opioid Selection in Postoperative Pain.” *The Korean Journal of Pain* 27 (3): 200–209.

Butwick, Alexander J, Cynthia A Wong, and Nan Guo. 2018. “Maternal Body Mass Index and Use of Labor Neuraxial Analgesia: A Population-Based Retrospective Cohort Study.” *Anesthesiology* 129 (3): 448–58.

Cai, Xiaoyun, Huizhen Huang, Marissa S Kuzirian, Lindsey M Snyder, Megumi Matsushita, Michael C Lee, Carolyn Ferguson, Gregg E Homanics, Alison L Barth, and Sarah E Ross. 2016. “Generation of a KOR-Cre Knockin Mouse Strain to Study Cells Involved in Kappa Opioid Signaling.” *Genesis* 54 (1): 29–37.

Cai, You-Qing, Wei Wang, Yuan-Yuan Hou, and Zhizhong Z Pan. 2014. “Optogenetic Activation of Brainstem Serotonergic Neurons Induces Persistent Pain Sensitization.” *Molecular Pain* 10 (November): 70.

Camarata, P J, and T L Yaksh. 1985. “Characterization of the Spinal Adrenergic Receptors Mediating the Spinal Effects Produced by the Microinjection of Morphine into the Periaqueductal Gray.” *Brain Research* 336 (1): 133–42.

Campos, Carlos A, Anna J Bowen, Carolyn W Roman, and Richard D Palmiter. 2018. “Encoding of Danger by Parabrachial CGRP Neurons.” *Nature* 555 (7698): 617–22.

Cano, Georgina, Alicia M Passerin, Jennifer C Schiltz, J Patrick Card, Shaun F Morrison, and Alan F Sved. 2003. “Anatomical Substrates for the Central Control of Sympathetic Outflow to Interscapular Adipose Tissue during Cold Exposure.” *The Journal of Comparative Neurology* 460 (3): 303–26.

Cao, Wei Hua, and Shaun F Morrison. 2003. “Disinhibition of Rostral Raphe Pallidus Neurons Increases Cardiac Sympathetic Nerve Activity and Heart Rate.” *Brain Research* 980 (1): 1–10.

Carlson, Jonathan D, Jennifer J Maire, Melissa E Martenson, and Mary M Heinricher. 2007. “Sensitization of Pain-Modulating Neurons in the Rostral Ventromedial Medulla after Peripheral Nerve Injury.” The Journal of Neuroscience 27 (48): 13222–31.

Carstens, E, B Stelzer, and M Zimmermann. 1988. “Microinjections of Glutamate or Morphine at Coincident Midbrain Sites Have Different Effects on Nociceptive Dorsal Horn Neurons in the Rat.” *Neuroscience Letters* 95 (1–3): 185–91.

Carstens, E, H Bihl, D R Irvine, and M Zimmermann. 1981. “Descending Inhibition from Medial and Lateral Midbrain of Spinal Dorsal Horn Neuronal Responses to Noxious and Nonnoxious Cutaneous Stimuli in the Cat.” *Journal of Neurophysiology* 45 (6): 1029–42.

Carter, Matthew E, Sung Han, and Richard D Palmiter. 2015. “Parabrachial Calcitonin Gene-Related Peptide Neurons Mediate Conditioned Taste Aversion.” *The Journal of Neuroscience* 35 (11): 4582–86.

Cechetto, D F, and C B Saper. 1988. “Neurochemical Organization of the Hypothalamic Projection to the Spinal Cord in the Rat.” *The Journal of Comparative Neurology* 272 (4): 579–604.

Chadwick, H S, and L B Ready. 1988. “Intrathecal and Epidural Morphine Sulfate for Post-Cesarean Analgesia--a Clinical Comparison.” *Anesthesiology* 68 (6): 925–29.

Chaplan, S R, F W Bach, J W Pogrel, J M Chung, and T L Yaksh. 1994. “Quantitative Assessment of Tactile Allodynia in the Rat Paw.” *Journal of Neuroscience Methods* 53 (1): 55–63.

Charuluxananan, S, O Kyokong, W Somboonviboon, S Lertmaharit, P Ngamprasertwong, and K Nimcharoendee. 2001. “Nalbuphine versus Propofol for Treatment of Intrathecal Morphine-Induced Pruritus after Cesarean Delivery.” *Anesthesia and Analgesia* 93 (1): 162–65.

Charuluxananan, S, W Somboonviboon, O Kyokong, and K Nimcharoendee. 2000. “Ondansetron for Treatment of Intrathecal Morphine-Induced Pruritus after Cesarean Delivery.” *Regional Anesthesia and Pain Medicine* 25 (5): 535–39.

Charuluxananan, Somrat, Oranuch Kyokong, Wanna Somboonviboon, Arunchai Narasethakamol, and Pissamai Promlok. 2003. “Nalbuphine versus Ondansetron for Prevention of Intrathecal Morphine-Induced Pruritus after Cesarean Delivery.” *Anesthesia and Analgesia* 96 (6): 1789–93.

Chavkin, Charles. 2011. “The Therapeutic Potential of κ-Opioids for Treatment of Pain and Addiction.” *Neuropsychopharmacology* 36 (1): 369–70.

Chen, Michael C, Ramalingam Vetrivelan, Chun-Ni Guo, Catie Chang, Patrick M Fuller, and Jun Lu. 2017. “Ventral Medullary Control of Rapid Eye Movement Sleep and Atonia.” *Experimental Neurology* 290 (January): 53–62.

Chen, QiLiang, Zachary Roeder, Ming-Hua Li, YangMiao Zhang, Susan L Ingram, and Mary M Heinricher. 2017. “Optogenetic Evidence for a Direct Circuit Linking Nociceptive Transmission through the Parabrachial Complex with Pain-Modulating Neurons of the Rostral Ventromedial Medulla (RVM).” *ENeuro* 4 (3).

Chen, Tao, Xiao-Lin Wang, Juan Qu, Wei Wang, Ting Zhang, Yuchio Yanagawa, Sheng-Xi Wu, and Yun-Qing Li. 2013. “Neurokinin-1 Receptor-Expressing Neurons That Contain Serotonin and Gamma-Aminobutyric Acid in the Rat Rostroventromedial Medulla Are

Involved in Pain Processing." *The Journal of Pain* 14 (8): 778–92.

Chestnut, David H. 2005. "Efficacy and Safety of Epidural Opioids for Postoperative Analgesia." *Anesthesiology* 102 (1): 221–23.

Chiang, Michael C, Eileen K Nguyen, Martha Canto-Bustos, Andrew E Papale, Anne-Marie M Oswald, and Sarah E Ross. 2020. "Divergent Neural Pathways Emanating from the Lateral Parabrachial Nucleus Mediate Distinct Components of the Pain Response." *Neuron*, April.

Chiravanich, Wirinda, Maliwan Oofuvong, and Nalinee Kovitwanawong. 2012. "Single Dose of Gabapentin for Prophylaxis Intrathecal Morphine-Induced Pruritus in Orthopedic Surgery: A Randomized Controlled Trial." *Journal of the Medical Association of Thailand = Chotmaihet Thangphaet* 95 (2): 186–90.

Cho, H J, and A I Basbaum. 1991. "GABAergic Circuitry in the Rostral Ventral Medulla of the Rat and Its Relationship to Descending Antinociceptive Controls." *The Journal of Comparative Neurology* 303 (2): 316–28.

Cleary, D R, M J Neubert, and M M Heinricher. 2008. "Are Opioid-Sensitive Neurons in the Rostral Ventromedial Medulla Inhibitory Interneurons?" *Neuroscience* 151 (2): 564–71.

Cohen, S E, E F Ratner, T R Kreitzman, J H Archer, and L R Mignano. 1992. "Nalbuphine Is Better than Naloxone for Treatment of Side Effects after Epidural Morphine." *Anesthesia and Analgesia* 75 (5): 747–52.

Colvin, Lesley A, Fiona Bull, and Tim G Hales. 2019. "Perioperative Opioid Analgesia-When Is Enough Too Much? A Review of Opioid-Induced Tolerance and Hyperalgesia." *The Lancet* 393 (10180): 1558–68.

Comoli, E, E R Ribeiro-Barbosa, and Newton Sabino Canteras. 2003. "Predatory Hunting and Exposure to a Live Predator Induce Opposite Patterns of Fos Immunoreactivity in the PAG." *Behavioural Brain Research* 138 (1): 17–28.

Cousins, M J, and L E Mather. 1984. "Intrathecal and Epidural Administration of Opioids." *Anesthesiology* 61 (3): 276–310.

Cowan, Alan, George B Kehner, and Saadet Inan. 2015. "Targeting Itch with Ligands Selective for κ Opioid Receptors." *Handbook of Experimental Pharmacology* 226: 291–314.

Dafny, N, W Q Dong, C Prieto-Gomez, C Reyes-Vazquez, J Stanford, and J T Qiao. 1996. "Lateral Hypothalamus: Site Involved in Pain Modulation." *Neuroscience* 70 (2): 449–60.

Dahan, Albert, Leon Aarts, and Terry W Smith. 2010. "Incidence, Reversal, and Prevention of Opioid-Induced Respiratory Depression." *Anesthesiology* 112 (1): 226–38.

Dahan, Albert, Raymonda Romberg, Luc Teppema, Elise Sarton, Hans Bijl, and Erik Olofsen. 2004. "Simultaneous Measurement and Integrated Analysis of Analgesia and Respiration after an Intravenous Morphine Infusion." *Anesthesiology* 101 (5): 1201–9.

Dampney, Roger A L, Teri M Furlong, Jouji Horiuchi, and Kamon Iigaya. 2013. "Role of Dorsolateral Periaqueductal Grey in the Coordinated Regulation of Cardiovascular and Respiratory Function." *Autonomic Neuroscience: Basic & Clinical* 175 (1–2): 17–25.

Davidson, Steve, and Glenn J Giesler. 2010. "The Multiple Pathways for Itch and Their Interactions with Pain." *Trends in Neurosciences* 33 (12): 550–58.

De Felice, Milena, Raul Sanoja, Ruizhong Wang, Louis Vera-Portocarrero, Janice Oyarzo, Tamara King, Michael H Ossipov, et al. 2011. "Engagement of Descending Inhibition from the Rostral Ventromedial Medulla Protects against Chronic Neuropathic Pain." *Pain* 152 (12): 2701–9.

DeSousa, Kalindi A. 2014. "Intrathecal Morphine for Postoperative Analgesia: Current Trends." *World Journal of Anesthesiology* 3 (3): 191.

DiGiusto, Matthew, Tarun Bhalla, David Martin, Derek Foerschler, Megan J Jones, and Joseph D Tobias. 2014. "Patient-Controlled Analgesia in the Pediatric Population: Morphine versus Hydromorphone." *Journal of Pain Research* 7 (August): 471–75.

Ding, H, K Hayashida, T Suto, D D Sukhtankar, M Kimura, V Mendenhall, and M C Ko. 2015. "Supraspinal Actions of Nociceptin/Orphanin FQ, Morphine and Substance P in Regulating Pain and Itch in Non-Human Primates." *British Journal of Pharmacology* 172 (13): 3302–12.

Dourish, C T, M F O'Neill, J Coughlan, S J Kitchener, D Hawley, and S D Iversen. 1990. "The Selective CCK-B Receptor Antagonist L-365,260 Enhances Morphine Analgesia and Prevents Morphine Tolerance in the Rat." *European Journal of Pharmacology* 176 (1): 35–44.

Dowell, Deborah, Tamara M. Haegerich, and Roger Chou. 2016. "CDC Guideline for Prescribing Opioids for Chronic Pain — United States, 2016." *MMWR. Recommendations and Reports* 65 (1): 1–49.

Drewes, A M, L Svendsen, S J Taagholt, K Bjerregård, K D Nielsen, and B Hansen. 1998. "Sleep in Rheumatoid Arthritis: A Comparison with Healthy Subjects and Studies of Sleep/Wake Interactions." *British Journal of Rheumatology* 37 (1): 71–81.

Drewes, Asbjørn Mohr, Poul Jennum, Arne Andreasen, Anette Sjøl, and Kim Dremstrup Nielsen. 1994. "Self-Reported Sleep Disturbances and Daytime Complaints in Women with Fibromyalgia and Rheumatoid Arthritis." *Journal of Musculoskeletal Pain* 2 (4): 15–31.

Dualé, C, C Frey, F Bolandard, A Barrière, and P Schoeffler. 2003. "Epidural versus Intrathecal Morphine for Postoperative Analgesia after Caesarean Section." *British Journal of Anaesthesia* 91 (5): 690–94.

Dunteman, E, M Karanikolas, and K S Filos. 1996. "Transnasal Butorphanol for the Treatment of Opioid-Induced Pruritus Unresponsive to Antihistamines." *Journal of Pain and Symptom Management* 12 (4): 255–60.

Edelmayer, Rebecca M, Todd W Vanderah, Lisa Majuta, En-Tan Zhang, Beatriz Fioravanti, Milena De Felice, Juliana G Chichorro, et al. 2009. “Medullary Pain Facilitating Neurons Mediate Allodynia in Headache-Related Pain.” *Annals of Neurology* 65 (2): 184–93.

Edvinsson, L, J Cervós-Navarro, L I Larsson, C Owman, and A L Rönnberg. 1977. “Regional Distribution of Mast Cells Containing Histamine, Dopamine, or 5-Hydroxytryptamine in the Mammalian Brain.” *Neurology* 27 (9): 878–83.

Eippert, Falk, Ulrike Bingel, Eszter D Schoell, Juliana Yacubian, Regine Klinger, Jürgen Lorenz, and Christian Büchel. 2009. “Activation of the Opioidergic Descending Pain Control System Underlies Placebo Analgesia.” *Neuron* 63 (4): 533–43.

Eisenach, James C, David D Hood, Regina Curry, and Steven L Shafer. 2003. “Cephalad Movement of Morphine and Fentanyl in Humans after Intrathecal Injection.” *Anesthesiology* 99 (1): 166–73.

Eldor, J, V Fishelev, S Levine, P Guedj, and I Dudakova. 1994. “Prevention of Epidural Morphine Pruritus by Intramuscular Promethazine in Parturients.” *Regional Anesthesia* 19 (6): 433–34.

Els, Charl, Tanya D Jackson, Diane Kunyk, Vernon G Lappi, Barend Sonnenberg, Reidar Hagtvedt, Sangita Sharma, Fariba Kolahdooz, and Sebastian Straube. 2017. “Adverse Events Associated with Medium- and Long-Term Use of Opioids for Chronic Non-Cancer Pain: An Overview of Cochrane Reviews.” *Cochrane Database of Systematic Reviews* 10 (October): CD012509.

Ennis, M, C Schneider, E Nehring, and W Lorenz. 1991. “Histamine Release Induced by Opioid Analgesics: A Comparative Study Using Porcine Mast Cells.” *Agents and Actions* 33 (1–2): 20–22.

Fang, F G, J L Moreau, and H L Fields. 1987. “Dose-Dependent Antinociceptive Action of Neurotensin Microinjected into the Rostroventromedial Medulla of the Rat.” *Brain Research* 420 (1): 171–74.

Fang, F, and H K Proudfit. 1996. “Spinal Cholinergic and Monoamine Receptors Mediate the Antinociceptive Effect of Morphine Microinjected in the Periaqueductal Gray on the Rat Tail, but Not the Feet.” *Brain Research* 722 (1–2): 95–108.

Faris, P L, B R Komisaruk, L R Watkins, and D J Mayer. 1983. “Evidence for the Neuropeptide Cholecystokinin as an Antagonist of Opiate Analgesia.” *Science* 219 (4582): 310–12.

Fassoulaki, A, V Gatzou, G Petropoulos, and I Siafaka. 2004. “Spread of Subarachnoid Block, Intraoperative Local Anaesthetic Requirements and Postoperative Analgesic Requirements in Caesarean Section and Total Abdominal Hysterectomy.” *British Journal of Anaesthesia* 93 (5): 678–82.

Fechir, M, M Breimhorst, S Kritzmann, C Geber, T Schlereth, B Baier, and F Birklein. 2012. “Naloxone Inhibits Not Only Stress-Induced Analgesia but Also Sympathetic Activation

and Baroreceptor-Reflex Sensitivity." *European Journal of Pain* 16 (1): 82–92.

Fields, H L, A Malick, and R Burstein. 1995. "Dorsal Horn Projection Targets of ON and OFF Cells in the Rostral Ventromedial Medulla." *Journal of Neurophysiology* 74 (4): 1742–59.

Fields, H L, and S D Anderson. 1978. "Evidence That Raphe-Spinal Neurons Mediate Opiate and Midbrain Stimulation-Produced Analgesias." *Pain* 5 (4): 333–49.

Fields, Howard. 2004. "State-Dependent Opioid Control of Pain." *Nature Reviews. Neuroscience* 5 (7): 565–75.

Flacke, J W, W E Flacke, B C Bloor, A P Van Etten, and B J Kripke. 1987. "Histamine Release by Four Narcotics: A Double-Blind Study in Humans." *Anesthesia and Analgesia* 66 (8): 723–30.

Follansbee, Taylor, Tasuku Akiyama, Masanori Fujii, Auva Davoodi, Masaki Nagamine, Milera Iodi Carstens, and Earl Carstens. 2018. "Effects of Pruritogens and Algogens on Rostral Ventromedial Medullary (RVM) ON and OFF Cells." *Journal of Neurophysiology* 120 (5): 2156–63.

Foo, H, and Peggy Mason. 2003. "Brainstem Modulation of Pain during Sleep and Waking." *Sleep Medicine Reviews* 7 (2): 145–54.

Foo, H, Katherine Crabtree, and Peggy Mason. 2010. "The Modulatory Effects of Rostral Ventromedial Medulla on Air-Puff Evoked Microarousals in Rats." *Behavioural Brain Research* 215 (1): 156–59.

Fornal, C, S Auerbach, and B L Jacobs. 1985. "Activity of Serotonin-Containing Neurons in Nucleus Raphe Magnus in Freely Moving Cats." *Experimental Neurology* 88 (3): 590–608.

François, Amaury, Sarah A Low, Elizabeth I Sypek, Amelia J Christensen, Chaudy Sotoudeh, Kevin T Beier, Charu Ramakrishnan, et al. 2017. "A Brainstem-Spinal Cord Inhibitory Circuit for Mechanical Pain Modulation by GABA and Enkephalins." *Neuron* 93 (4): 822-839.e6.

Galloway, K S, and M Yaster. 2000. "Pain and Symptom Control in Terminally Ill Children." *Pediatric Clinics of North America* 47 (3): 711–46.

Gan, T J, B Ginsberg, P S Glass, J Fortney, R Jhaveri, and R Perno. 1997. "Opioid-Sparing Effects of a Low-Dose Infusion of Naloxone in Patient-Administered Morphine Sulfate." *Anesthesiology* 87 (5): 1075–81.

Ganesh, Arjunan, and Lynne G Maxwell. 2007. "Pathophysiology and Management of Opioid-Induced Pruritus." *Drugs* 67 (16): 2323–33.

Gao, S, A Proekt, N Renier, D P Calderon, and D W Pfaff. 2019. "Activating an Anterior Nucleus Gigantocellularis Subpopulation Triggers Emergence from Pharmacologically-Induced Coma in Rodents." *Nature Communications* 10 (1): 2897.

Gao, Zheng-Run, Wen-Zhen Chen, Ming-Zhe Liu, Xiao-Jun Chen, Li Wan, Xin-Yan Zhang, Lei Yuan, et al. 2019. "Tac1-Expressing Neurons in the Periaqueductal Gray Facilitate the Itch-Scratching Cycle via Descending Regulation." *Neuron* 101 (1): 45-59.e9.

Gebhart, G F. 1982. "Opiate and Opioid Peptide Effects on Brain Stem Neurons: Relevance to Nociception and Antinociceptive Mechanisms." *Pain* 12 (2): 93–140.

George, Ronald B, Terrence K Allen, and Ashraf S Habib. 2009. "Serotonin Receptor Antagonists for the Prevention and Treatment of Pruritus, Nausea, and Vomiting in Women Undergoing Cesarean Delivery with Intrathecal Morphine: A Systematic Review and Meta-Analysis." *Anesthesia and Analgesia* 109 (1): 174–82.

Ghilardi, J R, C J Allen, S R Vigna, D C McVey, and P W Mantyh. 1992. "Trigeminal and Dorsal Root Ganglion Neurons Express CCK Receptor Binding Sites in the Rat, Rabbit, and Monkey: Possible Site of Opiate-CCK Analgesic Interactions." *The Journal of Neuroscience* 12 (12): 4854–66.

Goletiani, Nathalie V, Jack H Mendelson, Michelle B Sholar, Arthur J Siegel, Alicja Skupny, and Nancy K Mello. 2007. "Effects of Nalbuphine on Anterior Pituitary and Adrenal Hormones and Subjective Responses in Male Cocaine Abusers." *Pharmacology, Biochemistry, and Behavior* 86 (4): 667–77.

Graham, D T, H Goodell, and H G Wolff. 1951. "Neural Mechanisms Involved in Itch, Itchy Skin, and Tickle Sensations." *The Journal of Clinical Investigation* 30 (1): 37–49.

Grangier, L, B Martinez de Tejada, G L Savoldelli, O Irion, and G Haller. 2020. "Adverse Side Effects and Route of Administration of Opioids in Combined Spinal-Epidural Analgesia for Labour: A Meta-Analysis of Randomised Trials." *International Journal of Obstetric Anesthesia* 41: 83–103.

Grant, Calum R.K., and Matthew R. Checketts. 2008. "Analgesia for Primary Hip and Knee Arthroplasty: The Role of Regional Anaesthesia." *Continuing Education in Anaesthesia, Critical Care & Pain* 8 (2): 56–61.

Green, Carmen R, Karen O Anderson, Tamara A Baker, Lisa C Campbell, Sheila Decker, Roger B Fillingim, Donna A Kalauokalani, et al. 2003. "The Unequal Burden of Pain: Confronting Racial and Ethnic Disparities in Pain." *Pain Medicine* 4 (3): 277–94.

Grosman, N. 1981. "Histamine Release from Isolated Rat Mast Cells: Effect of Morphine and Related Drugs and Their Interaction with Compound 48/80." *Agents and Actions* 11 (3): 196–203.

Gudbjörnsson, B, J E Broman, J Hetta, and R Hällgren. 1993. "Sleep Disturbances in Patients with Primary Sjögren's Syndrome." *Rheumatology* 32 (12): 1072–76.

Gulhas, Nurcin, Feray Akgul Erdil, Ozlem Sagir, Ender Gedik, Turkan Togal, Zekine Begec, and M Ozcan Ersoy. 2007. "Lornoxicam and Ondansetron for the Prevention of Intrathecal Fentanyl-Induced Pruritus." *Journal of Anesthesia* 21 (2): 159–63.

Gulhas, Nurcin, Feray Akgul Erdil, Ozlem Sagir, Ender Gedik, Turkan Togal, Zekine Begec, and M Ozcan Ersoy. 2007. “Lornoxicam and Ondansetron for the Prevention of Intrathecal Fentanyl-Induced Pruritus.” *Journal of Anesthesia* 21 (2): 159–63.

Gunal, Ali Ihsan, Goksel Ozalp, Tahir Kurtulus Yoldas, Servin Yesil Gunal, Ercan Kirciman, and Huseyin Celiker. 2004. “Gabapentin Therapy for Pruritus in Haemodialysis Patients: A Randomized, Placebo-Controlled, Double-Blind Trial.” *Nephrology, Dialysis, Transplantation* 19 (12): 3137–39.

Gunter, J B, J McAuliffe, T Gregg, N Weidner, A M Varughese, and D M Sweeney. 2000. “Continuous Epidural Butorphanol Relieves Pruritus Associated with Epidural Morphine Infusions in Children.” *Paediatric Anaesthesia* 10 (2): 167–72.

Gutstein, H B, A Mansour, S J Watson, H Akil, and H L Fields. 1998. “Mu and Kappa Opioid Receptors in Periaqueductal Gray and Rostral Ventromedial Medulla.” *Neuroreport* 9 (8): 1777–81.

Hachisuka, Junichi, H Richard Koerber, and Sarah E Ross. 2020. “Selective-Cold Output through a Distinct Subset of Lamina I Spinoparabrachial Neurons.” *Pain* 161 (1): 185–94.

Hachisuka, Junichi, Kyle M Baumbauer, Yu Omori, Lindsey M Snyder, H Richard Koerber, and Sarah E Ross. 2016. “Semi-Intact Ex Vivo Approach to Investigate Spinal Somatosensory Circuits.” *ELife* 5 (December).

Hamity, M V, S R White, and D L Hammond. 2010. “Effects of Neurokinin-1 Receptor Agonism and Antagonism in the Rostral Ventromedial Medulla of Rats with Acute or Persistent Inflammatory Nociception.” *Neuroscience* 165 (3): 902–13.

Hammond, D L, G M Tyce, and T L Yaksh. 1985. “Efflux of 5-Hydroxytryptamine and Noradrenaline into Spinal Cord Superfusates during Stimulation of the Rat Medulla.” *The Journal of Physiology* 359 (February): 151–62.

Han, Sung, Matthew T Soleiman, Marta E Soden, Larry S Zweifel, and Richard D Palmiter. 2015. “Elucidating an Affective Pain Circuit That Creates a Threat Memory.” *Cell* 162 (2): 363–74.

Hargreaves, K, R Dubner, F Brown, C Flores, and J Joris. 1988. “A New and Sensitive Method for Measuring Thermal Nociception in Cutaneous Hyperalgesia.” *Pain* 32 (1): 77–88.

Häring, Martin, Amit Zeisel, Hannah Hochgerner, Puneet Rinwa, Jon E T Jakobsson, Peter Lönnerberg, Gioele La Manno, et al. 2018. “Neuronal Atlas of the Dorsal Horn Defines Its Architecture and Links Sensory Input to Transcriptional Cell Types.” *Nature Neuroscience* 21 (6): 869–80.

Hawi, Amale, Harry Alcorn, Jolene Berg, Carey Hines, Howard Hait, and Thomas Sciascia. 2015. “Pharmacokinetics of Nalbuphine Hydrochloride Extended Release Tablets in Hemodialysis Patients with Exploratory Effect on Pruritus.” *BMC Nephrology* 16 (1): 47.

Heinricher, M M, I Tavares, J L Leith, and B M Lumb. 2009. “Descending Control of Nociception: Specificity, Recruitment and Plasticity.” *Brain Research Reviews* 60 (1): 214–25.

Heinricher, M M, S McGaraughty, and V Tortorici. 2001. “Circuitry Underlying Antiopioid Actions of Cholecystokinin within the Rostral Ventromedial Medulla.” *Journal of Neurophysiology* 85 (1): 280–86.

Heinricher, Mary M, and Miranda J Neubert. 2004. “Neural Basis for the Hyperalgesic Action of Cholecystokinin in the Rostral Ventromedial Medulla.” *Journal of Neurophysiology* 92 (4): 1982–89.

Hellman, Kevin M, and Peggy Mason. 2012. “Opioids Disrupt Pro-Nociceptive Modulation Mediated by Raphe Magnus.” *The Journal of Neuroscience* 32 (40): 13668–78.

Hellman, Kevin M, Scott J Mendelson, Marco A Mendez-Duarte, James L Russell, and Peggy Mason. 2009. “Opioid Microinjection into Raphe Magnus Modulates Cardiorespiratory Function in Mice and Rats.” *American Journal of Physiology. Regulatory, Integrative and Comparative Physiology* 297 (5): R1400-8.

Helmstetter, F J, S A Tershner, L H Poore, and P S Bellgowan. 1998. “Antinociception Following Opioid Stimulation of the Basolateral Amygdala Is Expressed through the Periaqueductal Gray and Rostral Ventromedial Medulla.” *Brain Research* 779 (1–2): 104–18.

Hentall, I D, and H L Fields. 1979. “Segmental and Descending Influences on Intraspinal Thresholds of Single C-Fibers.” *Journal of Neurophysiology* 42 (6): 1527–37.

Hermens, J M, J M Ebertz, J M Hanifin, and C A Hirshman. 1985. “Comparison of Histamine Release in Human Skin Mast Cells Induced by Morphine, Fentanyl, and Oxymorphone.” *Anesthesiology* 62 (2): 124–29.

Hong, Daewha, Pamela Flood, and Geraldine Diaz. 2008. “The Side Effects of Morphine and Hydromorphone Patient-Controlled Analgesia.” *Anesthesia and Analgesia* 107 (4): 1384–89.

Hooke, L P, L He, and N M Lee. 1995. “Dynorphin A Modulates Acute and Chronic Opioid Effects.” *The Journal of Pharmacology and Experimental Therapeutics* 273 (1): 292–97.

Horta, M L, and P T G Vianna. 2003. “Effect of Intravenous Alizapride on Spinal Morphine-Induced Pruritus.” *British Journal of Anaesthesia* 91 (2): 287–89.

Horta, M L, L C L Morejon, A W da Cruz, G R Dos Santos, L C Welling, L Terhorst, R C Costa, and R U Z Alam. 2006. “Study of the Prophylactic Effect of Droperidol, Alizapride, Propofol and Promethazine on Spinal Morphine-Induced Pruritus.” *British Journal of Anaesthesia* 96 (6): 796–800.

Horta, M L, L Ramos, and Z R Gonçalves. 2000. “The Inhibition of Epidural Morphine-Induced

Pruritus by Epidural Droperidol." *Anesthesia and Analgesia* 90 (3): 638–41.

Hosobuchi, Y, J E Adams, and R Linchitz. 1977. "Pain Relief by Electrical Stimulation of the Central Gray Matter in Humans and Its Reversal by Naloxone." *Science* 197 (4299): 183–86.

Huang, Jing, Erika Polgár, Hans Jürgen Solinski, Santosh K Mishra, Pang-Yen Tseng, Noboru Iwagaki, Kieran A Boyle, et al. 2018. "Circuit Dissection of the Role of Somatostatin in Itch and Pain." *Nature Neuroscience* 21 (5): 707–16.

Ibironke, G F, and K S Rasak. 2013. "Forced Swimming Stress-Related Hypoalgesia:Nondependence on the Histaminergic Mechanisms." *Neurophysiology* 45 (4): 340–43.

Ikoma, Akihiko, Martin Steinhoff, Sonja Ständer, Gil Yosipovitch, and Martin Schmelz. 2006. "The Neurobiology of Itch." *Nature Reviews. Neuroscience* 7 (7): 535–47.

Inan, Saadet, Alvaro T Huerta, Liselotte E Jensen, Nae J Dun, and Alan Cowan. 2019. "Nalbuphine, a Kappa Opioid Receptor Agonist and Mu Opioid Receptor Antagonist Attenuates Pruritus, Decreases IL-31, and Increases IL-10 in Mice with Contact Dermatitis." *European Journal of Pharmacology* 864 (December): 172702.

Jackson, Cherry W, Amy Heck Sheehan, and Jennifer G Reddan. 2007. "Evidence-Based Review of the Black-Box Warning for Droperidol." *American Journal of Health-System Pharmacy* 64 (11): 1174–86.

Jannuzzi, Rose G. 2016. "Nalbuphine for Treatment of Opioid-Induced Pruritus: A Systematic Review of Literature." *The Clinical Journal of Pain* 32 (1): 87–93.

Jennings, Elaine M, Bright N Okine, Michelle Roche, and David P Finn. 2014. "Stress-Induced Hyperalgesia." *Progress in Neurobiology* 121 (October): 1–18.

Jensen, T S, and T L Yaksh. 1984. "Spinal Monoamine and Opiate Systems Partly Mediate the Antinociceptive Effects Produced by Glutamate at Brainstem Sites." *Brain Research* 321 (2): 287–97.

Jiang, C J, C C Liu, T J Wu, W Z Sun, S Y Lin, F Y Huang, and C C Chao. 1991. "Mini-Dose Intrathecal Morphine for Post-Cesarean Section Analgesia." *Ma Zui Xue Za Zhi = Anaesthesiologica Sinica* 29 (4): 683–89.

Jiang, M, and M M Behbehani. 2001. "Physiological Characteristics of the Projection Pathway from the Medial Preoptic to the Nucleus Raphe Magnus of the Rat and Its Modulation by the Periaqueductal Gray." *Pain* 94 (2): 139–47.

Jones, S L, and G F Gebhart. 1987. "Spinal Pathways Mediating Tonic, Coeruleospinal, and Raphe-Spinal Descending Inhibition in the Rat." *Journal of Neurophysiology* 58 (1): 138–59.

Jørgensen, H, J Wetterslev, S Møiniche, and J B Dahl. 2000. “Epidural Local Anaesthetics versus Opioid-Based Analgesic Regimens on Postoperative Gastrointestinal Paralysis, PONV and Pain after Abdominal Surgery.” *Cochrane Database of Systematic Reviews*, no. 4: CD001893.

Juneja, M M, W E Ackerman, and K Bellinger. 1991. “Epidural Morphine Pruritus Reduction with Hydroxyzine in Parturients.” *The Journal of the Kentucky Medical Association* 89 (7): 319–21.

Kamei, Junzo, and Hiroshi Nagase. 2001. “Norbinaltorphimine, a Selective κ-Opioid Receptor Antagonist, Induces an Itch-Associated Response in Mice.” *European Journal of Pharmacology* 418 (1–2): 141–45.

Kamei, Junzo, Shoko Hirano, Shigeo Miyata, Akiyoshi Saitoh, and Kenji Onodera. 2005. “Effects of First- and Second-Generation Histamine-H1-Receptor Antagonists on the Pentobarbital-Induced Loss of the Righting Reflex in Streptozotocin-Induced Diabetic Mice.” *Journal of Pharmacological Sciences* 97 (2): 266–72.

Kardon, Adam P, Erika Polgár, Junichi Hachisuka, Lindsey M Snyder, Darren Cameron, Sinead Savage, Xiaoyun Cai, et al. 2014. “Dynorphin Acts as a Neuromodulator to Inhibit Itch in the Dorsal Horn of the Spinal Cord.” *Neuron* 82 (3): 573–86.

Kaye, Alan David, Richard D Urman, Elyse M Cornett, Brendon M Hart, Azem Chami, Julie A Gayle, and Charles J Fox. 2019. “Enhanced Recovery Pathways in Orthopedic Surgery.” *Journal of Anaesthesiology, Clinical Pharmacology* 35 (Suppl 1): S35–39.

Kendrick, W D, A M Woods, M Y Daly, R F Birch, and C DiFazio. 1996. “Naloxone versus Nalbuphine Infusion for Prophylaxis of Epidural Morphine-Induced Pruritus.” *Anesthesia and Analgesia* 82 (3): 641–47.

Kerman, Ilan A, Lynn W Enquist, Stanley J Watson, and Bill J Yates. 2003. “Brainstem Substrates of Sympatho-Motor Circuitry Identified Using Trans-Synaptic Tracing with Pseudorabies Virus Recombinants.” *The Journal of Neuroscience* 23 (11): 4657–66.

Khasabov, S G, and D A Simone. 2013. “Loss of Neurons in Rostral Ventromedial Medulla That Express Neurokinin-1 Receptors Decreases the Development of Hyperalgesia.” *Neuroscience* 250 (October): 151–65.

Khasabov, Sergey G, Patrick Malecha, Joseph Noack, Janneta Tabakov, Keiichiro Okamoto, David A Bereiter, and Donald A Simone. 2015. “Activation of Rostral Ventromedial Medulla Neurons by Noxious Stimulation of Cutaneous and Deep Craniofacial Tissues.” *Journal of Neurophysiology* 113 (1): 14–22.

Kilkenny, Carol, William Browne, Innes C Cuthill, Michael Emerson, Douglas G Altman, and NC3Rs Reporting Guidelines Working Group. 2010. “Animal Research: Reporting in Vivo Experiments: The ARRIVE Guidelines.” *British Journal of Pharmacology* 160 (7): 1577–79.

Kim, Yu Shin, Yuxia Chu, Liang Han, Man Li, Zhe Li, Pamela Colleen LaVinka, Shuohao Sun, et al. 2014. “Central Terminal Sensitization of TRPV1 by Descending Serotonergic Facilitation Modulates Chronic Pain.” *Neuron* 81 (4): 873–87.

Kjellberg, F, and M R Tramèr. 2001. “Pharmacological Control of Opioid-Induced Pruritus: A Quantitative Systematic Review of Randomized Trials.” *European Journal of Anaesthesiology* 18 (6): 346–57.

Ko, M C H, M S Song, T Edwards, H Lee, and N N Naughton. 2004. “The Role of Central Mu Opioid Receptors in Opioid-Induced Itch in Primates.” *The Journal of Pharmacology and Experimental Therapeutics* 310 (1): 169–76.

Ko, M C Holden, Heeseung Lee, Michael S Song, Katarzyna Sobczyk-Kojiro, Henry I Mosberg, Shiroh Kishioka, James H Woods, and Norah N Naughton. 2003. “Activation of Kappa-Opioid Receptors Inhibits Pruritus Evoked by Subcutaneous or Intrathecal Administration of Morphine in Monkeys.” *The Journal of Pharmacology and Experimental Therapeutics* 305 (1): 173–79.

Ko, M C, and N N Naughton. 2000. “An Experimental Itch Model in Monkeys: Characterization of Intrathecal Morphine-Induced Scratching and Antinociception.” *Anesthesiology* 92 (3): 795–805.

Ko, Mei-Chuan, and Stephen M Husbands. 2009. “Effects of Atypical Kappa-Opioid Receptor Agonists on Intrathecal Morphine-Induced Itch and Analgesia in Primates.” *The Journal of Pharmacology and Experimental Therapeutics* 328 (1): 193–200.

Ko, Mei-Chuan. 2015. “Neuraxial Opioid-Induced Itch and Its Pharmacological Antagonism.” *Handbook of Experimental Pharmacology* 226: 315–35.

Koch, Josh, Renee Manworren, Lynn Clark, Charles T Quinn, George R Buchanan, and Zora R Rogers. 2008. “Pilot Study of Continuous Co-Infusion of Morphine and Naloxone in Children with Sickle Cell Pain Crisis.” *American Journal of Hematology* 83 (9): 728–31.

Koutsikou, Stella, Dilys M Parry, Frankie M MacMillan, and Bridget M Lumb. 2007. “Laminar Organization of Spinal Dorsal Horn Neurones Activated by C- vs. A-Heat Nociceptors and Their Descending Control from the Periaqueductal Grey in the Rat.” *The European Journal of Neuroscience* 26 (4): 943–52.

Koutsikou, Stella, Thomas C Watson, Jonathan J Crook, J Lianne Leith, Charlotte L Lawrenson, Richard Apps, and Bridget M Lumb. 2015. “The Periaqueductal Gray Orchestrates Sensory and Motor Circuits at Multiple Levels of the Neuraxis.” *The Journal of Neuroscience* 35 (42): 14132–47.

Kozono, Hideki, Hiroshi Yoshitani, and Ryoko Nakano. 2018. “Post-Marketing Surveillance Study of the Safety and Efficacy of Nalfurafine Hydrochloride (Remitch® Capsules 2.5 Mg) in 3,762 Hemodialysis Patients with Intractable Pruritus.” *International Journal of Nephrology and Renovascular Disease* 11 (January): 9–24.

Krajnik, M, and Z Zylicz. 2001. “Understanding Pruritus in Systemic Disease.” *Journal of Pain and Symptom Management* 21 (2): 151–68.

Kumagai, Hiroo, Toshiya Ebata, Kenji Takamori, Taro Muramatsu, Hidetomo Nakamoto, and Hiromichi Suzuki. 2010. “Effect of a Novel Kappa-Receptor Agonist, Nalfurafine Hydrochloride, on Severe Itch in 337 Haemodialysis Patients: A Phase III, Randomized, Double-Blind, Placebo-Controlled Study.” *Nephrology, Dialysis, Transplantation* 25 (4): 1251–57.

Kumar, Kamal, and Sudha Indu Singh. 2013. “Neuraxial Opioid-Induced Pruritus: An Update.” *Journal of Anaesthesiology, Clinical Pharmacology* 29 (3): 303–7.

Kung, Chia-Chi, Shiou-Sheng Chen, Hong-Jyh Yang, Chih-Jun Lai, and Li-Kuei Chen. 2018. “Pharmacogenetic Study of Pruritus Induced by Epidural Morphine for Post Cesarean Section Analgesia.” *Taiwanese Journal of Obstetrics & Gynecology* 57 (1): 89–94.

Kut, Elvan, Victor Candia, Jan von Overbeck, Judit Pok, Daniel Fink, and Gerd Folkers. 2011. “Pleasure-Related Analgesia Activates Opioid-Insensitive Circuits.” *The Journal of Neuroscience* 31 (11): 4148–53.

Kyriakides, K, S K Hussain, and G J Hobbs. 1999. “Management of Opioid-Induced Pruritus: A Role for 5-HT3 Antagonists?” *British Journal of Anaesthesia* 82 (3): 439–41.

LaBella, F S, R S Kim, and J Templeton. 1978. “Opiate Receptor Binding Activity of 17-Alpha Estrogenic Steroids.” *Life Sciences* 23 (17–18): 1797–1804.

Lagraize, S C, W Guo, K Yang, F Wei, K Ren, and R Dubner. 2010. “Spinal Cord Mechanisms Mediating Behavioral Hyperalgesia Induced by Neurokinin-1 Tachykinin Receptor Activation in the Rostral Ventromedial Medulla.” *Neuroscience* 171 (4): 1341–56.

Lansu, Katherine, Joel Karpiak, Jing Liu, Xi-Ping Huang, John D McCorvy, Wesley K Kroeze, Tao Che, et al. 2017. “In Silico Design of Novel Probes for the Atypical Opioid Receptor MRGPRX2.” *Nature Chemical Biology* 13 (5): 529–36.

Lapirot, Olivier, Raja Chebbi, Lénaic Monconduit, Alain Artola, Radhouane Dallel, and Philippe Luccarini. 2009. “NK1 Receptor-Expressing Spinoparabrachial Neurons Trigger Diffuse Noxious Inhibitory Controls through Lateral Parabrachial Activation in the Male Rat.” *Pain* 142 (3): 245–54.

Lawhorn, C D, J D McNitt, E E Fibuch, J T Joyce, and R J Leadley. 1991. “Epidural Morphine with Butorphanol for Postoperative Analgesia after Cesarean Delivery.” *Anesthesia and Analgesia* 72 (1): 53–57.

Laxenaire, M C, D A Moneret-Vautrin, S Widmer, C Mouton, J L Guéant, M C Bonnet, H Bricard, A Facon, F Lesage, and J Valfrey. 1990. “[Anesthetics Responsible for Anaphylactic Shock. A French Multicenter Study].” *Annales Francaises d’Anesthesie et de Reanimation* 9 (6): 501–6.

Lecea, Luis de, Matthew E Carter, and Antoine Adamantidis. 2012. “Shining Light on Wakefulness and Arousal.” *Biological Psychiatry* 71 (12): 1046–52.

Lee, Heeseung, Norah N Naughton, James H Woods, and Mei-Chuan Ko. 2007. “Effects of Butorphanol on Morphine-Induced Itch and Analgesia in Primates.” *Anesthesiology* 107 (3): 478–85.

Leon-Casasola, O A de, D Karabella, and M J Lema. 1996. “Bowel Function Recovery after Radical Hysterectomies: Thoracic Epidural Bupivacaine-Morphine versus Intravenous Patient-Controlled Analgesia with Morphine: A Pilot Study.” *Journal of Clinical Anesthesia* 8 (2): 87–92.

Leung, C G, and P Mason. 1999. “Physiological Properties of Raphe Magnus Neurons during Sleep and Waking.” *Journal of Neurophysiology* 81 (2): 584–95.

Levy, J H, N W Brister, A Shearin, J Ziegler, C C Hug, D M Adelson, and B F Walker. 1989. “Wheal and Flare Responses to Opioids in Humans.” *Anesthesiology* 70 (5): 756–60.

Lewis, J W, G Baldrighi, and H Akil. 1987. “A Possible Interface between Autonomic Function and Pain Control: Opioid Analgesia and the Nucleus Tractus Solitarius.” *Brain Research* 424 (1): 65–70.

Li, Yi, Jiawei Zeng, Juen Zhang, Chenyu Yue, Weixin Zhong, Zhixiang Liu, Qiru Feng, and Minmin Luo. 2018. “Hypothalamic Circuits for Predation and Evasion.” *Neuron* 97 (4): 911-924.e5.

Liang, Huazheng, Charles Watson, and George Paxinos. 2016. “Terminations of Reticulospinal Fibers Originating from the Gigantocellular Reticular Formation in the Mouse Spinal Cord.” *Brain Structure & Function* 221 (3): 1623–33.

Liao, Chia-Chih, Chieh-Szu Chang, Chi-Hao Tseng, Michael J Sheen, Shih-Chang Tsai, Yao-Lung Chang, and Shu-Yam Wong. 2011. “Efficacy of Intramuscular Nalbuphine versus Diphenhydramine for the Prevention of Epidural Morphine-Induced Pruritus after Cesarean Delivery.” *Chang Gung Medical Journal* 34 (2): 172–78.

Liebeskind, J C, G Guilbaud, J M Besson, and J L Oliveras. 1973. “Analgesia from Electrical Stimulation of the Periaqueductal Gray Matter in the Cat: Behavioral Observations and Inhibitory Effects on Spinal Cord Interneurons.” *Brain Research* 50 (2): 441–46.

Lin, J S, Y Hou, K Sakai, and M Jouvet. 1996. “Histaminergic Descending Inputs to the Mesopontine Tegmentum and Their Role in the Control of Cortical Activation and Wakefulness in the Cat.” *The Journal of Neuroscience* 16 (4): 1523–37.

Liu, Ming-Zhe, Xiao-Jun Chen, Tong-Yu Liang, Qing Li, Meng Wang, Xin-Yan Zhang, Yu-Zhuo Li, Qiang Sun, and Yan-Gang Sun. 2019. “Synaptic Control of Spinal GRPR+ Neurons by Local and Long-Range Inhibitory Inputs.” *Proceedings of the National Academy of Sciences of the United States of America*, December.

Liu, Spencer S., Paul D. Ware, Hugh W. Allen, Joseph M. Neal, and Julia E. Pollock. 1996. "Dose-Response Characteristics of Spinal Bupivacaine in VolunteersClinical Implications for Ambulatory Anesthesia." *Anesthesiology: The Journal of the American Society of Anesthesiologists*, October.

Liu, Tong, and Ru-Rong Ji. 2013. "New Insights into the Mechanisms of Itch: Are Pain and Itch Controlled by Distinct Mechanisms?" *Pflugers Archiv: European Journal of Physiology* 465 (12): 1671–85.

Liu, Xian-Yu, Zhong-Chun Liu, Yan-Gang Sun, Michael Ross, Seungil Kim, Feng-Fang Tsai, Qi-Fang Li, et al. 2011. "Unidirectional Cross-Activation of GRPR by MOR1D Uncouples Itch and Analgesia Induced by Opioids." *Cell* 147 (2): 447–58.

Lu, Yuefeng, Kimberly L Simpson, Kristin J Weaver, and Rick C S Lin. 2010. "Coexpression of Serotonin and Nitric Oxide in the Raphe Complex: Cortical versus Subcortical Circuit." *Anatomical Record* 293 (11): 1954–65.

Luo, Miaw-Chyi, Qingmin Chen, Michael H Ossipov, David R Rankin, Frank Porreca, and Josephine Lai. 2008. "Spinal Dynorphin and Bradykinin Receptors Maintain Inflammatory Hyperalgesia." The Journal of Pain 9 (12): 1096–1105.

Ma, Chao, and Yuguang Huang, eds. 2016. *Translational Research in Pain and Itch*. illustrated ed. Springer.

Maduka, U P, M V Hamity, R Y Walder, S R White, Y Li, and D L Hammond. 2016. "Changes in the Disposition of Substance P in the Rostral Ventromedial Medulla after Inflammatory Injury in the Rat." *Neuroscience* 317 (March): 1–11.

Mahowald, M W, M L Mahowald, S R Bundlie, and S R Ytterberg. 1989. "Sleep Fragmentation in Rheumatoid Arthritis." *Arthritis and Rheumatism* 32 (8): 974–83.

Manning, B H, and K B Franklin. 1998. "Morphine Analgesia in the Formalin Test: Reversal by Microinjection of Quaternary Naloxone into the Posterior Hypothalamic Area or Periaqueductal Gray." *Behavioural Brain Research* 92 (1): 97–102.

Marinelli, Silvia, Christopher W Vaughan, Stephen A Schnell, Martin W Wessendorf, and MacDonald J Christie. 2002. "Rostral Ventromedial Medulla Neurons That Project to the Spinal Cord Express Multiple Opioid Receptor Phenotypes." *The Journal of Neuroscience* 22 (24): 10847–55.

Marson, L, and K E McKenna. 1992. "A Role for 5-Hydroxytryptamine in Descending Inhibition of Spinal Sexual Reflexes." *Experimental Brain Research* 88 (2): 313–20.

Marson, L, K B Platt, and K E McKenna. 1993. "Central Nervous System Innervation of the Penis as Revealed by the Transneuronal Transport of Pseudorabies Virus." *Neuroscience* 55 (1): 263–80.

Martenson, Melissa E, Justin S Cetas, and Mary M Heinricher. 2009. "A Possible Neural Basis

for Stress-Induced Hyperalgesia." *Pain* 142 (3): 236–44.

Martins, Isabel, and Isaura Tavares. 2017. "Reticular Formation and Pain: The Past and the Future." *Frontiers in Neuroanatomy* 11 (July): 51.

Mason, P, I Escobedo, C Burgin, J Bergan, J H Lee, E J Last, and A L Holub. 2001. "Nociceptive Responsiveness during Slow-Wave Sleep and Waking in the Rat." *Sleep* 24 (1): 32–38.

Mason, P. 2001. "Contributions of the Medullary Raphe and Ventromedial Reticular Region to Pain Modulation and Other Homeostatic Functions." *Annual Review of Neuroscience* 24: 737–77.

Mason, Peggy, Keming Gao, and Jonathan R Genzen. 2007. "Serotonergic Raphe Magnus Cell Discharge Reflects Ongoing Autonomic and Respiratory Activities." *Journal of Neurophysiology* 98 (4): 1919–27.

Mason, Peggy. 2012. "Medullary Circuits for Nociceptive Modulation." *Current Opinion in Neurobiology* 22 (4): 640–45.

Maxwell, Lynne G, Sandra C Kaufmann, Sally Bitzer, Eric V Jackson, John McGready, Sabine Kost-Byerly, Lori Kozlowski, Sharon K Rothman, and Myron Yaster. 2005. "The Effects of a Small-Dose Naloxone Infusion on Opioid-Induced Side Effects and Analgesia in Children and Adolescents Treated with Intravenous Patient-Controlled Analgesia: A Double-Blind, Prospective, Randomized, Controlled Study." *Anesthesia and Analgesia* 100 (4): 953–58.

Mayer, D J, and J C Liebeskind. 1974. "Pain Reduction by Focal Electrical Stimulation of the Brain: An Anatomical and Behavioral Analysis." *Brain Research* 68 (1): 73–93.

Mayer, D J, T L Wolfle, H Akil, B Carder, and J C Liebeskind. 1971. "Analgesia from Electrical Stimulation in the Brainstem of the Rat." *Science* 174 (4016): 1351–54.

McGaraughty, Steve, and Mary M Heinricher. 2002. "Microinjection of Morphine into Various Amygdaloid Nuclei Differentially Affects Nociceptive Responsiveness and RVM Neuronal Activity." *Pain* 96 (1–2): 153–62.

McMahon, S B, and P D Wall. 1988. "Descending Excitation and Inhibition of Spinal Cord Lamina I Projection Neurons." *Journal of Neurophysiology* 59 (4): 1204–19.

McNicol, Ewan, Nathalie Horowicz-Mehler, Ruth A Fisk, Kyle Bennett, Maria Gialeli-Goudas, Priscilla W Chew, Joseph Lau, Daniel Carr, and Americal Pain Society. 2003. "Management of Opioid Side Effects in Cancer-Related and Chronic Noncancer Pain: A Systematic Review." *The Journal of Pain* 4 (5): 231–56.

Meixiong, James, Michael Anderson, Nathachit Limjunyawong, Mark F Sabbagh, Eric Hu, Madison R Mack, Landon K Oetjen, Fang Wang, Brian S Kim, and Xinzhong Dong. 2019. "Activation of Mast-Cell-Expressed Mas-Related G-Protein-Coupled Receptors

Drives Non-Histaminergic Itch." *Immunity* 50 (5): 1163–1171.e5.

Melo, Helvira, Lilian Basso, Mircea Iftinca, Wallace K MacNaughton, Morley D Hollenberg, Derek M McKay, and Christophe Altier. 2018. "Itch Induced by Peripheral Mu Opioid Receptors Is Dependent on TRPV1-Expressing Neurons and Alleviated by Channel Activation." *Scientific Reports* 8 (1): 15551.

Meng, I D, J P Johansen, I Harasawa, and H L Fields. 2005. "Kappa Opioids Inhibit Physiologically Identified Medullary Pain Modulating Neurons and Reduce Morphine Antinociception." *Journal of Neurophysiology* 93 (3): 1138–44.

Millan, M J. 1999. "The Induction of Pain: An Integrative Review." *Progress in Neurobiology* 57 (1): 1–164.

Millan, Mark J. 2002. "Descending Control of Pain." *Progress in Neurobiology* 66 (6): 355–474.

Miller, Jamie L, and Tracy M Hagemann. 2011. "Use of Pure Opioid Antagonists for Management of Opioid-Induced Pruritus." *American Journal of Health-System Pharmacy* 68 (15): 1419–25.

Millhorn, D E, T Hökfelt, K Seroogy, W Oertel, A A Verhofstad, and J Y Wu. 1987. "Immunohistochemical Evidence for Colocalization of Gamma-Aminobutyric Acid and Serotonin in Neurons of the Ventral Medulla Oblongata Projecting to the Spinal Cord." *Brain Research* 410 (1): 179–85.

Millington, G W M, A Collins, C R Lovell, T A Leslie, A S W Yong, J D Morgan, T Ajithkumar, et al. 2018. "British Association of Dermatologists' Guidelines for the Investigation and Management of Generalized Pruritus in Adults without an Underlying Dermatosis, 2018." *The British Journal of Dermatology* 178 (1): 34–60.

Mogil, J S, W F Sternberg, H Balian, J C Liebeskind, and B Sadowski. 1996. "Opioid and Nonopioid Swim Stress-Induced Analgesia: A Parametric Analysis in Mice." Physiology & Behavior 59 (1): 123–32.

Mokha, S S, J A McMillan, and A Iggo. 1986. "Pathways Mediating Descending Control of Spinal Nociceptive Transmission from the Nuclei Locus Coeruleus (LC) and Raphe Magnus (NRM) in the Cat." *Experimental Brain Research* 61 (3): 597–606.

Morales, M, E Battenberg, and F E Bloom. 1998. "Distribution of Neurons Expressing Immunoreactivity for the 5HT3 Receptor Subtype in the Rat Brain and Spinal Cord." *The Journal of Comparative Neurology* 402 (3): 385–401.

Moreau, J L, and H L Fields. 1986. "Evidence for GABA Involvement in Midbrain Control of Medullary Neurons That Modulate Nociceptive Transmission." *Brain Research* 397 (1): 37–46.

Mores, Kendall L, Benjamin R Cummins, Robert J Cassell, and Richard M van Rijn. 2019. "A Review of the Therapeutic Potential of Recently Developed G Protein-Biased Kappa

Agonists." *Frontiers in Pharmacology* 10 (April): 407.

Morgan, M M, J H Sohn, A M Lohof, S Ben-Eliyahu, and J C Liebeskind. 1989. "Characterization of Stimulation-Produced Analgesia from the Nucleus Tractus Solitarius in the Rat." *Brain Research* 486 (1): 175–80.

Morgan, Michael M, and Cecilea C Clayton. 2005. "Defensive Behaviors Evoked from the Ventrolateral Periaqueductal Gray of the Rat: Comparison of Opioid and GABA Disinhibition." *Behavioural Brain Research* 164 (1): 61–66.

Morgan, Michael M, Kelsey L Whittier, Deborah M Hegarty, and Sue A Aicher. 2008. "Periaqueductal Gray Neurons Project to Spinally Projecting GABAergic Neurons in the Rostral Ventromedial Medulla." *Pain* 140 (2): 376–86.

Morrison, S F, A F Sved, and A M Passerin. 1999. "GABA-Mediated Inhibition of Raphe Pallidus Neurons Regulates Sympathetic Outflow to Brown Adipose Tissue." *The American Journal of Physiology* 276 (2): R290-7.

Morrison, Shaun F. 2016. "Central Neural Control of Thermoregulation and Brown Adipose Tissue." *Autonomic Neuroscience: Basic & Clinical* 196 (February): 14–24.

Moruzzi, G, and H W Magoun. 1949. "Brain Stem Reticular Formation and Activation of the EEG." *Electroencephalography and Clinical Neurophysiology* 1 (4): 455–73.

Moser, Hannah R, and Glenn J Giesler. 2013. "Itch and Analgesia Resulting from Intrathecal Application of Morphine: Contrasting Effects on Different Populations of Trigeminothalamic Tract Neurons." *The Journal of Neuroscience* 33 (14): 6093–6101.

Mudumbai, Seshadri C, Elizabeth M Oliva, Eleanor T Lewis, Jodie Trafton, Daniel Posner, Edward R Mariano, Randall S Stafford, Todd Wagner, and J David Clark. 2016. "Time-to-Cessation of Postoperative Opioids: A Population-Level Analysis of the Veterans Affairs Health Care System." *Pain Medicine* 17 (9): 1732–43.

Mugabure Bujedo, Borja. 2012. "A Clinical Approach to Neuraxial Morphine for the Treatment of Postoperative Pain." *Pain Research and Treatment* 2012 (July): 612145.

Mulroy, M F, K L Larkin, and A Siddiqui. 2001. "Intrathecal Fentanyl-Induced Pruritus Is More Severe in Combination with Procaine than with Lidocaine or Bupivacaine." *Regional Anesthesia and Pain Medicine* 26 (3): 252–56.

Munanairi, Admire, Xian-Yu Liu, Devin M Barry, Qianyi Yang, Jun-Bin Yin, Hua Jin, Hui Li, et al. 2018. "Non-Canonical Opioid Signaling Inhibits Itch Transmission in the Spinal Cord of Mice." *Cell Reports* 23 (3): 866–77.

Nakamura, Kazuhiro, Kiyoshi Matsumura, Thomas Hübschle, Yoshiko Nakamura, Hiroyuki Hioki, Fumino Fujiyama, Zsolt Boldogköi, et al. 2004. "Identification of Sympathetic Premotor Neurons in Medullary Raphe Regions Mediating Fever and Other Thermoregulatory Functions." *The Journal of Neuroscience* 24 (23): 5370–80.

Nectow, Alexander R, Marc Schneeberger, Hongxing Zhang, Bianca C Field, Nicolas Renier, Estefania Azevedo, Bindiben Patel, et al. 2017. “Identification of a Brainstem Circuit Controlling Feeding.” *Cell* 170 (3): 429-442.e11.

Ngan Kee, Warwick D, Kim S Khaw, Floria F Ng, Karman K L Ng, Rita So, and Anna Lee. 2014. “Synergistic Interaction between Fentanyl and Bupivacaine given Intrathecally for Labor Analgesia.” *Anesthesiology* 120 (5): 1126–36.

Nguyen, Eileen, Grace Lim, Huiping Ding, Junichi Hachisuka, Mei-Chuan Ko, and Sarah E Ross. 2021. “Morphine Acts on Spinal Dynorphin Neurons to Cause Itch through Disinhibition.” *Science Translational Medicine* 13 (579).

Niiyama, Yukitoshi, Tomoyuki Kawamata, Hitoshi Shimizu, Keiichi Omote, and Akiyoshi Namiki. 2005. “The Addition of Epidural Morphine to Ropivacaine Improves Epidural Analgesia after Lower Abdominal Surgery.” *Canadian Journal of Anaesthesia* 52 (2): 181–85.

Norris, M C, W M Grieco, M Borkowski, B L Leighton, V A Arkoosh, H J Huffnagle, and S Huffnagle. 1994. “Complications of Labor Analgesia: Epidural versus Combined Spinal Epidural Techniques.” *Anesthesia and Analgesia* 79 (3): 529–37.

Ohgami, Yusuke, Carlyn C Zylstra, Lindsay P Quock, Eunhee Chung, Donald Y Shirachi, and Raymond M Quock. 2009. “Nitric Oxide in Hyperbaric Oxygen-Induced Acute Antinociception in Mice.” *Neuroreport* 20 (15): 1325–29.

Pacharinsak, Cholawat, Sergey G Khasabov, Alvin J Beitz, and Donald A Simone. 2008. “NK-1 Receptors in the Rostral Ventromedial Medulla Contribute to Hyperalgesia Produced by Intraplantar Injection of Capsaicin.” *Pain* 139 (1): 34–46.

Pagani, Martina, Gioele W Albisetti, Nandhini Sivakumar, Hendrik Wildner, Mirko Santello, Helge C Johannssen, and Hanns Ulrich Zeilhofer. 2019. “How Gastrin-Releasing Peptide Opens the Spinal Gate for Itch.” *Neuron* 103 (1): 102-117.e5.

Pan, Z Z, J T Williams, and P B Osborne. 1990. “Opioid Actions on Single Nucleus Raphe Magnus Neurons from Rat and Guinea-Pig in Vitro.” *The Journal of Physiology* 427 (August): 519–32.

Pan, Z Z, S A Tershner, and H L Fields. 1997. “Cellular Mechanism for Anti-Analgesic Action of Agonists of the Kappa-Opioid Receptor.” *Nature* 389 (6649): 382–85.

Pan, Z Z. 1998. “Mu-Opposing Actions of the Kappa-Opioid Receptor.” *Trends in Pharmacological Sciences* 19 (3): 94–98.

Pan, Z, N Hirakawa, and H L Fields. 2000. “A Cellular Mechanism for the Bidirectional Pain-Modulating Actions of Orphanin FQ/Nociceptin.” *Neuron* 26 (2): 515–22.

Pasternak, Gavril W. 2004. “Multiple Opiate Receptors: Déjà vu All over Again.” *Neuropharmacology* 47 Suppl 1: 312–23.

Pathan, Hasan, and John Williams. 2012. “Basic Opioid Pharmacology: An Update.” *British Journal of Pain* 6 (1): 11–16.

Peng, Y B, Q Lin, and W D Willis. 1996a. “Involvement of Alpha-2 Adrenoceptors in the Periaqueductal Gray-Induced Inhibition of Dorsal Horn Cell Activity in Rats.” *The Journal of Pharmacology and Experimental Therapeutics* 278 (1): 125–35.

Pérez, H, and S Ruiz. 1995. “Medullary Responses to Chemoreceptor Activation Are Inhibited by Locus Coeruleus and Nucleus Raphe Magnus.” *Neuroreport* 6 (10): 1373–76.

Pertovaara, Antti. 2006. “Noradrenergic Pain Modulation.” Progress in Neurobiology 80 (2): 53–83.

Pettini, Eleonora, Massimo Micaglio, Ubaldo Bitossi, Angelo R De Gaudio, Duccio R Degl’Innocenti, Lorenzo Tofani, Vittorio Limatola, Chiara Adembri, and Alessandro Di Filippo. 2018. “Influence of OPRM1 Polymorphism on Postoperative Pain after Intrathecal Morphine Administration in Italian Patients Undergoing Elective Cesarean Section.” *The Clinical Journal of Pain* 34 (2): 178–81.

Pfeiffer, A, V Brantl, A Herz, and H M Emrich. 1986. “Psychotomimesis Mediated by Kappa Opiate Receptors.” *Science* 233 (4765): 774–76.

Phan, Ngoc Quan, Tobias Lotts, Attila Antal, Jeffrey D Bernhard, and Sonja Ständer. 2012. “Systemic Kappa Opioid Receptor Agonists in the Treatment of Chronic Pruritus: A Literature Review.” *Acta Dermato-Venereologica* 92 (5): 555–60.

Philbin, D M, J Moss, C E Rosow, C W Akins, and J L Rosenberger. 1982. “Histamine Release with Intravenous Narcotics: Protective Effects of H1 and H2-Receptor Antagonists.” *Klinische Wochenschrift* 60 (17): 1056–59.

Plummer, Nicholas W, Irina Y Evsyukova, Sabrina D Robertson, Jacqueline de Marchena, Charles J Tucker, and Patricia Jensen. 2015. “Expanding the Power of Recombinase-Based Labeling to Uncover Cellular Diversity.” *Development* 142 (24): 4385–93.

Porebski, Grzegorz, Kamila Kwiecien, Magdalena Pawica, and Mateusz Kwitniewski. 2018. “Mas-Related G Protein-Coupled Receptor-X2 (MRGPRX2) in Drug Hypersensitivity Reactions.” *Frontiers in Immunology* 9 (December): 3027.

Potrebic, S B, H L Fields, and P Mason. 1994. “Serotonin Immunoreactivity Is Contained in One Physiological Cell Class in the Rat Rostral Ventromedial Medulla.” *The Journal of Neuroscience* 14 (3 Pt 2): 1655–65.

Prieto, G J, J T Cannon, and J C Liebeskind. 1983. “N. Raphe Magnus Lesions Disrupt Stimulation-Produced Analgesia from Ventral but Not Dorsal Midbrain Areas in the Rat.” *Brain Research* 261 (1): 53–57.

Reichling, D B, and A I Basbaum. 1990. “Contribution of Brainstem GABAergic Circuitry to Descending Antinociceptive Controls: II. Electron Microscopic Immunocytochemical

Evidence of GABAergic Control over the Projection from the Periaqueductal Gray to the Nucleus Raphe Magnus in the Rat." *The Journal of Comparative Neurology* 302 (2): 378–93.

Reiner, P B, and A Kamondi. 1994. "Mechanisms of Antihistamine-Induced Sedation in the Human Brain: H1 Receptor Activation Reduces a Background Leakage Potassium Current." *Neuroscience* 59 (3): 579–88.

Ren, K, A Randich, and G F Gebhart. 1991. "Spinal Serotonergic and Kappa Opioid Receptors Mediate Facilitation of the Tail Flick Reflex Produced by Vagal Afferent Stimulation." *Pain* 45 (3): 321–29.

Reszke, Radomir, and Jacek C Szepietowski. 2018. "End-Stage Renal Disease Chronic Itch and Its Management." *Dermatologic Clinics* 36 (3): 277–92.

Reynolds, D V. 1969. "Surgery in the Rat during Electrical Analgesia Induced by Focal Brain Stimulation." Science 164 (3878): 444–45.

Roeder, Zachary, QiLiang Chen, Sophia Davis, Jonathan D Carlson, Domenico Tupone, and Mary M Heinricher. 2016. "Parabrachial Complex Links Pain Transmission to Descending Pain Modulation." *Pain* 157 (12): 2697–2708.

Rosow, C E, J Moss, D M Philbin, and J J Savarese. 1982. "Histamine Release during Morphine and Fentanyl Anesthesia." *Anesthesiology* 56 (2): 93–96.

Ross, Sarah E, Alan R Mardinly, Alejandra E McCord, Jonathan Zurawski, Sonia Cohen, Cynthia Jung, Linda Hu, et al. 2010. "Loss of Inhibitory Interneurons in the Dorsal Spinal Cord and Elevated Itch in Bhlhb5 Mutant Mice." *Neuron* 65 (6): 886–98.

Roth, T, T Roehrs, G Koshorek, J Sicklesteel, and F Zorick. 1987. "Sedative Effects of Antihistamines." *The Journal of Allergy and Clinical Immunology* 80 (1): 94–98.

Rubelowski, J M, M Menge, C Distler, M Rothermel, and K P Hoffmann. 2013. "Connections of the Superior Colliculus to Shoulder Muscles of the Rat: A Dual Tracing Study." *Frontiers in Neuroanatomy* 7 (June): 17.

Rydenhag, B, and S Andersson. 1981. "Effect of DLF Lesions at Different Spinal Levels on Morphine Induced Analgesia." *Brain Research* 212 (1): 239–42.

Rzasa Lynn, Rachael, and J L Galinkin. 2018. "Naloxone Dosage for Opioid Reversal: Current Evidence and Clinical Implications." *Therapeutic Advances in Drug Safety* 9 (1): 63–88.

Safronov, Boris V, Vitor Pinto, and Victor A Derkach. 2007. "High-Resolution Single-Cell Imaging for Functional Studies in the Whole Brain and Spinal Cord and Thick Tissue Blocks Using Light-Emitting Diode Illumination." *Journal of Neuroscience Methods* 164 (2): 292–98.

Sakakibara, Satoshi, Noritaka Imamachi, Manabu Sakakihara, Yukiko Katsube, Mai Hattori, and

Yoji Saito. 2019. “Effects of an Intrathecal TRPV1 Antagonist, SB366791, on Morphine-Induced Itch, Body Temperature, and Antinociception in Mice.” *Journal of Pain Research* 12 (August): 2629–36.

Sakakihara, Manabu, Noritaka Imamachi, and Yoji Saito. 2016. “Effects of Intrathecal κ-Opioid Receptor Agonist on Morphine-Induced Itch and Antinociception in Mice.” *Regional Anesthesia and Pain Medicine* 41 (1): 69–74.

Samineni, Vijay K, Jose G Grajales-Reyes, Bryan A Copits, Daniel E O’Brien, Sarah L Trigg, Adrian M Gomez, Michael R Bruchas, and Robert W Gereau. 2017. “Divergent Modulation of Nociception by Glutamatergic and Gabaergic Neuronal Subpopulations in the Periaqueductal Gray.” *ENeuro* 4 (2).

Samineni, Vijay K, Jose G Grajales-Reyes, Saranya S Sundaram, Judy J Yoo, and Robert W Gereau. 2019. “Cell Type-Specific Modulation of Sensory and Affective Components of Itch in the Periaqueductal Gray.” *Nature Communications* 10 (1): 4356.

Sandkühler, J, Q G Fu, and M Zimmermann. 1987. “Spinal Pathways Mediating Tonic or Stimulation-Produced Descending Inhibition from the Periaqueductal Gray or Nucleus Raphe Magnus Are Separate in the Cat.” *Journal of Neurophysiology* 58 (2): 327–41.

Sardella, Thomas C P, Erika Polgár, Francesca Garzillo, Takahiro Furuta, Takeshi Kaneko, Masahiko Watanabe, and Andrew J Todd. 2011. “Dynorphin Is Expressed Primarily by GABAergic Neurons That Contain Galanin in the Rat Dorsal Horn.” *Molecular Pain* 7 (September): 76.

Sarma, V J, and U V Boström. 1993. “Intrathecal Morphine for the Relief of Post-Hysterectomy Pain--a Double-Blind, Dose-Response Study.” *Acta Anaesthesiologica Scandinavica* 37 (2): 223–27.

Sarvela, P J, P M Halonen, A I Soikkeli, J P Kainu, and K T Korttila. 2006. “Ondansetron and Tropisetron Do Not Prevent Intraspinal Morphine- and Fentanyl-Induced Pruritus in Elective Cesarean Delivery.” *Acta Anaesthesiologica Scandinavica* 50 (2): 239–44.

Sathyamurthy, Anupama, Kory R Johnson, Kaya J E Matson, Courtney I Dobrott, Li Li, Anna R Ryba, Tzipporah B Bergman, Michael C Kelly, Matthew W Kelley, and Ariel J Levine. 2018. “Massively Parallel Single Nucleus Transcriptional Profiling Defines Spinal Cord Neurons and Their Activity during Behavior.” *Cell Reports* 22 (8): 2216–25.

Satpute, Ajay B, Philip A Kragel, Lisa Feldman Barrett, Tor D Wager, and Marta Bianciardi. 2019. “Deconstructing Arousal into Wakeful, Autonomic and Affective Varieties.” *Neuroscience Letters* 693 (February): 19–28.

Scammell, Thomas E, Elda Arrigoni, and Jonathan O Lipton. 2017. “Neural Circuitry of Wakefulness and Sleep.” *Neuron* 93 (4): 747–65.

Schattauer, Selena S, Jamie R Kuhar, Allisa Song, and Charles Chavkin. 2017. “Nalfurafine Is a G-Protein Biased Agonist Having Significantly Greater Bias at the Human than Rodent

Form of the Kappa Opioid Receptor." *Cellular Signalling* 32 (January): 59–65.

Schmelz, M, R Schmidt, A Bickel, H O Handwerker, and H E Torebjörk. 1997. "Specific C-Receptors for Itch in Human Skin." *The Journal of Neuroscience* 17 (20): 8003–8.

Schmelz, Martin, and Ralf Paus. 2007. "Opioids and the Skin: 'Itchy' Perspectives beyond Analgesia and Abuse." *The Journal of Investigative Dermatology* 127 (6): 1287–89.

Schmidt-Rondon, Eric, Zhenping Wang, Shelle A Malkmus, Anna Di Nardo, Keith Hildebrand, Linda Page, and Tony L Yaksh. 2018. "Effects of Opioid and Nonopioid Analgesics on Canine Wheal Formation and Cultured Human Mast Cell Degranulation." *Toxicology and Applied Pharmacology* 338 (January): 54–64.

Schneeberger, Marc, Luca Parolari, Tania Das Banerjee, Varun Bhave, Putianqi Wang, Bindiben Patel, Thomas Topilko, et al. 2019. "Regulation of Energy Expenditure by Brainstem GABA Neurons." *Cell* 178 (3): 672-685.e12.

Scholten, Julia, Karin Hartmann, Alexander Gerbaulet, Thomas Krieg, Werner Müller, Giuseppe Testa, and Axel Roers. 2008. "Mast Cell-Specific Cre/LoxP-Mediated Recombination in Vivo." *Transgenic Research* 17 (2): 307–15.

Schubert, Nadja, Katharina Lisenko, Christian Auerbach, Anke Weitzmann, Shanawaz Mohammed Ghouse, Lina Muhandes, Christa Haase, et al. 2018. "Unimpaired Responses to Vaccination With Protein Antigen Plus Adjuvant in Mice With Kit-Independent Mast Cell Deficiency." *Frontiers in Immunology* 9 (August): 1870.

Schwenkgrub, Joanna, Evan R Harrell, Brice Bathellier, and Julien Bouvier. 2020. "Deep Imaging in the Brainstem Reveals Functional Heterogeneity in V2a Neurons Controlling Locomotion." *Science Advances* 6 (49).

Shah, M K, A T Sia, and J L Chong. 2000. "The Effect of the Addition of Ropivacaine or Bupivacaine upon Pruritus Induced by Intrathecal Fentanyl in Labour." *Anaesthesia* 55 (10): 1008–13.

Shamsizadeh, Ali, Neda Soliemani, Mohammad Mohammad-Zadeh, and Hassan Azhdari-Zarmehri. 2014. "Permanent Lesion in Rostral Ventromedial Medulla Potentiates Swim Stress-Induced Analgesia in Formalin Test." *Iranian Journal of Basic Medical Sciences* 17 (3): 209–15.

Sharon, Haggai, Adi Maron-Katz, Eti Ben Simon, Yuval Flusser, Talma Hendler, Ricardo Tarrasch, and Silviu Brill. 2016. "Mindfulness Meditation Modulates Pain through Endogenous Opioids." *The American Journal of Medicine* 129 (7): 755–58.

Sheen, Michael J, Shung-Tai Ho, Chian-Her Lee, Yu-Chi Tsung, and Fang-Lin Chang. 2008. "Preoperative Gabapentin Prevents Intrathecal Morphine-Induced Pruritus after Orthopedic Surgery." *Anesthesia and Analgesia* 106 (6): 1868–72.

Shim, Won-Sik, and Uhtaek Oh. 2008. "Histamine-Induced Itch and Its Relationship with Pain."

Molecular Pain 4 (July): 29.

Sia, Alex T, Yvonne Lim, Eileen C P Lim, Rachelle W C Goh, Hai Yang Law, Ruth Landau, Yik-Ying Teo, and Ene Choo Tan. 2008. "A118G Single Nucleotide Polymorphism of Human Mu-Opioid Receptor Gene Influences Pain Perception and Patient-Controlled Intravenous Morphine Consumption after Intrathecal Morphine for Postcesarean Analgesia." *Anesthesiology* 109 (3): 520–26.

Siddik-Sayyid, S M, V G Yazbeck-Karam, B W Zahreddine, A M B F Adham, C M Dagher, W A Saasouh, and M T Aouad. 2010. "Ondansetron Is as Effective as Diphenhydramine for Treatment of Morphine-Induced Pruritus after Cesarean Delivery." *Acta Anaesthesiologica Scandinavica* 54 (6): 764–69.

Siddik-Sayyid, Sahar M, Marie T Aouad, Samar K Taha, Mireille S Azar, Mona A Hakki, Romeo N Kaddoum, Viviane G Nasr, Vanda G Yazbek, and Anis S Baraka. 2007. "Does Ondansetron or Granisetron Prevent Subarachnoid Morphine-Induced Pruritus after Cesarean Delivery?" *Anesthesia and Analgesia* 104 (2): 421–24.

Sikand, Parul, Steven G Shimada, Barry G Green, and Robert H LaMotte. 2009. "Similar Itch and Nociceptive Sensations Evoked by Punctate Cutaneous Application of Capsaicin, Histamine and Cowhage." *Pain* 144 (1–2): 66–75.

Silva, Carlos, and Neil McNaughton. 2019. "Are Periaqueductal Gray and Dorsal Raphe the Foundation of Appetitive and Aversive Control? A Comprehensive Review." *Progress in Neurobiology* 177 (February): 33–72.

Sim, L J, and S A Joseph. 1992. "Efferent Projections of the Nucleus Raphe Magnus." *Brain Research Bulletin* 28 (5): 679–82.

Simmons, Scott W, Neda Taghizadeh, Alicia T Dennis, Damien Hughes, and Allan M Cyna. 2012. "Combined Spinal-Epidural versus Epidural Analgesia in Labour." *Cochrane Database of Systematic Reviews* 10 (October): CD003401.

Sjöström, S, A Tamsen, M P Persson, and P Hartvig. 1987. "Pharmacokinetics of Intrathecal Morphine and Meperidine in Humans." *Anesthesiology* 67 (6): 889–95.

Slappendel, R, E W Weber, B Benraad, J van Limbeek, and R Dirksen. 2000. "Itching after Intrathecal Morphine. Incidence and Treatment." *European Journal of Anaesthesiology* 17 (10): 616–21.

Smith, Howard S, Timothy R Deer, Peter S Staats, Vijay Singh, Nalini Sehgal, and Harold Cordner. 2008. "Intrathecal Drug Delivery." *Pain Physician* 11 (2 Suppl): S89–104.

Smith, Michael C, Julie Williamson, Myron Yaster, Geoffrey J C Boyd, and Eugenie S Heitmiller. 2012. "Off-Label Use of Medications in Children Undergoing Sedation and Anesthesia." *Anesthesia and Analgesia* 115 (5): 1148–54.

Snyder, Lindsey M, Michael C Chiang, Emanuel Loeza-Alcocer, Yu Omori, Junichi Hachisuka,

Tayler D Sheahan, Jenna R Gale, et al. 2018. “Kappa Opioid Receptor Distribution and Function in Primary Afferents.” *Neuron* 99 (6): 1274-1288.e6.

Somrat, C, K Oranuch, U Ketchada, S Siriprapa, and R Thipawan. 1999. “Optimal Dose of Nalbuphine for Treatment of Intrathecal-Morphine Induced Pruritus after Caesarean Section.” *The Journal of Obstetrics and Gynaecology Research* 25 (3): 209–13.

Stevens, R A, and S M Ghazi. 2000. “Routes of Opioid Analgesic Therapy in the Management of Cancer Pain.” *Cancer Control* 7 (2): 132–41.

Stuphorn, V, E Bauswein, and K P Hoffmann. 2000. “Neurons in the Primate Superior Colliculus Coding for Arm Movements in Gaze-Related Coordinates.” *Journal of Neurophysiology* 83 (3): 1283–99.

Sultan, Pervez, Maria Cristina Gutierrez, and Brendan Carvalho. 2011. “Neuraxial Morphine and Respiratory Depression: Finding the Right Balance.” *Drugs* 71 (14): 1807–19.

Sultan, Pervez, Stephen H Halpern, Ellile Pushpanathan, Selina Patel, and Brendan Carvalho. 2016. “The Effect of Intrathecal Morphine Dose on Outcomes After Elective Cesarean Delivery: A Meta-Analysis.” *Anesthesia and Analgesia* 123 (1): 154–64.

Sun, Eric C, Beth D Darnall, Laurence C Baker, and Sean Mackey. 2016. “Incidence of and Risk Factors for Chronic Opioid Use Among Opioid-Naive Patients in the Postoperative Period.” *JAMA Internal Medicine* 176 (9): 1286–93.

Sun, Yan-Gang, and Zhou-Feng Chen. 2007. “A Gastrin-Releasing Peptide Receptor Mediates the Itch Sensation in the Spinal Cord.” *Nature* 448 (7154): 700–703.

Sutton, Caitlin Dooley, and Brendan Carvalho. 2017. “Optimal Pain Management after Cesarean Delivery.” *Anesthesiology Clinics* 35 (1): 107–24.

Szarvas, Szilvia, Dominic Harmon, and Damian Murphy. 2003. “Neuraxial Opioid-Induced Pruritus: A Review.” *Journal of Clinical Anesthesia* 15 (3): 234–39.

Szarvas, Szilvia, Ramesh S Chellapuri, Dominic C Harmon, John Owens, Damian Murphy, and George D Shorten. 2003. “A Comparison of Dexamethasone, Ondansetron, and Dexamethasone plus Ondansetron as Prophylactic Antiemetic and Antipruritic Therapy in Patients Receiving Intrathecal Morphine for Major Orthopedic Surgery.” *Anesthesia and Analgesia* 97 (1): 259–63.

Szucs, Peter, Vitor Pinto, and Boris V Safronov. 2009. “Advanced Technique of Infrared LED Imaging of Unstained Cells and Intracellular Structures in Isolated Spinal Cord, Brainstem, Ganglia and Cerebellum.” *Journal of Neuroscience Methods* 177 (2): 369–80.

Tang, Jefferson, Leonid Churilov, Chong Oon Tan, Raymond Hu, Brett Pearce, Luka Cosic, Christopher Christophi, and Laurence Weinberg. 2020. “Intrathecal Morphine Is Associated with Reduction in Postoperative Opioid Requirements and Improvement in Postoperative Analgesia in Patients Undergoing Open Liver Resection.” *BMC*

Anesthesiology 20 (1): 207.

Tarcatu, Dana, Cristina Tamasdan, Natalie Moryl, and Eugenie Obbens. 2007. "Are We Still Scratching the Surface? A Case of Intractable Pruritus Following Systemic Opioid Analgesia." *Journal of Opioid Management* 3 (3): 167–70.

Tarcatu, Dana, Cristina Tamasdan, Natalie Moryl, and Eugenie Obbens. 2007. "Are We Still Scratching the Surface? A Case of Intractable Pruritus Following Systemic Opioid Analgesia." *Journal of Opioid Management* 3 (3): 167–70.

Tashiro, Manabu, Motohisa Kato, Masayasu Miyake, Shoichi Watanuki, Yoshihito Funaki, Yoichi Ishikawa, Ren Iwata, and Kazuhiko Yanai. 2009. "Dose Dependency of Brain Histamine H(1) Receptor Occupancy Following Oral Administration of Cetirizine Hydrochloride Measured Using PET with [11C]Doxepin." *Human Psychopharmacology* 24 (7): 540–48.

Ter Horst, G J, R W Hautvast, M J De Jongste, and J Korf. 1996. "Neuroanatomy of Cardiac Activity-Regulating Circuitry: A Transneuronal Retrograde Viral Labelling Study in the Rat." *The European Journal of Neuroscience* 8 (10): 2029–41.

Tershner, S A, J M Mitchell, and H L Fields. 2000. "Brainstem Pain Modulating Circuitry Is Sexually Dimorphic with Respect to Mu and Kappa Opioid Receptor Function." Pain 85 (1–2): 153–59.

Thakkar, Mahesh M. 2011. "Histamine in the Regulation of Wakefulness." *Sleep Medicine Reviews* 15 (1): 65–74.

Tiong, Sheena Y X, Erika Polgár, Josie C van Kralingen, Masahiko Watanabe, and Andrew J Todd. 2011. "Galanin-Immunoreactivity Identifies a Distinct Population of Inhibitory Interneurons in Laminae I-III of the Rat Spinal Cord." *Molecular Pain* 7 (May): 36.

Togashi, Yuko, Hideo Umeuchi, Kiyoshi Okano, Naoki Ando, Yoshitaka Yoshizawa, Toshiyuki Honda, Kuniaki Kawamura, et al. 2002. "Antipruritic Activity of the Kappa-Opioid Receptor Agonist, TRK-820." *European Journal of Pharmacology* 435 (2–3): 259–64.

Törn, K, M Tuominen, P Tarkkila, and L Lindgren. 1994. "Effects of Sub-Hypnotic Doses of Propofol on the Side Effects of Intrathecal Morphine." *British Journal of Anaesthesia* 73 (3): 411–12.

Torrecilla, Maria, Nidia Quillinan, John T Williams, and Kevin Wickman. 2008. "Pre- and Postsynaptic Regulation of Locus Coeruleus Neurons after Chronic Morphine Treatment: A Study of GIRK-Knockout Mice." *The European Journal of Neuroscience* 28 (3): 618–24.

Torrecilla, Maria, Nidia Quillinan, John T Williams, and Kevin Wickman. 2008. "Pre- and Postsynaptic Regulation of Locus Coeruleus Neurons after Chronic Morphine Treatment: A Study of GIRK-Knockout Mice." *The European Journal of Neuroscience* 28 (3): 618–24.

Tracey, Irene, and Patrick W Mantyh. 2007. “The Cerebral Signature for Pain Perception and Its Modulation.” *Neuron* 55 (3): 377–91.

Tsai, F F, S Z Fan, Y M Yang, K L Chien, Y N Su, and L K Chen. 2010. “Human Opioid μ-Receptor A118G Polymorphism May Protect against Central Pruritus by Epidural Morphine for Post-Cesarean Analgesia.” *Acta Anaesthesiologica Scandinavica* 54 (10): 1265–69.

Tubog, Tito D, Jennifer L Harenberg, Kristina Buszta, and Jennifer D Hestand. 2018. “Prophylactic Nalbuphine to Prevent Neuraxial Opioid-Induced Pruritus: A Systematic Review and Meta-Analysis of Randomized Controlled Trials.” *Journal of Perianesthesia Nursing : Official Journal of the American Society of PeriAnesthesia Nurses / American Society of PeriAnesthesia Nurses* 34 (3).

Tupone, Domenico, Christopher J Madden, and Shaun F Morrison. 2014. “Autonomic Regulation of Brown Adipose Tissue Thermogenesis in Health and Disease: Potential Clinical Applications for Altering BAT Thermogenesis.” *Frontiers in Neuroscience* 8 (February): 14.

Umeuchi, Hideo, Yuko Togashi, Toshiyuki Honda, Kaoru Nakao, Kiyoshi Okano, Toshiaki Tanaka, and Hiroshi Nagase. 2003. “Involvement of Central Mu-Opioid System in the Scratching Behavior in Mice, and the Suppression of It by the Activation of Kappa-Opioid System.” *European Journal of Pharmacology* 477 (1): 29–35.

Ummenhofer, W C, R H Arends, D D Shen, and C M Bernards. 2000. “Comparative Spinal Distribution and Clearance Kinetics of Intrathecally Administered Morphine, Fentanyl, Alfentanil, and Sufentanil.” *Anesthesiology* 92 (3): 739–53.

Urban, M O, and D J Smith. 1993. “Role of Neurotensin in the Nucleus Raphe Magnus in Opioid-Induced Antinociception from the Periaqueductal Gray.” *The Journal of Pharmacology and Experimental Therapeutics* 265 (2): 580–86.

Vaughan, C W, S L Ingram, M A Connor, and M J Christie. 1997. “How Opioids Inhibit GABA-Mediated Neurotransmission.” *Nature* 390 (6660): 611–14.

Vendruscolo, Leandro Franco, Fabrício Alano Pamplona, and Reinaldo Naoto Takahashi. 2004. “Strain and Sex Differences in the Expression of Nociceptive Behavior and Stress-Induced Analgesia in Rats.” Brain Research 1030 (2): 277–83.

Wagner, K M, Z Roeder, K Desrochers, A V Buhler, M M Heinricher, and D R Cleary. 2013. “The Dorsomedial Hypothalamus Mediates Stress-Induced Hyperalgesia and Is the Source of the Pronociceptive Peptide Cholecystokinin in the Rostral Ventromedial Medulla.” *Neuroscience* 238 (May): 29–38.

Walley, T J. 2000. “Davies Textbook of Adverse Drug Reactions.” *Postgraduate Medical Journal* 76 (901): 741E.

Wang, H, and M W Wessendorf. 1999. “Mu- and Delta-Opioid Receptor MRNAs Are Expressed

in Spinally Projecting Serotonergic and Nonserotonergic Neurons of the Rostral Ventromedial Medulla." *The Journal of Comparative Neurology* 404 (2): 183–96.

Wang, Jian, Hua Zhang, Yu-Peng Feng, Hua Meng, Li-Ping Wu, Wen Wang, Hui Li, Ting Zhang, Jin-Shan Zhang, and Yun-Qing Li. 2014. "Morphological Evidence for a Neurotensinergic Periaqueductal Gray-Rostral Ventromedial Medulla-Spinal Dorsal Horn Descending Pathway in Rat." *Frontiers in Neuroanatomy* 8 (October): 112.

Wang, Zilong, Changyu Jiang, Hongyu Yao, Ouyang Chen, Sreya Rahman, Yun Gu, Yul Huh, and Ru-Rong Ji. 2020. "Central Opioid Receptors Mediate Morphine-Induced Itch and Chronic Itch." *BioRxiv*, June.

Wang, Zilong, Changyu Jiang, Hongyu Yao, Ouyang Chen, Sreya Rahman, Yun Gu, Junli Zhao, Yul Huh, and Ru-Rong Ji. 2021. "Central Opioid Receptors Mediate Morphine-Induced Itch and Chronic Itch via Disinhibition." *Brain: A Journal of Neurology* 144 (2): 665–81.

Warner, M A, M P Hosking, J R Gray, D L Squillace, J W Yunginger, and T A Orszulak. 1991. "Narcotic-Induced Histamine Release: A Comparison of Morphine, Oxymorphone, and Fentanyl Infusions." *Journal of Cardiothoracic and Vascular Anesthesia* 5 (5): 481–84.

Warwick, J P, C F Kearns, and W E Scott. 1997. "The Effect of Subhypnotic Doses of Propofol on the Incidence of Pruritus after Intrathecal Morphine for Caesarean Section." *Anaesthesia* 52 (3): 270–75.

Watcha, M F, and P F White. 1992. "Postoperative Nausea and Vomiting. Its Etiology, Treatment, and Prevention." *Anesthesiology* 77 (1): 162–84.

Waters, Alexander J, and Bridget M Lumb. 2008. "Descending Control of Spinal Nociception from the Periaqueductal Grey Distinguishes between Neurons with and without C-Fibre Inputs." *Pain* 134 (1–2): 32–40.

Watkins, L R, G Griffin, G R Leichnetz, and D J Mayer. 1980. "The Somatotopic Organization of the Nucleus Raphe Magnus and Surrounding Brain Stem Structures as Revealed by HRP Slow-Release Gels." *Brain Research* 181 (1): 1–15.

Waxler, Beverly, Zerin P Dadabhoy, Ljuba Stojiljkovic, and Sara F Rabito. 2005b. "Primer of Postoperative Pruritus for Anesthesiologists." *Anesthesiology* 103 (1): 168–78.

Waxler, Beverly, Zerin P. Dadabhoy, Ljuba Stojiljkovic, and Sara F. Rabito. 2005a. "Primer of Postoperative Pruritus for Anesthesiologists." *Anesthesiology: The Journal of the American Society of Anesthesiologists*, July.

Weber, Franz, Shinjae Chung, Kevin T Beier, Min Xu, Liqun Luo, and Yang Dan. 2015. "Control of REM Sleep by Ventral Medulla GABAergic Neurons." *Nature* 526 (7573): 435–38.

Wei, F, K Ren, and R Dubner. 1998. "Inflammation-Induced Fos Protein Expression in the Rat Spinal Cord Is Enhanced Following Dorsolateral or Ventrolateral Funiculus Lesions."

Brain Research 782 (1–2): 136–41.

Wei, Feng, Ronald Dubner, Shiping Zou, Ke Ren, Guang Bai, Dong Wei, and Wei Guo. 2010. "Molecular Depletion of Descending Serotonin Unmasks Its Novel Facilitatory Role in the Development of Persistent Pain." *The Journal of Neuroscience* 30 (25): 8624–36.

Wells, J, M J Paech, and S F Evans. 2004. "Intrathecal Fentanyl-Induced Pruritus during Labour: The Effect of Prophylactic Ondansetron." *International Journal of Obstetric Anesthesia* 13 (1): 35–39.

Werawatganon, T, and S Charuluxanun. 2005. "Patient Controlled Intravenous Opioid Analgesia versus Continuous Epidural Analgesia for Pain after Intra-Abdominal Surgery." *Cochrane Database of Systematic Reviews*, no. 1 (January): CD004088.

Werner, W, S Dannenberg, and K P Hoffmann. 1997. "Arm-Movement-Related Neurons in the Primate Superior Colliculus and Underlying Reticular Formation: Comparison of Neuronal Activity with EMGs of Muscles of the Shoulder, Arm and Trunk during Reaching." *Experimental Brain Research* 115 (2): 191–205.

Werner, W. 1993. "Neurons in the Primate Superior Colliculus Are Active before and during Arm Movements to Visual Targets." *The European Journal of Neuroscience* 5 (4): 335–40.

Wiedenmayer, C P, and G A Barr. 2000. "Mu Opioid Receptors in the Ventrolateral Periaqueductal Gray Mediate Stress-Induced Analgesia but Not Immobility in Rat Pups." *Behavioral Neuroscience* 114 (1): 125–36.

Wiertelak, E P, B Roemer, S F Maier, and L R Watkins. 1997. "Comparison of the Effects of Nucleus Tractus Solitarius and Ventral Medial Medulla Lesions on Illness-Induced and Subcutaneous Formalin-Induced Hyperalgesias." *Brain Research* 748 (1–2): 143–50.

Wilson, Sarah R, Aislyn M Nelson, Lyn Batia, Takeshi Morita, Daniel Estandian, David M Owens, Ellen A Lumpkin, and Diana M Bautista. 2013. "The Ion Channel TRPA1 Is Required for Chronic Itch." *The Journal of Neuroscience* 33 (22): 9283–94.

Winkler, Clayton W, Sam M Hermes, Charles I Chavkin, Carrie T Drake, Shaun F Morrison, and Sue A Aicher. 2006. "Kappa Opioid Receptor (KOR) and GAD67 Immunoreactivity Are Found in OFF and NEUTRAL Cells in the Rostral Ventromedial Medulla." *Journal of Neurophysiology* 96 (6): 3465–73.

Wong, C A, R J McCarthy, J Blouin, and R Landau. 2010. "Observational Study of the Effect of Mu-Opioid Receptor Genetic Polymorphism on Intrathecal Opioid Labor Analgesia and Post-Cesarean Delivery Analgesia." *International Journal of Obstetric Anesthesia* 19 (3): 246–53.

Wong, C A, R J McCarthy, J Blouin, and R Landau. 2010. "Observational Study of the Effect of Mu-Opioid Receptor Genetic Polymorphism on Intrathecal Opioid Labor Analgesia and Post-Cesarean Delivery Analgesia." *International Journal of Obstetric Anesthesia* 19 (3): 246–53.

Wood, Patrick B. 2008. “Role of Central Dopamine in Pain and Analgesia.” *Expert Review of Neurotherapeutics* 8 (5): 781–97.

Woolf, Clifford J. 2009. “Mu and Delta Opioid Receptors Diverge.” *Cell* 137 (6): 987–88.

Wu, Christopher L, Robert W Hurley, Gerard F Anderson, Robert Herbert, Andrew J Rowlingson, and Lee A Fleisher. 2004. “Effect of Postoperative Epidural Analgesia on Morbidity and Mortality Following Surgery in Medicare Patients.” *Regional Anesthesia and Pain Medicine* 29 (6): 525–33; discussion 515.

Xie, Jennifer Y, David S Herman, Carl-Olav Stiller, Luis R Gardell, Michael H Ossipov, Josephine Lai, Frank Porreca, and Todd W Vanderah. 2005. “Cholecystokinin in the Rostral Ventromedial Medulla Mediates Opioid-Induced Hyperalgesia and Antinociceptive Tolerance.” *The Journal of Neuroscience* 25 (2): 409–16.

Yamamoto, Yumi, Pyry A Välitalo, Yin Cheong Wong, Dymphy R Huntjens, Johannes H Proost, An Vermeulen, Walter Krauwinkel, et al. 2018. “Prediction of Human CNS Pharmacokinetics Using a Physiologically-Based Pharmacokinetic Modeling Approach.” *European Journal of Pharmaceutical Sciences* 112 (January): 168–79.

Yazigi, Alexandre, Viviane Chalhoub, Samia Madi-Jebara, and Fadia Haddad. 2004. “Ondansetron for Prevention of Intrathecal Opioids-Induced Pruritus, Nausea and Vomiting after Cesarean Delivery.” *Anesthesia & Analgesia*, January, 264.

Yazigi, Alexandre, Viviane Chalhoub, Samia Madi-Jebara, Fadia Haddad, and Gemma Hayek. 2002. “Prophylactic Ondansetron Is Effective in the Treatment of Nausea and Vomiting but Not on Pruritus after Cesarean Delivery with Intrathecal Sufentanil-Morphine.” *Journal of Clinical Anesthesia* 14 (3): 183–86.

Yeh, H M, L K Chen, C J Lin, W H Chan, Y P Chen, C S Lin, W Z Sun, M J Wang, and S K Tsai. 2000. “Prophylactic Intravenous Ondansetron Reduces the Incidence of Intrathecal Morphine-Induced Pruritus in Patients Undergoing Cesarean Delivery.” *Anesthesia and Analgesia* 91 (1): 172–75.

Yesudian, P D, and N J E Wilson. 2005. “Efficacy of Gabapentin in the Management of Pruritus of Unknown Origin.” *Archives of Dermatology* 141 (12): 1507–9.

Yilmaz, Pinar, Martin Diers, Slawomira Diener, Mariela Rance, Michèle Wessa, and Herta Flor. 2010. “Brain Correlates of Stress-Induced Analgesia.” *Pain* 151 (2): 522–29.

Yoshida, Kyoko, Kazuhiro Nakamura, Kiyoshi Matsumura, Kazuyuki Kanosue, Matthias König, Heinz-Jürgen Thiel, Zsolt Boldogköi, et al. 2003. “Neurons of the Rat Preoptic Area and the Raphe Pallidus Nucleus Innervating the Brown Adipose Tissue Express the Prostaglandin E Receptor Subtype EP3.” *The European Journal of Neuroscience* 18 (7): 1848–60.

Yoshida, Kyoko, Megumi Maruyama, Takayoshi Hosono, Kei Nagashima, Yutaka Fukuda, Ruediger Gerstberger, and Kazuyuki Kanosue. 2002. “Fos Expression Induced by Warming

the Preoptic Area in Rats." *Brain Research* 933 (2): 109–17.

Young, A A, and N J Dawson. 1987. "Static and Dynamic Response Characteristics, Receptive Fields, and Interaction with Noxious Input of Midline Medullary Thermoresponsive Neurons in the Rat." *Journal of Neurophysiology* 57 (6): 1925–36.

Yurashevich, M, and A S Habib. 2019. "Monitoring, Prevention and Treatment of Side Effects of Long-Acting Neuraxial Opioids for Post-Cesarean Analgesia." *International Journal of Obstetric Anesthesia* 39 (April): 117–28.

Zaretsky, Dmitry V, Joseph L Hunt, Maria V Zaretskaia, and Joseph A DiMicco. 2006. "Microinjection of Prostaglandin E2 and Muscimol into the Preoptic Area in Conscious Rats: Comparison of Effects on Plasma Adrenocorticotrophic Hormone (ACTH), Body Temperature, Locomotor Activity, and Cardiovascular Function." *Neuroscience Letters* 397 (3): 291–96.

Zaretsky, Dmitry V, Maria V Zaretskaia, and Joseph A DiMicco. 2003. "Stimulation and Blockade of GABA(A) Receptors in the Raphe Pallidus: Effects on Body Temperature, Heart Rate, and Blood Pressure in Conscious Rats." *American Journal of Physiology. Regulatory, Integrative and Comparative Physiology* 285 (1): R110-6.

Zhang, Wenjun, Shannon Gardell, Dongqin Zhang, Jennifer Y Xie, Richard S Agnes, Hamid Badghisi, Victor J Hruby, et al. 2009. "Neuropathic Pain Is Maintained by Brainstem Neurons Co-Expressing Opioid and Cholecystokinin Receptors." *Brain: A Journal of Neurology* 132 (Pt 3): 778–87.

Zhang, Yi, Shengli Zhao, Erica Rodriguez, Jun Takatoh, Bao-Xia Han, Xiang Zhou, and Fan Wang. 2015. "Identifying Local and Descending Inputs for Primary Sensory Neurons." *The Journal of Clinical Investigation* 125 (10): 3782–94.

Zhao, Zhong-Qiu, Xian-Yu Liu, Joseph Jeffry, W K Ajith Karunarathne, Jin-Lian Li, Admire Munanairi, Xuan-Yi Zhou, et al. 2014. "Descending Control of Itch Transmission by the Serotonergic System via 5-HT1A-Facilitated GRP-GRPR Signaling." *Neuron* 84 (4): 821–34.

Zhuo, M, and G F Gebhart. 1992. "Characterization of Descending Facilitation and Inhibition of Spinal Nociceptive Transmission from the Nuclei Reticularis Gigantocellularis and Gigantocellularis Pars Alpha in the Rat." *Journal of Neurophysiology* 67 (6): 1599–1614.